The Heart in Sickle Cell Disease
Role of Non Invasive Cardiac Imaging by Advanced Echocardiography and Cardiac Magnetic Resonance Assessment of Myocardial Function

by

Inês Zimbarra Cabrita

A dissertation submitted in fulfilment of the
requirements for the degree of Doctor of Philosophy of
Imperial College London

National Heart and Lung Institute
Imperial College London
London, England

October, 2014

Declaration of Originality

I, Ines Zimbarra Cabrita, hereby declare that this thesis, Role of non-invasive cardiac imaging by advanced echocardiography and cardiac magnetic resonance assessment of myocardial function, is entirely my own work, except where otherwise acknowledged. The studies presented in this thesis have been conceived and designed with the assistance of my supervisor, Dr. J Simon R Gibbs, Professor Petros Nihoyannopoulos and Professor Fausto Pinto. The work was performed in the Department of Cardiovascular Sciences at Imperial College London. Statistical support was received from Mr. Paul Bassett and Mrs. Zélia Barroso. All published and unpublished material used in the thesis has been given full acknowledgment. This work has not been previously submitted, in whole or in part, to any other academic institution for a degree, diploma, or any other qualification.

Funding

My university fees were paid by FCT (Fundação Ciência e Tecnologia) from the Doctoral Grant Ref. SFRH / BD / 47751 / 2008

Abstract

Sickle cell disease (SCD) is one of the most prevalent genetic disorders worldwide that affects approximately 12,000 people in the United Kingdom. Raised tricuspid regurgitant velocity (TRV), which may be related to left ventricular diastolic dysfunction (LV DD), occurs in approximately 30% of adults with SCD, and has been shown to be an independent risk factor for death. This thesis examines aspects of the role of LV DD in the development of increased tricuspid regurgitant velocity and investigates the hypothesis that myocardial dysfunction, affecting the right and left ventricle, is an important cardiovascular risk factor in patients with SCD.

In the retrospective study, we determine the 5 year- survival of a cohort of patients with SCD based on their TRV. The association between raised TRV and mortality in a UK SCD population has been confirmed. Higher values of TRV were associated with a greater than 4 fold increased risk of death (HR: 4.48, 99%CI 1.01-19.8).

In the prospective study, sixty-one patients with SCD were included in the study (mean duration of follow-up 17.13±3 months). In the serial echocardiographic study , left ventricular average E/E´ ratio which is a predictor of increased left ventricular filling pressures, was independently associated with an increased tricuspid regurgitation velocity (p=0.007). In addition, blood urea nitrogen and global function index lateral showed independent association with an increased LV lateral E/E´ ratio. Biventricular myocardial deformation by 2D and 3D speckle tracking revealed significant changes in the serial measurements of systolic function.

These findings provide novel insight into the pathophysiology of the cardiovascular complications of SCD and support the implementation of echocardiographic screening of adult patients with SCD to identify high-risk individuals for further evaluation.

Publications Arising From This Thesis

The list of publications related to this research is as follows:

Peer Reviewed Journal Articles

ZIMBARRA CABRITA, I., MOHAMMED, A., LAYTON, M., GHORASHIAN, S., GILMORE A, CHO G., HOWARD J., ANIE, K.A., DESFORGES, L., BASSETT, P., GRAPSA, J., HOWARD, L., MAHALINGAM, G., DAWSON,D., PINTO, F.J., NIHOYANNOPOULOS, P., DAVIES, S.C. & GIBBS J. S. R. 2013. Tricuspid regurgitation velocity and 5 year survival in a North London population of patients with sickle cell disease in the United Kingdom, Br J Haematol. 2013 May 29. doi: 10.1111/bjh.12391. [Epub ahead of print]

ZIMBARRA CABRITA I., RUÍSANCHEZ C., GRAPSA J., DAWSON D., NORTH B., PINTO F.J., GIBBS J.S.R. & NIHOYANNOPOULOS P. 2013. Validation of the isovolumetric relaxation time for the estimation of pulmonary systolic arterial blood pressure in chronic pulmonary hypertension. Eur Heart J Cardiovasc Imaging. Jan;14(1):51-5.

ZIMBARRA CABRITA I., GRAPSA J., DAWSON D., PINTO F.J., GIBBS J.S.R. & NIHOYANNOPOULOS P. 2012. Anomalous insertion of the papillary muscle in a patient with sickle cell disease: a normal variant with no left ventricular outflow obstruction. Rev Port Cardiol, Oct;31(10):683-4.

GRAPSA, J., GIBB,S J.S.R., **ZIMBARRA CABRITA, I.**, WATSON, G.F., PAVLOPOULOS, H., DAWSON, D., GIN-SING, W., HOWARD, L.S.G.E. & NIHOYANNOPOULOS, P. 2012. The Association of Clinical Outcome with Right Atrial and Ventricular Remodelling in Patients with Pulmonary Arterial Hypertension: Study with Real Time 3D Echocardiography. Eur Heart J Cardiovasc Imaging doi: 10.1093/ehjci/jes003

ZIMBARRA CABRITA I., VILLAR, C., DAWSON, D., GRAPSA, J., NORTH, B., HOWARD, L., PINTO, F.J., NIHOYANNOPOULOS, P. & GIBBS, J.S.R. 2010. Right ventricular function in patients with pulmonary hypertension. The value of myocardial performance index measured by tissue Doppler imaging. Eur J Echocardiogr. Sep;11(8): 719-24

Published Abstracts

GRAPSA, J., **ZIMBARRA CABRITA, I.**, AFILALO, J., PASCHOU, S.A., DAWSON, D., DURIGHEL, G., O'REGAN, D., HOWARD, L.S.G.E., GIBBS, J.S.R & NIHOYANNOPOULOS, P. 2012. Regression of right ventricular mass in idiopathic pulmonary arterial hypertension: indicator of poor prognosis? two year follow-up study with 3D echocardiography and cardiac magnetic resonance. Eur J Echocardiography Abstracts Supplement 13 (S1), i169

GRAPSA, J., AFILALO, J., **CABRITA, I.Z.**, REGAN, D.O., DURIGHEL, G., LEVINE, R.A., NIHOYANNOPOULOS, P. 2012. The learning curve of CMR and 3D echocardiography for right ventricular assessment in idiopathic pulmonary arterial hypertension. Eur Heart J Cardiovasc Imaging 13(suppl 1): i76-i99 doi:10.1093/ehjci/jes257

ZIMBARRA CABRITA INÊS, GRAPSA JULIA, NIHOYANNOPOULOS PETROS, HOWARD LUKE, R. GIBBS SIMON. 2012 The prognostic implication of tricuspid regurgitation in idiopathic pulmonary arterial hypertensive patients, Rev Port Cardiol; 31(Espec Congr):5

ZIMBARRA CABRITA, I., GRAPSA, J., MOHAMMED, A., LAYTON, M., CHO, G., PINTO, F.J., NIHOYANNOPOULOS P. & GIBBS J.S.R. 2012 Left ventricular ejection fraction: may different methods be used interchangeably? Rev Port Cardiol; 31(EspecCongr):5

GRAPSA, J., REGAN, D.O., **CABRITA, I.Z.**, DAWSON, D., HORWAD, L.S.G.E., GIBBS, S.J.R. & NIHOYANNOPOULOS, P. 2011. Learning curve of real time 3D echocardiography and cardiac magnetic resonance on right ventricular remodeling: be fast and accurate. Eur Heart J 32(suppl 1): 935-1118 doi:10.1093/eurheartj/ehr325

GRAPSA, J., GIBBS, J.S.R., **CABRITA, I.Z.**, DAWSON, D., WATSON, G., GIN-SING, W., HOWARD, L.S.G.E. & NIHOYANNOPOULOS, P. 2011 Clinical outcome and right atrial remodeling inpatients with pulmonary arterial hypertension: study with real time 3D Echocardiography. Eur Heart J 32(suppl 1): 313-631 doi:10.1093/eurheartj/ehr323

GRAPSA, J., **ZIMBARRA CABRITA, I.**, DAWSON, D., HORWAD, L., GIBBS, S.J.R. & NIHOYANNOPOOULOS, P. 2011. Application of 3D Echocardiography in Pulmonary Hypertensive Patients: which indices associate with right heart catheterization? Rev Port Cardiol ; vol 30; Supplement I

ZIMBARRA CABRITA, I., GRAPSA, J., DAWSON, D., HORWAD, L., GIBBS S.J.R. & NIHOYANNOPOOULOS, P. 2011. Right ventricular speckle tracking in pulmonary hypertension: study of load influence. Rev Port Cardiol; vol 30; Supplement I

ZIMBARRA CABRITA, I., GRAPSA, J., DAWSON, D., HORWAD, L., GIBBS S.J.R. & NIHOYANNOPOOULOS, P. 2011 Left ventricular speckle tracking in pulmonary

hypertension: the study of interventricular strain dependence. Rev Port Cardiologia ; vol 30; Supplement I

ZIMBARRA CABRITA, I., RUISANCHEZ, C., SULEMANE, S., NIHOYANNOUPOLUS, P. & GIBBS, S.J.R. 2009. Função ventricular direita em doentes com hipertensão pulmonar: contributo do índice de performance miocárdica medido por Doppler tecidular. Rev Port Cardiol; vol 28; Supplement I

ZIMBARRA CABRITA, I., RUISANCHEZ, C., LAYTON, M., PINTO, F.J., NIHOYANNOPOULOS, P., GIBBS, S.J.R. 2009 Cardiovascular complications in sickle cell disease: echocardiographic features" European Heart Journal 30 (Abstract Supplement), 57

ZIMBARRA CABRITA, I., ABUBAKAR, M., LAYTON, D.M., GILMORE, A., CHO, G., HOWARD, J., NIHOYANNOPOULOS, P., GIBBS, J.S.R. 2009. Survival of patients with pulmonary hypertension and sickle cell disease in the United Kingdom, European Heart Journal, 30 (Abstract Supplement), 258

Presentations by invitation

ZIMBARRA CABRITA, I. New echocardiographic assessment in pulmonary hypertension, Simpósio Inovações em Cadiopneumologia, Escola Superior de Saúde da Cruz Vermelha Portuguesa, Lisbon, Portugal (May 2011)

ZIMBARRA CABRITA, I. Echocardiography in sickle cell disease, Pulmonary Hypertension Physicians Forum, Chelsea Physic Garden, London, United Kingdom (Nov 2010)

ZIMBARRA CABRITA, I. UK vs USA: Mortality of adults with sickle cell disease and pulmonary hypertension, Research in Progress meeting, Institute of Education, London, United Kingdom (Dec 2009)

ZIMBARRA CABRITA, I. Advanced echocardiography and magnetic resonance imaging in assessing patients with drepanocitosis, Symposium Research in Cardiopneumology, XXX Congresso Português de Cardiologia, Vilamoura, Portugal (April 2009)

Acknowledgements

It is amazing to me when I realize that I have made it to the point where I must thank all of the individuals and friends who have supported me to help me get to where I am.

I would like to begin by thanking my supervisors, Dr. Simon Gibbs, Prof. Petros Nihoyannopoulos and Prof. Fausto Pinto, whose knowledge has been invaluable in helping me complete this thesis. Their guidance, encouragement and fantastic mentoring have been of vast importance for this major work.

I must thank my family foremost for their support. My parents and sister Catarina have made research and writing more enjoyable than it would have been without their constant love and distractions.

A special thanks to my parents for the long days in taking care of my son António. Also to my adorable niece Maria and António´s brothers for giving me extra strength by making António smile every day!

Many friends assist me in so many ways and I truly appreciate them.
Gaia Mahalingam with whom I spent the first three years of this journey that always gave me her friendship and motivation in this adventure. Julia Grapsa, a great friend who always gave me her support and a great help with the scientific revision of the thesis. To Susana Gonçalves for her friendship and motivational coffee breaks!

Of course I would like to also thank everyone who has helped to make this research a success through their advising, motivation and support: Declan O´Regan, Ben Ariff, Mark Layton, Ani Bakalov, David Matthews & Cheever, Claire Andrews, Sir John McMichael Centre staff, David Dawson, Ornella Punzo, Wing-See, Taryn Coulter, Cristina Ruisanchez, Francisca Patuleia and Marcial Barros for the "accommodation" during my UK visits.

I am also very grateful to all patients and study participants.

I am especially grateful to Rute Lança, Manuela Medina and once more my mother, who helped me with the thesis formatting and editing.

I would like to acknowledge Fundação Ciência e Tecnologia for the chance and financial support provided to realise this research. To Emma Watson, special thanks, for her encouragement and support throughout these years.

Finally, I express my special gratitude to my partner Gonçalo for his love and dedicated assistance and to my little son António, who became part of this project two years ago. This thesis is dedicated to them! Without their love and assistance this thesis would not have been completed.

Obrigada a todos!

"Perfection is achieved not when there is nothing left to add, but when there is nothing left to take away."

Antoine de Saint-Exupéry

Table of Contents

List of Figures

Chapter 1

Chapter 2

Chapter 3

Chapter 4

Chapter 6

List of Tables

List of Abbreviations

2DE	2-dimensional echocardiography
2DSTE	2-dimensional speckle tracking
3DSTE	3-dimensional speckle tracking
6 MWT	6 minute walk test
BMI	Body mass index
BNP	Brain natriuretic peptide
BSA	Body surface area
CI	Confidence interval
CMR	Cardiac magnetic resonance imaging
CO	Cardiac output
DD	Diastolic Dysfunction
DTI	Doppler tissue imaging
ECC	Eulerian circumferencial
ECG	Electrocardiogram
EDV	End-diastolic volume
EF	Ejection fraction
ESV	End- systolic volume
GFI	Global function index
GLS	Global longitudinal strain
Hb	Haemoglobin
HbA	Adult haemoglobin
HbF	Fetal haemoglobin
HbS	Sickle haemoglobin
HCT	Haematocrit
HR	Hazard ratio
HRate	Heart rate
ICC	Intra-class correlation
IQR	Interquantile range
IVRT	Isovolumic relaxation time
LA	Left atrial
LDH	Lactate dehydrogenase
LGE	Late gadolinium enhancement
LV	Left ventricle
LVEDD	Left ventricular end-diastolic diameter
LVEF	Left ventricle ejection fraction
LVOT	LV outflow tract
MCV	Mean cell volume
MRI	Magnetic resonance imaging
MV DT	Mitral valve decelaration time
NHLBI	National Heart, Lung and Blood Institute
NHS	National Health Service
NIH	National Institute of Health
NYHA	New York Heart Association
PAH	Pulmonary arterial hypertension
PASP	Pulmonary arterial systolic pressure
PH	Pulmonary hypertension
PVR	Pulmonary vascular resistance
RA	Right atrial
RBC	Red blood cells
RR	Risk ratio
RT3DE	Real time 3 dimensional echocardiography
RV	Right ventricle
RVOT	Right ventricular outflow tract
SCD	Sickle cell disease
SD	Standard deviation
SR	Strain rate
STE	Speckle tracking echocardiography
SV	Stroke volume
TAPSE	Tricuspid annular peak systolic excursion
tET	Ejection timeby Tissue Doppler
tIVC	Isovolumic contraction time by Tissue Doppler
tIVR	Tissue Doppler isovolumic relaxation time
tMPI	Myocardial performance index by Tissue Doppler
TRV	Tricuspid regurgitant jet velocity
UK	United Kingdom
US	United States
VTI	Velocity-time integral

Introduction

Thesis overview

The Thesis includes two major studies:

- A **retrospective survival study consisting** of 5 years of follow-up, in which data from 170 Sickle Cell Disease (SCD) patients from Hammersmith Hospital and Central Middlesex Hospital were analysed. The population in the retrospective study included patients who were referred to the Echocardiographic Laboratory of Hammersmith Hospital and Central Middlesex Hospital from the Sickle Cell or Haematology Clinic. The clinical indication was either a clinical decision to screen for raised TRV or follow-up of previously elevated TRV. The aim of the retrospective study was to determine the survival cohort of patients with SCD based on their TRV and describe differences between those with elevated and normal TRV (Chapter 2).
- A **prospective study** of 61 patients with SCD who were identified from the 126 patients who participated in the Screening Phase of the WALK-PHaSST study. The patients were followed up for a mean period of 17 months. The 11 patients included in the Main Interventional Trial (sildenafil versus placebo) were not invited to participate in the prospective study. All of these 11 patients had TRV ≥ 2.7 m/s by echocardiogram, and 6MW distance of 150-500 m.
- The primary aim of this study was to assess the impact of cardiovascular complications in patients with SCD and to prospectively evaluate the clinical and echocardiographic predictors of short term clinical outcomes (Chapter 3).

Nature of study populations

The retrospective and prospective studies were conducted simultaneously with no overlap or repeated use of data. In the retrospective survival study, clinical and echocardiographic data was assessed at only 1 time point (data obtained between 2004 and 2005). Of the 161 patients included, 27 patients were subsequently included in the prospective study where new clinical echocardiographic data was assessed at 2 time points (data obtained between 2008-2010).

Scope and structure

The Thesis is structured into 9 chapters, divided into sections and sub-sections.

In Chapter 1 I briefly introduce to scope and structure of the thesis, the hypothesis of the study and the literature review on the subject giving an overview of SCD, the latest cardiac imaging technologies and recent developments to study myocardial function in this disease, specifically Echocardiography and Cardiac Magnetic Resonance. In addition, it also describes the previous research that has been conducted in respect to SCD and the Heart. Chapter 2presentes the data analysis and results from the retrospective survival study of 5 years follow-up. Chapter 3 describes the methodology used, the aims and research questions of the study, a description of the recruitment of the patients and healthy volunteers, the statistical methods and the imaging protocols used. In Chapter 4 the results are discussed with aim to answer the research questions according to the findings. We characterise the left and right ventricles myocardial function, the interventricular dependence in the patients group, the relationship between estimated pulmonary systolic pressures and biventricular function. Chapter 5 describes the associations between different variables with short term clinical outcomes. Chapter 6 reportes the reproducibility and reliability data regarding the test re-test results from the real time three-dimensional echocardiography (RT3DE) analysis of the left ventricle strain imaging and right ventricle volumes by 4D echocardiography. Chapter 7 includes the discussion of the results and a debate considering the initial research questions of the project. Finally, in Chapter 8, I give a summary of the results and conclusions, with consideration giving to the limitations of the study and suggestions for future research. Chapter 9 include the References of the thesis.

Hypotheses of the study

The hypotheses of this research are:

- Mortality rates in patients with SCD and Pulmonary Hypertension (PH) are lower in the United Kingdom (UK) when compared to the United States (US) population.
- Cardiac manifestations in SCD are related to age.
- Myocardial dysfunction, affecting the right and left ventricles, is an important cardiovascular risk factor in patients with sickle cell disease and its severity differs according to sickle genotypes.
- Right ventricle dysfunction is associated with a poor outcome in SCD.
- Advanced echocardiographic techniques such as myocardial deformation analysis may add additional value in understanding abnormalities of myocardial function in patients with SCD.

Chapter 1: Background and Context of the Research

Chapter 1 Background and Context of the Research

1.1. Overview of Sickle cell Disease

Sickle cell disease is the name given to a group of inherited conditions that affect haemoglobin (Hb) formation in the blood and is one of the most common haemoglobinopathies worldwide.

Also known as sickle cell anaemia, SCD is a genetic disorder of haemoglobin that is transmitted on an autosomal recessive basis that results from mutations in both copies of the β-globin gene (Frenette and Atweh, 2007, Bunn, 1997), a major subunit of haemoglobin. Haemoglobin is the iron-containing oxygen-transport protein found in the red blood cells (RBC). Adult haemoglobin (HbA) is the normal and most common type of haemoglobin (Fig.1.1) seen in adults while newborn infants have predominantly fetal haemoglobin (HbF). HbF is mostly replaced by adult haemoglobin by the age of one year (Oni, 2006). SCD occurs when an infant inherits the gene for sickle haemoglobin (HbS) from both parents or the gene for sickle haemoglobin from one parent and another abnormal haemoglobin gene, from the other parent (Brawley et al., 2008) . The characteristic phenotype of SCD includes an altered polymerization of haemoglobin resulting in a "sickled" shape to the red blood cells (Bunn, 1997) (Fig.1.2). Individuals with only one mutated β-globin gene and one normal working copy are known as sickle cell trait carriers. Sickle cell trait carriers are healthy and will not develop SCD.

The sickle mutation is characterized as a glutamine-to-valine substitution at the sixth residue of the β-globin polypeptide (Ingram, 2004) resulting in the synthesis of HbS, a structural variable that is far less soluble than normal haemoglobin when deoxygenated(Bunn, 1997).

Homozygosity for the HbS allele (homozygous sickle disease: haemoglobin SS disease) is responsible for the most common and most severe variant of SCD. Some patients are heterozygous resulting from several other genetic variants. This is related to the

interaction of different mutations of the human β-globin genes (De Montalembert, 2008). When the β^s gene interacts with the β^C gene, the resulting sickling disorder will be HbSC disease which is typically mild. Mutation such as HbC or β-thalassemia will result in haemoglobin SC and $S\beta^o$ and $S\beta^+$, respectively. When a β^s gene interacts with a β-thalassemia gene, the severity of the resulting sickling disorder depends on the severity of the co inherited β-thalassemia mutation. A $S\beta^o$ -thalassemia tends to be of a severity similar to that of homozygous HbSS. In contrast, when the resulting sickling disorder is $S\beta^+$thalassemia it can be clinically mild if the β^{+-}thalassemia mutation is mild(Kato et al., 2007).

The deoxygenated HbS molecules initially polymerize without forming fibres and subsequently polymerize into long fibres which deform the red cell into the typical sickle shape (Fig.1.3) (N.C. Hughes-Jones, 2004).

SCD is characterized by chronic haemolytic anaemia, with high susceptibility to infections, end-organ damage and intermittent episodes of vascular occlusion causing both acute and chronic pain (Frenette and Atweh, 2007).

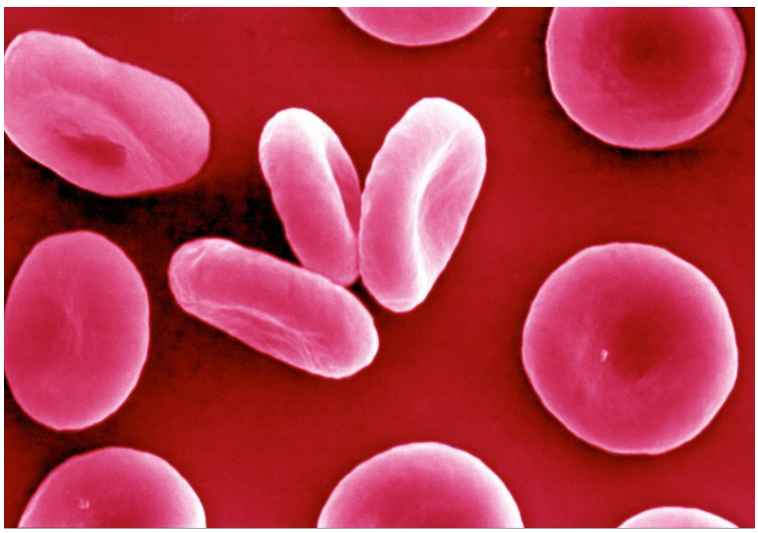

Fig. 1.1: Normal red blood cells.

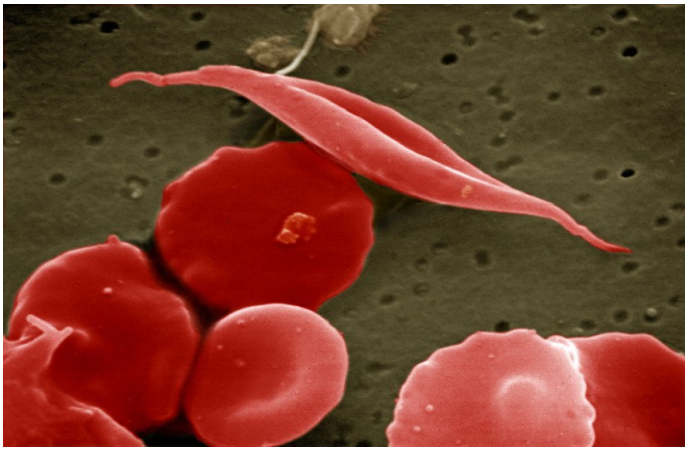

Fig. 1.2: Sickle red blood cells. The figure shows a classical sickle-shaped erythrocyte.

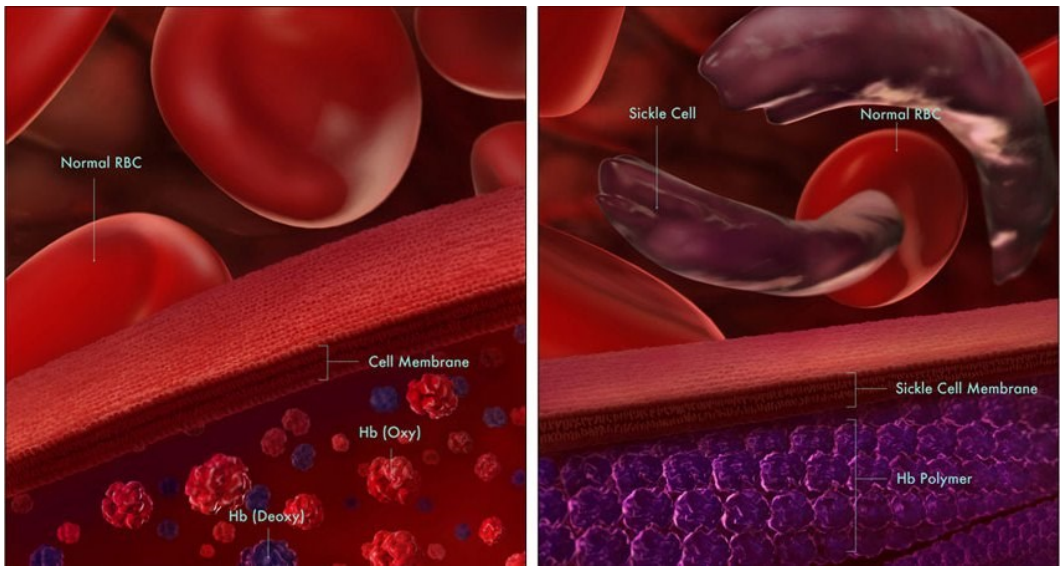

Fig. 1.3: The bottom half of the image (left) is a sectioned RBC. In a normal RBC, Hb is free to bind to oxygen. The red HbA are haemoglobin where oxygen has binded to the heme component of Hb. The purple proteins are deoxygenated forms of Hb. The bottom half of the image (right) is a sectional sickle cell within a blood vessel. It is shown that the Hb proteins form polymers due to a point mutation in the 6th position in the β-globin chain. The mutation causes glutamic-acid to be replaced with hydrophobic amino acid valine. The polymers within the cell tent and stretch the cell membrane which changes RBC into a sickle shape.

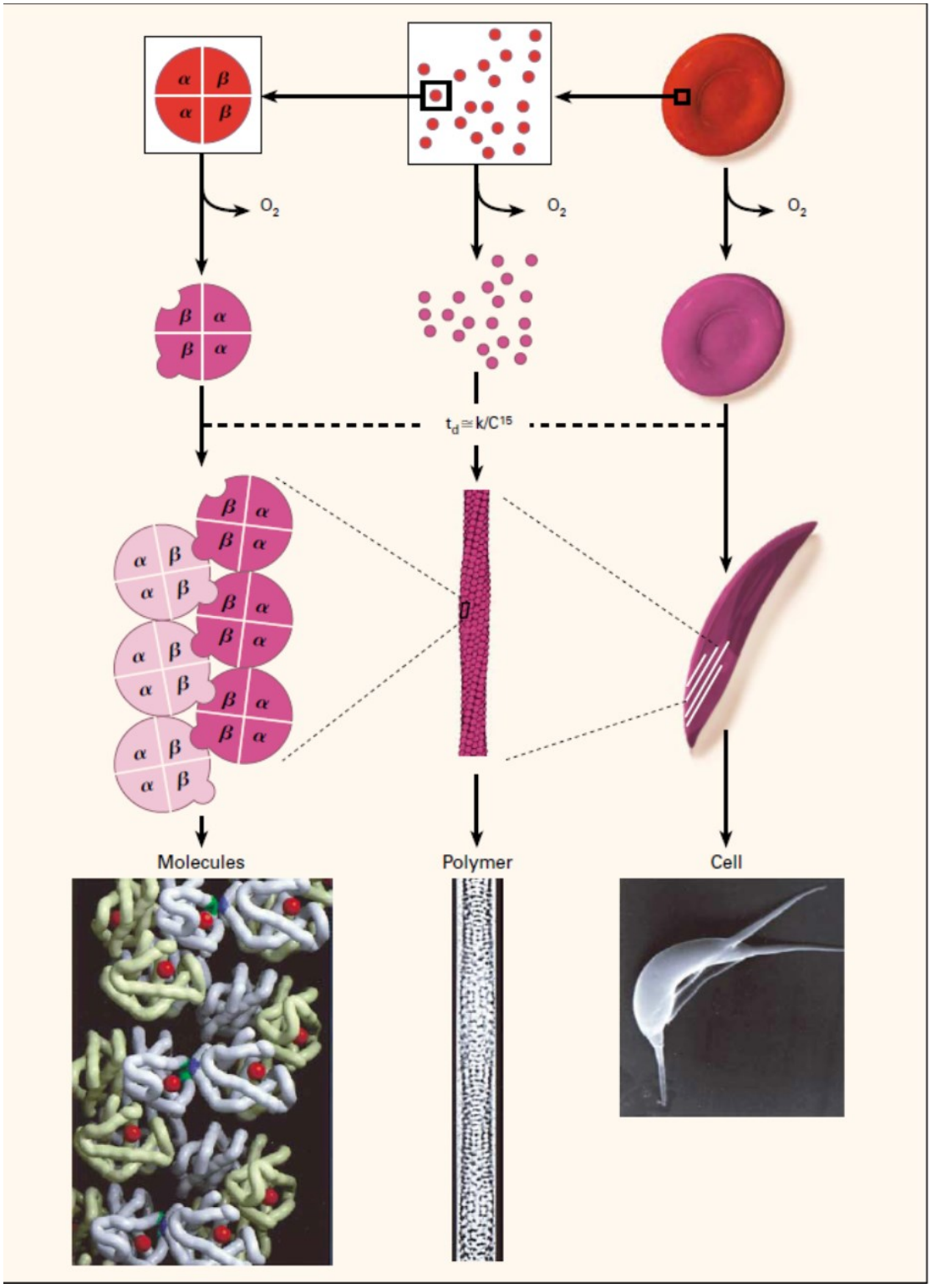

Fig. 1.4: Induction of Red-Cell Sickling by Polymerization of Deoxyhaemoglobin S.

As red cells traverse the microcirculation, oxygen is released from oxyhaemoglobin (red circles), generating deoxyhaemoglobin (purple circles). The diagram at the left of the figure (Fig. 1.4.) shows molecules of haemoglobin S, with the globular a 2 b S 2 tetramer shown as a flat circle. Deoxygenation of haemoglobin S induces a change in

conformation in which the b subunits move away from each other. The hydrophobic patch at the site of the b 6 valine replacement, shown as a projection, can bind to a complementary hydrophobic site on a b subunit of another haemoglobin tetramer, shown as an indentation. This interaction is necessary for the formation of polymer, depicted as the interaction of three deoxyhaemoglobin S molecules on one strand (dark purple) with three deoxyhaemoglobin S molecules on an- other strand (light purple). At the bottom, a high-resolution model, shows the interaction of three deoxyhaemoglobin S molecules on one strand with three deoxyhaemoglobin S molecules on another strand. The *a* subunits are pale yellow- green, and the *b* subunits are grey (lighter in the foreground and darker in the background). The heme groups are shown as red spheres. Also shown are contacts between foreground b subunits involving b 6 valine (blue) on one strand and the hydrophobic acceptor site (bright green) on the other strand. Only one of the two b 6 valine sites in each haemoglobin S tetramer makes this contact. The diagram in the middle shows the assembly of deoxyhaemoglobin S into a helical 14-strand fiber, shown as a twisted rope- like structure. The equation shows the time that elapses, or delay time (t d), between the deoxygenation of haemoglobin S and the concerted formation of polymer. The delay time is inversely proportional to the intracellular haemoglobin concentration (C), raised to about the 15th power; k denotes an experimental constant. The photograph at the bottom is a high-resolution electron micrograph of a fiber, provided by Dr. Stuart Edelstein. As deoxyhaemoglobin S polymerizes and fibers align, the red cell is distorted into an elongated banana or "sickle" shape, as shown in the diagram at the right. (Bunn, 1997)

1.1.1. History of Sickle Cell Disease

In 1846, an American doctor, R. Lebby wrote an article entitled "Case of Absence Spleen". The case report was about an African American slave who has been executed for murder. One hour after the execution, the autopsy reported "unusual body builds", describing a strange phenomenon of a man having lived without a spleen (Lebby, 1846). The following published reports of SCD appear later in the 1870's where scientist began to investigate for causes of the disease (Bloom, 1995).

Progress in the study of SCD, lead to the discovery of sickle cell disease in 1910 by James B. Herrick. A dental student with complaints of pain episodes, and symptoms of anaemia went to Dr. Herrick who assigned a resident, Dr. Ernest Irons to the case. Dr. Irons examined the student´s blood under the microscope and saw red blood cells he described as "having the shape of a sickle". The term "sickle-shaped" was coined to describe the uncharacteristic appearance of the red blood cells of this patient (Herrick, 1910). Nevertheless, Herrick was not sure if the patient's symptoms were related to a specific disease or any manifestations of another type of disease (Herrick, 1924.).

In 1927, Hahn and Gillespie discovered the role of deoxygenation when it was found that red blood cells from persons with the disease could be made to sickle by removing oxygen (Rosenthal, 2006). The peculiar elongated forms seen on oxygenated blood smears were irreversible sickle cells, which were later recognized as having an acquired membrane defect causing them to retain an abnormal shape even after the Hb is oxygenated. In 1949, two doctors, Dr. Col. E. A. Beet (Beet, 1949) and Dr. James V. Neel, an American geneticist, published independently two articles showing conclusively the hereditary nature of SCD (Neel, 1949a).

Later on, in 1945, the famous Nobel Prize-winning chemist Linus Pauling hypothesized that the disease might originate from an abnormality in the haemoglobin molecule with an abnormal electrophoretic mobility. This hypothesis was validated in 1949 by the demonstration through gel electrophoresis of the differential migration of sickle versus normal haemoglobin (Pauling and I.C., 1949) which encouraged Pauling and his colleagues to name sickle cell disease "a molecular disease" (Pauling, 1964). It was also in 1949 that the autosomal recessive inheritance of the disease was demonstrated (Neel, 1949b).

Later in 1958, Ingram and colleagues demonstrated that Hb S differed from normal haemoglobin A by a single amino acid (Ingram, 1958). Further studies analysed the structure and physical properties of Hb S, reporting that the mutant sickle haemoglobin formed intracellular polymers upon deoxygenation (Ferrone, 2004) .

1.1.2. Incidence and prevalence

SCD is most common in people whose ancestors come from Africa, South or Central America, Caribbean islands, Mediterranean countries (such as Turkey, Greece, and Italy), India, and Saudi Arabia. The World Health Organisation estimates that sickle cell disease causes nine percent of deaths in under five year olds in Africa (up to 15% in some countries in West Africa), with infection being the main cause of death (WHO, 2006 October). In certain areas of sub-Saharan Africa, an estimated 40 to 60% of the population is heterozygous, suggesting that 1 to 4% of babies born in this region may have the disease (Aliyu et al., 2008). In the US the disease affects between 50,000 and 100,000 people (Brawley et al., 2008) with an estimated one in every 375 individuals of African American descent affected. Approximately 1 in every 12 African Americans carries a SCD β-globin mutation (Wethers, 2000).

It is estimated that approximately 250,000 children are born with SCD worldwide every year (Serjeant, 1997). According to the National Health Service (NHS) Thalassemia and Sickle Cell screening programme there are approximately 240,000 carriers and an estimated 12,500 sickle cell patients in the UK (Streetly, 2000) (Lucas et al., 2008) being London one of the largest cohorts of haemoglobinopathy patients in the UK. The highest prevalence is among Black Africans and Black Caribbean's (Streetly et al., 2010). Although there is the lack of a National registry in UK, it has been reported that the number of new sickle cell patients in England is approximately 250 per annum, and it is expected this will increase through the raising of migration (Streetly, 2000).

The Cooperative Study of Sickle Cell Disease (Gaston and Rosse, 1982) made an important contribution for the study of the natural history of this disease. This study was commissioned in 1978 by the National Heart, Lung and Blood Institute (NHLBI) to characterize prospectively the clinical course of SCD in a cohort involving 4,000 patients from 23 centres across the US. This study defined the incidence and characteristics of virtually all the complications in SCD. Interestingly, it was found that over 20% of the adults suffered from fatal pulmonary complications of the disease.

1.1.3. Pathophysiology

Sickle-cell disease covers a wide spectrum of illness. Most affected people have chronic anaemia with a haemoglobin concentration of around 8 g/dl.

Clinical expression of SCD is very heterogeneous, ranging from a mild phenotype with survival between 60s years of age and 70s to a more severe disease with significant organ damage and early death (De Montalembert, 2008).

When sickle haemoglobin (haemoglobin S) is deoxygenated, the replacement of b 6 glutamic acid with valine results in a hydrophobic interaction with another haemoglobin molecule, triggering an aggregation into large polymers. The primary event in the molecular pathogenesis of sickle cell disease is the polymerization of deoxygenated haemoglobin S which results in a distortion of the shape of the RBC and a marked decrease in its deformability. The RBC became rigid cells and will be responsible for the vaso occlusive phenomena that are the hallmark of SCD (O'Malley, 2006).

Through high resolution electron microscopy and advanced methods for imaging reconstruction, the fiber's three dimensional structure has been demonstrated. The rate and extent of polymer formation in a circulating SS red cell depend primarily on three independent variables: the cell's degree of deoxygenation, the intracellular haemoglobin concentration, and the presence or absence of haemoglobin F (O'Malley, 2006). Several studies have focused on study of the pathogenesis of the vaso-occlusive events in sickle cell disease, which have demonstrated by rigorous measurements of the kinetics of polymer formation, in haemoglobin solutions as well as in sickle erythrocytes (Asakura et al., 1994, Rodgers, 1997).

The severity of sickle cell disease is mainly determined by the extent of haemoglobin S polymerization(Brittenham et al., 1985) and is proportional to the degree and duration of haemoglobin deoxygenation and to the concentration of intracellular haemoglobin S raised to approximately the 15th power.(Bunn, 1997)

Haemoglobin polymerization and erythrocyte sickling shape, where red blood cells are rigid, sticky and elongated, can lead to small vessel obstruction, ischemia and ultimately necrosis, due to the decreased lifespan of these cells. Clinical manifestations of this process are well known in the bone, lung, spleen, retina and central nervous system and are highly prevalent manifestations in these patients.

Several studies have described the wide-ranging manifestations and complications that affect every aspect of the life of afflicted SCD patients (Bunn, 1997, Claster and Vichinsky, 2003). SCD complications are not until now all well understood, however the understanding of the pathophysiology of SCD has increased resulting in more effective treatment with reduced morbidity and mortality. This is largely because of the variable degree of severity, the variability of the various manifestations, and the complexity of the interaction of the disease process with other health-related events(Schultz WH, 2003).

Acute complications include stroke, acute chest syndrome, splenic sequestration, severe pain crisis, an increased risk of sepsis or other infections (Platt et al., 1994b, Fitzhugh et al., 2010). The extent to which SCD affects the heart and its function is unclear and remains under recognised.

1.1.4. The heart in sickle cell disease

Clinical manifestations of cardiovascular abnormalities in patients with SCD have been previously documented (Ng et al., 1967, Uzsoy, 1964, Covitz et al., 1995). Interestingly the earliest description of the cardiac manifestations in SCD, has been made by Jammes Herrick, who detected a precordial murmur and cardiac enlargement (Herrick, 1910).

Lindsay, in a extended review on this subject, has referred that in patients with SCD, cardiac abnormalities are more frequent than in those with other forms of anaemia (Lindsay J, 1974). Maybe this is attributed to the chronicity and severity of the anaemia (Varat et al., 1972), especially in homozygous form of the disease. Theoretically, severe anaemia leads to inadequate oxygen delivery to tissues and the circulatory system is strained by sickled erythrocyte's propensity to occlude small blood vessels which in the heart may perhaps cause myocyte dysfunction. In a study by Hedge et al. it has been described that iron deficiency anaemia can produce left ventricular dysfunction and overt heart failure (Hegde et al., 2006).

Low haemoglobin levels are associated with elevated cardiac output at rest, cardiac enlargement and heart murmurs due to an increased stroke volume (Serjeant, 1997). Many patients with SCD have elevated left-heart filling pressures as a result of a chronically elevated cardiac output and/or diastolic dysfunction.

Although not in agreement with some researchers (Lester et al., 1990, Gerry Jr et al., 1978) a specific SCD cardiomyopathy has been described (Oliveira and Gómez-Patino, 1963, Rubler and Fleischer, 1967, Patel et al., 2012), which may in part be related to the abnormal properties of sickle cell haemoglobin, by either affecting left ventricular (LV) function due to its differing oxygen carrying properties, through intravascular sickling, long-standing anaemia or intravascular thrombosis.

The mechanism of vaso-occlusion and the sequelae of chronic intravascular haemolysis have addressed the highly variable clinical manifestations of SCD. The existence of a specific myocardial abnormality is intuitively attractive since gross cardiomegaly is commonly observed in these patients. The marked desaturation of coronary venous flow is in favour of the appearance of this vaso-occlusive phenomena that might injure the myocardium.

Myocardial scintigraphic imaging using isotopes such as thallium have been used to detect myocardium perfusion abnormalities in children with SCD (Wang et al., 2004, Sherman and Sule, 2004). Several studies have reported cases of myocardial infarction in patients with SCD (Barrett et al., 1984, Martin et al., 1996, Mansi and Rosner, 2002), however this entity has been frequently overlooked since these patients often have few or no traditional risk factors for coronary artery disease (Pannu et al., 2008, Martin et al., 1996).

Myocardial perfusion abnormalities in SCD have been found in 23 (61%) patients aged 12±5 years old, using scintigraphy (Acar et al., 2003). Another study was performed using contrast echocardiography for evaluation and quantification of myocardial perfusion. Twenty-six patients aged 23±5 years, all homozygotic SS were studied where it was found abnormal myocardial microvasculature reserve in 13 patients (Almeida et al., 2008). Raman et al. hypothesised in a subset of adults SCD patients, that these patients may have myocardial ischemia in the absence of infracted myocardium, myocardium iron overload or coronary artery disease. It was also described in this study, right ventricular dysfunction despite normal pulmonary arterial pressures (Raman et al., 2006).

Despite the long-standing interest in studying the heart in SCD, precise definition of the pathophysiologic mechanisms and clear characterization of the cardiac manifestations

in these patients is needed. Moreover, cardiovascular abnormalities appear to be less common in the heterozygous sickle patients than in homozygous sickle state and this is expected since in most such patients the anaemia is less severe.

1.1.5. Diastolic function in Sickle Cell Disease

Diastolic function is often referred as the ability of the left ventricle to accept blood at low pressures during diastole. Its impairment is characterized by abnormal ventricular distensibility and relaxation which leads to the incapacity to maintain normal ventricular filling, unless there is an increase in the left atrial pressure, is called diastolic dysfunction (Di Tullio, 2008). In SCD, it has been described that diastolic function may be a consequence of relative systemic hypertension, increased preload, decrease ventricular compliance, impaired left ventricle contractile state or direct myocardial damage from microvascular vaso-oclusive disease as a result of sickling episodes.

Diastolic dysfunction, diagnosed by Doppler echocardiography has become the primary tool for identifying and grading the severity of diastolic dysfunction in SCD which has been reported in several studies. Due to the non-uniform use of echocardiographic parameters and also the no uniform classification of diastolic dysfunction, this entity has not been comprehensively analysed and contradictory results have been found. The use of echocardiographic measurements is to a great extent variable.

In a paediatric study including 37 children, diastolic function was found in 95% according to conventional echocardiographic criteria (El-Beshlawy et al., 2006). In contrast, Sachdev et al reported an echocardiographic evidence of diastolic dysfunction in 18% of SCD adult patients contributing to PH in only one third of patients with a tricuspid regurgitan jet velocity (TRV) of 2.5 m/s or greater (Sachdev et al., 2007).
Interestingly, echocardiographic signs of left ventricular diastolic dysfunction (evidenced by a low E/A ratio) and PH (evidenced by an elevated TRV) are independent and additive risk factors for death in this National Institute of Health (NIH) PH screening study cohort. Nevertheless, no advanced echocardiographic assessment for myocardial function was used in this study.

Another study performed in 107 patients (between 3 and 18 years old) with SCD, showed early systolic and diastolic dysfunction in the left ventricle (68%) and in the right ventricle (17%). In this study, there was no correlation with haemoglobin level or number of transfusions (Caldas et al., 2008a).
More recently, a study from Knight-Perry et al. found that SCD adult patients when compared to a control group had larger left and right heart chambers and higher estimated LV and right ventricle (RV) filling pressures, whereas DTI derived measures of LV and RV relaxation were similar between the groups. Furthermore, noninvasive measures of LV ventricular relaxation or stiffness or compliance (i.e., isovolumic relaxation time (IVRT), E velocities, mitral E/A ratio, and mitral valve deceleration time (MV DT) did not differ between patients with SCD and controls, suggesting that the intrinsic myocardial properties in subjects with SCD remain preserved (Knight-Perry et al., 2011).

Doppler-derived diastolic parameters do not provide specific information on intrinsic passive diastolic properties, thus, diastolic dysfunction cannot be diagnosed solely by Doppler echocardiography (Maurer et al., 2004). In fact, several authors have reported the need of consistency and uniformization in the use tissue Doppler imaging and myocardial deformation parameter for the use of load-independent echocardiographic parameters (Zilberman et al., 2007, Sachdev et al., 2007).

Cardiac iron overload can contribute for the abnormal myocardial relaxation but it has been rarely reported to SCD patients (Wood, 2008) . Nevertheless, early detection of myocardial iron overload is important and this is possible with the application of magnetic resonance imaging (MRI) in combination with tissue Doppler echocardiography and deformation imaging, a promising technique enabling the detection of wall motion abnormalities despite preserved global heart function (Vogel et al., 2003).

Besides some controversy among literature, it is well established that patients with SCD have some degree of diastolic dysfunction, however, it is not yet clear whether the patients have subtle and sub-clinical LV systolic dysfunction despite preserved ejection

fraction and a growing interest among researchers has been developed during the last years, with the use of more advanced cardiovascular imaging modalities.

1.1.6. Pulmonary hypertension in sickle cell disease

Pulmonary hypertension is a disorder characterized by increased pulmonary artery pressure and has been defined in the latest Guidelines for the diagnosis and treatment of pulmonary hypertension (Authors/Task Force Members et al., 2009) by a mean pulmonary artery pressure ≥ 25 mm Hg which based on cardiac catheterisation measurement, considered the gold standard definition of pulmonary hypertension. The echocardiographic correlate of this diagnostic criterion based on tricuspid regurgitation estimates systolic pulmonary arterial pressure and a cut off value of TRV≥2.5 m/s, has been widely used (Lee et al., 2009, Sachdev et al., 2007, Gladwin et al., 2004, Parent et al., 2011, De Castro et al., 2008).

For pulmonary arterial hypertension, additionally should be a normal cardiac output (to reject a hyperdynamic state, and a wedge pressure ≤ 15 mmHg to exclude causes of left sided-cardiac disease).

Pulmonary hypertension may occur as a consequence of raised pulmonary vascular resistance or high cardiac output. Raised pulmonary vascular resistance may occur as a consequence of pre-capillary pulmonary arterial disease, post capillary disease (pulmonary venous disease or left heart disease) or both (J Simon R Gibbs, 2009).
While severe pulmonary hypertension is normally a straightforward echocardiographic diagnosis, it is possible to miss mild cases especially when right ventricular function is preserved and the remainder of the echocardiographic examination at rest appears normal.

PH has been increasingly recognised as a complication of SCD and its development heralds a severe clinical phenotype associated with sudden death (Fitzhugh et al., 2010, Gladwin et al., 2004).

The aetiology of PH in SCD is probably multifactorial, including haemolysis, impaired nitric oxide biovailability, chronic hypoxemia, thromboembolism, splenic infarction, portal hypertension, lung fibrosis, HIV and schistosomiasis, all considered risk factors for pulmonary hypertension (Roberto F. Machado, 2005).

Autopsy studies suggest that 75% of patients with SCD have histological findings of pulmonary arterial hypertension (PAH) at the time of death (Odd et al., 2009), suggesting that PAH may be clinically silent or poorly recognized for a late manifestation.

One of the controversies in relation to PH in SCD is the inappropriate use of TRV for defining PH. The use of TRV obtained from echo only allows for the diagnosis of suspected PH, being a widely and successfully tool for screening test for elevation of pulmonary arterial pressure (Hatle et al., 1981, Lanzarini et al., 2002) since it has a low false-negative rate. The diagnoses of PH still requires right heart catheterization due to the high negative predictive rate as stated in the latest consensus report (Authors/Task Force Members et al., 2009, McLaughlin et al., 2009) and evidence-based analysis (Hoeper et al., 2009) (Parent et al., 2011, Fonseca et al., 2012)

The ability to highlight a subgroup of patients with a high predicted mortality by use of a non-invasive measurement such as TRV represents a significant clinical advance and has rightly generated a lot of research interest. Raised TRV as assessed by Doppler echocardiography, whether or not associated with pulmonary arterial hypertension, is commonly found in sickle cell disease in approximately 32 to 40% of patients (Ataga et al., 2004, Fitzhugh et al., 2010, Gladwin et al., 2004, Liem et al., 2007b) and has been reported as a marker of mortality in several major studies from the United States (Anthi et al., 2007b, De Castro et al., 2008, Ataga et al., 2006, Machado and Gladwin, 2010, Lorch et al., 2011, Gladwin et al., 2012) .

Sutton and colleagues reported a 40% mortality rate at 22 months, with an odds ratio for death of 7.86 (2.63-23.4)(Sutton et al., 1994). Powars and colleagues reported a mean 2.5-year survival in SCD patients with chronic lung disease with PH (Powars et al., 1988). De Castro and colleagues similarly reported a 50% 2-year mortality rate in SCD-PH patients (De Castro, 2004).

Regarding SCD, PH has been defined based on the tricuspid regurgitant jet velocity (TRV) using the modified Bernoulli's equation (4*TRV plus central venous pressure estimate), whereas in other PH diseases have used catheterisation for diagnosis of PH. Whether increase TRV in SCD is of increased risk from PAH and/or from vasculopathy or other associated complications of SCD, e.g. proteinuria (prevalence of 20 to 25 %), is important to identify.

In the NIH PH screening study, a TRV of at least 2.5 m/s, as compared with a velocity of less than 2.5 m/s, was independently associated with a marked increased risk of death (Risk Ratio (RR) = 10.1; 95% Confidence Interval (CI) = 2.2-47; P < .001)(Gladwin et al., 2004). The 18-month mortality was 16% for patients with a TRV of 2.5 m/s or greater and was less than 2% in patients without PH. In addition, a study by Castro and colleagues reported a similar prevalence of PH (36% in patient with HbSS and S-beta0 thalassemia and 25% in SC and S-beta+thalassemia) and a remarkably similar 17% mortality rate for patients with PH over 2 years compared with approximately 2% for subjects without PH(Castro et al., 2003). Ataga and colleagues have also shown a 10% mortality rate for patients with PH over 26 months in comparison to 1% in those patients without PH (Kenneth I. Ataga, 2006).

The high prevalence of PH in the population and associated high mortality demand worldwide non-invasive screening of all adults with Doppler echocardiography. There are limited data on specific screening procedures and echocardiographic assessment, which uses different limits when compared to other forms of PH, probably due to the central controversy of whether intensification of specific therapy will contribute to decrease mortality and morbidity associated with the most severe cases of the disease. Although the precise aetiology and severity of the pulmonary hypertension in patients with SCD has not been well defined, several studies (Table 1) have shown that even modestly elevated pulmonary artery pressures when compared to other forms of PH, as assessed by right heart catheterization or by echo-Doppler, indicate a poor prognosis(Gladwin et al., 2004, Castro et al., 2003). A controversy in this field is related to the contribution of left ventricular dysfunction to increased pulmonary pressures. Castro et al has shown with invasive hemodynamic measurements a varied picture of high pulmonary artery pressures and elevated pulmonary capillary wedge pressure, suggesting that LV dysfunction (systolic or diastolic) may contribute to the high pulmonary artery systolic pressure (Castro et al., 2003) . In the French study by Parent

et al, a total of 385 patients were included and has been reported that 25% of these patients had elevated TRV (≥ 2,5 m/s), however, the catheterization showed that only 24 patients (6% of the total population) had real PH and from this ones , only 6 had PAH, while over 75% were explained by pulmonary venous hypertension or a hyperdynamic state. On the other hand, it is important to refer, that in this study, the exclusion criteria were not similar to most of the studies, and patients where pulmonary hypertension would be expected, were excluded. This inconsistency of selection criteria among SCD studies regarding pulmonary hypertension, warrants the need for further investigations to understand the impact of left-sided cardiovascular disease in these patients, which apparently may be more frequent than what has been reported.

Table 1.0.1 - Pulmonary hypertension SCD studies with the use of tricuspid regurgitant jet velocity.

First Author (Publication year)	Type of study	Criteria for PH	Exclusions	Number of patients screened	Disease phenotype — no. (%)	% of patients with PH	Follow-up time (months)	Overall mortality	Mortality in PH group	P-value (mortality in PH vs non-PH)
Cabrita et al. (2013)	Retrospective	TRV≥2.5 m/s	Unstable patients > 2W from vaso-occlusive crisis >4W from ACS	164	102 HbSS(62%) 41 HbSC (25%) 8 HbS-β^0 (5.5%) 1 HbS-β^+ (6%) 2 Other (1.2%)	29%	68.1*	9.1%	14.5%	0.06 NS
Fonseca G. et al (2012)	Prospective	RHC in patients with TRV≥2.5 m/s	Unstable patients, History of ACS >2W from a transfusion Valvular heart disease LV systolic dysfunction	80	HbSS HbS-β^0 (not specified %)	81% of 26 pts who underwent RHC; 40% by TRV≥2.5 m/s	31.9*	8.75%	15.6%	0.07 NS
Parent et al. (2011)	Prospective	TRV≥2.5 m/s or RHC	Unstable patient, Severe renal insufficiency Chronic restrictive lung disease severe liver disease	398	379 HbSS (98%) 6 HbS-β^0 (2%)	25% (24/96 who underwent RHC) ; 27% by TRV≥2.5 m/s	26±6**	2,00%	12.5%	**0.002**
Gladwin et al. (2009)	Prospective	TRV≥2.5 m/s	Unstable patients > 2W from vaso-occlusive crisis > 4W from ACS	195	132 HbSS (69%) 35 HbSC (18%) 23 HbS-$\beta^{0,+}$ (12%) 5 unknown	32%	18.3 for TR<2.5; 17.3 for TR≥2.5*	5.3%	12.9%	**<0.001**
Lee M. (2009)	Prospective	TRV≥2.5 m/s	Unstable patients ≥2W from an acute illness ≥3 weeks from transfusion	94	23 HbSC (26%) 1 HbS-β+ (1%) 4 HbS-β^0 (5%)	20%	39.4 ± 8.7 PH group ;36.1 ± 13.7 non Ph group **	no deaths	NA	NA
Castro L.M. et al (2008)	Retrospective	TRV>2.5 m/s or by RHC	Acute vaso occlusion symptoms Any other acute complication of SCD	125	77 HbSS (62%) 33 HbSC (26%) 11 HbS-β+ (9%) 2 HbS-β^0 (2%)	32%	62.4 **	9.6%	21.4%	**<0.05**
Ataga et al. (2006)	Prospective	PASP+Age+BMI +Gender	Unstable patients >4W from ACS Evidence of CHF	93	70 HbSS (75%) 10 HbSC (11%) 6 HbS-β^0 (6%) 7 HbS-β+ (8%)	39%	33.6 *	13.1%	11%	**0.01**
Castro O. et al (2003)	Retrospective	Right Heart Cath. MPAP>25 mmHg	None (all patients were hospitalized)	34	28 HbSS (82%) 4 HbSC (12%) 1 HbS-β+ (3%) 1 HbSD (3%)	58%	45 for non-PH; 23 for PH*	41%	55%	**0.04**

ACS: acute chest syndrome;CHF: congestive heart failure; Pts: patients; PH: pulmonary hypertension; TRV: tricuspid regurgitant jet velocity ;RHC: right heart catheterization; W: weeks; * Median . ** Mean

1.2. Echocardiography

Echocardiography was first used in 1954 by Edler, a Swedish cardiologist and Hertz, a physicist (Edler I Fau - Hertz and Hertz) to record movement of heart structures and since than it has evolved considerably from the single spatial and temporal resolution of M-mode echocardiography to the 3-dimensional imaging systems.

Echocardiography is considered one of the most commonly performed non-invasive diagnostic tests in patients with known or suspected cardiovascular abnormalities and it is an increasingly important investigative tool in cardiology. The assessment of cardiac function is becoming progressively sophisticated and the recent developments in cardiac ultrasound permit the utilization of many newer physical concepts with currently available echocardiographic machines.

Unlike most medical diagnostic tests, diagnostic ultrasound exists in nature and the sonic imaging capability in some mammals is remarkable. True clinical use of echocardiography began in the mid 1970's (Gramiak and Shah, 1971, POPP and HARRISON, 1970, Feigenbaum, 1996). Interestingly, studies using echocardiography for the evaluation of cardiac performance, started to rise in the late 1970's where several reports have been published (Lindsay J, 1974) (Gerry Jr et al., 1978).
Echocardiography provides comprehensive evaluation of the cardiovascular structure, regional and global function, and hemodynamics that be possible to provide comprehensive measurements to fully understand the cardiovascular structure and myocardial function (Thomas and Popovic, 2006, Lamers et al., 2006, Caldas et al., 2008b).

M-mode was the first clinical application of ultrasound. M-mode or motion-mode images are a continuous 1-dimensional graphic display that can be derived by selecting any of the individual sector lines from which a 2-dimensional image is constructed.
M-mode echocardiography is useful for quantitating single dimensions of walls and chambers in normally shaped ventricles, with the important advantage of its high temporal resolution, which makes it useful for example timing valve motion(Gottdiener et al., 2004) and annular motion. Although some limitations of its use are related to the

single dimension which may not be representative in distorted ventricles and the beam orientation is frequently off-axis.

Two-dimensional (2D) echocardiography is the spine of echocardiography. It allows for the comprehensive visualization of the components of the beating heart, by displaying in real-time tomographic images. The distance of ultrasound echoes along the vertical axis represents the depth of echo-producing structures, with brightness indicating the intensity of the returning echo. It gives information regarding cardiac chamber size, wall thickness, global and regional systolic function, and valvular and vascular structures (Lang et al., 2005).

The motion of the stars caused a change in the wavelength (or frequency shift) of the light reaching the observer. The phenomenon has been termed “Doppler effect” and applies to any wave in which the source or receiver is mobbing to respect to other. This principle was first described by Christian Doppler an Austrian physicist who noted that stars appeared on different colours when observed from a stationary point at earth(Gorcsan and Tanaka, 2011).

This principle has been applied to echocardiography for detecting the direction and velocity of moving blood within the cardiac chambers, across the valves and in great vessels(Kleijn et al., 2012b).

Although 2D echocardiography is the most frequent used imaging modality for LV quantification, its limitations are well known for the estimation of ventricular volumes. Two-dimensional assessment of global LV volumes and ejection fraction (EF) with biplane method of discs relies on geometric assumptions and has some limitations due to chamber foreshortening and subsequent underestimation of LV volumes.

The visual assessment of LV ejection fraction and regional wall motion abnormalities still requires extensive skill and expertise of the reader and eventually remains subjective (Quiñones et al., 2003, Blondheim et al., 2010).

Imaging technology has advanced considerably during the last decade, considering equipment, software, and image processing where the advent of modalities such as real-time 3 Dimensional echocardiography (RT3DE), tissue Doppler strain imaging and speckle tracking has been widely valued (Oh et al., 2006, Teske et al., 2008, Hung et al., 2007).

Much of the progress witnessed in these techniques can be attributed to their application to complex problems, such as the quantification of global and regional LV systolic and diastolic function, as well as response to cardiac resynchronization therapy. The need to understand a new language is fundamental for the selection of diagnostic and therapeutic strategies in patients with SCD and co-existent cardiac dysfunction.

Three-dimensional imaging techniques such as computed tomography and cardiac magnetic resonance imaging (CMR) overcome limitations posed by other methods in that images planes are precisely defined and geometric assumptions are unnecessary. However, these imaging modalities are expensive, time-consuming and have limited availability.

The acquisition of the first 3D cardiac ultrasound images was reported in 1974. Developments in 3D echocardiography started in the late 1980s with the introduction of off-line 3D medical ultrasound imaging systems. Several review articles have been published, assessing the progresses and limitations of 3D ultrasound technology for clinical screening (Gopal et al., 1993, Sugeng et al., 2003, Jenkins et al., 2004). These articles reflect the diversity of 3D systems that were developed for both image acquisition and reconstruction. One of them was the introduction of the matrix phased array transducers that scan a true three-dimensional volume at each pulse. This technology, pioneered by Von Ramm at Duke University with the volumetric transducer, was fundamentally different from the former generations of 3D systems as the entire cardiac volume was acquired in real-time (1 scan for 1 cardiac cycle), enabling the cardiologist to view moving cardiac structures from any given plane over a single cardiac cycle (Kisslo et al., 2000). Since then, a variety of computer-based 3-dimensional reconstruction techniques have been developed to replace the subjective mental reconstruction of complex cardiac geometry.

With a linear 1D array, the transducer controls the direction within a slice in 3D space, referred to as the azimuth. With this 2D matrix array, the steering is controlled in both the azimuth and the elevation directions, allowing the acquisition of an entire pyramidal-shape (Kühl et al., 2004) . Samples are acquired slice by slice at evenly spaced depths. The spacing between each scanning depth is equal to 0.308 mm in radial coordinates. This spacing determines the resolution in the receive line direction. A maximum of 512 slices can be acquired with the transducer. The RT3DE transducer array operates at frequencies between 2.0 MHz and 3.5 MHz. The particular design of the transmitter and receiver lines achieves a 16:1 parallel processing mode allowing extremely fast acquisition.

RT3DE imaging facilitates the display of simultaneous multiple-plane display on the same screen to convey the 3-dimensional nature of the ultrasound data and it has been used in several clinical settings (Sachpekidis et al., 2011, Kapetanakis et al., 2011). It automatically acquires the image of the entire cardiac structure along 4 cardiac cycles while the transducers is kept fixed on a point. 3-D images are thus easier to obtain and are theoretically more precise than complex non-real time methods.

Real-time 3D echocardiography using second-generation matrix-array transducers retain all the advantages of echocardiography but provide 3D spatial registration. Image quality is improved, therefore offering a practical approach for assessment of the RV and LV function and quantification of volumes, of outmost importance evaluation in the SCD population.

1.2.1. Assessment of Left Ventricular Volumes and Function by RT3DE

The need for a more reproducible assessment of LV volumes and function, prompt to the development of three-dimensional echocardiography (Monaghan, 2006). During the last decade, several studies using CMR as the current gold standard technique have shown the accuracy and reliability of 3D over 2D echocardiography (Jacobs et al., 2006, Jenkins et al., 2006).

Since it does not require any geometric assumptions and it can guard against image foreshortening, the direct volumetric assessment of LV size is preferable to calculations made from 2D or M-Mode (Atsumi et al., 2013).

A wide number of software packages are currently available to calculate 3D LV volumes. They use semi-automated border tracking techniques to create a mathematical cast of the whole ventricle throughout the cardiac cycle, where EF and volumes are derived (Fig. 1.5).

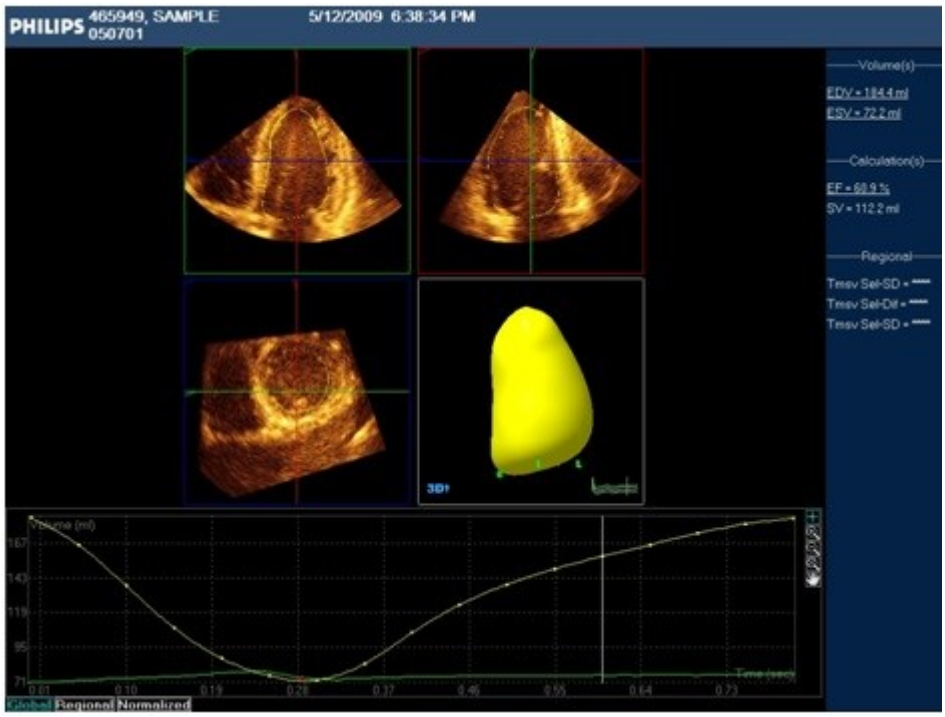

Fig. 1.5: Real time 3D echocardiographic dataset showing LV endocardial cast. LV volume rendered representation with cut-planes of short-axis, 4 and 2-chamber views are displayed. The global volume curve is display on the bottom.

1.2.2. Assessment of Right Ventricular Volumes and Function by RT3DE

Right ventricular systolic dysfunction has been identified as a key element in determining prognosis of patients afflicted with pulmonary hypertension(Lopez-Candales et al., 2005). Although echocardiography has proved invaluable to noninvasively assess pulmonary artery pressures, evaluation of right ventricular size and systolic function by echocardiography is somewhat more difficult, largely because of the complex RV anatomy that limits its evaluation (Ho and Nihoyannopoulos, 2006).

The high prevalence of PH in SCD population and associated high mortality demand universal non-invasive screening of all adults with Doppler echocardiography. Sachdev

et al (Sachdev et al., 2007), reported that echocardiographic evidence of diastolic dysfunction is common in SCD patients, but contributes to PH in only one third of patients with a TRV of 2.5 m/s or greater. Interestingly, echocardiographic signs of left ventricular diastolic dysfunction (evidenced by a low E/A ratio) and PH (evidenced by an elevated TRV) are independent and additive risk factors for death in the NIH PH screening study cohort (Gladwin et al., 2004). Therefore, identification of early right ventricular dysfunction is of outmost clinical importance.

A study comparing 2D and 3D echocardiography found that 2D significantly overestimated right heart volume assessments compared with 3D by a factor of 45% and showed a greater reproducibility of 3D (Schindera et al., 2002). In other study (Niemann et al., 2007) a recent technology by TomTec Imaging Systems has been used to validate RV volumes and EF by 3D echo. The results showed a good reproducibility and accuracy in measuring RV volumes in healthy adult subjects.

This recent software uses three-dimensional ultrasound data sets to combine the simplicity and speed of echocardiography with the accuracy of MRI. The software calculates a three-dimensional right ventricular surface model using a semiautomated border detection algorithm with manual correction options based on in vivo normal as well as pathologic RV modelling (Fig. 1.6). The model will therefore measure right ventricular end diastolic and systolic volumes and ejection fraction. To our knowledge no study was performed in SCD population with the use of 3D echocardiography with specific software for RV analysing.

The high prevalence of PH in the SCD population and previous described high mortality, demand universal non-invasive screening of all adults with echocardiography and an accurate quantification of right and left ventricular volume and function is necessary for a better understanding of this complex disease.

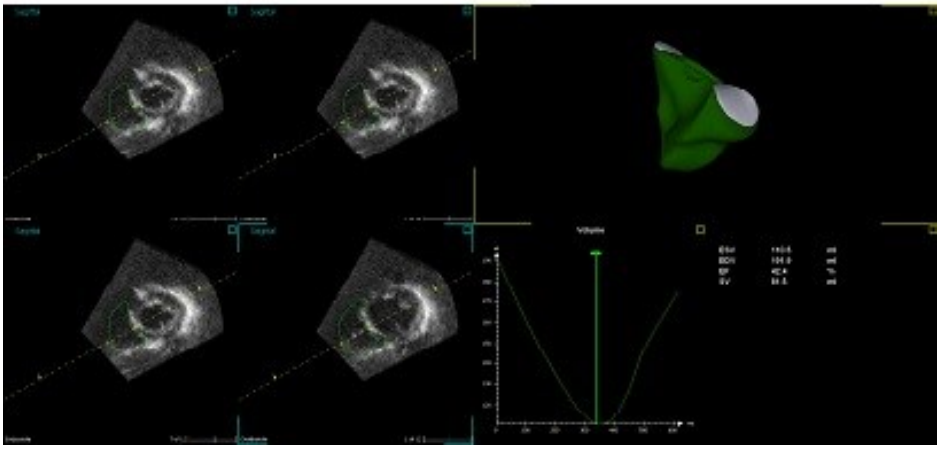

Fig. 1.6: Three dimensional analysis of the right ventricular volumes, stroke volume and ejection fraction. Display of 3D images in sagital views in systole (top) and diastole (bottom), with manual tracing and adjustments in all planes.

1.2.2.1. Limitations of RT3D

The limitations of 3D echocardiography are well known. One of the limitations is concerning the additional training which is need to capture 3D images and also for the correct use of the dedicated software. This may be related with the fact that RT3D is not yet so currently available and included as a routine as is 2D imaging

RT3D images are not yet fully integrated with data storage systems used for 2D echocardiography. In addition, it is not fully incorporated into major society guidelines and differences in data derived from different software packages need to be further delineated. As in 2D imaging, patients with poor acoustic windows secondary to body habitus, chest deformities or lung pathology remain a challenge(Atsumi et al., 2013).

Technically, 3DRT has reduced temporal and spatial resolution which may be a limitation especially when trying to image larger ventricles and/or at higher heart rates. Also “stiching” artefacts particularly in those with arrhythmia or those unable to breathhold for a sufficient period, need careful check on the images prior to analysis.

Left ventricular volumes quantification, which is currently the most clinically applicable RT3D technique, appears to have a significant underestimation of volumes. Although, this limitation maybe overcome by experience and was independent of software use (Aessopos et al., 2007).

It has been described, that this is mainly related to the difficultly in differentiating left ventricular trabeculations from true myocardium. There is an urgent need for widely agreed cut-off values for certain analyses according to software programs.
Concerning the assessment of RV, there are reported difficulties in imaging the near field by 3D echo which results in poor definition of the anterior free wall of the right ventricle with potential inaccuracies for extrapolation of the endocardial contour. (Seo et al., 2009)

1.2.3. Myocardial deformation imaging

Myocardial deformation imaging is a novel echocardiographic method for assessment of global and regional myocardial function. The assessment of the contractile function of the heart has traditionally been restricted to volumetric assessments of left and right ventricles and the estimation of ejection fraction. The regional wall motion abnormalities have been evaluated with visual estimation which undoubtedly, it's a method that lacks of reproducibility and standardization.

Myocardial imaging can be performed with 3 methods: Doppler Tissue Imaging (DTI), 2-dimensional speckle tracking (2DSTE) or 3-dimensional speckle tracking (3DSTE).

1.2.3.1. Doppler Tissue Imaging

DTI has proven to be effective in measuring ventricular function (Sohn et al., 1997, Yu et al., 2007) (Teske et al., 2008). The method of strain rate imaging by tissue Doppler was developed at the Norwegian University of Science and Technology in Trondheim. The derived parameters from DTI, strain and strain rate (SR), offer a quantitative evaluation of regional myocardial deformation and deformation rate. The myocardial time-velocity curve can be reconstructed either on line as spectral pulsed DTI or off line from 2D colour-coded DTI image loops(Yu et al., 2007) . Importantly, the peak systolic velocity is a sensitive marker of mildly impaired LV systolic function, even in those with a normal

ejection fraction or apparently preserved LV systolic function, a common finding in SCD (Thomas H Marwick, 2009, George R. Sutherland, 2006)

Tissue Doppler use the velocity gradient along the length of the myocardium in order to calculate strain rate, which is afterwards integrate to derive strain (as percentage) (Heimdal et al., 1998).

The concept of strain is complex, but linear strain can be defined by the Lagrangian formula:

$$\varepsilon = \frac{L - L_0}{L_0} = \frac{\Delta L}{L_0}$$

Where ε is strain, L_0 = baseline length and L is the instantaneous length at the time of measurement. Thus strain is deformation of an object, relative to its original length. By this definition, strain is a dimensionless ratio, and is often expressed as percentage.
It is important to refer, that strain and strain rate only describe the part of the myocardial relating to volume changes and not to pressure, and both systolic and diastolic deformation is load dependent. The assessment of regional dysfunction, have to take into account the segment interaction and the load dependency, so it may enable us for assessing relatively contractility, since contractility cannot be measured directly.

One of the limitations of DTI method for strain analysis is the angle dependency since it assesses only the plane incident with the ultrasound beam. The second limitation is the requirement for the acquisition of images with high frame rate.

1.2.3.2. 2D Speckle Tracking

Speckle tracking echocardiography (STE) is a new developed technique for the assessment of LV and RV global and regional function. It analyses motion by tracking speckles in the ultrasonic image in two dimensions (Perk et al., 2007). During the systole, the ventricular myocardium simultaneously shortens in the longitudinal and circumferential planes and thickens in the radial plane. Reciprocal changes are found during diastole.

STE analyses myocardial motion by frame-by-frame tracking of natural acoustic markers (≈20 to 40 pixels in size and variably referred to as “speckles,” “patterns,” or “fingerprints”) that are produced by constructive and destructive interference (i.e., reflections, interference, scattering) between ultrasound and myocardium within a user-defined region of interest.

The movement of individual speckles towards or away from one another represents regional myocardial shortening or lengthening and thus giving information regarding the strain and strain rate (Shah and Solomon, 2012, Perk et al., 2007). Longitudinal and circumferential shortening results in negative strain values, while radial thickening results in a positive strain value (Fig. 1.7). Unlike DTI, 2-STE analyses Lagrangian strain. Speckle tracking is an offline technique that is applied to previously acquired 2D images, attention is therefore needed for the acquisition of the images since Frame rates of ≈40 to 80 are required to avoid speckle decorrelation, and good image quality is needed for accurate tracking(Marwick et al., 2009a). Usually, the myocardium is analysed in six different planes: three short-axis views (basal, mid-ventricular, and apical) and three other apical views (four-chamber, two-chamber, and three-chamber).

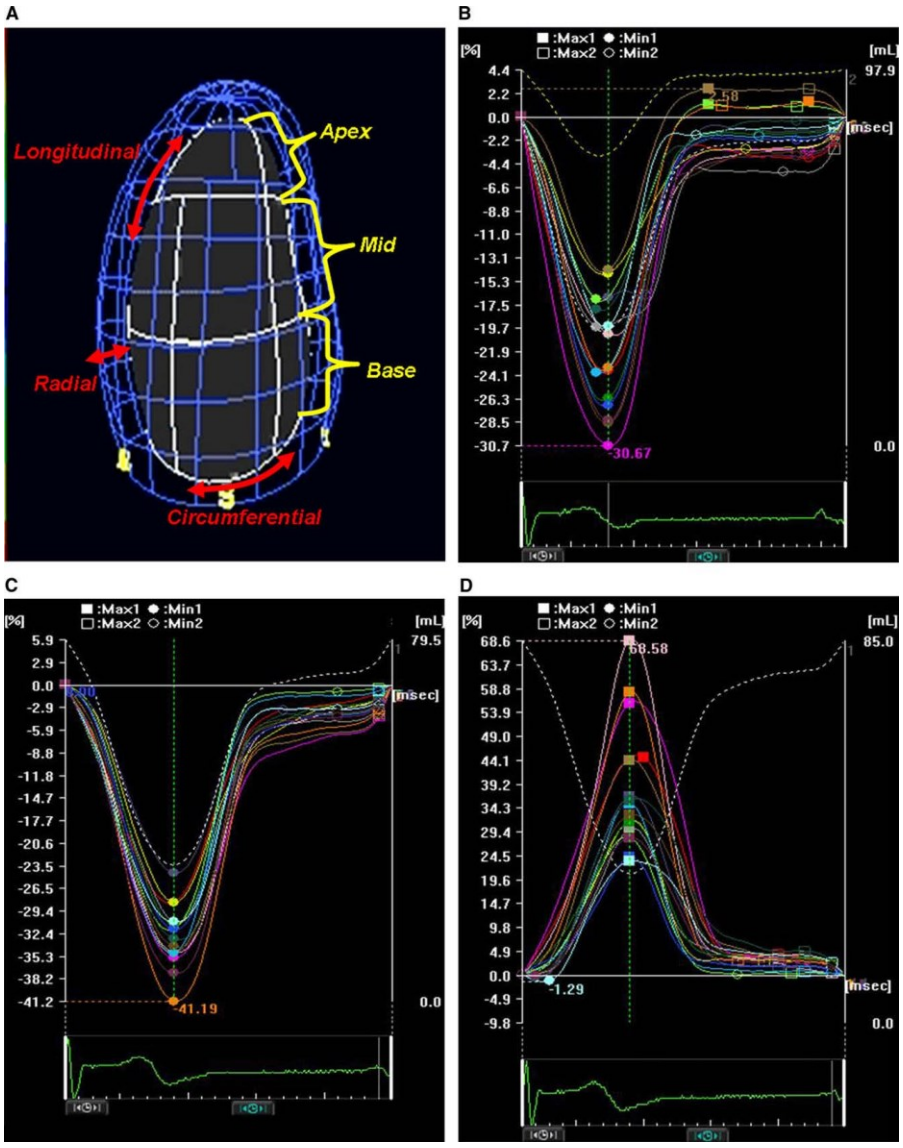

Fig. 1.7: Myocardial motion and deformation. A-motion components that can be assessed based on echocardiographic imaging. B-contains both normal deformation (longitudinal shortening/lengthening, radial thickening/thinning and circumferential shortening/lengthening) and *shear(base-apex twisting) C*- longitudinal velocity and displacement D- deformation (strain) and speed of deformation(strain-rate)

STE gives information regarding myocardial deformation in the 3 principal planes: transmural (also referred as radial), circumferential and longitudinal (Fig. 1.8) and because it is performed in 2-dimensional B-Mode images, it is independently of both cardiac translation and the angle of incidence (Wang et al., 2007a). STE has been validated by reference sonomicrometry (Urheim et al., 2000), tagged cardiac magnetic resonance (Amundsen et al., 2006) and in an animal model (Pirat et al., 2008).

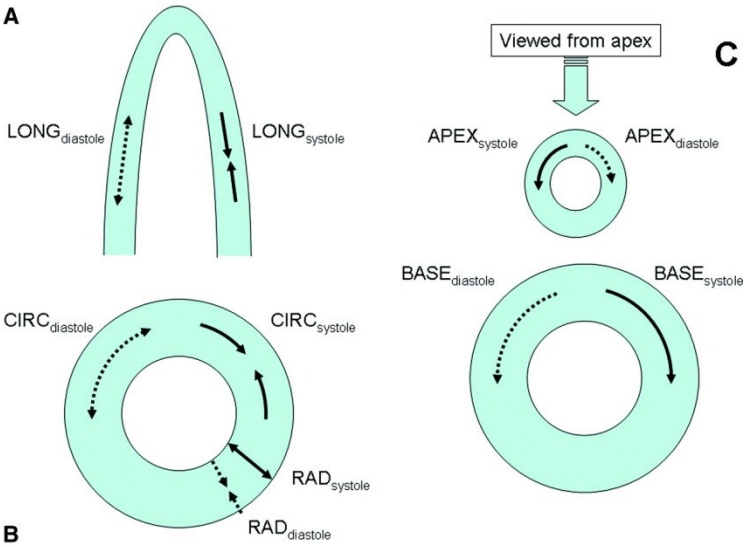

Fig. 1.8: Graphic representation of the principal myocardial deformations: longitudinal (A), radial and circumferential (B), and torsion (C). The direction of deformation in systole is shown as solid lines and that in diastole is shown as dashed lines. LONG indicates longitudinal; RAD, radial; and CIRC, circumferential.

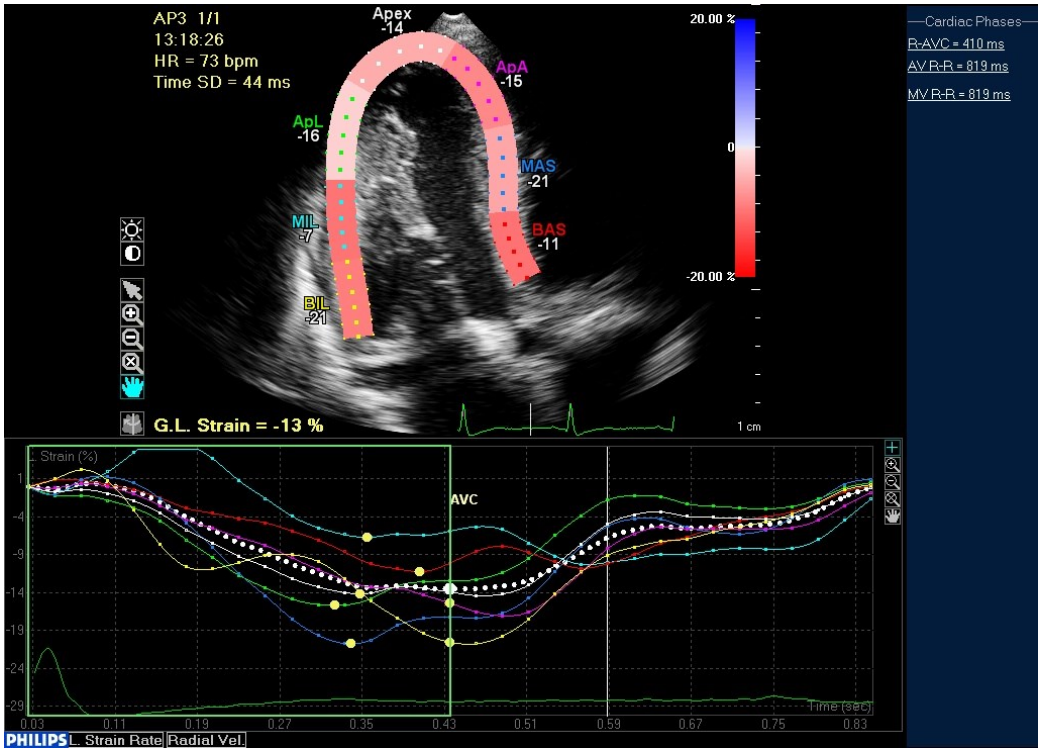

Fig. 1.9: Two dimensional longitudinal strain analysis of the left ventricle by speckle tracking (4 chambers apical view).

2DSTE overcomes in part the strain derived DTI limitations since uses the movement of the uniform ultrasound backscatter speckle pattern, within 2D images, to assess myocardial strain throughout the cardiac cycle (Fig. 1.9). Another advantage of 2DSTE over DTI is the time required to complete analysis, where less time is required with 2DSTE.

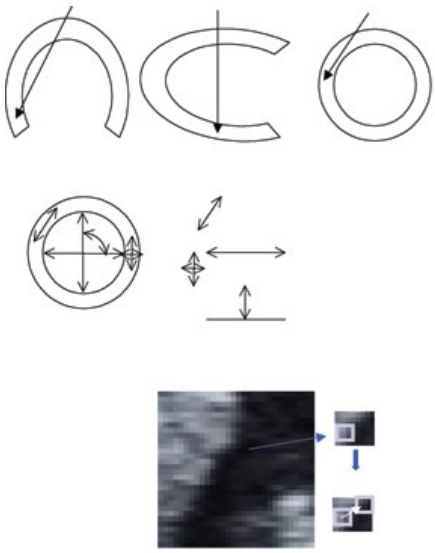

Fig. 1.10: Doppler versus Speckle Tracking Approach for Tissue Motion Analysis.

The limitations of the technique are known and are related with the myocardial deformation measurements being affected by loss of speckles due to motion outside the imaging plane. Since the technique follows speckles in 2D planes, but speckle moves in three dimensions, only a portion of the real motion can be detected. In addition, the technique possesses limited reproducibility, especially when applied to suboptimal images and there is poor intervendor agreement, attributed to a lack of standardization in image analysis (Zimbarra Cabrita et al., 2013a).

1.2.3.3. 3D Speckle Tracking

Recent developments in RT3DE imaging resulted in improved image quality and higher frame rates allowing an automated endocardial tracking and a quantitative assessment not only on LV volumes and EF but also on both global and regional myocardial deformation of the entire LV (Mor-Avi et al., 2011) which has been studied more commonly using 2-dimensional speckle tracking echocardiography. Although, few studies(Maffessanti et al., 2009) have shown that 2DSTE may underestimate myocardial strain because of its inability to see through-plane motion. Both technologies use ultrasound image data to detect movement of the myocardium, 2D tracking tracks 2D movement or the projection of 3D movement into a 2D plane, while 3D tracking assesses real movement in 3D space (Perez de isla, 2008). Therefore, translation remains a problem using 2DSTE, as error is introduced to strain measurements when the heart

swings out of the imaging plane and out-of-plane motion occurs as the result of rotation and motion of the heart; as a result, only a portion of the real motion can be detected.

3DSTE is a purely 3D technology, having the capability of displaying the entire myocardium using a single set; with a great benefit for truly assess global left ventricular function. When using 3DSTE, a speckle particle moves through a volume and so the vector can be detected along the movement (Fig.1.11).

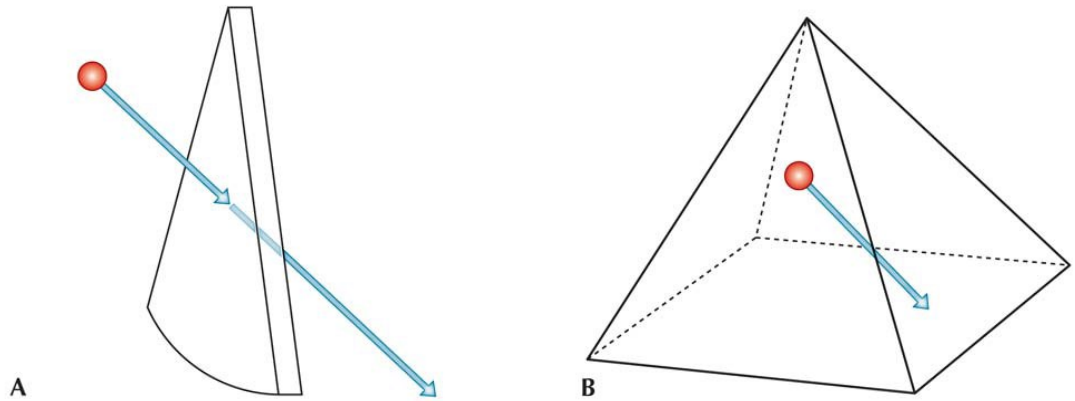

Fig. 1.11: Advantages of three-dimensional speckle tracking. A - When using two-dimensional tracking, a speckle particle can move through the scan plane. B- Three-dimensional speckle tracking avoids this limitation.

Has can be demonstrated in Fig. 1.12 , 3D tracking allows for the 3D dataset to include the total area in which the speckle may move, therefore the accuracy in detection of tissue movement is improved.

3D tracking generates more than 3000 vectors per volume, and the temporal resolution is the same as the volume rate of cardiac 4D datasets (20-30 volumes per second). Being currently still a research tool, it provides new insights in the assessment of LV function, in particular for strain analysis, rotation and twist estimations, with the advantage of simultaneous calculations of 3D LV volumes and EF, presenting nowadays as a potential clinical tool for assessing myocardial strain in SCD patients.

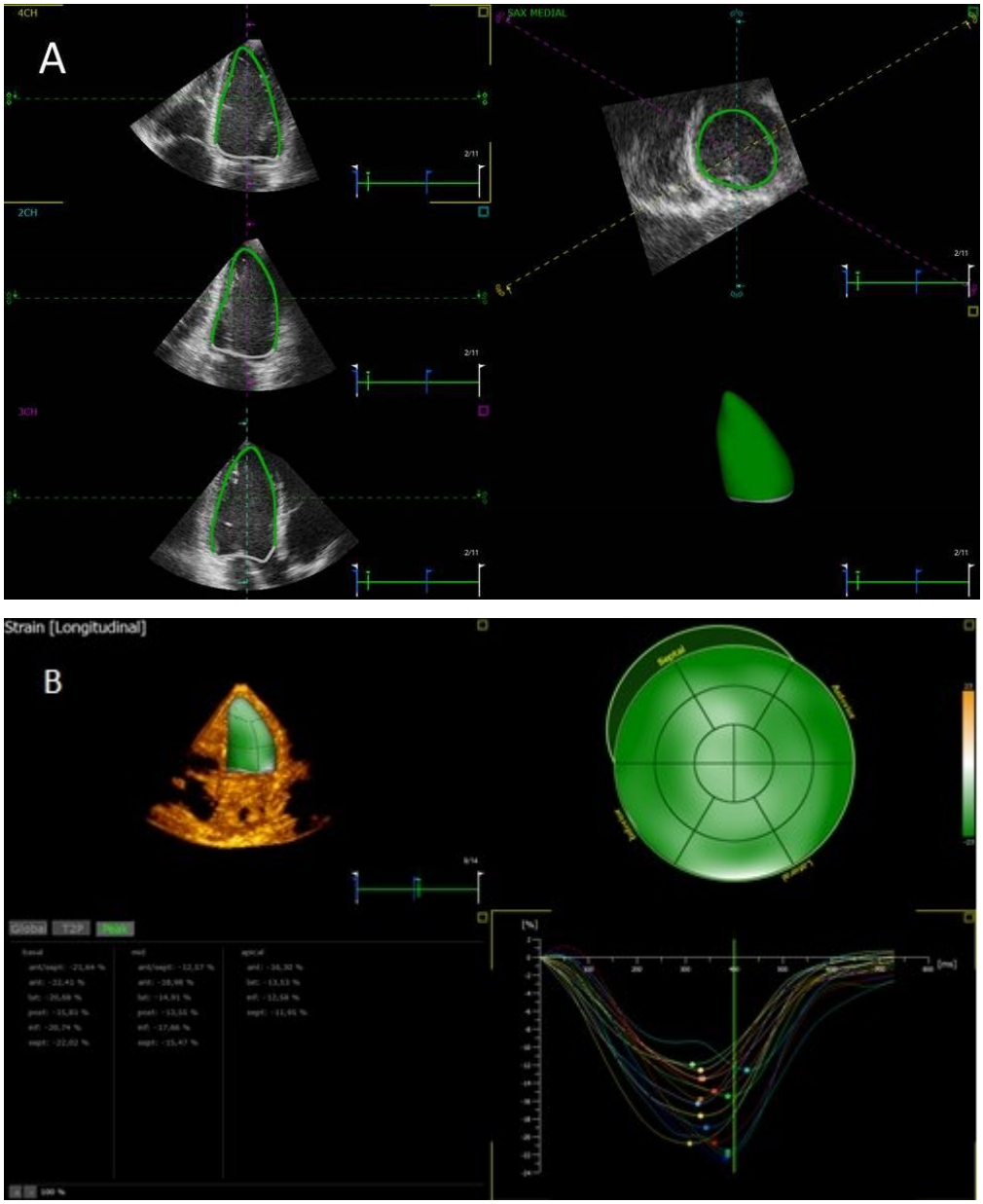

Fig. 1.12: A- Tracing endocardium in apical four, three and two-chamber views. The tracked mesh in end diastole at apical views and its intersections with three short-axis. B- Three-dimensional speckle tracking display of longitudinal strain.

Area strain is a novel parameter obtained by 3DSTE, with a high potential clinical application. The new parameter combines an analysis of both the longitudinal and circumferential shortening of the left ventricle(Støylen, 2011) providing an estimate of the subendocardial surface deformation, which is inversely proportional to the radial deformation of the ventricular wall (Fig. 1.13).

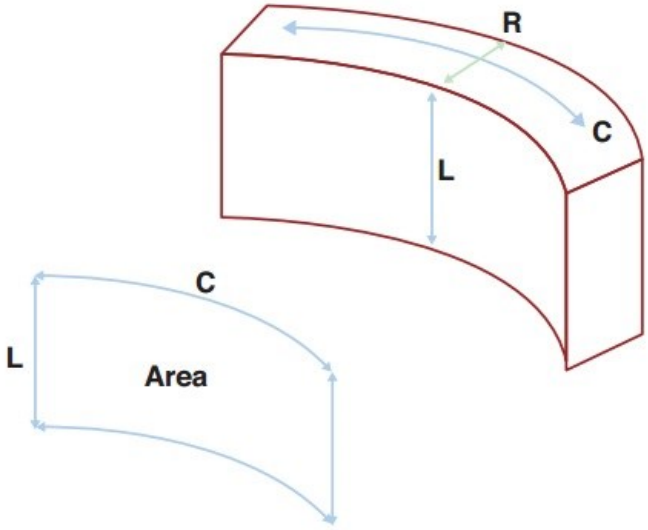

Fig. 1.13: Area strain. As the ventricle contract, the end diastolic area of the selected region (red) would be reduced in both the longitudinal and circumferential direction, the area reduction being the product of longitudinal and circumferential shortening. Thus, the magnitude of the area change would be greater than the circumferential or longitudinal shortening alone

Importantly, the relatively low frame rates used in 3DSTE have been referred as a potential limitation. In a recent study by Yodwut et al, it has been demonstrated that 3DSTE assessment of myocardial deformation is not compromised by low frame rates when derived from 18 or 25 frames/sec data sets but it may be underestimated with lower frame rates (Yodwut C 2012).

Kleijn et al. in a recent study with 45 consecutive healthy subjects, shown that even though 3DSTE-derived underestimates LV volumes (when comparing with MRI), measurement of the left ventricle ejection fraction (LVEF) revealed excellent accuracy (Kleijn et al., 2012a).

1.2.3.3.1. Limitations of 3DSTE

One of the limitation of the 3DSTE technique is related to the concern that 3D STE–derived strain measurements may be underestimated because the frame rates of real-time 3D echocardiography are not sufficiently high to accurately capture all phases of the cardiac cycle. It has been described that loss of deformation information occurs somewhere between 10 and 18 frames/sec, below which frame rates are not sufficient to accurately capture all phases of the cardiac cycle (Victor and Barron, 2010).

Furthermore, this technique is not yet interchangeable among different manufacturers, so its use in the clinical setting is still limited.

Left ventricular torsion (or twist) plays an important role with respect to LV ejection and filling. Streeter et al (STREETER et al., 1969). has described fiber orientation in the canine in the lates 1960's and since then, interest in fiber architecture and the resulting LV torsional deformation during contraction, has developed significantly in the last years (Rüssel et al., 2009). During the cardiac cycle, there is a systolic twist and an early diastolic untwist of the LV about its long axis because of oppositely directed apical and basal rotations (Fig. 1.14). As viewed from the LV apex, systolic apical rotation is counter clockwise and basal rotation, clockwise. LV torsion is followed by rapid untwisting of the ventricle which contributes to active suction of blood from the atria (Wu and Kovács, 2006). The way of contraction for subendocardial fibers is right-hand orientated while subepicardial fibers are left-handed and because of its direct relation to fiber orientation, LVtor is considered a valuable addition to strain measures such as transversal, circumferential or longitudinal thickening.

The characteristics of this torsional deformation have been described in different clinical and experimental studies (Helle-Valle et al., 2005, Amundsen et al., 2006), and it is well established that LV rotation is sensitive to changes in both regional and global LV function (Rüssel et al., 2009). During the past decades, tissue tagging magnetic resonance imaging has enable noninvasive measurement of LV myocardial deformation in 3D space (Buchalter et al., 1990, Moore et al., 2000b) and has driven several investigations of LV torsion in various diseases, including SCD (Ahmad et al., 2012) 2DSTE estimation of LV torsion (LVtor) has been validated by tagged MRI and the results have provided evidence that LVtor by STE is concordant with those analysed by MRI (Notomi et al., 2005). With its better temporal resolution and widespread availability, 2DSTE LVtor may lead to a fast introduction of LV torsion as an effective noninvasive index of global LV contractility (Kim et al., 2009)

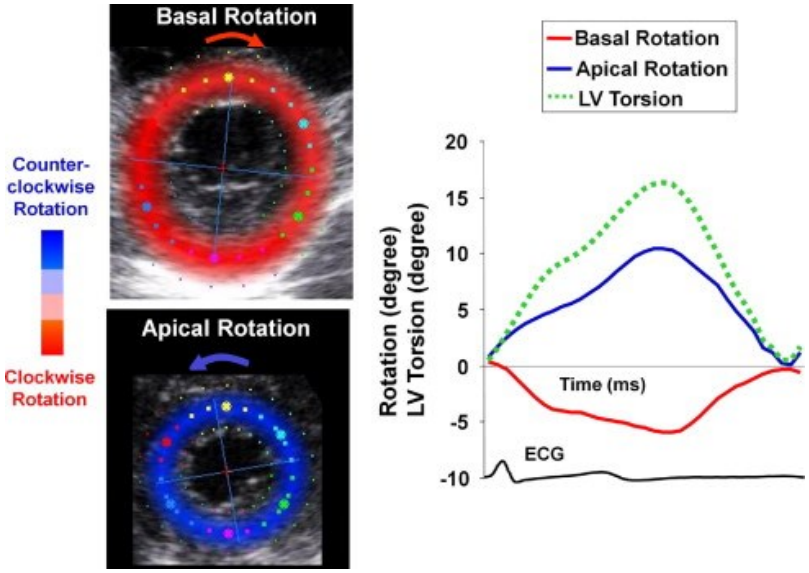

Fig. 1.14: (Left) - (Right) - Corresponding rotation and torsion (circumferential-longitudinal shear angle) curves, starting at end-diastole and showing the entire cardiac cycle.

The effect of preload and afterload on LV torsion have been widely studied (Buchalter et al., 1990, Kroeker et al., 1995) and it has been shown that an increase in preload (increased end-diastolic volume) caused an increase in twist angles and twist angles decreased under increasing afterload (increased end-systolic volumes). The understanding of the influence of LVtor in the cardiovascular system of patients with sickle cell disease need to be better understood, in particular in patients with suspected pulmonary hypertension which has not been fully explored.

The classification of diastolic dysfunction (DD) is debatable.

The ability of the left ventricle to accept blood at low pressures during diastole is often referred to as “diastolic function”. Abnormal ventricular distensibility and relaxation and the consequent inability to maintain a normal ventricular filling (unless the left atrial pressures increases), is called diastolic dysfunction. The basic mechanisms of DD may be intrinsic to the cardiomyocite, due to abnormalities in the extracellular matrix, neurohormonal influences and cardiac endothelial dysfunction (Gaasch, 1994). The study of DD, had a great improvement in the 1990’s with the introduction of echocardiography and Doppler based techniques, which provided a noninvasive assessment of the diastolic performance of the LV and its application in larger cohorts of patients.

Cardiac complications are a common feature of SCD and more recently, has been considered an important cause of associated morbidity and mortality (Fitzhugh et al., 2010). The chronic anaemia results in an increase in cardiac output, and has been widely demonstrated that LV dilatation is closely linked to the degree of anaemia (Ahmed et al., 2004).

Recent studies have shown that LV diastolic dysfunction is common in children. Importantly, Schadev et al found in a study with 235 adults with SCD, that LV diastolic dysfunction, reflected by a low E/A ratio, was an independent risk factor for mortality with a risk ratio of 4.8 (95% CI: 1.9 to 12.1, $p< 0.001$) (Sachdev et al., 2007). Additionally, the same study found that the combination of diastolic dysfunction measures and suspected PH (TRV≥2.5 m/s), increases the mortality risk ration to above 12.

As it has been observed the diastolic manifestations are associated with age, increases in blood pressure, increased LV mass and higher creatinine levels. Although, the presence of a systemic vasculopathy affecting after load, is not well understood. Microvascular disease may reflect directly on myocardial function. In addition, on the same NIH study (Sachdev et al., 2007) significant associations between systolic blood pressure and both increased pulmonary pressures and LV filling pressures have been found.

Anthi et al., in a study with invasive right heart catheterization measurements in patients with suspected PH, have shown evidence of LV diastolic dysfunction in 33% of the PH diagnoses with pulmonary venous hypertension(Anthi et al., 2007a) Castro et al.

The difficult in the assessment of diastolic function is well-know and its difficulty increases in the setting of preserved LV systolic function, which is find out in the majority of patients with SCD. Doppler-derived E/E' ratio above 15 has been accepted as a predictor of high LV filling pressure, however, milder degrees of LV dysfunction are more commonly found.

The possibility of racial/ethnic differences is susceptibility to the development of DD has received far less attention.

The Anglo-Scandinavian Cardiac Outcomes Trial has reported a decrease in left ventricular diastolic performance in African-Caribbean hypertensive patients, when

compared to European matching patients(Sharp et al., 2008). Importantly, the effect of African-Caribbean ethnicity on diastolic function persisted after adjustment for the most important confounding factors (age, gender, systolic blood pressure, pulse pressure, cholesterol, smoking, ejection fraction, left ventricular mass index, and diabetes mellitus), leading the hypothesis of the existence of an intrinsic difference in the diastolic function of the left ventricle between the 2 racial groups. Interestingly, in a study by Russo et al, performed in unselected sample of a multi-ethnic population, disparities in modifiable cardiovascular risk factors and sociodemographic variables, rather than intrinsic race-ethnic differences, seemed to account for most of the differences observed is diastolic dysfunction, suggesting a role for risk factor control in reducing race-ethnic disparities in diastolic function (Russo et al., 2010).
Studies with patients living in the same geographic area and with similar access to health care may help minimize this important confounding factor and improve comparability between the racial/ethnic groups particular in SCD.

In patients with heart failure, anaemia has been linked to more severe cardiac dysfunction, increased plasma BNP (brain natriuretic peptide) and a worse prognosis, even after adjustment for conventional risk factors such as coronary heart disease, smoking, hypertension, Dyslipidaemia and renal function. Amin et al have found that anaemia has a range of effects on cardiac structure, including myocyte hypertrophy and interstitial fibrosis, leading ultimately to left ventricle hypertrophy (Amin et al., 2004). More understanding is needed in which extend anaemia reflects the diastolic dysfunction observed in SCD.

Although it is important to mention, that the majority of the studies in SCD, use conventional echocardiographic parameters for assessing diastolic function. The more extensive use of Tissue Doppler and Myocardial deformation has been lacking and prospective studies for profounder understanding of the mechanics behind diastolic dysfunction are needed for a better comprehension the impact of impairment of ventricular filling as opposed to a decrease in contractile function. The detection of both sub-clinical systolic and/or diastolic impairment provides the clinical with an opportunity to act before clinical symptoms develop.

Two-dimensional, Doppler, colour flow imaging, and myocardial (tissue Doppler) imaging are currently the most practical diagnostic modality, with good reproducibility, to identify patients with diastolic dysfunction.

Furthermore, a recent study that combined global myocardial strain rate during the isovolumetric relaxation period (by speckle tracking) and transmitral flow velocities showed that the mitral E velocity/global myocardial strain rate ratio predicted LV filling pressure in patients in whom the E/e´ ratio was inconclusive and was more accurate than E/e´ in patients with normal EFs and those with regional dysfunction (Wang et al., 2007b). Therefore, a more complete evaluation of diastolic function by deformation imaging is necessary in SCD and its incremental clinical value has not been fully investigated.

1.3. Cardiovascular Magnetic Resonance

1.3.1. General overview

Since the acquisition of the first magnetic resonance signal in the 1952 by Herman Carr, and the first magnetic resonance images in the early 1970s by the Nobel laureates Paul Lauterbur and Sir Peter Mansfield, MRI has progressed enormously to become a popular technique in the medical community. MRI is most frequently useful in the evaluation of the nervous and musculoskeletal systems, but can be applied to the cardiovascular system as well. This chapter comprehends the basic principles of MRI, image acquisition of the moving heart, and general applications to the cardiovascular system.

Cardiac magnetic resonance imaging has an increasingly valuable role to play as an adjunct to routine cardiovascular imaging modalities (De Vinuesa et al., 2008, Duerden et al., 2006). CMR is an accurate and reproducible method to provide non-invasive myocardial-tissue characterization at a high spatial resolution is still considered the gold standard for measuring ejection fraction and ventricular volumes(Task Force of the European Society of Cardiology, 1998).

1.3.2. Synchronising with the cardiac cycle

For routine CMR, cardiac synchronization with the electrical activity is required for both pulse sequence and signal acquisition. The electrocardiogram (ECG) tracing is transmitted by a wireless system to the CMR console for processing. Computer software is programmed to detect the R wave of the QRS complex, which marks the electrical systole and the beginning of the cardiac cycle (Lanzer et al., 1985). Based on the ECG information, images of the beating heart can either be obtained at a single time point (still imaging) or at multiple time points throughout the cardiac cycle (cine imaging) (Ridgway, 2010).

1.3.3. Cine Imaging

Cine imaging can be accomplished by using gradient echo-based pulse sequences with very short repetition times. It involves data acquisition at multiple time points, known as cardiac phases, throughout the cardiac cycle (Ridgway, 2010). Data acquired within each cardiac phase fills a separate k-space (*temporary image space)* resulting in the reconstruction of a separate image corresponding to each cardiac phase. The combined images can then be displayed as a movie, thus enabling functional assessment of the heart.

1.3.4. Perfusion imaging

Myocardial perfusion imaging is commonly used in coronary artery disease to assess the blood flow in the myocardium (Greenwood et al., 2012) It requires ultra-fast imaging techniques able to acquire several images of the myocardium (usually 3-5 short-axis slices) per cardiac cycle while a gadolinium based contrast agent transits through the coronary arteries. The single shot images are usually presented as a movie where the resulting myocardial signal correlates with the coronary blood flow and gadolinium concentration in the myocardium. Regional imbalances in contrast concentration under maximal pharmacological dilatation may evidence areas of hypoperfusion indicating myocardial ischemia. The sequences normally employed for perfusion images are based

on spoiled gradient echo, balanced steady stated free precession, and hybrid-echo planar imaging (efficient method of filling k-space via a combination of radiofrequency pulses and gradients). T1-weighting and a saturation recovery preparation pulse are necessary to maximise the effect of the contrast agent (Biglands et al., 2012)

1.3.5. Volumes and function

CMR is currently the most reliable method for volume assessment, and is frequently used as the benchmark for validation of other imaging modalities (Hoffmann et al., 2003). Ejection fraction (derived from the end-diastolic and end-systolic volumes) is the parameter measured by CMR to assess systolic function. Diastolic ventricular function can also be assessed by CMR, but is not usually performed as echocardiography remains the preferred approach.

1.3.6. Myocardial tissue tagging

One of the reference modality for measuring myocardial deformation is tagged MRI.

In 1988, Zerhouni et. al(Zerhouni et al., 1988) introduced a magnetic resonance based noninvasive imaging method for tracking myocardial motion: myocardial tissue tagging. The method allows for automatically extracting of local/global deformation parameters at the pixel and myocardial segment scales (Petitjean et al., 2004). Non-invasive markers, known as tags, are created within the tissue by locally induced perturbations of the magnetization with selective radiofrequency saturation of multiple, thin tag planes in a plane perpendicular to the imaging plane prior to image acquisition (Shehata et al., 2009). These perturbations then produce regions of reduced signal intensity that appear as dark lines in the acquired images. Improving this technique Axel and Dougherty (Axel and Dougherty, 1989) then developed spatial modulation of magnetization to allow the application of tags in two orthogonal directions that, combined, form a grid of sharp intrinsic tissue markers (Fig.15). One of the approaches to measure myocardial motion from tagged MRI image sequences is the phased-based optical flow methods such as harmonic phase analysis (Harmonic phase analysis) (O'Regan et al., 2012), which are in some extent, sensitive to artefacts.

Mid wall LV circumferential strain (*ECC*) is the most frequently computed parameter for quantifying regional function. ECC measure is preferred due to myocardial geometry contributing an abundance of tagging data around the mid wall myocardial circumference compared to along the width of radial wall thickness (Moore et al., 2000a). This makes *ECC* data less sensitive to noise and more suitable for assessing the transmural strain gradient. In the normal heart, circumferential strain increases gradually from the base towards the apex. With respect to transverse regions, the greatest shortening is consistently observed in the anterior and lateral myocardial segments with the least deformation seen in the inferior wall. Moreover, *ECC* appears to increase from epicardium towards endocardium (Zwanenburg et al., 2005).

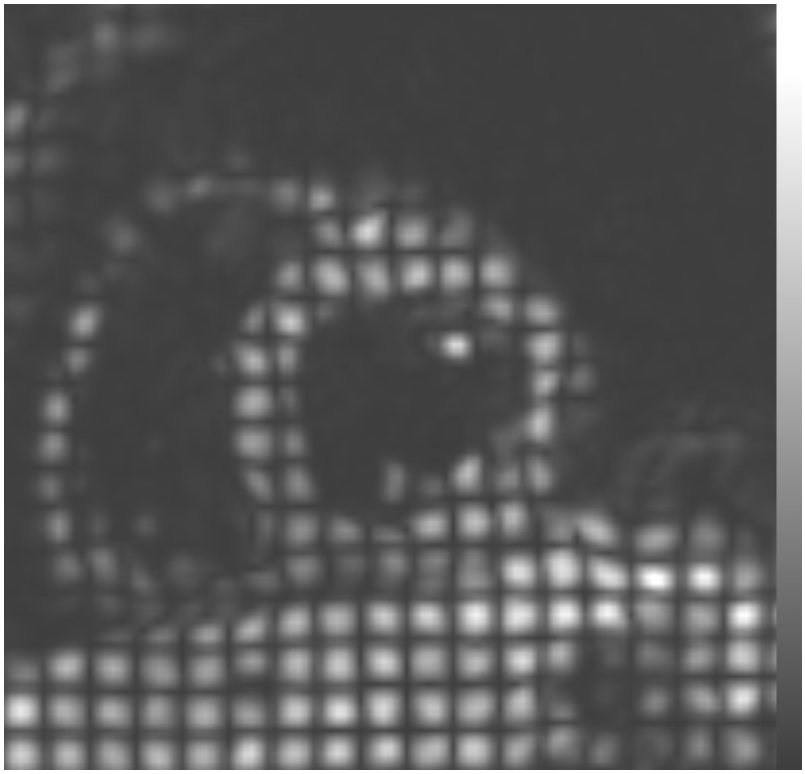

Fig. 1.15: Short-axis tagged image

The application of CMR tagging in the RV includes several technical challenges. The very thin wall (<5 mm) of the normal RV offers less than the minimum optimal tag spacing (≥6 mm) and therefore limits the number of tag stripes that would be required for accurate quantification (Fayad et al., 1998). An attempt to overcome these limitations

has been done and several studies have been investigating RV patterns of mechanical deformation.

1.3.7. CMR in Secondary Cardiomyopathies

The heart can be affected by a number of systemic conditions, such as sarcoidosis, amyloidosis, Anderson-Fabry and other metabolic storage disorders, muscular dystrophies, iron-overload cardiomyopathy and in transfusion-dependent hemoglobinopathies. These patients are usually referred to CMR when there is suspected cardiac involvement, although sometimes these conditions can be detected unexpectedly in the evaluation of heart failure or left ventricular hypertrophy (Alpendurada et al., 2012). Late gadolinium enhancement (LGE) imaging is extremely helpful in this setting, where infiltration or fibrosis depicted by LGE shows good correlation with endomyocardial biopsy (Smedema et al., 2005, Vogelsberg et al., 2008). Iron overload cardiomyopathy is a peculiar condition in this group of systemic diseases because diagnosis by CMR is not based on the presence of LGE (Kirk et al., 2011), but rather by documentation of iron deposition in the myocardium. This is possible by assessment of T2* relaxation, which has an inverse correlation with the amount of tissue iron (Carpenter et al., 2011). CMR has the unique ability of investigating iron deposition and ventricular function at the same time, and has contributed to the significant decline in mortality of iron-overload cardiomyopathy in the United Kingdom(Modell et al., 2008) and can be considered as the reference technique for *in vivo* quantification of infarct size in SCD. In a study performed in 47 patients with SCD, it has been shown by CMR that LV changes are partly result of a chronic anemia, however a homogeneous fibrotic disorder affecting the LV could not be excluded (Westwood et al., 2007).
Accurate quantification and timing of regional myocardial function allows early identification of dysfunction and its etiology, and therefore becomes increasingly important for clinical risk assessment, SCD patients management, and evaluation of therapeutic efficacy.

Despite providing the most comprehensive information, CMR is an expensive technique and not readily available in most institutions. Image acquisition is technically challenging and image interpretation requires adequate training. In CMR studies, scans

times are relatively long, patients have to lie flat, and monitoring or perfusion devices inside the magnet room have to be magnetic resonance-compatible. Therefore, CMR is not suitable for the very unstable patient and should be avoided in these patients if other studies can give similar information. Despite pacemakers and implantable electronic devices being regarded as contra-indications, CMR can potentially be safely performed in experienced centres when appropriate precautions are taken(Naehle et al., 2009) .

CMR currently offers the most comprehensive cardiovascular information of all imaging techniques. Extensive research in the last decade has validated this technique in several clinical settings and supports its use in daily practice. However, lack of availability, medical training and cost constrains a more widespread use of this technique. Therefore, it is regarded as complement to echocardiography, since most of the general indications are similar.

1.4. Potential benefits from this research

Investigations into how the heart is affected in patients with SCD are widely reported as shown earlier in the critical review of the literature. Although, there is a certain amount of variability in the results and methodology approach and a thorough understanding of the subject is needed.

Importantly, the majority of these previous investigations used conventional cardiac imaging techniques and were mainly performed in the US population, which may have different results. We believe that the use of the latest imaging techniques in echocardiography may benefit these patients for the identification of early manifestations of subclinical myocardial dysfunction and its relation to the presence of elevated tricuspid regurgitant jet by Doppler echocardiography.

This thesis represents the first prospective investigation to study a group of patients with SCD, followed up at SCD referral UK centres, with the latest cardiac imaging technologies for the understanding of the cardiac function and existence of early markers of myocardial dysfunction. This study may defines the normal ranges and

variability of myocardial deformation derived from 3-dimensional speckle tracking and speckle tracing in a SCD population.

In addition, we will study the variability of the different softwares packages for the assessment of myocardial deformation and ventricular volumes quantification which plays an important role in the clinical and research settings.

Chapter 2: A 5-year survival study in a North West London population of patients with sickle cell disease.

Chapter 2 A 5-year survival study in a North West London population of patients with sick cell disease

2. Introduction

This Chapter describes the retrospective survival study which was the first part of the research described in this thesis. The retrospective study has been published in the British Journal of Haematology (doi: 10.1111/bjh.12391), as mentioned in Introduction.

2.1. Background of retrospective study

Sickle cell disease is one of the most prevalent genetic disorders worldwide, affecting approximately 12,000 people in the United Kingdom (Fitzhugh et al., Hickman et al., 1999, Lucas et al., 2008). Although life expectancy is reduced in SCD (Platt et al., 1994a, Schultz WH, 2003), advances in management has led to a significant improvement in survival (Telfer et al., 2007, Quinn et al., 2010).

The development of pulmonary arterial hypertension in SCD heralds a severe clinical phenotype, and is associated with death (Fitzhugh et al., 2010, Gladwin et al., 2004). Autopsy studies suggest that 75% of patients with SCD have histological findings of PAH at the time of death (Odd et al., 2009), suggesting that PAH may be clinically silent or poorly recognized. A raised TRV on echocardiography is predictive of a raised systolic pulmonary arterial pressure (Hatle et al., 1981, Lanzarini et al., 2002), although this has a high negative predictive rate (13) and cardiac catheterization is required to confirm the diagnosis of pulmonary hypertension (Parent et al., 2011, Fonseca et al., 2012). The ability to highlight a subgroup of patients with a high predicted mortality by use of a non-invasive measurement such as TRV represents a significant clinical advance and has rightly generated a lot of research interest. Raised TRV as assessed by Doppler echocardiography, whether or not associated with pulmonary arterial hypertension, is commonly found in sickle cell disease (Ataga et al., 2004) and has been reported as a marker of mortality in several major studies from the United States (De Castro et al., 2008, Ataga et al., 2006, Machado and Gladwin, 2010, Lorch et al., 2011, Gladwin et al., 2012, Anthi et al., 2007a) . Raised TRV has been

found in 32 to 42% of patients with SCD (Gladwin et al., 2004, Fitzhugh et al., Akgul et al., 2007, Liem et al., 2007a, Parent et al., 2011).

Studies in the UK using similar measurements and valuations have not been carried out, where differences in organization of health services and socio-demographics may lead to different findings.

The purpose of this study was to determine the survival of a cohort of patients with sickle cell disease, attending two hospitals in North West London, based on their TRV and describe differences between those with elevated and normal TRV.

2.2. Material and Methods

2.2.1. Patient population

All patients with SCD who were referred to the echocardiography laboratory of Hammersmith Hospital or Central Middlesex Hospital, London from the Sickle Cell or Haematology Clinics between August 2004 and May 2012 were studied retrospectively. The clinical indication for requesting the echocardiogram was either a clinical decision by their haematologist to screen for raised TRV or follow-up of previously elevated TRV. Only patients in stable condition were included; patients who had a vaso-occlusive crisis within the preceding two weeks or an episode of acute chest syndrome within four weeks were excluded.

The local research ethics committee issued a consent waiver to allow the review of the medical records. The authors had full access to the data and take responsibility for its integrity. All authors have read and agreed to the manuscript as written.

2.2.2. Laboratory and Clinical data

Laboratory data used for analysis were those recorded at the date closest to that of the echocardiogram. Only steady state results were included. The cause of death when known was obtained from the death certificate, medical records or general practitioner of the patient.

2.2.3. Transthoracic echocardiography

All studies were performed by an experienced sonographer using the Philips Sonos 7500, equipped with a transducer S3 1.8-3 MHz.

An electrocardiogram was simultaneously recorded from all subjects. Images were recorded and stored in digital format for subsequent off-line review and frame-by-frame analysis with ProSolv CardioVascular Analyzer 3.5 (FUJIFILM, USA). Two-dimensional echocardiographic examination and colour Doppler data were collected according to the recommendations of the American Society of Echocardiography (Gottdiener et al., 2004, Lang et al., 2005) using a standardized protocol.

Paraesternal long axis, short axis, right ventricular inflow, apical four, three and two chamber views were obtained. Transvalvular flow, Doppler determinations of the severity of the valvular regurgitation and left ventricular diastolic function were assessed.

Tricuspid regurgitation velocity was assessed in a minimum of four views and five sequential complexes were recorded. Continuous-wave Doppler of the peak regurgitant jet velocity was used to estimate the right-ventricular systolic pressure gradient using the modified Bernoulli equation (4x [tricuspid regurgitant velocity]). Pulmonary arterial systolic pressure (PASP) was estimated by adding the estimated mean right atrial pressure. The mean right atrial pressure was calculated according to the degree of collapse of the inferior vena cava with inspiration (Howard et al., 2012).

Left ventricular diastolic dysfunction was assessed using conventional echocardiographic parameters: mitral inflow peak early (E) and peak late (A) flow velocities, the E/A ratio, the deceleration time of early mitral flow velocity (DT), and IVRT at rest and during the Valsalva manoeuvre. LV diastolic dysfunction was characterized either normal (E/A ratio 0.9 to 1.5, DT 160 to 240 ms, IVRT 70 to 90 ms), restrictive (E/A ratio >2, DT<160 ms, IVRT < 70 ms), or delayed relaxation (E/A ratio<0.9, DT>240 ms, IVRT > 90 ms). (Quinones et al., 2002, Lester et al., 2008) . Left atrial (LA) diameter was obtained from the paraesternal long axis view at the end-ventricular systole when the LA chamber was at its greatest dimension. Right atrial volume was calculated by 2D-mode apical 4-chamber view using the area – length method. (Lang et al., 2005, Quinones et al., 2002)

2.2.4. Statistical analysis

Statistical analysis was performed using the Stata software (version 9.2, StataCorp, USA).

Normally distributed variables were compared between groups using an unpaired t-test, while variables which lacked a normal distribution were compared using a Mann-Whitney test.

Distributions of continuous variables were shown by the mean ± standard deviation (SD) for normally distributed data or median and interquartile range for skewed data. Demographic, clinical and echocardiographic findings were compared according to TRV <2.5 versus TRV ≥2.5 m/s by the Student's *t*-test for normally distributed continuous variables or the Kruskal-Wallis test for skewed continuous variables.

The relationship between two qualitative variables was analysed using the two sided Fisher's exact test. The association between variables and TRV was examined using linear regression.

Patient survival was illustrated graphically using a Kaplan-Meier plot. Additionally the effect of clinical and laboratory variables (Table 5) on patient survival was examined using Cox regression analysis. Subsequently the joint effect of the explanatory variables upon survival was examined in a multivariate analysis. This multivariate analysis was restricted to those variables which showed some evidence of a significant effect from the univariate analyses ($p<0.1$). A backwards selection procedure was used to retain only those variables that were statistically significant. Before performing the multivariate analyses, the colinearity between variables was examined using variance inflation factors.

Due to large number of factors analysed, p-values of less than 0.01 were considered significant for the univariate analyses. A higher significance level of 0.05 was used for the multivariable analyses, so as not to omit potentially important predictors from the final model.

2.3. Results

2.3.1. Clinical characteristics of study population

A total of 170 adults with SCD were referred to the echocardiography laboratory and evaluated at Hammersmith and Central Middlesex hospital between August 2004 and May 2012. Echocardiogram and laboratory data were complete in 164 cases. Echocardiographic measurements of left ventricular diastolic dysfunction were complete in 145 patients.
The median age of the 164 patients was 42.3 years (range 15–82 years) where 114 were female (70%) and the median PASP was 28.0 mmHg (IQR 22.9-32.6) One hundred and two patients had HbSS (62.2%), 41 HbSC (25%), 8 *HbS-β^0 thalassaemia* 4.9%), 11 *HbS-β^+ thalassaemia* (6.7%), and 2 had other genotypes, *S-D Punjab* and S/HPFH, (1.2%). The median follow-up interval was 68.1months (IQR 48, 78) (Table 2.1).

Elevated TRV was present in 29.1 % of patients (n=48): 12.8 % had TRV ≥ 2.5 – 2.69 m/s, 10% had TRV 2.7 – 2.99 m/s and 6.1% had TRV ≥ 3.0 m/s. Left ventricular dilatation was seen in 8 patients (5%) and reduced LV systolic function (ejection fraction <55%) in 2 patients. Twenty-six patients (16%) were on hydroxycarbamide therapy, of whom 19 had a TRV<2.5 m/s and 7 patients had a TRV≥2.5 m/s (p=0.814).
Five patients (3%) out of the 145 patients had echocardiographic evidence of left ventricular diastolic dysfunction.

2.3.2. Associations with tricuspid regurgitation velocity

Results of the univariate analyses show that age, LA diameter and right atrial (RA) volume were significantly associated with TRV and a trend for an association with haemoglobin, ferritin and creatine (Table 2.2).
Multivariate analysis indicated that both age and LA diameter were significantly associated with TRV (Table 3). An increase in both of these two variables was associated with an increase in TRV. A 10-year increase in age was associated with a 0.06 unit (m/s) increase in TRV, while a 10-mm increase in LA diameter was associated with TRV values increasing by 0.18.

Patients in the study were further categorized according to TRV <2.5 m/s versus TRV≥2.5 m/s. The results suggested that there was some evidence of a difference in SCD genotype between groups. HbSS or *HbS-β^0 thalassaemia* genotype was more common (80%) in patients with a TRV ≥ 2.5 when compared to a TRV< 2.5 (64%), although the result was of borderline statistical significance (p=0.05). Age, left ventricular end-diastolic diameter (LVEDD), LA diameter, RA volume, haemoglobin and haematocrit were all found to vary significantly between the two groups (TRV <2.5 m/s versus TRV≥2.5 m/s or more) (Table 2.4). The LV ejection fraction was within normal limits in both groups. There were no differences in lung function tests between the two TRV groups.

Table 2.1- a) Clinical characteristics of SCD patients**.**

Clinical characteristics	N	SCD patients
		Mean (SD)/Median (IQR)*
Age (years)	164	42.3 (33,50)*
Sex (male/female) %	164	(30/70)
Systolic blood pressure (mmHg)	136	120 (113,129)*
Diastolic blood pressure (mmHg)	136	71.7 (11.6)
Body mass index (kg/m^2)	125	24 (22,)*
Hydroxycarbamide therapy (%)	162	16
White cell count (x10E^9/l)	157	9.1 (7.4,10.9) *
Haemoglobin (g/l)	155	94 (80,110)*
Ferritin (ug/L)	116	173 (83,474)
Haematocrit (ratio)	150	0.27 (0.24,0.32)*
Red blood cell (10^12/l)	153	3.32 (0.97)
Mean corpuscular volume (fl)	154	86.15 (79,92)*
Creatinine (µmol/L)	156	70 (59,85)*
Lactate dehydrogenase (IU/L)	102	606 (385,879)*
Bilirubin (µmol/L)	149	35 (20-52)*
Tricuspid regurgitant velocity (m/s)	164	2.28 (0.42)
Pulmonary artery systolic pressure (mmHg)	164	28.04 (24,33)*

SD: standard deviation, * Median , IQR: interquartile range

Table 2.2 - b) Clinical associations with tricuspid regurgitation velocity in a univariate analysis of all patients.

Variable	Category	Coefficient (99% CI)	P-value
Age (***)		0.10 (0.03, 0.16)	**<0.001**
Systolic Blood Pressure (***)		0.03 (-0.03, 0.10)	0.18
Genotype	HbSS / *HbS-β⁰*	0	
	Other genotypes	-0.09 (-0.28, 0.10)	023
Interventricular septum		0.04 (-0.02, 0.10)	0.09
Left ventricular posterior wall		0.02 (-0.03, 0.08)	0.26
Mitral valve E/A		-0.08 (-0.30, 0.13)	0.30
Mitral valve decelaration time(****)		0.06 (-0.04, 0.16)	0.10
Left atrium diameter (***)		0.22 (0.08, 0.36)	**<0.001**
Right atrium volume (***)		0.09 (0.01, 0.17)	**0.006**
Body mass index (**)		-0.03 (-0.13, 0.07)	0.42
White cell count (**)		-0.02 (-0.16, 0.13)	0.73
Haemoglobin		-0.03 (-0.07, 0.01)	0.06
Fetal haemoglobin		-0.02 (-0.07, 0.03)	0.30
Platelet (****)		-0.01, (-0.05, 0.02)	0.26
Ferritin (†)		0.16 (-0.05, 0.38)	0.05
Creatinine (†)		0.48 (-0.02, 0.98)	0.01

(**) Coefficients given for a 5 unit increase in explanatory variable
(***) Coefficients given for a 10 unit increase in explanatory variable
(****) Coefficients given for a 50 unit increase in explanatory variable
(†) Variable analysed on the log scale (to base 10)

Table 2.3 - Clinical associations with tricuspid regurgitant velocity in a multivariate analysis of all patients.

Variable	Coefficient (95% CI)	P-value
Age (***)	0.06 (0.01, 0.11)	0.02
Left atrium diameter (***)	0.18 (0.07, 0.29)	0.001

(***) Coefficients given for a 10 unit increase in explanatory variable. Variables entered into the analysis were age, left atria diameter, right atria volume, haemoglobin, ferritin and creatinine.

Table 2.4 - Clinical characteristics of all SCD patients without and with raised TRV.

Variable	TRV < 2.5m/s n=116; Mean (SD)	TRV ≥ 2.5m/s n=48; Mean (SD)	P-value
Age (years)	41 (12)	46 (13)	**0.04**
Systolic Blood pressure (mmHg)	121 (14)	123 (15)	0.40
Diastolic blood pressure (mmHg)	72 (12)	72 (11)	0.76
Interventricular septum(mm)	8.6 (1.5)	9.0 (1.3)	0.10
Left ventricular posterior wall(mm)	9 (8, 10)*	9 (8, 10)*	0.21
Left ventricular end-diastolic diameter (mm)	49 (5)	51 (6)	**0.02**
Left ventricular ejection fraction (%)	72 (7)	73 (6)	0.22
Mitral valve E/A	1.49 (0.35)	1.41 (0.56)	0.26
Mitral valve deceleration time (ms)	180 (160, 200)*	200 (162, 210)*	0.06
Left atrium diameter(mm)	37.2 (5.9)	40.7 (6.2)	**0.001**
Right atrial volume (cm^3)	53 (16)	69 (21)	**0.003**
Body mass index (Kg/m^2)	25 (5)	24 (6)	0.20
Haemoglobin (g/l)	99 (20)	91 (21)	**0.04**
Haematocrit (ratio)	0.29 (0.06)	0.26 (0.07)	**0.05**
Red blood cell (10^12/l)	3.4 (0.9)	3.1(1.1)	0.06
Automated absolute reticulocyte count (10^9/l)	214 (96)	216(100)	0.91
White cell count ($x10E^9/l$)	9.1 (7.7, 10.8)*	9.3 (7.3, 11.6)*	0.80
Fetal Haemoglobin (%)	4.2 (2.6, 8.6)*	3.5 (1.5, 6.0)*	0.41
Platelet (10^9/l)	317 (213, 393)*	301(203, 390)*	0.73
Ferritin (ug/L)	155 (85, 395)*	267(63, 692)*	0.19
Lactate dehydrogenase (IU/L)	562 (355, 816)*	784 (500, 993)*	0.06
Bilirubin (µmol/L)	34 (19, 48)*	44 (23, 62)*	0.08
Creatinine (µmol/L)	70 (58,83)*	70 (61,91)*	0.23
Hydroxycarbamide (%)	15.5	17.5	0.81
Number of admissions	0 (0, 1)*	0 (0, 2)*	0.38
Follow-up duration (months)	72.5 (47-79)	49.5 (33.7-76.7)	0.11†

SD, standard deviation,* Median (Interquartile range) † deceased cases not considered.

2.3.3. Survival analysis

There were 15 deaths during follow-up (9.1 %). Seven of these patients had increased TRV giving a mortality, in the high TRV group, of 16.67% (8 out of 48) after 68 months median of follow up time (range 4.0-84.3 months) compared to 6.9% in the lower TRV group (8 out of 116). In addition, A Kaplan-Meier analysis of the 5-year survival rates was 95.0% (with 95% CI of 89.7% to 97.6%).
The causes of death of patients with and without raised TRV are shown in (Table 2.5). One patient with an unknown cause of death did not have an elevated TRV.

The effect of each variable upon survival was examined separately. When TRV was considered a continuous variable, there was a statistically significant association with survival (p=0.009). Higher values of TRV were associated with an increased risk of death (hazard ratio (HR): 4.48, 99%CI 1.01-19.8). A one-unit (1 m/s) increase in TRV was associated with the risk of death at any time increasing by more than four-fold.
When TRV was considered as a categorical variable (TRV <2.5 m/s and TRV≥2.5 m/s) as reported in previous studies, there was a trend to reduced survival in the group with raised TRV (p=0.06), conforming with the association of TRV with an increased risk of death when assessed as a continuous variable (Fig. 2.1).
Higher values of Hb, haematocrit (HCT) and RBC were all associated with a decreased risk of death at any time in the univariate analysis. A 0.1 unit increase in HCT was associated with the hazard of death being only 20% as large (Table 2.6).
The results of the multivariable analysis indicated that decreased Hb, increased mean cell volume (MCV) and increased MV DT were all still significantly associated with reduced patient survival (Table 2.7). The effects of TRV after adjusting for these three significant variables, has showed that there is no additional effect of TRV upon patient outcome. TRV was not found to be an independent risk factor for death.

Table 2.5 - Cause of death and clinical characteristics in patients with SCD.

ID	Gender	Age	Follow up time (months)	Phenotype	TRV (m/s)	Cause of death
159	F	42	68	HbSS	1.8	Respiratory failure
062	F	40	53	HbSS	1.9	Sudden death from sickle cell disease
059	F	35	80	HbSS	2.0	Intracerebral haemorrhage
123	M	58	74	HbSS	2.1	Liver failure (secondary to iron overload)
161	F	54	38	S-HPFH	2.1	Renal failure
124	0	75	71	HbSC	2.2	Post surgery complications
048	F	82	20	HbS-β^0	2.4	Unknown cause
078	M	49	70	HbSS	2.4	Cirrhosis Liver failure
069	F	42	69	HbSS	2.7	Cardiomyopathy Renal failure
120	F	49	43	HbSS	2.7	Hepatocellular cancer
037	0	25	20	HbSS	2.8	Road traffic accident
122	M	62	5	HbSS	3.0	Decompensated alcoholic liver disease ; other problems : sepsis, haemolysis secondary to SCD
014	F	32	4	HbSS	3.1	Multiple organ failure,sepsis
030	F	68	70	HbSS	3.2	Cardiac failure
170	F	50	70	HbSS	3.4	Cardiac failure

Table 2.6 - Proportional hazards (Cox) regression analysis of mortality.

Variable	Category	Hazard Ratio (99% CI)	P-value
Age (***)		1.48 (-0.92, 2.38)	0.03
Systolic Blood Pressure (***)		0.61 (0.31,1.20)	0.06
Diastolic Blood Pressure (***)		0.54 (0.25,1.18)	0.04
Genotype	HbSS / *HbS-β^0 thalassemia*	1	
	Other genotypes	0.30(0.04,2.11)	0.11
Body Mass Index (**)		0.58 (0.28,1.21)	0.06
Hydroxycarbamide (%)		1.35(0.26,7.22)	0.641
White cell count (**)		0.70 (0.20,2.42)	0.46
Haemoglobin		0.62 (0.404,0.97)	**0.006**
Fetal Haemoglobin		1.04 (0.86, 1.27)	0.59
Platelet (****)		0.95 (0.72,1.26)	0.64
Ferritin (†)		2.77 (0.79,9.80)	0.04
Creatinine		5.24 (0.18,158)	0.21
Haematocrit (*)		0.20 (0.05,0.76)	**0.002**
Red blood count		0.33 (0.11, 0.93)	**0.006**
Mean Corpuscular Volume (***)		1.59 (1.06, 2.41)	**0.004**
LDH (****)		0.99 (0.89, 1.11)	0.91

Variable	Category	Hazard Ratio (99% CI)	P-value
Bilirubin (†)		1.02 (0.11, 9.56)	0.98
LVEDD (***)		1.24 (0.36, 4.17)	0.65
LVESD (***)		1.79 (0.43, 7.42)	0.29
Left atrium diameter (***)		2.24 (0.79, 46.35)	0.05
Right atrium volume (***)		0.81 (0.38, 1.71)	0.47
Mitral valve E/A		0.39 (0.06, 2.46)	0.19
Mitral valve DT (****)		1.89 (1.23, 2.90)	**<0.001**
TRV (continuous)		4.48 (1.01, 19.8)	**0.009**
TRV	< 2.5	1	
	≥ 2.5	2.71 (0.71, 10.4)	0.06

LDH: Lactate dehydrogenase , LVEDD: left ventricular end-diastolic diameter , LVESD: left ventricular end-systolic diameter, DT: deceleration time, TRV: tricuspid regurgitant velocity
(*) Hazard ratios given for a 0.1 unit increase in explanatory variable
(**) Hazard ratios given for a 5 unit increase in explanatory variable
(***) Hazard ratios given for a 10 unit increase in explanatory variable
(****) Hazard ratios given for a 50 unit increase in explanatory variable
(†) Variable analysed on the log scale (to base 10)

Table 2.7 - Multivariate analysis of mortality**.**

Variable	Hazard Ratio (95% CI)	P-value†
Haemoglobin	0.58 (0.37, 0.93)	0.03
MCV (***)	1.89 (1.50, 2.77)	0.001
MV DT (****)	2.69 (1.74, 4.17)	<0.001

(***) Hazard ratios given for a 10 unit increase in explanatory variable
(****) Hazard ratios given for a 50 unit increase in explanatory variable
† P-value used based on the Wald method.

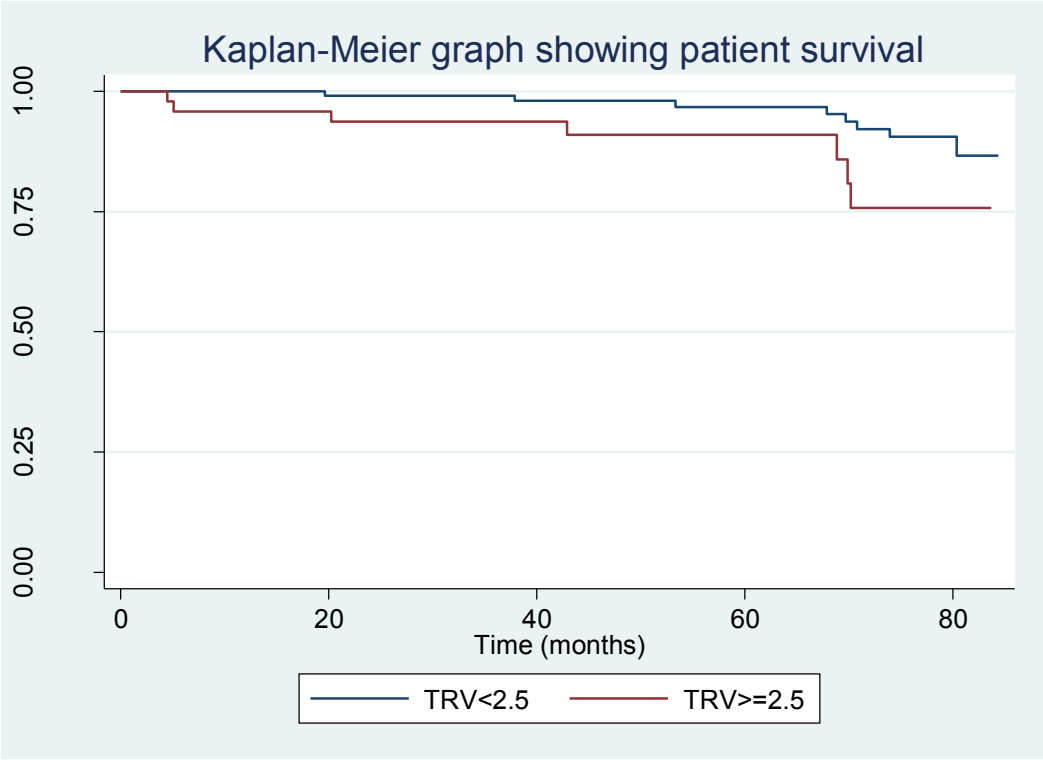

Fig. 2.1: Kaplan-Meier Survival curves according to the tricuspid regurgitant velocity. The upper line is the survival estimate for SCD patients without PH (TRV<2.5 m/s). The lower line is the survival estimate for SCD patients with PH (TRV≥2.5 m/s).The number of patients at risk at the time of each death is shown for both groups. (p=0.06).

2.4. Discussion

The major findings of this retrospective follow-up study of adults with sickle cell disease are a mortality of 16.67% in patients with a TRV ≥2.5 m/s after a median of 68 months follow-up, compared to a mortality of 6.9% in the lower TRV group, and the association between raised TRV and mortality with a greater than 4 fold increased risk of death when TRV was analysed as a continuous variable.

Although this association of increased mortality rate in patients with a raised TRV reflects previous studies from the US (Gladwin et al., 2004, Sutton et al., 1994), the overall mortality rates are much less marked in our study.

Three contemporary cohort studies in the US have reported a relationship between survival and raised TRV. Gladwin et al (Gladwin et al., 2004) reported that a TRV of ≥2.5 m/s, as compared with a velocity <2.5 m/s, was independently associated with a marked increased risk of death (RR = 10.1; 95% CI = 2.2-47; P < .001). During 18.3 months mean follow-up the mortality was 16% for patients with a TRV of ≥2.5 m/s and was less than 2% in patients with a TRV < 2.5 m/s. Follow-up data from this cohort

continues to be updated and demonstrates that raised TRV remains a strong independent risk factor for death and carries a 40% mortality rate at 45 months. The estimated risk ratio of death for patients with TRV 2.5-3.0 m/s was 4.4 (95%CI= 1.6-12.2; P<.001) and for a TRV >3.0 m/s was 10.6 (95%CI = 3.3-33.6; P < .001). With regard to hydroxycarbamide use, 37 % of the patients of the US cohort were on hydroxycarbamide therapy whilst in our cohort only 16% patients were on this treatment. In addition, we did not find an association with hydroxycarbamide use and mortality.

Castro et al (De Castro, 2004) reported a similar prevalence of raised TRV (36% in patients with HbSS and *HbS-β⁰ thalassemia* and 25% in HbSC and *HbS-β⁺ thalassemia* and a similar 17% mortality rate at 24 months for patients with raised TRV after 2 years compared with approximately 2% mortality for patients without raised TRV. This last study used a different definition of raised TRV from other studies which was corrected for age, sex and body mass index, and the TRV was measured whilst the patient was hospitalized, not in steady state. Castro et al. (Castro et al., 2003) in a study with 34 adults patients, reported a 2 year mortality rate of 55% in patients with a raised mean pulmonary artery pressure (> 25 mmHg) obtained by right heart catheterization, compared to a mortality rate of 21% in SCD without raised mean pulmonary artery pressure (≤25 mmHg) .

Two older studies also reported increased mortality. Sutton et al found that a raised TRV was associated with a 40% mortality rate at 22 months in 60 patients, with an odds ratio for death of 7.86 (2.63-23.4) (Sutton et al., 1994). Powars et al found a mean survival of 2.5 years in patients with chronic lung disease and elevated TRV (Powars et al., 1988). Recently, a large multinational study with unselected 632 screened patients (Gladwin et al., 2012) where a more conservative cut-off value of TRV ≥ 3.0 m/sec was used, showed that the association between TRV and mortality remained significant after adjustment for all other risk factors. In this study, 22 deaths were observed over median follow/up time of 29 months, of which, 11 patients had TRV of at least 3.0 m/sec. Current hydroxycarbamide use was not associated with mortality in this cohort.
In addition, we have re-analysed the data using the conservative cut off value of TRV ≥ 3 m/s. We have found no change in the results. Of the 164 patients included in our study, only 10 patients (6,1%) had a TRV value of 3.0 m/s or higher. Using the same time point

as Gladwin´s Study (24 months) we have found similar survival estimates of 99% for TRV<3.0 m/s and 80% for TRV≥3.0 m/s. Nonetheless, using a time point of 68 months, there was no significant difference (p=0.125) in the survival estimates: 95% for TRV<3.0 m/s and 80% for TRV≥3.0 m/s. We also found that patients with higher TRV values had a higher risk of death (HR: 6.52; 95% CI 2.97-20.6; p=0.001) when other factors are not considered (in comparison to a HR of 11.14 found in Gladwin's Study), however this risk disappears after adjustment for other variables associated with survival.

The lower mortality in our United Kingdom cohort raises the possibility that we studied a lower risk group of patients. On the other hand, our patients were selected randomly from those at higher risk attending out-patients clinics, whereas in Gladwin's study patients were recruited from the community through multimedia advertisements, community outreach, and regional clinics, and it was not certain if these patients were receiving comprehensive care for SCD. In the Castro paper (Castro et al., 2003) the selected patients were all hospitalized. This study preceded routine echo screening in the UK, so any selection bias is likely to have been positive rather than negative (ie patients who had symptoms of shortness of breath, or were thought to be at higher risk of pulmonary hypertension, or had a previous abnormal echo) were more likely to be referred for an echo, and this should have increased, not decreased mortality rates. In addition comparing our results to those of Gladwin et al., our study had significantly higher percentage of female patients and older patients, with a mean age of 42 years compared to 36 years and the latter should have biased the results in favour of increased mortality.

There was no significant difference in the sickle cell genotypes between the two studies (HbSS p=0.45; HbSC p=0.7; *HbS β thalassemia* p=0.68) and no significant difference in the mean TRV (p=0.15). In both studies the overall number of deaths was small which is reflected by the width of the CI for TRV ≥2.5 m/s relative to TRV<2.5 m/s. This means that the true hazard ratio in Gladwin's study could be from 2.2 to 47 (p<0.001), whereas in our study the limits are from 0.71 to 10.4 although not significant (p=0.06), when TRV was categorized in the two groups (TRV<2.5 m/s. and TRV ≥2.5 m/s). One explanation could be that the National Health Service in the UK ensures that health care is free at the point of access and this may lead to patients with milder phenotypic disease being more likely to attend outpatients clinic and increase the numbers of

patients with milder disease (and lower mortality) in the UK cohorts. On the other hand, easier NHS access to specialist sickle cell centres in the UK may result in better outcomes in terms of severity and overall quality of life. In addition, the mortality figures from the US data seem very high when compared with the UK experience. Although there are not sufficient longitudinal data for mortality of patients with SCD in the UK, the recent National Confidential Enquiry into Patient Outcome and Death (Lucas et al., 2008) report which collected data on all deaths in patients with haemoglobinopathies between January 2005 and December 2006 had only 81 reported deaths (including 7 patients with thalassaemia), which in an estimated population of 12,000 for SCD in the UK, is a very low mortality rate. In essence, the reasons for this difference in mortality with United States cohorts is not explained by the clinical measurements which were made and further studies to confirm our findings are warranted.

In our study, the effect of TRV on outcome was dependent on markers of haemolysis such as Hb and MCV. This is in contrast to the US studies which found raised TRV was an independent risk factor for death even after adjusting for causal factors such as those related to haemolysis. This and the greater overall mortality suggest a greater severity of SCD in these US patient cohorts. Why should this influence TRV as a marker of mortality? In the context of less severe SCD, end organ damage may be more directly related to haemolysis, whereas processes such as inflammation, endothelial hypertrophy and fibrosis may be more prominent in severe disease. These factors may in turn have influenced the relationship between haemolysis and survival.

In conclusion, we have confirmed the association between raised TRV and mortality in a UK SCD population attending two North West London specialist SCD centres, whose disease severity appears less than that reported in previous studies. Importantly, we did not find TRV as an independent risk factor for death. Nonetheless, of key importance to our study is the difference between mortality rates in this UK SCD population as compared to the US. Further prospective studies will enable us to more clearly characterize which patient factors modify survival in SCD patients with raised TRV.

2.5. Study limitations

In our study, a limited number of echocardiographic measurements were made at the time of these clinical studies and early studies did not include tissue Doppler. The assessment of RV function and dimensions was qualitative. The value of the mitral valve E/A ratio in evaluating left ventricular diastolic dysfunction may be limited and is dependent on intravascular volume status. Its results in SCD may be confounded by volume overload and may not accurately reflect the diastolic function of the left ventricle. Since this is a retrospective study, the selection of patients was not controlled so selection bias may have arisen. However, this remains one of the largest cohorts published to date and to the best of our knowledge with the longest follow-up period reported.

Chapter 3: General Methodology: Prospective Study

Chapter 3 General Methodology: Prospective Study

3.1. Regulatory Procedures

This study received ethical approval from the Hammersmith, Queen Charlotte's and Chelsea Research Ethics Committee of the National Research Health Service (Ref. 09/H0707/73) (see Appendix I). It was registered with the Research and Development department of the Hammersmith Hospital NHS Trust (Project reference: ZIMI1001). All participants, patients and healthy volunteers, gave written informed consent before participation and the research was conducted in accordance with Good Clinical Practice guidelines. Copies of the ethical approval letters, Research and Development approval, patient information sheets and consent forms are included in Appendix I and II.

The patients included in the screening visit were participants recruited from the observational study of Walk–PHaSST (Treatment of Pulmonary Hypertension and Sickle Cell Disease with Sildenafil Therapy) , a multicentre trial looking at the treatment of pulmonary hypertension in SCD patients with sildenafil therapy (http://www.clinicaltrials.gov; unique identifier, NCT00492531). The Walk-PHaSST trial was conducted in 9 US centres and 1 UK Centre, which was the National Heart and Lung Institute (Hammersmith Hospital). All participants gave written informed consent for the use of their clinical data in this study. No patients who participated in the interventional part of Walk-PHaSST were included in this study.

3.2. Aims of the project

The primary aim of the project described in this thesis is to assess the impact of cardiovascular complications in patients with sickle cell disease.

3.2.1. Specific Aims

This thesis has the following specific aims:

1. To conduct a retrospective mortality study in a cohort of 164 patients with SCD and pulmonary hypertension in a North West London population. This study has been described in Chapter 2
2. To describe a cardiovascular phenotype according to age in a cross-sectional study of cardiac abnormalities in patients with SCD from the age of 18 years old upwards in a UK cohort.
3. To assess left and right ventricle function, both systolic and diastolic, by new advanced echocardiographic techniques. In particular to study the impact of myocardial deformation, torsion, function and volumes in a longitudinal study. Test the clinical importance and association of echocardiographic findings with markers of haemolysis, clinical history and disease severity. Describe the associations of cardiac findings with 6 minute walk test (6MWT) and brain natriuretic peptide.
4. To prospectively evaluate the clinical and echocardiographic predictors of short-term clinical outcomes in patients with SCD in an Observational Follow-up Study.
5. To assess the relationship between elevated tricuspid velocity regurgitation and biventricular function by 2D and 3D Speckle Tracking.
6. To assess ventricular volumetry, ejection fraction and mass, iron overload and myocardial fibroses by cardiac magnetic resonance in a subgroup of SCD patients with LV diastolic dysfunction.
7. To assess the correlation between LV 2D Strain by speckle tracking and LV 3D Strain and LV 3D Strain with LV MRI Strain by myocardial tagging.
8. To assess the inter-observer, intra-observer and test re-test reproducibility of LV 3D Strain and RV 4D volumetry quantification with a novel semi-automated border detection software.

3.3. Recruitment of Study Participants

All study visits and data collection was carried out at Hammersmith Hospital, Imperial College NHS Trust, London. Participants in the study included patients with SCD (Group A) and a group of Healthy Volunteers to act as controls (Group B).
Subjects who agreed to participate were registered and booked at the Sir John McMichael Clinical Research Centre for the study visit and asked to sign three separate research consent forms: participant copy, participant clinical notes copy and study file copy (Appendix II).

All information sheets and consent forms had been approved by the local research committee. Participants were also clearly informed that they were free to withdraw from the study at any time. In order to reduce travelling costs and facilitate recruitment, all participants were offered reimbursement of their travel expenses

3.3.1. Group A: Patients with Sickle Cell Disease

Patients with a diagnosis of Sickle Cell Disease who had participated in the WALK-PHaSST study and who met the study inclusion criteria were invited at random to participate in this observational study. The WALK-PHaSST was conducted between June 2007 and October 2009, in collaboration with the National Institutes of Health with the SCD clinic and the Pulmonary Hypertension Service at Hammersmith Hospital as one of the Centres.

The recruitment of the patients in this study was conducted between January 2010 and June 2010. The WALK-PHaSST Executive Committee approved the use of study data in this study. There was no overlap between studies, patients were invited to participate after WALK-PHaSST has been completed.

An informal research consultation to inform patients of the study's aims and design was conducted by the investigator by phone or on the day of their appointment at the SCD Clinic. If they were interested in participating the relevant information sheet (see Appendix II) was provided explaining the purpose of the research. This information sheet was given in person if the consultation was done at the hospital or sent by post to

their home address with a cover letter (see Appendix II). Patients were given at least 24 hours to read the information sheet and they were contacted at their convenience to discuss the study and given the opportunity to ask any questions. Patients who agreed to participate were booked at the Sir John McMichael Clinical Research Centre for the follow-up visit and asked to sign three separate research consent forms listed: patient copy, patient clinical notes copy and study file copy (see Appendix II).

An additional information letter was also sent to the general practitioner/consultant of each patient, once they consented for this purpose.

All information sheets and consent forms had been approved by the local research committee. Patients were also clearly informed that they were free to withdraw from the study at any time.

In order to reduce travelling costs and facilitate recruitment, all participants were offered reimbursement of their travel expenses and the study visit was booked, when possible, to coincide with prearranged outpatient clinic appointments.

3.3.1.1. Inclusion criteria

The inclusion criteria were chosen with the aim of recruiting a heterogeneous cohort of SCD patients and a range of disease severity.

The inclusion criteria for this study were as follows:

- Males or females aged 18 years or older with a diagnosis of sickle cell disease (documentation of sickle cell disease, including but not limited to, HbSS, HbSC, HbSD, or Sβ°/+ thalassemia phenotype).
- Steady state patients.
- Able to provide written informed consent prior to any study-mandated procedures.

3.3.1.2. Exclusion criteria

The exclusion criteria for this study were as follows:

Unwilling or unable to give written informed consent.

A recent (less than 3 weeks) vaso-occlusive crisis, episode of acute chest syndrome, severe anaemic events or any other acute complications of SCD.

Admission to hospital or acute transfusion within 3 weeks.

At least moderate valvular heart disease.

Evidence of systolic heart failure (LV Ejection fraction <= 40%)

Congenital heart disease.

Known cardiac diseases

Uncontrolled atrial fibrillation.

3.3.2. Group B: Healthy volunteers

Healthy, age and race matched volunteers with no clinical or echocardiographic evidence of cardiovascular disease were included in the study to serve as control subjects.

The healthy volunteers participants were recruited at the Hammersmith Hospital by local advertisement (see Appendix II) or word of mouth and included relatives and acquaintances of participants with no SCD or SCD trait, who were not hospitalised or who had not presented to a doctor in the previous 3 weeks.

Healthy volunteers were given at least 24 hours to read the Information Sheet (see Appendix II) and they were contacted at their convenience to discuss the study and given the opportunity to ask any questions.

3.4. Method of data collection

3.4.1. Screening visit: patients

Participants in **Group A** underwent a baseline study which included:

Self reported medical history
Physical examination
Standard laboratory tests (including documentation of haemoglobin phenotype and cardiac biomarker)
A 6 minute walk test (6MW)
Transthoracic 2D and 3D echocardiogram

No patients were excluded for poor echocardiographic imaging quality. This means that the study population resembled that of everyday clinical practice, so the precision limits were the level of precision to be expected in a clinical setting.

After analysis of the transthoracic echocardiogram at the screening visit, patients were split according to a cut off value of 2.5 m/s for the TRV velocity. Subsequently, they were included in two groups in relation to the LV diastolic function status (with and without LV diastolic dysfunction) according to the European Association of Echocardiography/American Society of Echocardiography recommendations for the evaluation of LV diastolic function (Nagueh et al., 2009a) which will be described later in this Chapter.

The groups were defined as:

Group A1 –SCD patients with normal left ventricular diastolic function

Group A2 –SCD patients with abnormal left ventricular diastolic function

One year after the screening visit, there was a follow-up visit and the procedures undertaken will be described later in this Chapter.

3.4.2. Screening visit: Healthy Volunteers

All participants underwent a structured interview
These subjects were assessed for:

Self reported medical history

Physical examination

Transthoracic 2D and 3D echocardiogram

3.4.3. Follow-up visit

A second visit was conducted approximately after 1 year (mean 17.14±3 months) after the screening visit.

Patients who had participated in the observational study of the Walk-PhASST trial, were consecutively assigned to this study until the sample size was completed to achieve a sample size that gives 80% power at the 0.05 level of significance (two- sided).

Twelve patients declined to participate and 7 patients were excluded due to the exclusion criteria.

Follow-up investigations included a health status interview, laboratory tests, collection of blood for brain natriuretic peptide, and a transthoracic 2D and 3D echocardiogram. All participants underwent the transthoracic echocardiogram performed by I.Z.C. at the screening visit.

Additionally, patients from Group A2 (with LV diastolic dysfunction diagnosed by echocardiography), were invited to perform a cardiac magnetic resonance for assessment of concomitant causes of diastolic function (e.g. ischemic heart disease, left ventricular hypertrophy, myocardial infarction).

All patients were given a study ID number with 4 digits: the first two digits corresponding to consecutive numbers in sequence from 01 to 61 following the first and last name initials) so all data was anonymised on the ultrasound equipment and when transferred to the computer.

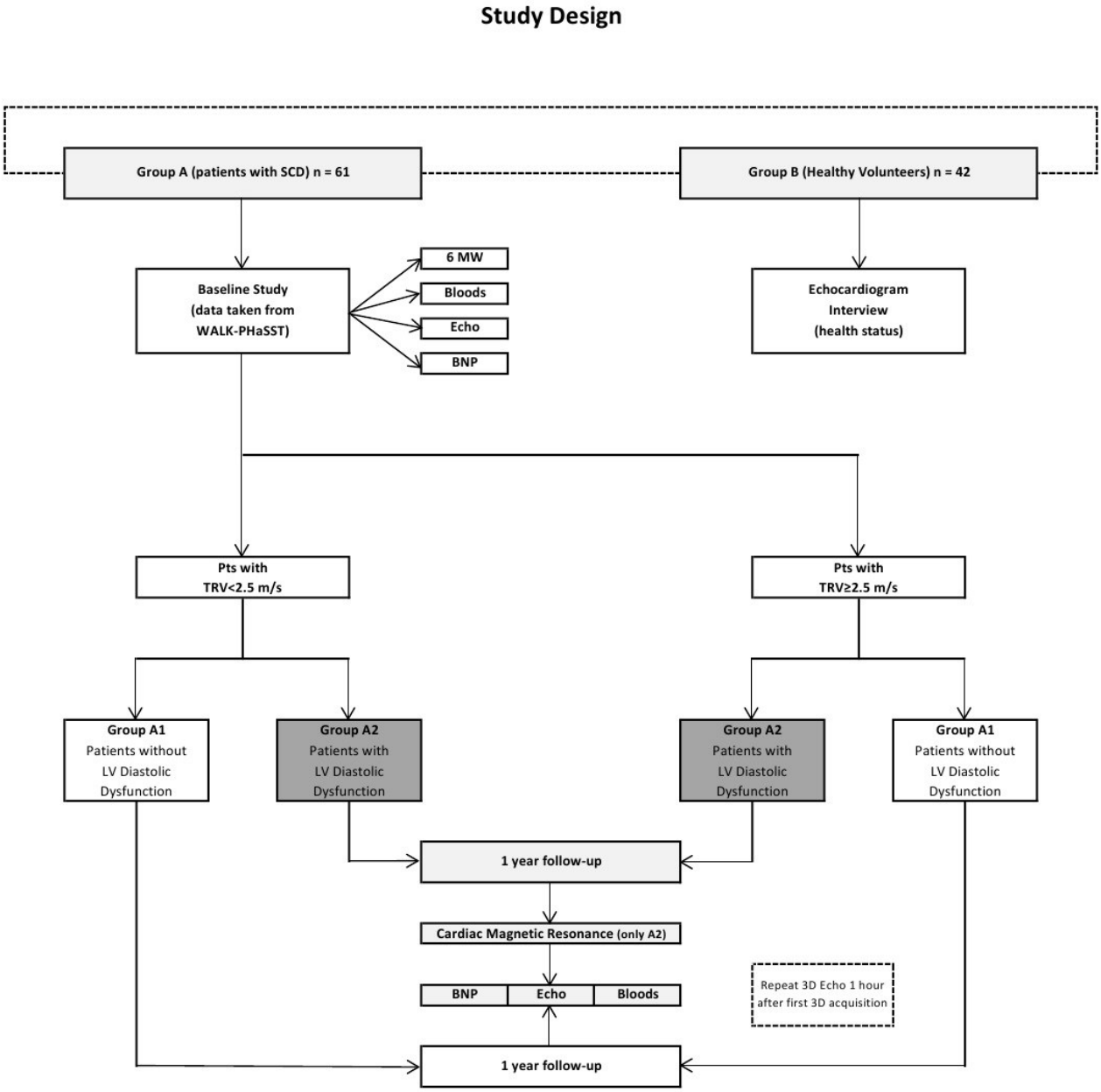

Fig. 3.1: Study design

3.5. Measurements and data confidentiality

The screening visit included the assessment of vital signs, self-reported medical history, medication, functional class by New York Heart Association Classification (NYHA), standard laboratory tests, a 6MWT and a transthoracic 2D and 3D echocardiogram. These data were taken from the WALK-PHaSST study patient´s record after informed consent had been obtained.

The follow-up visit included the recording of clinical events, number of hospital admissions, standard laboratory tests, functional classification system by NYHA and the evaluation of the echocardiogram. Additionally, the 3D echocardiogram was repeated after 1 hour of the first 3D image acquisition (test re-test), in order to evaluate the ability of the test to yield the same result for a single patient at 2 different test periods, which are closely spaced so that any variation detected reflects reliability of the test rather than changes in the patient status.

Data regarding laboratory tests was obtained from the Electronic Patient Record (ICHIS and ICE) from the Hammersmith Hospital. A study spread sheet was used to collect data from the screening visit and the follow-up visit. Three patient identifiers (patient ID, initials and date of birth) were used on all spread sheets. A database of demographics, echocardiography data, cardiac magnetic resonance and laboratory tests was generated.

3.5.1. Vital Signs

The assessment of the vital signs included the measurements of heart rate, blood pressure and oxygen oximetry.

Heart rate and blood pressure were measured at the time of the echocardiogram using an electronic blood pressure measuring device after the patient had been seated for five minutes. Regarding blood pressure, if the difference between 3 readings was greater than 10 mmHg systolic or diastolic, the measurements were repeated. The left arm was used in all readings.

Haemoglobin oxygen saturation was measured by finger pulse oximetry, using a finger clip oximeter probe. Oximetry provides a measure of the average oxygen saturation of haemoglobin. It relies on the principle that the light absorption characteristics of haemoglobin are altered by the binding of oxygen. An oximeter probe contains two LEDs emitting light at red (660nm) and infrared (910nm) wavelengths, and a photo detector to measure transmitted light. When an oximeter probe is applied to the fingertip a constant proportion of emitted light will be absorbed by the soft tissues. The absorption of light by blood constituents can be determined from changes in the

quantity of transmitted light occurring during fluctuations in arterial volume with each cardiac cycle.
The ratio of red and infrared light absorbed is used to calculate the oxygen saturation of haemoglobin.

3.5.2. Self-reported medical history and additional information

Details of each participant's medical history were collected, including history of vaso occlusive pain, acute chest syndrome, leg ulcers, total number of transfusion in lifetime, transfusion treatment, and record of history of multi organ disease (heart, kidney, lungs, spleen, liver, neurological problems). Alcohol, drugs and tobacco intake were also assessed.
A record was also made of all prescribed and over the counter medications.

3.5.3. New York Heart Association Classification

The functional class of the patients was assessed according to the NYHA.
The NYHA classification is based upon symptoms and exercise capacity reported by the patient (Table 3.1) (The Criteria Committee of the New York Heart Association, 1994). It is a commonly used measure to asses.
functional capacity in several diseases and the NYHA class has been shown to be a strong predictor of mortality in PAH (2008).

Table 3.1 - New York Heart Association Classification of Heart.

Class I	No limitation of physical activity. Ordinary physical activity does not cause undue fatigue, palpitation, or dyspnoea.
Class II	Slight limitation of physical activity. Comfortable at rest, but ordinary physical activity results in fatigue, palpitation, or dyspnoea.
Class III	Marked limitation of physical activity. Comfortable at rest, but less than ordinary activity results in fatigue, palpitation, or dyspnoea.
Class IV	Unable to carry on any physical activity without discomfort. Symptoms at rest. If any physical activity is undertaken, discomfort is increased.

3.5.4. Laboratory measurements: blood sample collection

Laboratory tests were performed at the Hammersmith Hospital laboratory and were undertaken in accordance with quality assured and approved techniques.
Blood samples were collected at the screening and the follow-up visit. An experienced research nurse was responsible for the collection and preparation of laboratory samples. Routine laboratory tests included a complete blood count, reticulocyte count, serum chemistry profile, and lactate dehydrogenase). After blood collection, results were obtained from the Electronic Patient Record (ICHIS and ICE) from the Hammersmith Hospital.

At the screening visit, Serum N-terminal pro-brain natriuretic peptide concentration was measured by a sandwich immunoassay using polyclonal antibodies that recognize epitopes located in the N-terminal segment (1– 6) of pro-BNP (1–108) (Elecsys analyser; Roche Diagnostics, Mannheim, Germany).

At follow-up visit, the biomarker assessment included the brain natriuretic peptide levels. All samples were collected by venepuncture into EDTA tubes. The blood samples were kept at room temperature and analysed within 4 hours of the draw time (Abbott i2000SR instrument reagents). Before analysis, each tube was inverted several times to ensure homogeneity.

3.5.5. 6 Minute Walk Test

The 6MWT was performed during the screening visit at the Sir John McMichael Clinical Research Centre by an experienced research nurse, in a 30 metre hallway. This test measured the distance that the patient could walk on a flat, hard surface in a period of 6 minutes (2002). It evaluates the global and integrated responses of all the systems involved during exercise, including the pulmonary and cardiovascular systems, systemic circulation, peripheral circulation, blood, neuromuscular units, and muscle metabolism. The 6MWT was done at least one hour before the echocardiogram.

3.5.6. Cardiac Imaging Analysis

3.5.6.1. Two-dimensional echocardiography

3.5.6.1.1. Image Acquisition and Processing

Transthoracic 2-dimensional echocardiography (2DE) was performed by the same experienced sonographer (certified by the European Association of Cardiovascular Imaging) at both visits (screening and follow-up) using a digital commercial harmonic imaging ultrasound system with an S 5-1MHz variable frequency phased-array transducer (Philips IE33, Philips Medical Systems, Bothell, WA, USA).

A single channel electrocardiogram (ECG) recording was performed, with ECG electrodes (Blue sensor, Ambu Ltd., Cambridgeshire, UK) placed below the right sternoclavicular joint and in the left axilla (modified lead II position). The ECG was sampled at 256 Hz.

All the studies were saved with the study Patient ID and were stored after digital acquisition to guarantee a high image quality and reproduction off line of the images without loss of information. The recorded echocardiography files were transmitted to a computer, and stored on DVD for off-line analysis of the ultrasound images. Off-line analysis of standard echocardiographic variables was performed with the use of dedicated software (Prosolv CV Analyser 3.0; Prosolv CardioVascular, Indianapolis, IN, USA).

3.5.6.1.2. Protocol overview

Echocardiography was the investigation of choice for the non-invasive assessment of cardiac structure and function. The scanning time was approximately 30-40 minutes which included the acquisition of the full volume images for 3D quantification. The participant was required to rest (lay supine) for 10 minutes before the scan was conducted. The sonographer verified the optimal ultrasound window with the patient in

supine position and when requested, the participant was asked to lay on his/her side with their left arm on the pillow.

During 2DE, we practiced the following protocol: two- dimensional images and Doppler blood flow measurements were obtained from four-, two- and three chamber, as well as parasternal long-axis (including RV inflow and outflow tract) , sub costal views and suprasternal view by manually rotating and angulating the transducer according to the guidelines of the American Society of Echocardiography (Lang et al., 2005) and the European Association of Echocardiography (Gordeuk et al., 2008). All patients were examined using greyscale second-harmonic 2D imaging technique with adjustment of image contrast, frequency, depth and sector size for adequate frame rate and optimal LV and RV border visualization. The recorded loops had at least 3 beats in each frame. All Doppler measurements were performed at 100mm/second sweep with low filter; with an average over three consecutive beats, to account for variations in heart rate. No measurements were performed at a premature beat of after following a premature beat.

The 2D-echocardiography study protocol included standard echocardiographic measurements of LV size, geometry, mass, systolic and diastolic function, right ventricular function, estimation of RV systolic pressure, qualitative and quantitative analysis of valvular regurgitation. Care was taken to avoid LV foreshortening in apical views and image acquisition was done during breath hold to minimize respiratory movements.

3.5.6.1.3. Standard echocardiography

The following echocardiographic parameters were assessed for chamber quantification: LV end-systolic and end-diastolic diameters, LV wall thickness, LV mass, LV ejection fraction, left atrial volume, RV diameter and fractional area change, right atrium volume and bi-ventricular global and regional wall motion abnormalities.

LV dimensions were obtained in the parasternal long axis view, with measurement of interventricular septal and posterior wall thickness. We estimated LV end-diastolic,

end-systolic volume and ejection fraction from the biplane Simpson method by tracing a contour around the LV cavity during end-diastole and end-systole in apical 4- and 2-chamber views (Lang et al., 2005). LV mass and LV mass index waere calculated using the area-length formula at short-axis view as described in the 1989 ASE document on LV Quantitation (Schiller et al., 1989). Relative wall thickness was calculated as septal + posterior wall thickness/LV end-diastolic diameter.

Left atrial volume was measured with the biplane method of disks incorporating apical 4- and 2-chamber views. Global and regional assessment of any wall motion abnormalities was performed visually by the sonographer in all views.

RV assessment was performed based on the echocardiographic protocol described in the Standard Operating Procedure of the Hammersmith Hospital for the Echocardiographic Assessment of Pulmonary Hypertension(Howard et al., 2012) . RV dimensions were obtained in the apical 4-chambers view, with measurements of the end-diastolic and end-systolic area which were derived by manually tracing the endocardial borders at end-diastole (onset of the QRS complex) and end-systole (smallest ventricular area). Before making any measurements, care was taken to obtain a true no foreshortened apical-4 chamber view, oriented to obtain the maximum RV dimension. RV fractional area change was calculated as: 100x (RV diastolic area-RV systolic area)/RV diastolic area. RV dysfunction was defined by a fractional area change < 32%. Global and regional assessment of any wall motion abnormalities was performed visually by the sonographer in all views. Additional measurements included the tricuspid annular peak systolic excursion (TAPSE), presence of pericardial effusion, RV myocardial performance index, tricuspid annulus assessment and inferior vena cava diameter. TAPSE was calculated using M-mode echocardiography with the cursor placed through the lateral tricuspid annulus in real-time. TAPSE (reference value < 0.16 cm) was measured as the total displacement of the tricuspid annulus from end diastole to end systole (Ghio et al., 2000).

Right atrium volume was measured with the area-length method with 4 chambers apical view (4C Apical), where RA volume = 0.85 X (RA area)2 / (RA systolic diameter).

The valvular assessment included the evaluation of morphology and function of the mitral, aortic, pulmonary and tricuspid valves in multiple views following the recommendations of the European Society of Echocardiography/American Society of Echocardiography (Zoghbi et al., 2003, Baumgartner et al., 2009).

Indexed parameters (e.g., LV diastolic volume, LV mass) were calculated by dividing each parameter by body surface area (BSA). BSA was calculated as follows: BSA (m2) = 0.20247 × ht (m) 0.725 × wt (kg) 0.425, where ht is height and wt is weight. Parameters such as RVOT acceleration time and IVRT were indexed to heart rate (HRate).

3.5.6.1.4. Conventional Doppler

Standard continuous-wave and pulsed wave Doppler examinations were performed in mitral, aortic, pulmonary and tricuspid valves in multiple views.

Mitral inflow assessment

Mitral inflow recordings were obtained with the pulsed Doppler from the apical four chamber view, with the Doppler sample volume being placed at the level of the mitral valve leaflet tips during maximal opening in diastole in order to measure peak early (E) wave and atrial contraction (A) wave velocities and early filling deceleration time. Isovolumic relaxation time was measured by placing the Doppler sample volume at the LV outflow tract. Pulmonary vein flow analysis was also recorded. Mitral inflow propagation velocity by Colour-M mode was measured. From the apical view, colour flow imaging was used to demonstrate mitral inflow. A cursor was placed along the centre of the mitral inflow colour jet, and the colour baseline was shifted upward until the centre of the jet became blue.

Estimation of right ventricular systolic pressure

Continuous-wave Doppler sampling of the tricuspid peak regurgitant jet velocity was used to estimate the right-ventricular-to-right-atrial systolic pressure gradient with the use of the modified Bernoulli equation (4x[tricuspid regurgitant velocity]^2). Velocity of

the TR jet was assessed, comparing the quality and peak measurements of the continuous-wave Doppler waves, obtained from different views, in particular the parasternal long-axis and apical 3-chamber view (modified) where the RV was visualised by tilting the probe anteriorly.

Careful attention was paid in obtaining optimal Doppler signals for both tricuspid and pulmonary regurgitation. The TR signal by continuous-wave Doppler was recorded initially from the low parasternal right ventricular inflow view, and it was optimised in multiple other views including parasternal short-axis and apical views. Apical views were optimised by moving the transducer medially towards the sternum in order to improve alignment with the TR jet. The wave with the highest quality and deepest peak was considered the most accurate. The mean right atrial pressure was calculated according to the degree of collapse of the inferior vena cava with inspiration (Lang et al., 2005).

No estimation of RV systolic pressure was done in cases of severe free-flow tricuspid regurgitation or RV outflow obstruction. A cut-off value of 2.5 m/s was used since it has been the most widely used approach in patients with sickle cell disease as described in Chapter 1 of this thesis. There was not sufficient pulmonary regurgitation in all patients to provide an adequate RV-end-diastolic pressure measurement.

Valvular assessment

Regarding valvular assessment, colour Doppler echocardiography was performed in all views after optimising gain and Nyquist limit. Valvular regurgitation was graded as absent/physiological trace (grade 1), mild (grade 2), moderate (grade 3) or severe (grade 4) using multiple parameters (Evangelista et al., 2008).

Stroke volume, Cardiac Output and Pulmonary Vascular Resistance

Echocardiography uses the combination of 2D and pulsed-wave Doppler imaging to measure cardiac output. Stroke volume (SV) can be derived from the product of the velocity-time integral (VTI) of the Doppler profile and the cross-sectional area of the LV outflow tract (LVOT). Cardiac output (CO) is the product of SV and HRate.

$$\mathbf{SV = VTI_{(LVOT)} \times cross\text{-}sectional\ area_{(LVOT)}} \quad ; \quad \mathbf{CO = SV \times HR}$$

Similarly, right ventricular SV and CO can be measured from the proximal right ventricular outflow tract (RVOT), just within the pulmonary valve from the parasternal short-axis view. Care should be taken to ensure that the Doppler cursor is in line with the axis of theRVOT, otherwise a significant error will appear in the measurements. In order to calculate pulmonary vascular resistance (PVR), continuous-wave Doppler is used to determine the peak tricuspid regurgitant velocity as described above: the highest velocity is used. In patients with atrial fibrillation, the average of five measurements should be taken.

$$\textbf{PVR (Wood units)} = 10(TRV/VTI_{RVOT}) + 0.16$$

This measurement has been shown to correlate well with PVR measured at cardiac catheterisation over a range of right and left atrial pressures (Scapellato et al., 2001, Abbas et al., 2003). A value of TRV/VTI_{RVOT} less than 0.2 has 94% sensitivity for a PVR of less than two Wood Units at catheterisation[26].

3.5.6.1.5. Tissue Doppler Imaging

Longitudinal myocardial function was assessed using TDI with a real-time pulse wave tissue Doppler technique. Tissue Doppler recordings of the left ventricle were measured with sample volumes at both septal and lateral mitral annulus. Measurements of the mean peak systolic (s´), early diastolic (e´) and late diastolic (a´) myocardial velocities, were recorded. The ratio of early diastolic LV inflow velocity to both septal and lateral mitral annular velocity (LV lateral E/e´) was calculated as an estimate of LV filling pressure. All the values were analysed but for specific analysis we have used the LV lateral E/e´ to estimate left ventricular diastolic diameter in this study, as has been used previously in SCD(Sachdev et al., 2011). Its use has also been suggested in the setting of non-cardiac pulmonary hypertension (Nagueh et al., 2009a). Global function index (GFI), is defined as a ratio between a diastolic parameter (E mitral inflow/e´) measured at one point and the peak systolic tissue Doppler velocity (GFI= [Emi/e´]/s´ [s x cm^{-1}]),

where E is E wave, s is systolic wave, and mi is mitral inflow. GFI was determined at septal and lateral levels (Núñez et al., 2004).

Right ventricular myocardial tissue velocities were also derived from the junction of the RV lateral wall and tricuspid valve annulus. Peak annular RV lateral wall velocities during systole (S wave) and E´ and A´ for early and late diastolic velocities were measured by the same method. Tissue Doppler RV isovolumic relaxation time (tIVR) was obtained between cessation of S-wave and onset of E´wave (Zimbarra Cabrita et al., 2013b)(Fig. 3.2).

Myocardial performance measured with Tissue Doppler Imaging (tMPI) was the parameter used for the evaluation of RV global function. MPI is defined as the sum of isovolumetric contraction and relaxation intervals divided by ejection time. Isovolumic contraction time (tIVC) was measured between cessation of A' wave and onset of S-wave; TDI ejection time (tET) was obtained between onset and cessation of S wave; TDI isovolumic relaxation time was obtained between cessation of S wave and onset of E' wave. tMPI was calculated as the sum of isovolumic contraction time and isovolumic relaxation time divided by ejection time (tIVC+tIVR)/ (tET). Special attention was paid to keep the best possible alignment between the tricuspid annulus motion and the ultrasound beam. tMPI is relatively unaffected by heart rate, loading conditions and RV geometry and importantly has the advantage of simultaneously recording the systolic and diastolic velocity patterns from the same cardiac cycle (Zimbarra Cabrita et al., 2010).

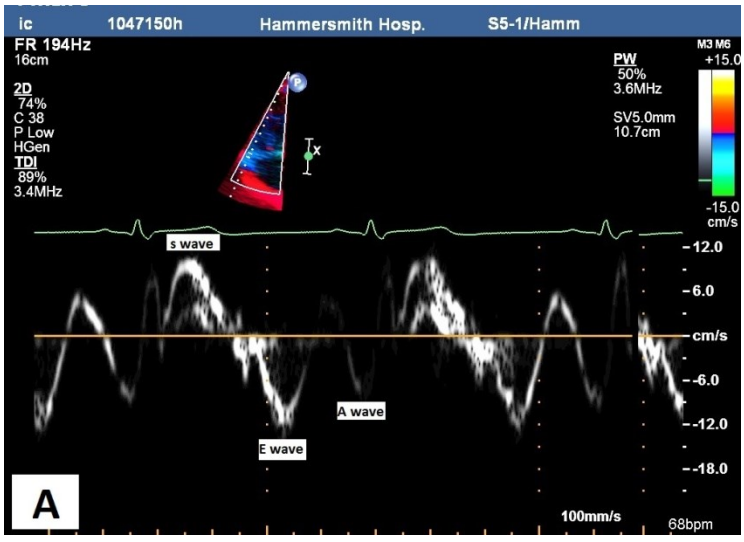

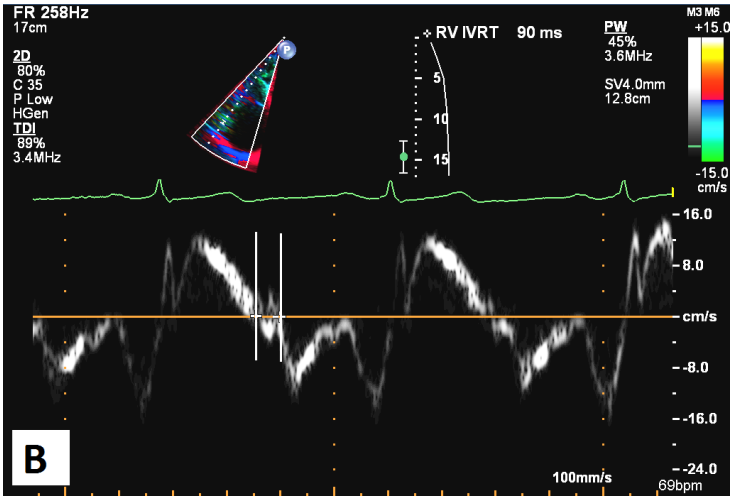

Fig. 3.2: A- Right ventricle measurements from tissue Doppler obtained from the lateral tricuspid annulus. A - Peak annular RV free wall velocities during systole (S wave) and E´ and A´ for early and late diastolic. B- Right ventricle isovolumic relaxation time measured from pulsed tissue Doppler

3.5.6.1.6. Left ventricular diastolic function

Diastolic function was assessed in all patients using pulsed Doppler where peak E and A velocities, E/A ratio, deceleration time and IVRT were assessed (Quinones et al., 2002).

Transmitral flow: the mitral flow velocities were recorded at sweep speed of 100 cm/s, using pulse waved Doppler with the sample volume placed at the tip of the mitral valve leaflets in the apical view. From the mitral valve inflow velocity curve the following measurements were made: peak E-wave velocity and its deceleration time; peak A-wave velocity; ratio of E-wave to A-wave (E/A) velocities and the IVRT was measured from the aortic valve closure to mitral valve opening.

Pulmonary venous flow was assessed from 4-chambers apical view, rotating the probe slightly anticlockwise (towards left) and ante-flexing the probe at a scan angle of 30 to visualize the LA appendage and left upper pulmonary vein. Sample volume was positioned about 1 cm into the pulmonary vein and spectral Doppler was recorded to measure peak S wave height, peak D wave height, peak atrial reversal wave depth, atrial reversal duration and blunting or S wave reversal.

LA volume was calculated from three measurements of LA dimension taken at ventricular end-systole using the formula for an ellipse. Indexation to body surface area was then performed.

Mitral inflow propagation velocity was obtained by colour M-mode of the mitral inflow. From the apical view, colour flow imaging was used to demonstrate mitral inflow. A cursor was placed along the centre of the mitral inflow colour jet, and the colour baseline shifted upward until just the centre of the jet turned blue.

Tissue Doppler imaging was also assessed since there have been several reports of elevated pulmonary capillary wedge pressure in SCD patients undergoing cardiac catheterisation (Gladwin et al., 2004, Castro et al., 2003). The longitudinal diastolic function and estimate of end-diastolic pressure were assessed by measuring the early (e´) and late (a´) diastolic velocities were measured from the basal lateral annulus and basal septal myocardial segments. Using the same tissue Doppler pulsed wave signal, the systolic myocardial velocity was measured. An estimate of LV filling pressure could then be obtained from the ratio of the transmitral E-wave velocity to the tissue Doppler Ea velocity (E/e´ ratio). LV diastolic function was not assessed in patients in atrial fibrillation. As it has been described (Lester et al., 2008, Nagueh et al., 2009b) , the assessment of diastolic function in patients with atrial fibrillation have limited accuracy where the loss of atrial contraction and relaxation reduces pulmonary venous systolic flow regardless of filling pressures, The Doppler estimation of LV filling pressures is limited by the variability in cycle length, the absence of organised atrial activity, and the frequent occurrence of LA enlargement.

In order to classify the various patterns for LV diastolic filling we used previously published criteria (Nagueh et al., 2009c) and divided the patients into four groups: Group 0 = normal filling pattern, Group 1 = abnormal relaxation, Group 2 = pseudonormal flow pattern, and Group 3 = restrictive flow pattern (Fig. 3.3).

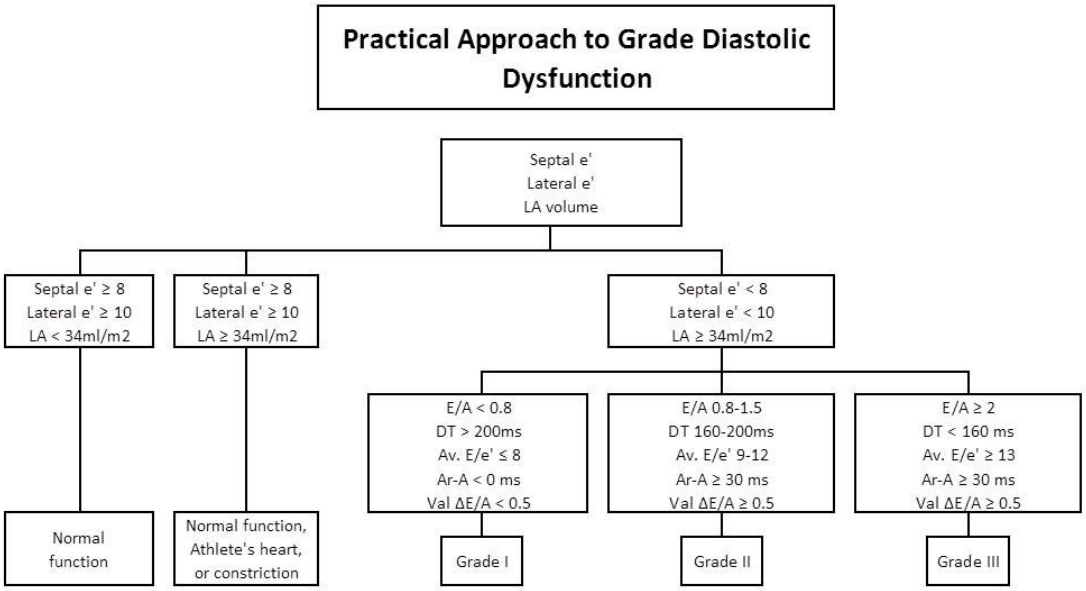

Fig. 3.3: Scheme for grading diastolic dysfunction. Av., Average; LA, left atrium; Val., Valsalva

3.5.6.1.7. 2D Speckle tracking imaging

Greyscale images for offline speckle-tracking analysis were acquired at frame rates of 55 to 90 frames/sec during breath-hold, usually with forced expiration. Parasternal short-axis images were acquired at the basal, mid and apical ventricular level and from standard apical two-three- and four-chamber views. At least three cardiac cycles were stored for offline analysis.

2D Left Ventricular Strain

LV longitudinal and circumferential strains were assessed using the 2D speckle tracking method at the follow-up visit. The apical four-,two-, and three-chamber images and short axis views at the papillary muscles, mid and apical level were analysed off line (Q-Lab 8.1, Philips Medical System) by automated tracking analysis after visual inspection of the tracking result. LV end-systolic longitudinal and circumferential strain for basal, mid and apical segments of the anterior, antero-septal, lateral, posterior, inferior and infero-septal segments were assessed. The LV was divided according to the 16-segment model (6 basal, 6 mid-LV, and 4 apical) of the American Society of Echocardiography, and each segment was individually analysed.

Apical 4C view was used to determine global strain by manually positioning three reference points: one on each side of the mitral valve annulus and the third at the apical endocardial border. Immediately, the software creates a region of interest (template) with the automatic delineation of endocardial and epicardial borders, tracking the speckles throughout the cardiac cycle, thus deriving the transmural global strain.

The thickness of the region of interest was adjusted to include the entire myocardium. The software used automatically tracks the myocardial deformation on the subsequent frame. If the tracking was not satisfactory, manual adjustments were made to the tracking points throughout the cardiac cycle. If satisfactory tracking was not accomplished after attempting 3 times, the non-tracking segments were excluded from analysis. Lagrangian strain curves were provided by the software. Aortic valve closure was measured with the use of electrocardiographic trace to estimate the timing of end-systole and early diastole. (Fig. 3.20). All offline measurements with QLAB were performed by the same observer (I.Z.C.).

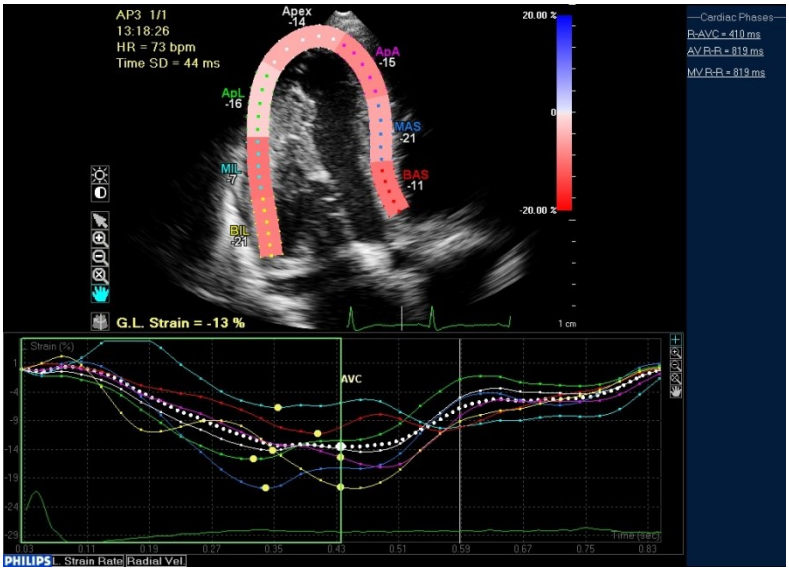

Fig. 3.4: Two-dimensional LV longitudinal myocardial left ventricle strain in an apical three-chamber view. Top: template originated by dedicated software after the points defined by the operator. Bottom: the curves of deformation, colored according to the corresponding segment depicted in the template; the points at the nadir of each curve correspond to peak systolic strain

The software was able to represent myocardial deformation in time–strain graphs to identify the different phases of cardiac cycle. When myocardial deformation was graphically represented as time–strain curves, cardiac cycle phases were recognised as follows: from the original length, during systole there is a negative wave which reaches

its negative peak at the aortic valve closure, representing the maximal longitudinal myocardial shortening during contraction (Fig. 3.4)(Marwick et al., 2009b). In diastole, strain values progressively increase towards the original length.

2D Right Ventricular Strain

The apical four-chamber view was obtained using the same ultrasound system with the same probe used for standard echocardiography; end-systole was chosen as the single frame for the endocardial-to-epicardial region of interest to include maximum RV lateral wall thickness for strain calculation. The reference points were manually inserted: first point on the basal septum and second point on the basal RV lateral wall. The region of interest then included the entire RV myocardial wall and the epicardial border was then adjusted to correspond closely to the RV lateral wall thickness. The tracking algorithm followed the endocardium from this frame through the cardiac cycle. For RV longitudinal strain, myocardial thickening was represented with a negative value colour coded as red and thinning was represented as a positive value colour coded as blue. These were superimposed in the conventional 2D image, with the mean values for each segment showing on the display. Longitudinal strains for each individual segment were measured and averaged for RV septal and lateral walls. In addition, the software calculated the RV Global longitudinal strain by averaging segmental strains along the entire RV (Fig. 3.5).

Fig. 3.5: Two-dimensional right ventricle strain in an apical four-chamber view.

3.5.6.2. Three-dimensional echocardiography

Real-time 3D echocardiography data set acquisition was obtained from an apical window using a matrix array ultrasonic transducer with 2,400 elements (X3-1 transducer, Philips IE33, Philips Medical Systems, Bothell, WA, USA). ECG tracing was optimised before images acquisitions to increase R wave peaks.

Images were gathered over four cardiac cycles during breath-hold. Care was taken to avoid a Valsalva manoeuvre while on breath-hold, which could degrade image quality and alter cardiac volumes. Full volume and harmonic imaging was used. Depth, time gain compensation and focus position were adjusted to obtain best image quality and care was taken to encompass the entire LV cavity in the data set. The quality of the acquisition was verified in each patient to exclude artefact motions and to ensure the entire LV was included in the full volume. When necessary, the data set was re-acquired. Data sets were stored digitally and exported to a DVD. The DICOM files were later exported to a separate workstation equipped with a commercially available software for off line analysis of LV volumes and Ejection fraction (Q-Lab 9.0, CMQ, Philips Medical System) and to a dedicated software for 3D Strain myocardial deformation analysis (4D LV-Analysis, TOM-TEC, Germany). All 3D images were acquired in the beginning of the study and repeated in 38 patients after 1 hour of the first acquisition to provide measures of reproducibility for inter-observer and test-re test variability.

3.5.6.2.1. Left Ventricle Volumetric Acquisition

Frames for end-diastolic and end systolic volumes were identified by the same method as for 2-D echocardiography. Contour tracing was performed with semi-automatic border detection after first identifying the apex and mitral annulus, a pre-configured ellipse was fitted to the endocardial borders of each frame and adjusted as required. All examinations were performed by the same operator (I.Z.C.).

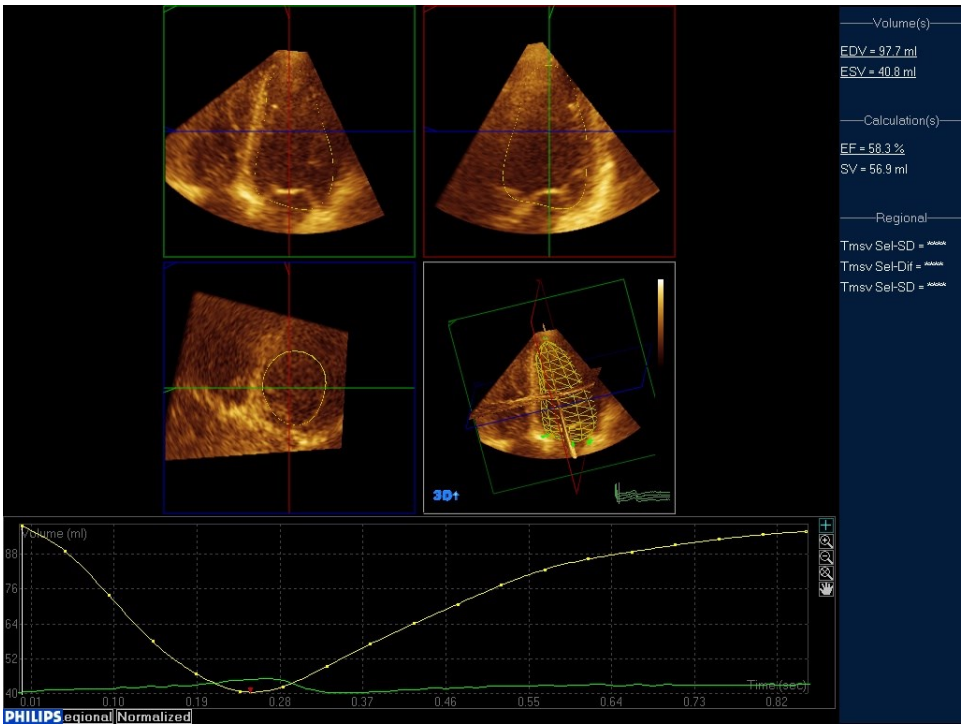

Fig. 3.6: 3D LV echocardiographic image, slice plane view with global volume curve display.

3.5.6.2.2. Right Ventricle Volumetric Acquisition

Images were acquired from apical four chamber views with the patient in the left decubitus position breath hold. Through careful manipulation and rotation of the probe the optimal projections were obtained. The best window available was used in a modified apical transducer location to centre the RV on the display and the RV lateral wall was visible within sector.

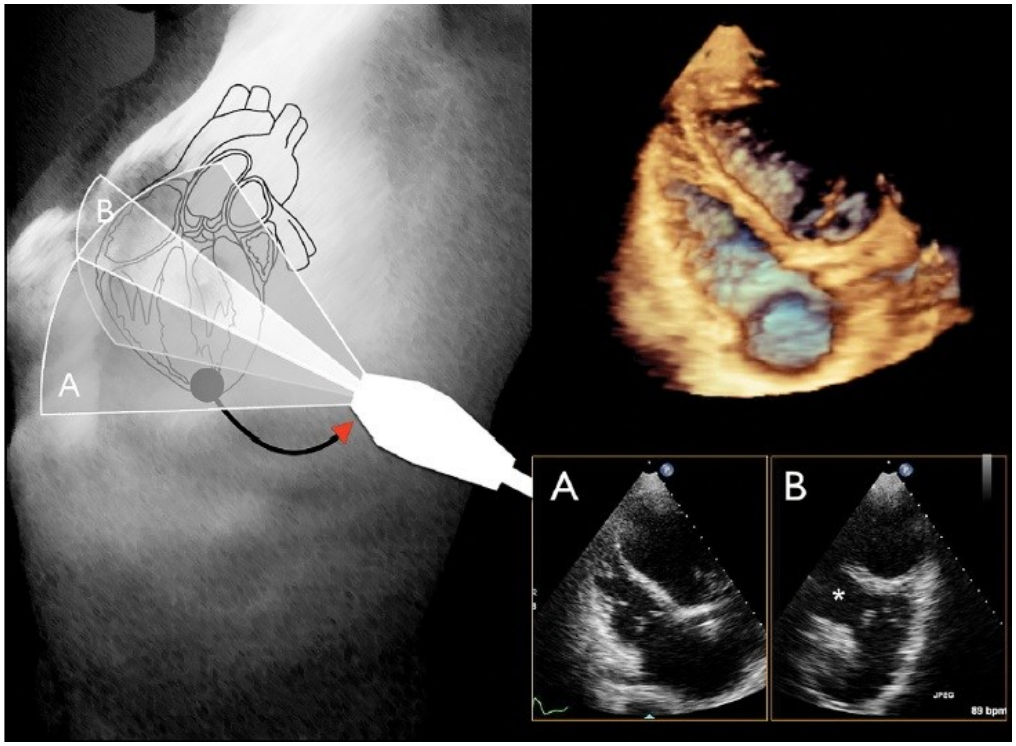

Fig. 3.7: RT3DE imaging of the right ventricle. (Left) For full coverage of the right ventricle by the 3D pyramidal data volume, (Top right) Colour-coded 3D image of the right ventricle. (Bottom right) (A) Modified 4-chamber view of the right ventricle. (B) Corresponding 90_ rotated image with good visualization of the outflow tract (asterisk).

Acquisitions were performed using a modified apical view to enable full coverage of the entire RV by pyramidal volume. Care was taken to the upper anterior Wall and RV outflow tract (Fig.3.7).

The optimisation of the position of the probe was achieved by stepwise 360^{o} rotation of the modified apical view. To obtain the highest possible frame rate, the sector size and depth were set up carefully. The data set was recorded over 4 cardiac cycles and at least 4 data sets were acquired per patient. The data set with the highest quality image was used for analysis.

The 3D data sets were posteriorly analysed offline using a novel dedicated software (4DRV-function CAP1.1; TomTec Imaging Systems, Inc, Unterschleissheim, Germany) and a software platform for data management (Research Arena 2.0; TomTec Imaging Systems, Inc.).

The analyses of the images were peformed as follows (3.8):

Step 1: within the 3D data set, 3 orthogonal main cut planes were selected and the operator defined the end-diastolic and end-systolic frames within the sequence as well as several landmarks.

Step 2: according to the previous view, the program automatically provided 4-chamber, sagittal, and coronal views of the right ventricle. The observer draws the end-diastolic and end-systolic contours manually in each view. In case of suboptimal endocardial visualisation of this region, contours of the RV outflow tract were extrapolated on the basis of the adjacent endocardium with improved visualisation to close the envelope and to advance within the predefined steps of the software. Trabeculations were included in the RV volume.

Step 3: the application defined a dynamic polyhedron model of the right ventricle on the basis of the initial contours. This model is automatically adapted to the endocardial surface of the ventricle over all frames of the cardiac cycle. If necessary, the observer manually corrected the contours

Step 4: finally, the RV analysis display offers the dynamic model and a table with the values of RV volumes and functions

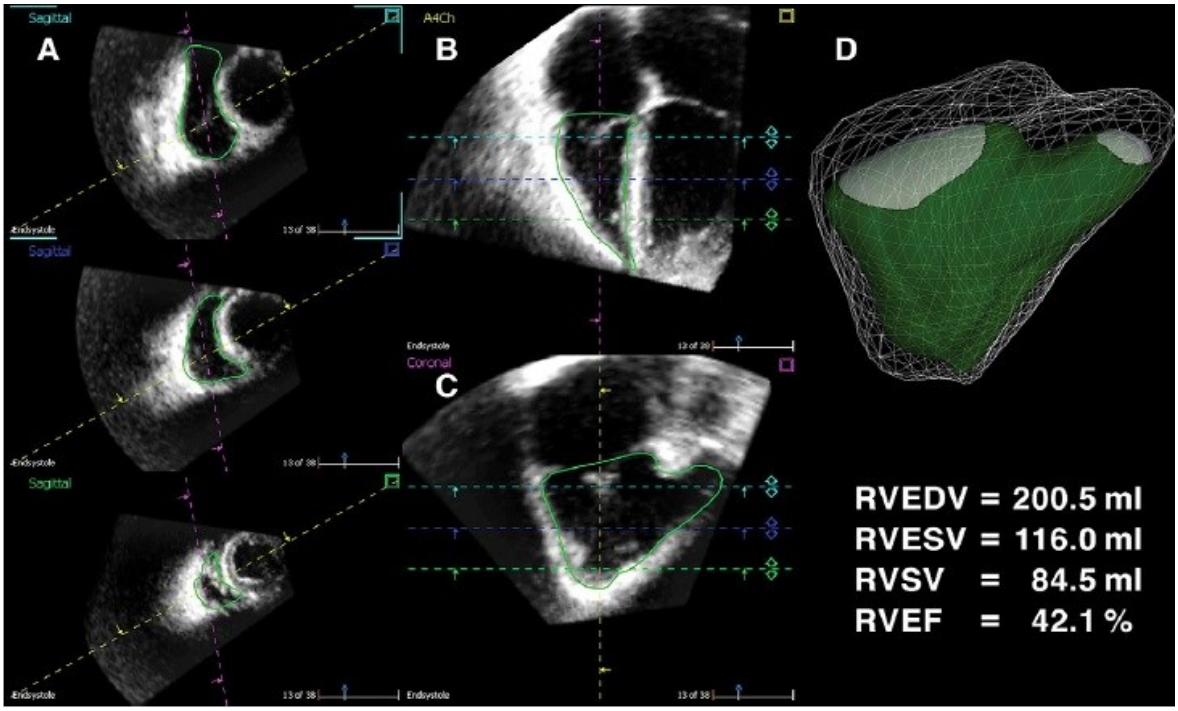

Fig. 3.8: Contour revision and final reconstruction of the dynamic RV polyhedron model of a dilated right ventricle. (A) Three different short-axis views of the right ventricle (base, middle, and apex). (B) Four-chamber view. (C) Coronal view depicting the inflow/outflow tract of the right ventricle. (D) The final reconstruction results in a polyhedron model of the right ventricle. Display of the end-diastolic volume as white polyhedron mesh and the end-systolic volume as green body surface RVEDV, RV end-diastolic volume; RVEF, RV ejection fraction; RVESV, RV end-systolic volume; RVSV, RV stroke volume.

3.5.6.2.3. Left Ventricle 3D Speckle Tracking Imaging

3DT was performed with an X3-1 transducer, Philips IE33 (Philips Medical Systems, Bothell, WA, USA). The 3D data sets were posteriorly analysed offline using a novel dedicated software (4D-LV-analysis 3.0 ; TomTec Imaging Systems, Inc, Unterschleissheim, Germany) and a software platform for data management (Research Arena 2.0; TomTec Imaging Systems, Inc).

Apical full volume acquisition was obtained in all patients to visualize the entire LV in a volumetric image. For acquisitions of a full-volume data set, 4 smaller real-time volumes, acquired from alternate cardiac cycles, are combined to provide a larger pyramidal volume. In this study, a frame rate of 20 to 30 Hz was used. To optimise the frame rate of acquisition, depth was minimised to include only the LV. Data sets were stored digitally for offline analysis.

After the LV long axis was manually aligned in the three apical views (four, three, and two chamber), the software automatically identified the LV endocardial border (Fig.3.9). No foreshortened apical views were identified by finding the largest long-axis dimensions. The LV boundaries were initialised by manually pointing at a small number of anatomic landmarks (mitral annulus and LV apex). In all cases, papillary muscles were included in the LV cavity. Endocardial contours were manually adjusted when necessary to optimise boundary position and tracking. Then, the 3D endocardial surface was automatically reconstructed and tracked in 3D space throughout the cardiac cycle.

The 3D images of the LV wall were automatically divided into 16 segments using standard segmentation. The software automatically tracked the contour on the subsequent frames in 3 different vectors simultaneously to calculate each strain data and resulting in a dynamic cast of the LV cavity. The following parameters of global LV deformation were evaluated: global longitudinal strain (GLS), LV twist and LV torsion. LV twist was calculated as the difference between basal and apical rotation measured in LV short-axis images. To measure basal rotation, the image plane is placed just distal to the mitral annulus and for apical rotation just proximal to the level with luminal closure at end-systole. LV torsion was defined by LV Twist normalized to LV end-diastolic length.

The time curves of the three principal components of segmental myocardial strain, longitudinal, circumferential and radial), as well as the corresponding strain rates were obtained using the standard 16-segment model. In addition, for each segment, a time curve of 3D strain was calculated as the vector sum of the longitudinal and circumferential components. The strain rates values were obtained by calculating the difference between strain values for each two consecutive points and dividing by the time interval as follows: $SR(t) = dS(t)/dt$ (Fig. 3.10).

The peak value of each index was defined as its maximum absolute value with the sign. All time curves were interpolated, resulting in effective temporal resolutions of 150 to 200 samples/sec.

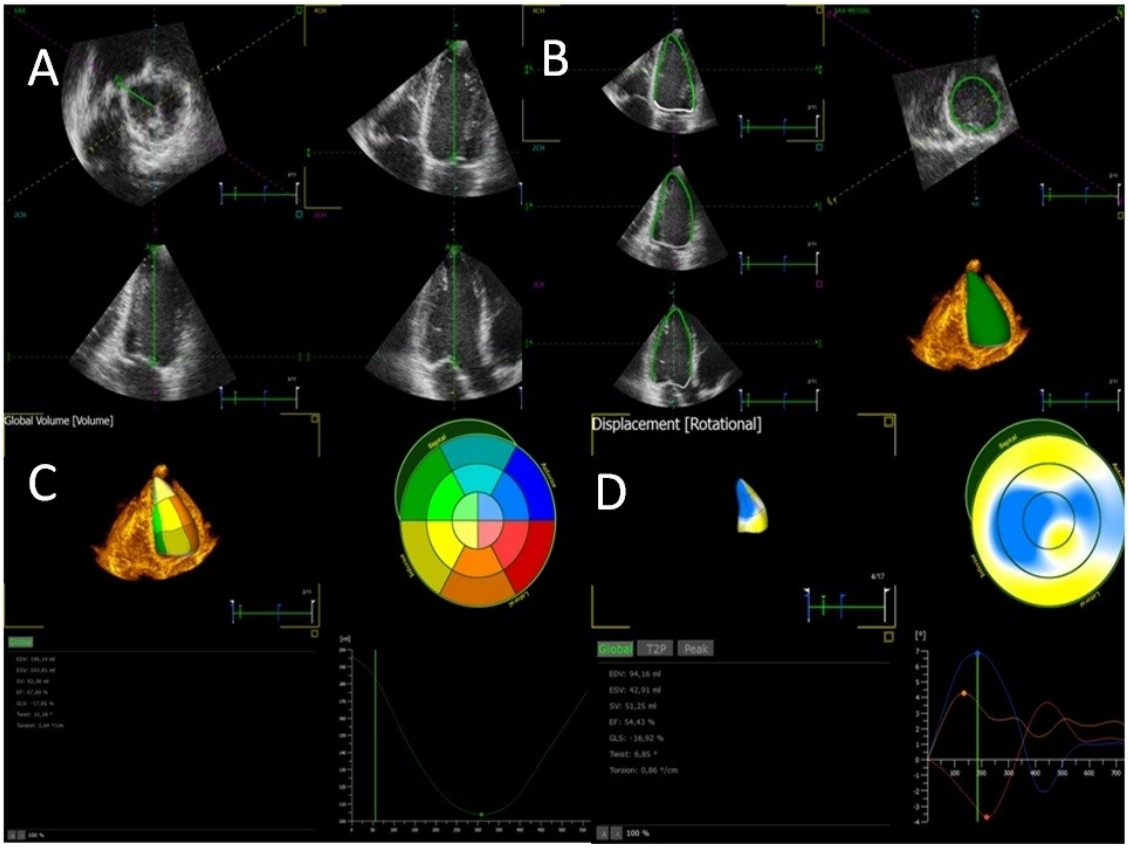

Fig. 3.9: Four dimensional speckle tracking left ventricle analysis. A) Standard long axis views and positioning of the landmarks (mitral valve, apex and aortic orientation). B) Four-, three- and two chamber views with the initialized LV boundaries. The system automatically tracks the complete endocardium. C) LV model with global volume curve. D) LV twist graph display.

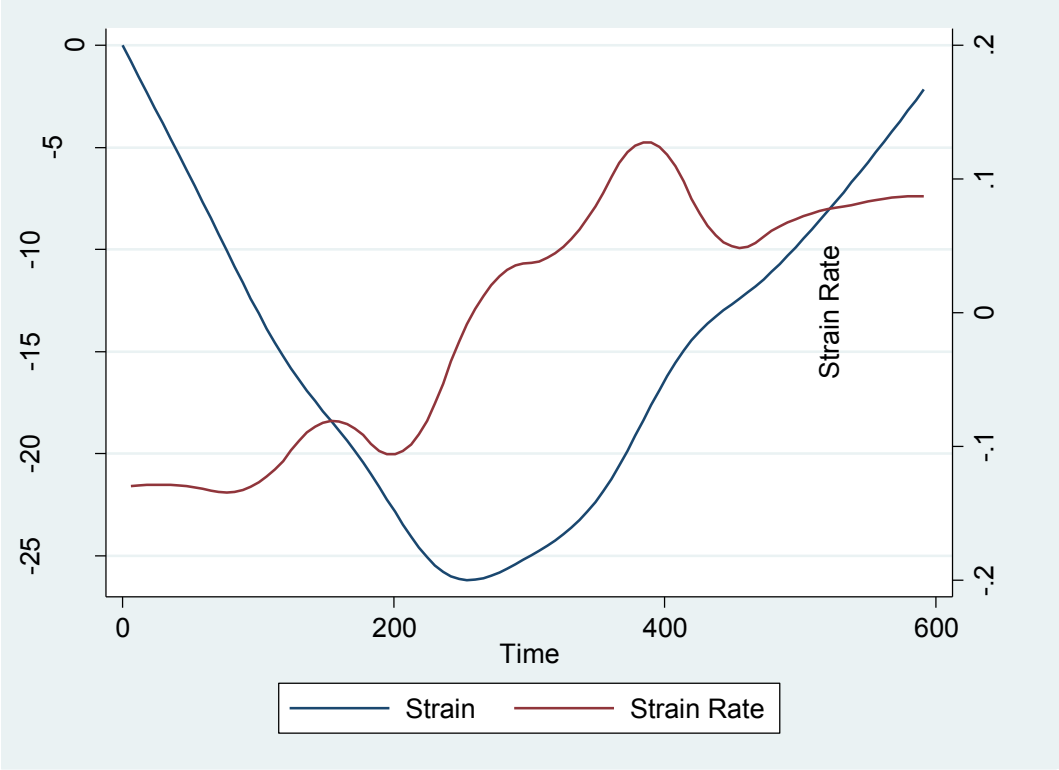

Fig. 3.10: Examples of strain (blue line, primary y axes) and the corresponding strain rate (red line, secondary y axes) over time throughout the cardiac cycle obtained in a patient with sickle cell disease.

3.5.6.3. Reproducibility

The reproducibility of the 2DE and RT3DE strain measurements was evaluated by calculating the intra- and inter-observer variability of both techniques. Analysis of the 2DE and RT3DE images obtained in all patients was repeated 2 weeks later by the primary reader and by an additional expert reader, who were both blinded to the previous measurements and the CMR-derived volumes when appropriate.
Intra- and inter-observer variability was assessed for each technique by calculating the absolute difference between the corresponding repeated measurements, which was also expressed in per cent of their mean. Absolute differences between repeated measurements were subjected to Bland–Altman analysis.

In addition, the inter- examination variability of the RT3DE technique for LV Strain data and RV Volumes was studied by repeating image acquisition 1 hour later in a group of 40 patients selected at random.

3.6. Cardiac magnetic resonance acquisitions

3.6.1. Protocol overview

Cardiac magnetic resonance was performed in the group of patients with LV diastolic dysfunction (Group A2). All acquisitions were obtained by the same radiologist at consultant level, expert in CMR imaging using a 1.5T Philips Achieva system (Best, Netherlands). A 32-element cardiac phased-array coil was used for signal reception. A retrospective cardiac gating was achieved with a vector-ECG system.
Coil sensitivity based uniformity correction was performed to correct signal variation within the heart (Bydder et al., 2002). Cine balanced steady-state free precession images used the following parameters: field of view, 320×320 mm; matrix, 160×151; repetition time, 3.0 ms; echo time, 1.5 ms; in-plane resolution,2.0×2.2 mm; number of cardiac phases, 30; section thickness, 8 mm. Myocardial oedema was imaged with a navigator-gated black blood T2-weighted turbo spin echo sequence with spectrally selective inversion recovery fat suppression using the following parameters: field of view, 350×280 mm; matrix, 256×123; repetition time 2 R–R intervals; echo time, 100

ms; in-plane resolution, 1.4×2.3 mm; section thickness, 8 mm. Strain mapping was performed using a grid pattern of tag lines (complementary spatial modulation of magnetisation (Fischer et al., 1993) with the following parameters: field of view, 350×350 mm; matrix, 144×144; repetition time, 30 ms; echotime, 2.2 ms; in-plane resolution, 2.4×2.4 mm; section thickness, 8 mm; tag line spacing, 7 mm. An intravenous bolus of gadobutrol 1.0 mmol/mL (Gadovist; Bayer Schering Pharma, Berlin, Germany) was administered at a dose of 0.15 mmol/kg. Early enhancement imaging was performed to assess microvascular obstruction with a single breath hold 3D inversion recovery gradient echo sequence within 1 min of contrast medium injection using the following parameters: field of view, 350×290 mm; matrix, 252×135; repetition time, 4.4 ms; echo time, 1.3 ms; inversion time, 400 ms; in-plane resolution, 1.4×2.1 mm; section thickness, 8 mm. LGE imaging was performed to assess necrosis after a 10-min delay with a 2D inversion recovery gradient echo sequence using the following parameters: field of view, 320×320 mm; matrix, 200×147; repetition time, 5.5 ms; echo time, 2.5 ms; in-plane resolution,1.6×2.2 mm; section thickness, 8 mm.

Contraindications to CMR were as follows:

- Pregnancy: Pregnant women were excluded as were women who planned to become pregnant during the menstrual cycle of the CMR study. We also excluded women who had no effective measure of birth control.
- Mental handicap, incompetence or confusion
- Cardiac pacemaker
- Mechanical heart valve
- Intra-ocular foreign body
- Orthopaedic implant within 8 weeks
- Surgical clips in the brain
- Intrauterine contraceptive devices
- Vascular stents (these were assessed on a case by case basis)
- Surgical clips in the body (these were assessed on a case by case basis)
- Intolerance of confined spaces
- Inability to lie supine for 60 minutes

- Clinical instability
- Significant arrhythmias

3.6.2. Magnetic resonance image analysis

Analyses of the MRI data sets were performed with the system implemented standard software (Philips View Forum R.4.1.) by an experienced observer who is blinded to patient details and to the results of existing examinations.

Axial slices of the RV from base to apex were planned from horizontal and vertical long axis images of the heart in the plane of the atrioventricular groove (short axis) (Fig.3.11). At the basal slice, non-trabeculated atrium was excluded from the RV cavity measurement (Lorenz et al., 1999) (Pattynama et al., 1995)

Image window and level settings were individually adjusted for each examination to achieve the best contrast between the myocardium and blood as well as adjacent pericardial tissue. All analysis was performed by an investigator experienced in the interpretation of CMR images (with level III accreditation) who was not aware of the echocardiographic measurements.

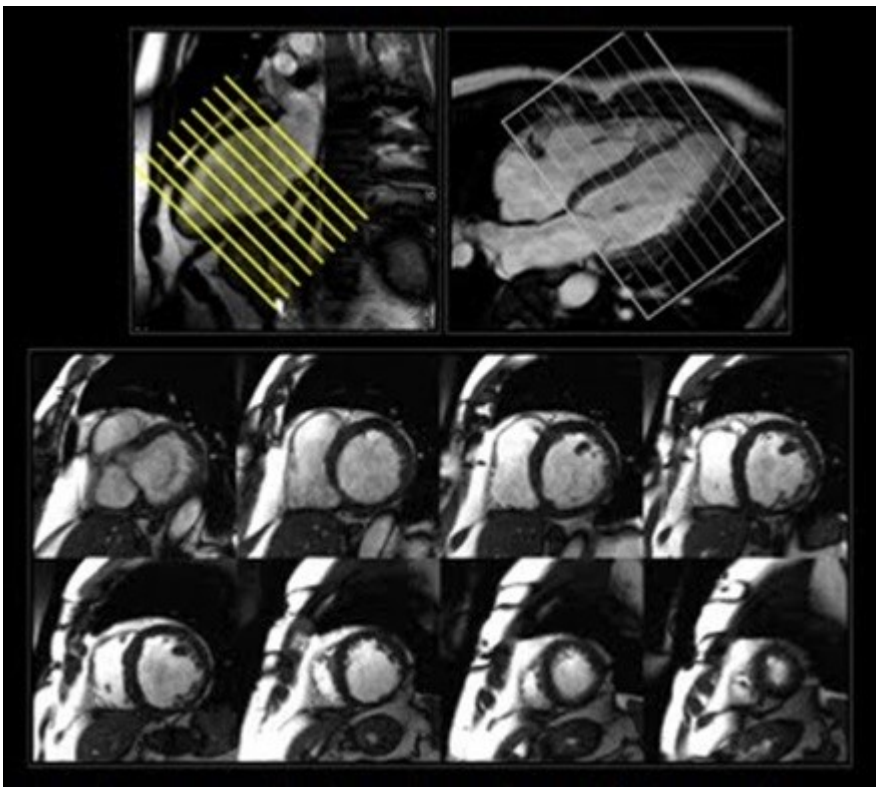

Fig. 3.11: CMR short-axis view. The plane is cut perpendicular to long axis on 2C view, and parallel to atrial-ventricular valves (between anterior & posterior groves) and almost perpendicular to interventricular septum on 4C views.

3.6.3. Left ventricular function and volumetric assessment

The endocardial and epicardial borders were traced semi-automatically at both end-diastole and end-systole on short-axis cine images and were then corrected manually at the base of the heart. Corrections to other images were allowed if visual inspection revealed obviously incorrect borders. The papillary muscles were included in the blood pool and excluded from the LV mass measurement. All image contours were checked by a cardiac MR physician after contouring was finished by the technologist.

LV end-diastolic volume and LV end-systolic volume were calculated using Simpson's rule (the summation of areas on each separate slice multiplied by the sum of slice thickness and image gap) in order to follow the same protocol as with echocardiography. LV mass was determined by the sum of the myocardial area (the difference between endocardial and epicardial contour) times slice thickness plus image gap in the end-diastolic phase multiplied by the specific gravity of myocardium (1.05 g/mL).

3.6.4. Right ventricular function and volumetric assessment

Assessment of the RV volumes/mass was performed using steady state free precession techniques. Imaging parameters were: repetition time/echo time of 3.4/1.7 ms, in-plane pixel size of 2.3 × 1.4 mm, section thickness of 8.0 mm, flip angle of 70º, and acquisition time of 12 heartbeats. Breath-hold scout images and subsequent vertical and horizontal long-axis cine images were initially acquired. Short-axis sequential slices were piloted from these, starting from the atrioventricular ring, covering both ventricles to beyond the apex.

Manual delineation was used to generate areas for RV endocardium and epicardium in end-diastole and endocardium in end-systole. These time points were defined by the largest and smallest endocardial areas. The method of disk summation was then employed to provide volumetric and mass data for the RV. Trabeculations were not included in the RV myocardium and they were included in blood pool.

3.6.5. Myocardial tagging

Tagging is created from the QRS complex detection of the electrocardiogram. Myocardial motion is followed during the cardiac cycle, thus reflecting the underlying myocardial deformation. However, fading of the tag lines close to end-diastole, as a result of T1 tissue relaxation, has limited its application to the systolic part of the cardiac cycle. Although spoiled gradient echo imaging is the commonly used sequence for tag generation at the widely available 1.5T magnets, recent studies have proposed implementing steady state free precession to achieve better contrast and longer tag persistence. Using high field strength magnets for tagging acquisition may also reduce the problem of tag fading. In fact, despite the potential increase in susceptibility effects during cardiac imaging, applying myocardial tagging at higher field strength appears to provide a better contrast to noise ratio as well as improve tag persistence (Fig.3.12).

Strain calculations were performed at LV mid-level (short-axis) using harmonic phase analysis (Harmonic phase analysis, Diagnosoft, NC, USA) (Osman et al., 1999). Peak Eulerian circumferential (Ecc) strain (midwall, transmural, epicardial and endocardial) was measured and an Ecc of greater than −15 % was considered as dysfunctional (Fig.3.13) (O'Regan et al., 2013).

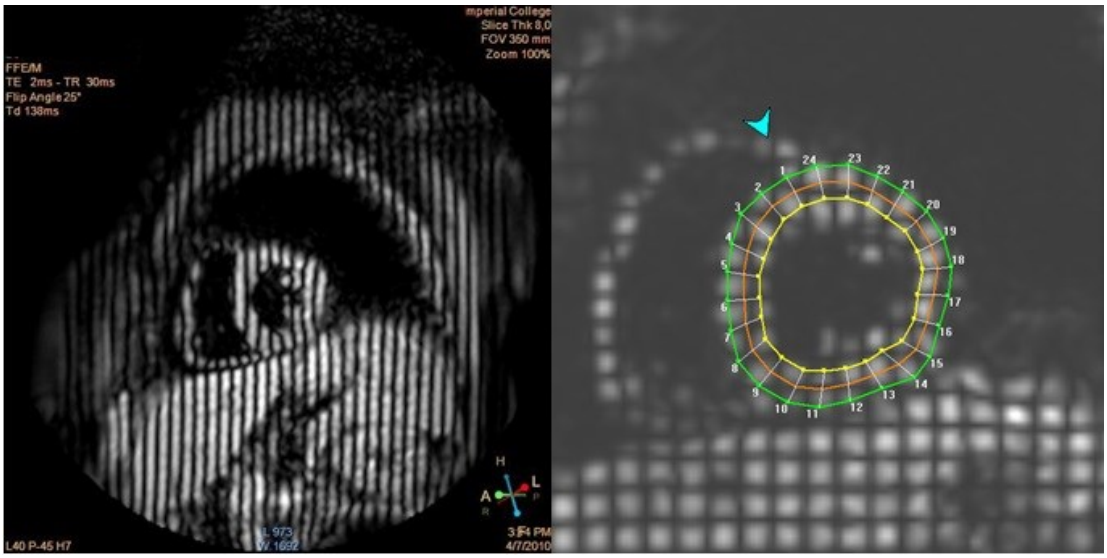

Fig. 3.12: (Left) Parallel tags on a systolic spin-echo ECG gated image in the four-chamber plane. (Right). Short axis tagging at the mid ventricular level, tagging is applied upon detection of QRS complex at end diastole. Tag lines follow the myocardial deformation during systole; a mesh model derived from manually segmented myocardium surfaces is represented.

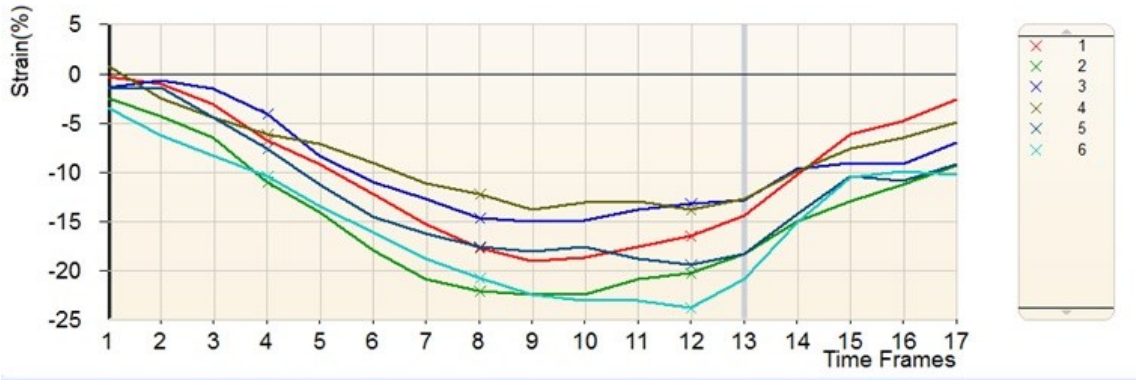

Fig. 3.13: Circumferential Strain curves from 6 segments, obtained from myocardial tagging.

3.7. Statistical Analysis

Data processing

Data were entered in Excel spreadsheets prior to statistical analysis and SPSS v20.00 (SPSS, Inc., Chicago, IL) was used for the analysis.

Power calculation

The PS power and sample size windows based calculator was used to calculate sample size and/or power.

Power is normally set at a modest 80 %. Since power is the chance of rejecting the null hypothesis when it is indeed false, as it increases, the chance of making a mistake decreases. Increasing sample size often means a better more powerful analysis but other factors such as the magnitude of difference (which can be obtained from previous similar studies), the frequency of the event amongst controls, variability of the observations and the ratio of controls to cases are also taken into consideration. The purpose of a power analysis is to find an appropriate balance among these factors by taking into account the substantive goals of the study, and the resources available to the researcher.

Sample size was determined regarding the evaluation of left ventricular diastolic function in pediatric sickle cell disease patients. According to Zilberman (Zilberman et

al., 2007) we would need a total of 60 patients to detect a difference of 1.8 on E/Ea ratio for the assessment of diastolic dysfunction, where the SD in each group is 2 with power of 80% using an unpaired 2 sample t-test at significance level 5%.

Data presentation and analysis

Data are presented as absolute numbers, percentages, mean (±standard deviation, SD), or median and interquartile range. The continuous variables were assessed for normality. The best transformation was then used to change to a normal distribution. The student t-test and the Kruskal-Wallis test (whichever was appropriate) were used to compare continuous variables between patients with SCD and control subjects, and the Pearson Chi square test and the Man-Whitney test was used to compare dichotomous variables Stepwise linear regression.Pearson and Spearman rank correlation was used to assess the relationship between echocardiogram parameters and clinical variables in patients with SCD. Group comparisons between a continuous and a dichotomous variable were evaluated using the Wilcoxon rank-sum test. Logistic regression was used for evaluating the ability of LV E/E´ to identify increased TRV. The diagnostic use of LV E/E´ was assessed through the use of receiver operating characteristic (ROC) curve. Multiple linear regression modelling was used to identify sets of independent variables that were associated with increased elevated E/E´ratio and predictors of increased pulmonary pressures. This modelling used a stepwise procedure in which a potential independent variable was considered if it had a p value <0.10 for bivariate association with TRV; the final model included variables with p≤ 0.05 in multiple regression. Multiple regression using ranks for all variables was used to confirm the most important correlates.
Multiple linear regression modeling is going to be used to identify sets of variables that are independently associated.

Due to the large number of comparisons there was an increased risk of finding significant results due to chance. As a result the level of statistical significance was reduced from 5% to 1%, consequently, p-values of less than 0.01 were considered to be statistically significant. Cox regression analyses identified prognostic predictors. Variables were removed at p>0.10.

For comparison of the difference in values between the screening and follow-up timepoints the normality of the changes from screening to follow-up were examined. Where the changes over time were approximately normally distributed, the paired t-test was used to compare the two set of measurements. Where the changes were not normally distributed, the Wilcoxon matched-pairs test was used instead.
Binary variables were compared between timepoints using the paired exact test. Categorical variables with more than two categories were analysed using the McNemar-Bowker test.

Reproducibility study

Inter-observer and intra-observer variability of the echocardiographic measurements was assessed by calculating the standard deviation of the differences between measurements of the volumes performed by two independent observers blinded to the results achieved by the other observer. One observer (I.Z.C.) analysed all of the images twice, leaving at least a one week gap and blinded to the previous results, providing intra-observer variability.

The study of reproducibility index between the measurements of intra-observer and inter-observer was done using the Altman and Bland method for calculation of limits of agreement. (Bland and Altman, 1986).

TEST re-test of LV 3D Strain analysis

Repeatability of the echocardiographic parameters (Test re-test) were done using the intra class correlation coefficient. All LV 3D strain outcomes were measured on a continuous scale. Two methods of analyses, were used to assess the agreement between the test and re-test values.

The first method of agreement used was the Bland-Altman limits of agreement method. This method measures, in real terms, the size of differences between test and re-test values on the same patients that are likely to occur.

The measure is obtained by first calculating the difference between the two values for each patient. The 95% limits of agreement (within which 95% of all differences between values should occur) are then calculated as follows:

Mean difference +/- 1.96*(standard deviation of differences)

Clinical judgement were required to decide whether the level of differences between the pairs of measurements is acceptable or not.

The second method of agreement was the intra-class correlation (ICC) method. This method involves splitting the total variation in the data into two sources, variation between patients, and variation within patients (i.e. variation between the test and re-test values for the same patient). The ICC is the proportion of the total variation that is between patients. If there is good agreement, there should be very little within patient variability, and so most variability should between patients, and thus the ICC values should be close to 1.

Two different analyses of the strain variables were produced. Initially the mean value of each of the 16 segments was calculated, and only this mean value was analysed. Subsequently, the agreement between the results of individual segments were analysed.

All calculations were performed with SPSS 20.0 (SPSS, Inc., Chicago, IL).

Chapter 4: Study Results

Chapter 4 Study results

4. Study subjects characterisation: general overview

The population studied in the prospective study included two groups of subjects: a group of patients with SCD and a group of healthy volunteers (race, age and sex matched). The 2 groups were comparable for the main traditionally cardiovascular risk factors. Eleven patients who were invited to participate in the study were not recruited The reasons were due to: recent hospitalization or SCD crisis (2), failure to keep an appointment (5), failure to agree to follow up (2) and no interest in participation in the study (2). Subject's characterisation will be described in the following points.

4.1. Baseline descriptive data of study cohort

4.1.1. Sociodemographics and Clinical characteristics

Of sixty one patients with SCD (55.7% female; mean age 40.22±11.79), the vast majority (96.7%) had *non Hispanic* or *latino* ethnicity. Africa was the most frequent country regarding ancestry (45.9%). Thirty two patients were born in Europe (52.2%), and 18 patients were born in West Africa (29.5%). Regarding the genotype, 44 patients (72.1 %) were Homozygous (HbSS), following HbSC in 15 patients, and representing 24.6% (Fig.4.1). All patients were of black race. Thirty-one patients (51%) were on Class I of the NYHA , twenty four (39%) on class II and six patients (10%) on Class III.

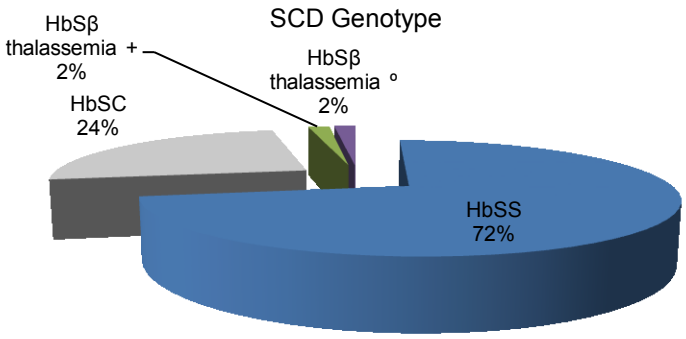

Fig. 4.1. Distribution of SCD genotype in study subjects

Baseline patient demographic characteristics for all 61 patients recruited are detailed in Table 4.1

Table 4.1 - Subjects demographic characteristics of patients.

	All SCD patients N (%)
Gender	
Female	34 (55.7%)
Male	27 (44.3%)
Ethnicity	
Not Hispanic or Latino	59 (96.7%)
Hispanic or Latino	2 (3.3%)
Country of Birth	
Europe	32 (52.5%)
West Africa	18 (29.5%)
West Indies	8 (13.1%)
Central Africa	3 (4.9%)
Sickle Cell Genotype	
HbSS	44 (72.1%)
HbSC	15 (24.6%)
HbSβ thalassemia $^{+}$	1 (1.6%)
HbSβ thalassemia^{o}	1 (1.6%)
NYHA functional class	
Class I	31 (50.8%)
Class II	24 (39.3%)
Class III	6 (9.8%)

The participant's clinical history was collected during the study interview at the screening visit. Nine patients (14.8%) never had a transfusion during their lifetime. Information regarding the patients' clinical history (common SCD complications and related organ disease) is detailed in Table 4.2.

Table 4.2 - Subjects clinical history at screening (data refers to events over lifetime)

Clinical History	N	(%)
Total number of transfusion in lifetime		
0	9	(14.8%)
1-5	23	(37.7%)
6-20	16	(26.2%)
21-100	6	(9.8%)
>100	7	(11.5%)
History of smoking		
None	40	(65.6%)
Former smoker	12	(19.7%)
Current smoker	9	(14.8%)
History of Alcohol		
None	28	(45.9%)
Formerly drank alcohol	4	(6.6%)
Currently drink alcohol	29	(47.5%)
History of drug use		
None	50	(82.0%)
Former drug use	7	(11.5%)
Current drug use	4	(6.6%)
History of Neurologic or Stroke Sequelae Present	1	(1.6%)
Vaso-Occl, Pain Crisis	45	(73.8%)
Leg Ulcers since Screening	20	(32.8%)
Kidney/urinary/genital problems	29	(47.5%)
Liver problems	28	(45.9%)
Spleen problems	23	(37.7%)
Lung Problems	48	(78.7%)
Lung, pneumonia/acute chest syndrome	40	(65.6%)
Lung, pulmonary embolism	2	(3.3%)
Lung, pulmonary hypertension	9	(14.8%)
Heart problems	28	(45.9%)
Splenomegaly	1	(1.6%)
Hepatomegaly	10	(16.4%)
Gastrointestinal, other	9	(14.8%)
Neurological problems	31	(50.8%)
Blood problems, other than sickle cell	10	(16.4%)
Infections	9	(14.8%)
Other diseases/aliments	30	(49.2%)

The baseline clinical characteristics of the 61 patients and the 42 age and sex matched black control subjects are summarised in Table 4.3. The median age of the SCD patients was 40.2 years (range 18–72 years) where 34 were female (55.7%) and the mean BMI was 24.34 mmHg (range 18.39-33.38). Forty two healthy volunteers (mean age 37.8±11.5 years; range, 19–71 years) were included in the study. Significant differences between patients and healthy volunteers were observed regarding the weight, body surface area, body mass index and systolic blood pressure. Compared with controls, subjects with SCD had lower systolic blood pressures, lower body weight and higher body mass index. We found no significant difference in heart rate between SCD patients

and control patients, despite the fact that, as expected, haemoglobin levels were decreased in SCD patients.

Table 4.3 - Baseline clinical characteristics of patients versus healthy.

Labels	Sickle Cell Patients					Healthy volunteers					*P value* *
	N	Mean ± SD	Min	Max	99%CI	N	Mean ± SD	Min	Max	99%CI	
Demographics											
Female (%)	61	55.70	*na*	*na*	*na*	42	52.40	*na*	*na*	*na*	0.73
Age(years)	61	40.2 ± 11.8	18.4	72.0	36.2 - 44.2	42	37.9 ± 11.6	19.0	71.0	33.0 - 42.7	0.32
Height (cm)	61	168.8 ± 9.8	151.0	192.0	165.5 - 172.2	42	1.7 ± 0.1	1.5	1.9	1.6 - 1.7	0.54
Weight (kg)	61	69.2 ± 10.8	50.6	93.5	65.6 - 72.9	42	75.8 ± 13.9	45.0	110.9	70.0 - 81.6	**0.01**
Body surface area	61	1.8 ± 0.2	1.5	2.2	1.7 - 1.9	42	1.9 ± 0.2	1.4	2.2	1.8 - 2.0	0.04
Body Mass Index (kg/m^2)	61	24.3 ± 3.6	18.4	33.4	23.1 - 25.6	42	22.6 ± 4.3	14.0	36.2	20.9 - 24.4	**0.02**
Heart rate (bpm)	61	76.0 ± 10.1	56.0	109.0	72.6 - 79.4	42	70.7 ± 10.5	47.0	96.0	66.3 - 75.1	0.12
Oxygen saturation on air (%)	61	97.2 ± 3.4	84.0	100.0	96.0 - 98.4	42	98.4 ± 1.6	94.0	100.0	97.9 - 98.9	0.16
Systolic BP (mmHg)	61	119.1 ± 14.3	93.0	163.0	114.2 - 123.9	42	124.4 ± 15.2	96.0	169.0	118.1 - 130.8	**0.04**
Diastolic BP (mmHg)	61	70.4 ± 11.4	43.0	98.0	66.5 - 74.3	42	75.5 ± 8.9	59.0	108.0	72.8 - 78.3	0.16

*Two-sided P values for continuous variables were calculated with the use of the t-test and and P values for categorical variables were calculated with the use of Mann-Whitney U test. BP: blood pressure.

4.1.2. Medication at screening

The patients' history of medication use is detailed in Table 4.4. Fourteen patients (23%) were receiving hydroxyurea therapy. Fifty nine patients (96.7%) were on folic acid and 54 patients (88.5%) were on treatment with penicillin (prophylactic) or other antibiotics. Only 2 patients (3.3%) were on chronic transfusion therapy at the time of the study.

Table 4.4 - Patient's medication at Screening.

Medication	N (%)
Anticooagulants	
Past	14 (23.0%)
Current	3 (4.9%)
Anticonvulsants	
Past	2 (3.3%)
Current	0 (0.0%)
Antidepressants	
Past	3 (4.9%)
Current	2 (3.3%)
Erythropoietin/darbopoietin	
Past	1 (1.6%)
Current	0 (0.0%)
Folic Acid	
Past	1 (1.6%)
Current	59 (96.7%)
Hydroxyurea	
Past	7 (11.5%)
Current	14 (23.0%)
Hydroxyurea, Cumulative	
Never	40 (65.6%)
< 1 Year	10 (16.4%)
1-5 Years	5 (8.2%)
> 5 Years	6 (9.8%)
Inhalers	
Past	6 (9.8%)
Current	8 (13.1%)
Iron Chelation therapy	
Past	5 (8.2%)
Current	1 (1.6%)
Oxygen at home	
Past	2 (3.3%)
Current	4 (6.6%)

Medication (Cont.)	N (%)
Prophylactic penicillin or other antibiot	
Past	1 (1.6%)
Current	54 (88.5%)
NSAIDS	
Past	5 (8.2%)
Current	4 (6.6%)
Other Pain Medications	
Past	1 (1.6%)
Current	8 (13.1%)
PDE-5 inhibitor	
Past	1 (1.6%)
Current	2 (3.3%)
Ace inhibitors	
Past	2 (3.3%)
Beta Blockers	
Past	1 (1.6%)
Current	2 (3.3%)
Calcium Chanel Blockers	
Past	6 (9.8%)
Diuretics	
Past	2 (3.3%)
Vasodilators	
Current	0 (0.0%)
Pulmonary Hypertension, Other, Specify	
aspirin (for transient ischemic attack)	1 (1.6%)
digoxin	1 (1.6%)
irbesartan	1 (1.6%)
losartan	2 (3.3%)
pulmicort inhaler	1 (1.6%)
On chronic transfusion therapy	2 (3.3%)
Type Simple	26 0.426
Type Exchange	26 (42.6%)

4.1.1. Laboratory results and 6 minute walking test

Among subjects with SCD, the mean hemoglobin was 9.14 g/dL (range 6-14 g/dL), the red blood cell count was 3.09 x10^6/U (range 1.72-5.06). The reticulocyte count is increased with a mean of 8.66 (%) (range 1.60 -21.9). ProBNP was abnormal in 9 patients (15%). Full haematological and biochemical characteristics of all patients are presented in table 4.5.

Pro-BNP measured at screening, was considered elevated (≥ 160 pg/ml) in 9 patients (15%). Lactate dehydrogenase (LDH) mean was 414.85 IU/L (range 167 -1323) and the mean 6 minute walking test distance was 406.4 meters (range 180 -615 meters).

Table 4.5 - Patients baseline clinical characteristics: laboratory tests and 6MW test.

Variables	Sickle Cell Patients				
	N	Mean ± SD	Min	Máx	99% CI
Full blood count					
Absolute neutrophil count	59	4.83 ± 2.69	1.90	17.30	(3.90 - 5.77)
Absolute Reticulocyte Count (x10^3 cells/uL)	60	238.81 ± 108.64	42.90	456.90	(201.48 - 276.14)
Hematocrit (SI units)	59	0.26 ± 0.05	0.16	0.38	(0.24 - 0.28)
Haemoglobin(g/dl)	60	9.14 ± 1.73	6.00	14.10	(8.55 - 9.74)
Mean cell hemoglobin concentration (g/L)	60	352.12 ± 13.30	317.00	382.00	(347.55 - 356.69)
Mean cell volume (fl)	60	86.89 ± 14.48	57.70	122.90	(81.92 - 91.87)
Neutrophils (%)	16	55.30 ± 9.52	40.40	76.50	(48.28 - 62.31)
Platelet count (x10^3 cells/ul)	60	331.47 ± 171.64	86.00	936.00	(272.49 - 390.45)
Red cell distribution width (%)	58	19.95 ± 3.30	14.20	26.60	(18.79 - 21.10)
Red blood count (x10^6/ul)	60	3.09 ± 0.88	1.72	5.06	(2.79 - 3.40)
Reticulocytes (%)	60	8.66 ± 5.05	1.60	21.90	(6.92 - 10.39)
White blood cell count (x10^3 cells/ul)	60	9.02 ± 3.76	3.20	22.80	(7.73 - 10.31)
Mean corpuscular haemoglobin (pg)	59	35.26 ± 1.54	31.70	42.00	(34.73 - 35.80)
Laboratory tests and 6MW test					
Chemistry Albumin (g/L)	58	41.69 ± 3.10	34.00	48.00	(40.61 - 42.77)
Alkaline Phosphatase (U/L)	58	100.34 ± 61.13	30.00	403.00	(78.95 - 121.74)
Alanine aminotransferase	58	24.98 ± 17.84	7.00	92.00	(18.74 - 31.22)
Aspartate aminotransferase (u/l)	57	40.95 ± 23.75	14.00	131.00	(32.56 - 49.34)
Blood urea nitrogen (mmol/L)	60	4.02 ± 3.07	0.90	23.00	(2.97 - 5.08)
Calcium (mmol/L)	55	2.32 ± 0.08	2.13	2.51	(2.29 - 2.35)
Chloride	60	106.97 ± 2.48	99.00	115.00	(106.11 - 107.82)
Bicarbonate (mmol/L)	58	20.48 ± 2.28	15.00	25.00	(19.68 - 21.28)
Creatinine (umol/l)	60	70.65 ± 28.01	29.00	252.00	(61.03 - 80.27)
Lactate dehydrogenase (IU/l)	53	414.85 ± 211.40	167.00	1323.00	(337.21 - 492.49)
Magnesium (si units)	59	0.86 ± 0.07	0.71	1.03	(0.83 - 0.88)
Phosphate (SI)	54	1.18 ± 0.18	0.74	1.73	(1.12 - 1.25)
Potassium (mmol/L)	60	4.44 ± 0.46	3.70	5.90	(4.28 - 4.60)
Albumin/creatinine ratio	40	18.49 ± 34.10	1.00	199.80	(3.89 - 33.09)
Sodium	60	138.43 ± 2.27	134.00	145.00	(137.65 - 139.21)
Total bilirubin (umol/l)	58	47.69 ± 37.15	10.00	171.00	(34.69 - 60.69)
Total protein (SI)	58	78.78 ± 5.29	69.00	95.00	(76.93 - 80.63)
Urea (mmol/l)	49	3.61 ± 1.46	0.90	10.10	(3.05 - 4.17)
ProBNP (pg/ml)	60	118.59 ± 317.35	6.60	2483.00	(9.54 - 227.64)
ProBNP, log 10	60	1.77 ± 0.43	0.82	3.40	(1.63 - 1.92)
6 minute walk total distance (m)	61	406.41 ± 74.29	180.00	615.00	(381.11 - 431.71)

Data are presented as mean±SD

4.1.2. Echocardiography Derived Parameters of Cardiac Structure and Function

4.1.2.1. Right and Left Cardiac Structure

All studied subjects were in sinus rhythm. Measurements of cardiac structure, including LA and RA volumes indexed to BSA, LV mass, endsystolic and end-diastolic volume indexed, were significantly higher in the SCD group compared with the control group. Twenty seven patients (44%) had LV end-diastolic dilation. According to gender, female patients had increased LV volumes, systolic and diastolic, when compared to males. In the group of 33 patients with increased LV mass (indexed to BSA), 42% had concentric hypertrophy and 57% had eccentric hypertrophy defined by the regional left ventricular wall thickness index ≥ 0.41.

Left atrium dilatation was present in 53 patients (87%), where in 34 patients (64%) the dilatation was severe (> 40 ml/m2), in 16 patients (30%) was moderately abnormal and in 3 patients (6%) was mild. Right atrium dilatation was present in 80% of the total patients.

RV end-diastolic and end-systolic areas, as well as RV 3D end-diastolic and end-systolic volumes were larger in the SCD group compared with controls. According to RV 3D volumetric assessment, 28 patients, of the 58 patients where RV volumes were measured (48%), had end-diastolic dilatation (≥101 ml/m2) (Table 4.6).

Table 4.6 – Left ventricular dilatation according to gender in all patients.

Variable	Count	Gender		All Patients
		Female	Male	
LV 2D diastolic volume indexed (ml/m2)				
Reference range (<75)	N (%)	24 (71%)	10 (37%)	34 (56%)
Mildly abnormal (76 - 86)	N (%)	7 (21%)	6 (22%)	13 (21%)
Moderately abnormal (87 - 96)	N (%)	2 (6%)	4 (15%)	6 (10%)
Severely abnormal (>=97)	N (%)	1 (3%)	7 (26%)	8 (13%)
Total	N (%)	34 (100%)	27 (100%)	61 (100%)
LV 2D systolic volume indexed (ml/m2)				
Reference range (12 - 30)	N (%)	28 (82%)	14 (52%)	42 (69%)
Mildly abnormal (31 - 36)	N (%)	5 (15%)	7 (26%)	12 (20%)
Moderately abnormal (37 - 42)	N (%)	1 (3%)	1 (4%)	2 (3%)
Severely abnormal (>=43)	N (%)	0 (0%)	5 (19%)	5 (8%)
Total	N (%)	34 (100%)	27 (100%)	61 (100%)

4.1.2.2. LV and RV Systolic Function.

Parameters of global LV function, including LV ejection fraction and global function index, were normal in both groups. Only 9.8% of patients had evidence of systolic dysfunction with an ejection fraction ≤55%. LV S´ wave septal (cm/s) was significantly different between patients and controls. As expected, the SCD group had greater Doppler-derived LV stroke volumes and cardiac output when compared with healthy volunteers (Table 4.7).

Table 4.7 - Cardiac structure and function in patients with SCD compared with healthy volunteers.

Variable	Patients		Healthy volunteers		Diff. Mean	99% CI of Difference		p-value ŧ
	(N)	Mean ± SD	(N)	Mean ± SD		Lower	Upper	
LV Structure								
LV septum diameter (mm)	61	2.78 ± 11.73	42	9.19 ± 1.38	-6.41	0.00	1.46	0.01
LV posterior wall diameter (mm)	61	10.08 ± 1.62	42	9.45 ± 1.49	0.63	-0.20	1.45	0.05
LV 2D end-diastolic diameter (mm)	61	50.85 ± 6.70	42	44.45 ± 5.39	6.40	3.14	9.66	**<0.001**
LV 2D end-systolic diameter (mm)	61	32.82 ± 5.41	42	29.26 ± 4.70	3.56	0.85	6.26	**0.001**
LV 2D diastolic volume indexed (ml/m2)	61	74.04 ± 21.79	42	49.58 ± 11.61	24.46	15.75	33.18	**<0.001**
LV 2D systolic volume indexed (ml/m2)	61	26.25 ± 10.56	42	17.67 ± 4.53	8.58	4.56	12.58	**<0.001**
LV mass index (g/m2)	53	91.12 ± 29.59	38	51.10 ± 15.20	40.02	27.49	52.57	**<0.001**
RV structure								
RV base to apex diamater (cm)	59	7.62 ± 1.05	42	6.36 ± 0.99	1.27	0.72	1.81	**<0.001**
RV mid diamater (cm)	59	3.17 ± 0.49	41	2.90 ± 0.49	0.27	0.01	0.54	0.01
RV base diameter (cm)	59	3.50 ± 0.58	42	3.33 ± 0.42	0.17	-2.10	1.18	0.46
RV diastolic area apical view (cm2)	61	21.04 ± 5.62	42	16.54 ± 3.86	4.50	1.88	7.12	**<0.001**
RV systolic area apical view (cm2)	61	11.87 ± 3.23	42	10.05 ± 2.36	1.82	0.29	3.35	**0.002**
3D RV end diastolic volume	58	109.93 ± 33.63	32	88.53 ± 18.51	21.40	6.93	35.87	**<0.001**
3D RV end systolic volume	58	49.70 ± 17.55	32	36.48 ± 8.78	13.22	5.90	20.53	**<0.001**
LA/RA structure								
Left atrium volume indexed (ml/m2)	60	44.28 ± 15.20	42	22.75 ± 7.31	21.53	15.58	27.49	**<0.001**
RA volume indexed (ml/m2)	57	37.89 ± 11.82	42	20.11 ± 6.95	17.79	12.80	22.78	**<0.001**
LV systolic function								
Global function index lateral	60	0.98 ± 0.32	41	0.74 ± 0.31	0.24	0.07	0.41	**<0.001**
Global function index septal	60	1.21 ± 0.32	39	1.08 ± 0.32	0.13	-0.04	0.31	0.04
LV 2D Ejection Fraction (%)	61	66.17 ± 7.24	42	63.95 ± 5.36	2.22	-1.22	5.67	0.09
LV 2D cardiac output (L/min)	61	6.35 ± 2.04	41	4.34 ± 0.95	2.01	1.23	2.81	**<0.001**
LV 2D stroke volume (mL)	60	83.42 ± 24.41	41	62.72 ± 14.47	20.70	10.51	30.89	**<0.001**
LV S´ wave lateral (cm/s)	60	9.42 ± 2.30	41	9.34 ± 1.89	0.08	-1.06	1.22	0.85
LV S' wave septal (cm/s)	60	8.28 ± 1.07	39	7.69 ± 0.72	0.59	0.08	1.11	**0.003**
RV systolic function								
Estimated PASP (mmHg)	61	31.84 ± 6.81	38	15.69 ± 1.85	16.15	13.71	18.59	**<0.001**
Pulmonary valve accelaration time (ms)	60	127.82 ± 26.75	42	134.96 ± 23.47	-7.15	-20.59	6.30	0.17
PVR (Woods unit)	52	1.55 ± 0.32	36	1.32 ± 0.20	0.23	0.07	0.39	**<0.001**
RV myocardial performance index by TDI	57	0.34 ± 0.11	42	0.25 ± 0.07	0.09	0.04	0.14	**<0.001**
RV S´wave (cm/s)	61	14.81 ± 2.70	40	12.50 ± 2.39	2.32	0.94	3.70	**<0.001**
Tricuspid annular systolic motion (mm)	60	29.20 ± 5.59	42	24.10 ± 3.81	5.10	2.66	7.55	**<0.001**
RV fractional area change (%)	61	43.21 ± 8.72	42	38.74 ± 7.66	4.47	0.10	8.84	0.01
3D RV Ejection fraction (%)	58	54.90 ± 7.18	32	58.91 ± 4.17	-4.01	-7.16	-0.86	**0.001**
TRV velocity (m/sec)								
TRV screening (m/s)	61	2.54 ± 0.30	38	1.96 ± 0.05	0.58	0.43	0.73	**<0.001**

Parameters of RV systolic function, including RV myocardial performance index by DTI and RV 3D ejection fraction (%), were significantly different between the SCD group and healthy volunteers. Patients with SCD had lower RV EF, increased values of RV tMPI and RV S wave velocity when compared to controls. Tricuspid annular systolic motion was normal in both groups and significantly higher in patients with SCD.

4.1.2.3. Diastolic Function Assessment

Pulsed-wave Doppler–derived transmitral E-wave velocity was higher in subjects with SCD compared with controls. Mitral deceleration time and LV E/A ratio, were similar between the groups, however LV isovolumic relaxation time and LV E/E´ both septal and average values, were increased in the SCD group as seen in Table 4.8.

Comprehensive diastolic assessment using tissue Doppler was available and we have found that the prevalence of diastolic dysfunction in the patients groups was 14 patients (23%) with SCD had mild diastolic dysfunction (Grade I), 4 (7%) had moderate diastolic dysfunction (Grade II), and none had severe diastolic dysfunction, using the current classification guidelines recommended by the American Society of Echocardiography (Nagueh et al., 2009b).

Table 4.8 - Left and right ventricular diastolic function in patients with SCD compared with healthy volunteers.

Variable	Patients		Healthy volunteers		Diff. Mean	99% CI of Difference		p-value ŧ
	(N)	Mean ± SD	(N)	Mean ± SD		Lower	Upper	
LV diastolic function								
LV E wave (cm/s)	61	88.53 ± 14.57	42	73.76 ± 14.04	14.77	7.21	22.33	**<0.001**
LV E/A ratio	55	1.52 ± 0.54	38	1.46 ± 0.37	0.06	-0.16	0.34	0.36
MV deceleration time (ms)	60	201.42 ± 38.93	42	187.90 ± 24.70	13.52	-3.04	30.09	0.03
LV Isovolumic relaxation time (ms)	55	95.00 ± 17.04	38	83.50 ± 15.64	11.5	2.53	20.35	**0.001**
Pulmonary veins a wave duration (ms)	38	113.61 ± 19.86	25	112.64 ± 20.11	0.97	-12.70	14.63	0.85
Pulmonary veins a wave reversal (cm/s)	45	23.76 ± 5.96	26	21.76 ± 4.20	2	-1.52	5.52	0.14
Duration a wave LV	45	118.08 ± 24.59	14	109.00 ± 29.05	9.08	-11.86	30.02	0.25
LV E´ lateral wall	60	11.72 ± 2.88	41	12.11 ± 2.74	-0.39	-1.89	1.12	0.50
LV E/E' lateral	60	7.99 ± 2.36	41	6.46 ± 1.89	1.53	0.37	2.69	**0.001**
MV E´ septal (cm/s)	60	9.26 ± 1.95	40	9.46 ± 2.22	-0.2	-1.30	0.91	0.64
LV E/E´septal	55	9.82 ± 2.10	38	8.08 ± 1.86	1.74	0.62	2.73	**<0.001**
LV E/E´avg	59	8.91 ± 2.00	41	7.33 ± 1.70	1.58	0.58	2.58	**<0.001**
RV diastolic function								
RV E wave (cm/s)	55	47.37 ± 10.50	38	44.66 ± 10.09	2.71	-3.03	8.44	0.22
RV E/A	47	1.53 ± 0.44	40	1.36 ± 0.33	0.16	-0.06	0.39	0.06
RV E´wave (cm/s)	60	12.14 ± 3.46	40	10.94 ± 3.15	1.20	-0.59	2.99	0.08
RV E´/A´	55	1.12 ± 0.45	36	1.25 ± 0.59	-0.12	-0.41	0.16	0.26
RV E/E´	55	4.23 ± 1.71	37	4.30 ± 1.38	-0.07	-0.96	0.82	0.84
RV isovolumic relaxation time (ms)	46	60.26 ± 35.91	34	53.44 ± 22.69	6.82	-11.70	25.34	0.33

Further analysis were performed to characterise LV diastolic function regarding gender and mean age (≤ 40 years and > 40 years) (Nagueh et al., 2009b). No other age groups were possible to be compared due to the characteristics of the studied subjects (only 4 patients were ≥ 60 years and 4 ≤ 20 years).

No differences in LV diastolic parameters were observed regarding both gender, however, as expected, age played an important role as it is detailed in Appendix VI.

Interestingly, the RV E/E´ ratio, a surrogate of RV filling pressures, was not significantly different among subjects with SCD compared with controls, as well as all the other RV parameters for assessing right ventricular diastolic function.

4.1.2. LV Strain quantification by 3D speckle tracking

Forty-three patients were eligible for LV Strain quantification by 3D speckle tracking. The quality tracking was not acceptable in 1197 segments (out of the total 3904 segments analysed), which corresponds to 31 % of non trackable LV strain values.
The mean frame rate of the RT3DE data sets in our study subjects was 18.05±1.65 frames per second in the patients group. The mean analysis duration was 10.5±1.28 minutes in the patients groups, which was significantly higher than in the healthy subjects (8.54±1.30 min).

LV volume time curves had similar general shape in subjects with SCD and healthy volunteers, although measurements of LV diastolic and systolic volumes were significantly different in the two study groups, which was consistent with the findings with 2D echocardiography.

All global LV myocardial strain quantifications (3D, longitudinal, circumferential and radial strain) were preserved in patients with SCD (Table 4.9), with Table 4.9 shows longitudinal, radial, and circumferential components of the 3DSTE-derived strain obtained in patients with SCD and normal subjects. As expected, the shape of the strain curves was similar to that of LV volume curves, with the exception of the radial strain curves which were inverted. Particularly, radial strain was positive throughout the cardiac cycle, reflecting a systolic increase in myocardial thickness, while the longitudinal and circumferential strains were negative reflecting systolic shortening of the ventricle in these two dimensions (Fig. 4.2).

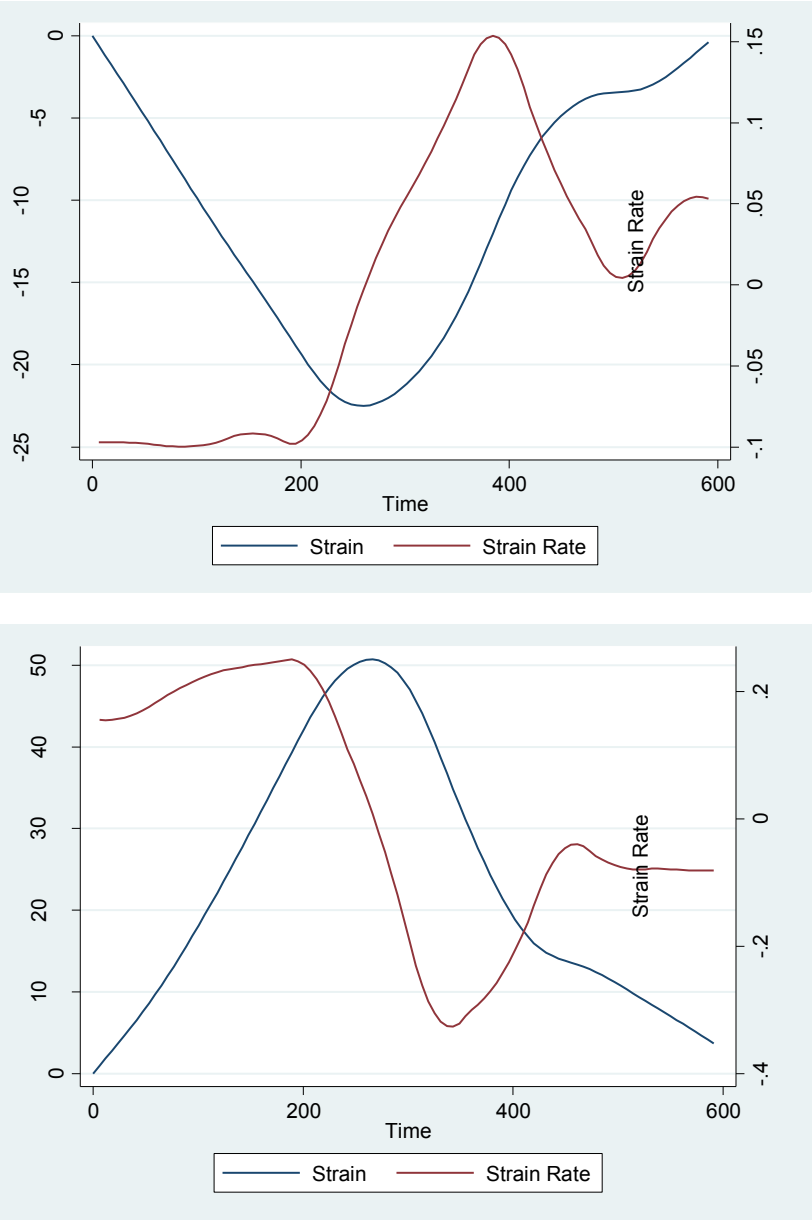

Fig. 4.2 - Examples of time curves of the longitudinal (top) and radial (bottom) components of 3D strain obtained in the same two subjects at the lateral segment (mid-level of the left ventricle).

Considering LV Global longitudinal strain, 10 patients (23%) had decreased values of strain (defined as ≥ -16%). However, no significant difference was found in the mean global strain between the patients with SCD and the normal subjects. Mean values of the 3DSTE-derived indices of LV systolic function also showed no significant differences between the two groups for either twist angle or torsion (Table 4.9). In addition, patients with SCD showed a trend toward an increase in both longitudinal and radial strains. When regional myocardial function was assessed, a significant difference between patients and healthy volunteers was found in LV circumferential median segments and in LV longitudinal basal segments, but both had normal values. A further

analysis concerning the segmental analysis (total of 64 segments) has showed an increase in the mean strain values of 29 segments (45%), when compared to healthy subjects. Nevertheless, only in 5 segments the mean difference was significant (Appendix V). No differences in strain values were observed regarding gender and age (Appendix VI). In addition, further analyses were taken to assess LV strain rate and no significant differences between patients and controls, which may reflect normal LV filling pressure on both groups, were found.

Table 4.9 - 3-Dimensional Strain Indices of Systolic LV Function

Variable	Patients		Healthy volunteers		Diff. Mean	99% CI of Difference		p-value ł
	(N)	Mean ± SD	(N)	Mean ± SD		Lower	Upper	
LV Strain								
3D Frame rate (Hz)	43	18.05 ± 1.65	26	17.23 ± 1.30	0.82	-0.19	1.82	0.04
3D analysis duration (min)	40	10.50 ± 1.28	26	8.54 ± 1.30	1.96	1.10	2.82	**<0.001**
LV 3D end diastolic volume (ml)	43	124.36 ± 39.48	26	96.30 ± 25.36	28.06	5.09	51.04	**0.002**
LV 3D end systolic volume (ml)	43	61.34 ± 22.90	26	46.63 ± 13.13	14.71	1.65	27.76	**0.004**
LV 3D stroke volume (ml)	43	63.02 ± 18.64	26	49.66 ± 13.85	13.36	2.15	24.56	**0.002**
LV 3D ejection fraction (%)	43	51.24 ± 4.96	26	51.52 ± 4.75	-0.28	-3.50	2.93	0.82
Global longitudinal strain (%)	43	-17.81 ± 3.00	26	-17.23 ± 2.77	-0.58	-2.50	1.34	0.43
3D LV strain twist (degree)	43	10.53 ± 6.40	26	10.43 ± 3.97	0.10	-3.60	3.80	0.94
3D LV strain torsion (degree/cm)	43	1.28 ± 0.85	26	1.34 ± 0.56	-0.06	-0.55	0.44	0.76
LV 3D Strain (%)								
Basal segments avg	43	-28.84 ± 3.03	26	-30.05 ± 3.38	1.21	-0.88	3.29	0.13
Median segments avg	43	-34.11 ± 4.91	26	-33.76 ± 3.93	-0.36	-3.36	2.65	0.75
Apical segments avg	43	-35.18 ± 7.26	26	-33.61 ± 5.68	-1.57	-6.00	2.85	0.35
Global (avg of all segments)	43	-32.40 ± 3.83	26	-32.33 ± 3.16	-0.07	-2.44	2.30	0.94
LV Circumferential Strain (CS%)								
Basal segments avg	43	-18.48 ± 3.00	26	-19.22 ± 3.13	0.74	-1.27	2.75	0.33
Median segments avg	43	-26.52 ± 4.87	26	-26.05 ± 4.29	-0.46	3.58	11.77	**<0.001**
Apical segments avg	43	-26.75 ± 7.17	26	-25.44 ± 5.12	-1.31	-5.58	2.96	0.42
Global (avg of all segments)	43	-23.48 ± 3.73	26	-23.38 ± 3.51	-0.10	-2.50	2.31	0.92
LV Longitudinal Strain (%)								
Basal segments avg	43	-17.31 ± 2.83	26	-19.80 ± 2.56	2.49	0.69	4.29	**<0.001**
Median segments avg	43	-18.61 ± 3.42	26	-17.89 ± 2.51	-0.72	-2.77	1.33	0.36
Apical segments avg	43	-18.45 ± 4.01	26	-17.73 ± 4.24	-0.72	-3.41	1.98	0.48
Global (avg of all segments)	43	-18.10 ± 2.79	26	-18.36 ± 2.05	0.26	-1.41	1.94	0.68
LV Radial Strain (%)								
Basal segments avg	43	53.61 ± 9.93	26	55.44 ± 8.67	-1.82	-8.07	4.42	0.44
Median segments avg	43	77.26 ± 20.61	26	71.10 ± 12.16	6.16	-5.64	17.97	0.17
Apical segments avg	43	83.67 ± 31.48	26	72.85 ± 22.23	10.82	-7.87	29.51	0.13
Global (avg of all segments)	43	69.79 ± 15.67	26	65.61 ± 9.99	4.18	-4.93	13.28	0.23
LV 3D Strain Rate (%/ms)								
Basal segments avg	43	-0.19 ± 0.02	26	-0.20 ± 0.04	0.01	-0.01	0.03	0.24
Median segments avg	43	-0.20 ± 0.03	26	-0.20 ± 0.03	-0.01	-0.03	0.01	0.41
Apical segments avg	43	-0.22 ± 0.07	26	-0.20 ± 0.04	-0.03	-0.07	0.01	0.06
Global (avg of all segments)	43	-0.20 ± 0.03	26	-0.20 ± 0.03	-0.01	-0.02	0.01	0.46
LV circumferential Strain Rate (%/ms)								
Basal segments avg	43	-0.11 ± 0.02	26	-0.12 ± 0.02	0.00	-0.01	0.02	0.40
Median segments avg	43	-0.16 ± 0.03	26	-0.16 ± 0.03	-0.01	-0.03	0.01	0.32
Apical segments avg	43	-0.17 ± 0.06	26	-0.15 ± 0.03	-0.02	-0.05	0.01	0.13
Global (avg of all segments)	43	-0.10 ± 0.15	26	-0.10 ± 0.01	0.00	-0.02	0.01	0.23
LV Longitudinal Strain Rate (%/ms)								
Basal segments avg	43	-0.11 ± 0.02	26	-0.11 ± 0.02	0.00	-0.01	0.02	0.67
Median segments avg	43	-0.10 ± 0.02	26	-0.10 ± 0.01	0.00	-0.01	0.01	0.26
Apical segments avg	43	-0.10 ± 0.02	26	-0.09 ± 0.02	-0.01	-0.02	0.01	0.22
Global (avg of all segments)	43	-0.10 ± 0.01	26	-0.10 ± 0.01	0.00	-0.01	0.01	0.42
LV Radial Strain Rate (%/ms)								
Basal segments avg	43	0.30 ± 0.05	26	0.32 ± 0.07	-0.02	-0.06	0.02	0.23
Median segments avg	43	0.44 ± 0.14	26	0.39 ± 0.07	0.04	-0.02	0.11	0.08
Apical segments avg	43	0.55 ± 0.50	26	0.40 ± 0.11	0.14	-0.12	0.41	0.15
Global (avg of all segments)	43	0.41 ± 0.16	26	0.37 ± 0.06	0.04	-0.05	0.13	0.22

ł Two-sided P values for continuous variables were calculated with the use of the t-test

4.1.3. RV Strain quantification by 2D speckle tracking

Data for the assessment RV Longitudinal Strain was obtained in 49 patients out of 61, by 2D speckle tracking and this is summarised in Table 4.10. The quality of tracking was not acceptable in 100 segments (out of the total 366 segments), which corresponds to 27.3 % of non trackable RV strain values.

Table 4.10 - Right ventricular 2-Dimensional Strain.

Variable	Patients		Healthy volunteers		Diff. Mean	99% CI of Difference		p-value ł
	(N)	Mean ± SD	(N)	Mean ± SD		Lower	Upper	
RV 2D Longitudinal strain (Free wall)								
Basal free wall	43	-21.58 ± 7.52	22	-18.59 ± 1.33	-2.99	-6.16	0.18	0.01
Median free wall	44	-24.89 ± 8.89	22	-19.32 ± 2.85	-5.57	-9.49	-1.65	**<0.001**
Apical free wall	43	-24.23 ± 7.89	22	-17.82 ± 3.38	-6.41	-10.14	-2.69	**<0.001**
All free wall segments_avg	49	-23.54 ± 5.33	22	-18.58 ± 1.70	-4.96	-7.20	-2.73	**<0.001**
RV 2D Longitudinal strain (septum)								
Basal septum	42	-13.76 ± 6.67	22	-15.45 ± 4.34	1.69	-2.49	5.88	0.29
Median septum	48	-17.67 ± 5.36	22	-16.45 ± 3.02	-1.21	-4.46	2.04	0.33
Apical septum	46	-15.87 ± 7.48	22	-16.86 ± 3.89	0.99	-2.67	4.66	0.47
All septum segments_avg	49	-15.85 ± 4.83	22	-16.26 ± 3.32	-2.35	-2.23	3.04	0.68
RV Global strain	49	-19.60 ± 4.12	22	-17.25 ± 1.86	-2.35	-4.23	-0.47	**0.001**

ł Two-sided P values for continuous variables were calculated with the use of the t-test. Significant difference between groups when p<0.01

As is shown, RV longitudinal strain was universally increased in all free wall segments (basal, median and apical levels) when compared to healthy subjects. As it can be observed, the RV strain in septum had lower values, however these were not significantly different from those of the healthy subjects. It may be assumed that the interventricular dependence may influence the septum strain assessment, which should be analysed individually.

The results for the RV Global Strain in patients with SCD, were within normal limits, with significant increased values when compared to healthy subjects (mean -19.60±4.12 versus -17.52±1.86) (Fig. 4.3). There was no systematic variation in strain values (mean) between the different RV segments or from base to apex.

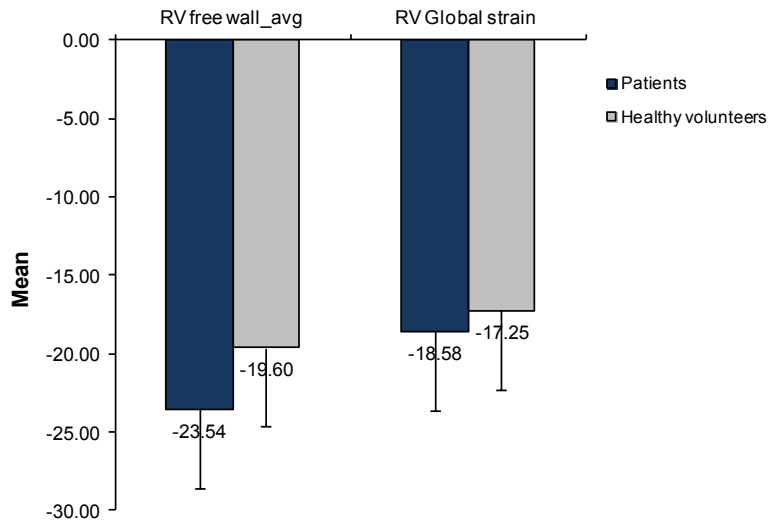

Fig. 4.3 – Mean values of RV free wall strain (average of basal, mid and apical segments) and RV Global strain in patients with SCD and Healthy volunteers.

4.1.4. Tricuspid regurgitant jet velocity

RV systolic pressure was estimated from tricuspid regurgitation peak velocity in all 61 patients and in 38 healthy volunteers. TRV was not detectable in 4 healthy subjects.
In forty eight patients with SCD (78.7%), tricuspid regurgitation was graded as mild and in 13 patients (21.3%) was graded as trace tricuspid regurgitation. Regarding other valves, 9 patients (14.8%) had mild mitral regurgitation, 1 patient (1.6%) had mild aortic regurgitation and 4 patients (6.6%) had mild pulmonary regurgitation. Distribution of patients according to TRV and NYHA functional class was as follows:

Table 4.11 – Distribution of TRV groups according to NYHA functional class.

		NYHA at screening			Mann-Whitney U test	
TRV Group	N	Class I n=31	Class II n=24	Class III n=6	Test	P-value
< 2.5 m/s	30	19 (63%)	11 (37%)	0 (0%)	317,5	0,018
>= 2.5 m/s	31	12 (39%)	13 (42%)	6 (19%)		

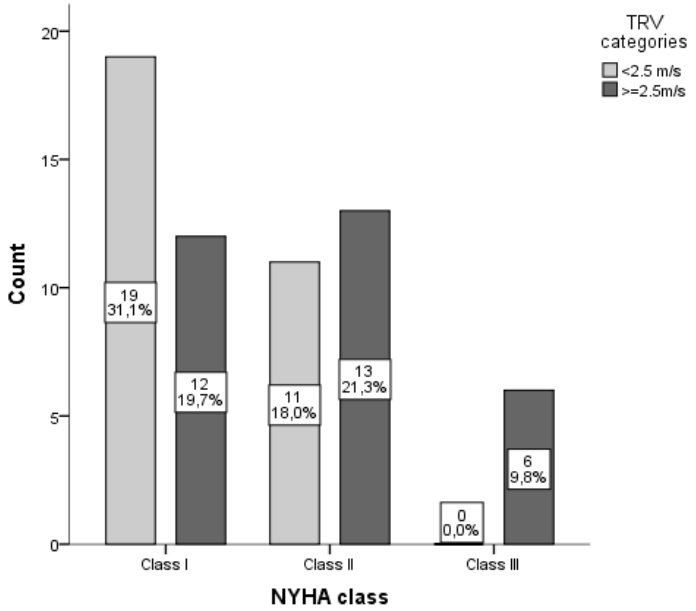

Fig. 4.4 - Distribution of TRV groups according to NYHA functional class.

TRV was higher in patients with SCD (mean 2.54±0.30 m/s; range 2.01-3.30 m/s) compared with healthy subjects (mean 1.96±0.23 m/s; p <0.001) and increased TRV (≥ 2.5 m/sec) was present in 31 patients (51%) compared to 2 (5%) healthy volunteers. Five subjects with SCD (16%) had TRV ≥ 3.0 m/s as is detailed in Fig. 4.5.

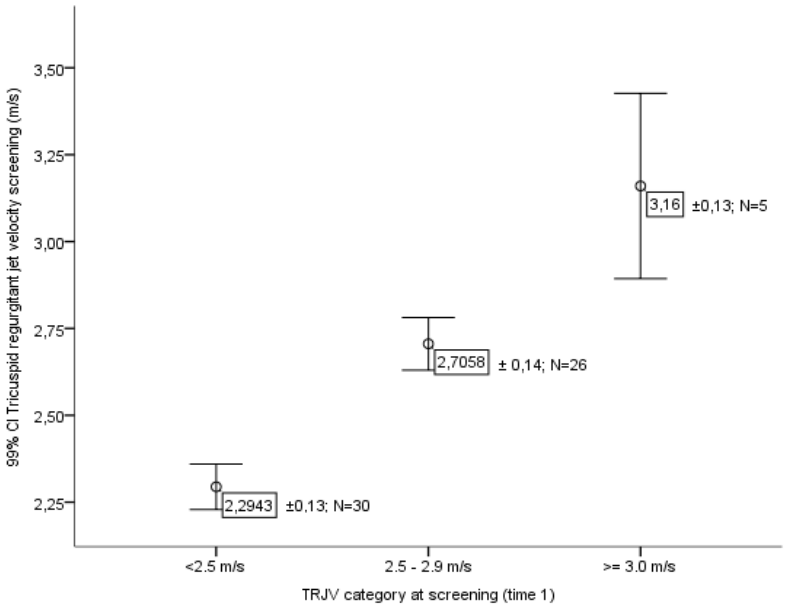

Fig. 4.5 – Detailed distribution by TRV group in patients with SCD.

4.1.5. Cardiac Magnetic Resonance

From the 18 patients from Group A2 (LV diastolic dysfunction), only 11 patients had a CMR for further analysis regarding myocardial fibroses early diagnosis of iron overload. The reasons for not performing the CMR were: claustrophobia (2), failure to commit with appointment(3) and unstable on the day of the appointment (2). Therefore, results of comparison between 2DSTE and tagging MRI for quantification of LV circumferential strain by tagged CSPAMM images were available in 10 patients, since 1 patients requested an early termination during the MRI (Table 4.12).

Table 4.12 – Cardiac Magnetic Resonance characterization in patients with LV diastolic dysfunction.

Cardiac magnetic resonanse	N	Mean ± SD	Min	Max	Percentiles	
					25	75
LV and RV Structure						
LV end diastolic volume (ml)	11	179.27 ± 63.82	114.00	329.00	129.00	223.00
LV end systolic volume (ml)	11	66.00 ± 37.59	37.00	159.00	42.00	86.00
LV ejection fraction (%)	11	64.45 ± 8.77	47.00	75.00	61.00	71.00
LV mass (gr)	10	137.70 ± 34.13	93.00	194.00	108.00	163.25
Iron (ms)	7	37.57 ± 8.70	31.00	56.00	32.00	39.00
RV end diastolic volume (ml)	10	159.50 ± 42.70	114.00	230.00	116.75	194.75
RV end systolic volume (ml)	10	72.00 ± 26.93	43.00	123.00	49.50	88.50
RV ejection fraction (%)	10	60.50 ± 7.21	49.00	72.00	56.25	66.75
RV mass (gr)	10	40.90 ± 14.47	19.00	68.00	27.50	50.25
Midwall Circunferencial Strain (%)						
Anterior Segment	10	-22.53 ± 3.20	-25.36	-16.03	-24.92	-19.29
Antero-septal segment	10	-20.81 ± 2.68	-22.96	-14.53	-22.81	-19.04
Infero-septal segment	10	-17.81 ± 3.63	-21.27	-9.06	-20.02	-15.71
Inferior segment	10	-16.51 ± 3.74	-20.90	-7.37	-18.53	-15.40
Infero-lateral segment	10	-20.89 ± 2.33	-24.67	-17.70	-23.03	-19.41
Antero-lateral segment	10	-24.50 ± 2.47	-29.97	-20.98	-25.91	-22.90
Strain_Average	10	-20.50 2.38	-22.55	-14.33	-21.95	-20.18
Transmural Circumferential Strain (5)						
Anterior Segment	10	-21.77 ± 2.72	-24.75	-16.38	-23.96	-19.51
Antero-septal segment	10	-20.06 ± 2.32	-22.50	-14.74	-21.75	-18.92
Infero-septal segment	10	-17.54 ± 3.52	-21.49	-9.05	-19.71	-15.87
Inferior segment	10	-16.11 ± 3.95	-20.59	-6.81	-18.79	-13.77
Infero-lateral segment	10	-18.95 ± 2.04	-21.64	-15.74	-21.19	-17.00
Antero-lateral segment	10	-22.71 ± 2.09	-26.86	-18.81	-23.71	-21.99
Strain_Average	10	-19.52 2.15	-21.62	-13.89	-20.31	-19.52

The time required for 2DSTE acquisition and analysis of all studied LV parameters was generally 10 minutes, whereas acquisition and analysis by MRI required approximately 15 to 20 min for LV volumes and EF, and at least 45 minutes for circumferential strain. No agreement was found between since the number of patients in these groups is very

small, no attempt was made to compare the parameters obtained with different methods. None of the patients had signs of myocardial fibroses or iron overload (mean 37.6, range 31-56 ms).

4.2. Distribution of Clinical and Echocardiography Variables According to TRV Groups

Sickle cell disease genotype (p=0.83) and clinical conditions (i.e. Alcohol History, Smoking history Total Number of Transfusion In Lifetime, Leg ulcers, Vaso occlusive pain episodes Lung Problems Acute Chest Syndrome and Spleen Problems) were not statistically significant different between TRV groups (Table 4.13) . Although the level of statistical significance in this study was 1%, there was a tendency to an association of increased TRV with the presence of leg ulcers (p=0.03), smoking history (p=0.02) and lung problems (p=0.03).

Table 4.13 - Clinical conditions in patients with SCD according to TRV groups

Variable	TRV < 2.5 m/s		TRV ≥ 2.5 m/s		*p* -value Mann-Whitney
	(N)	Mean Rank	(N)	Mean Rank	
Clinical conditions					
Alcohol History	30	28,58	31	33,34	0,24
Total Number of Transfusion In Lifetime	30	27,50	31	34,39	0,11
Leg ulcers	30	26,50	30	34,50	0,03
Vaso occlusive pain episodes	28	27,00	28	30,00	0,32
Smoking history	30	26,40	31	35,45	0,02
Lung Problems	30	27,33	31	34,55	0,03
Spleen Problems	30	27,63	31	34,26	0,08
Lung Pneumonia/Acute Chest Syndrome	30	30,32	31	31,66	0,72

In patients with TRV of 2.5 m/s or more, LV structure, chamber size, LV ejection fraction and LA volume, did not differ from patients with TRV < 2.5 m/s (Appendix VII). LV Global function index lateral that evaluates both systole and diastole function, was significantly reduced in patients with increased TRV (mean 0.86±0.21 versus mean 1.10±0.36) (Table 4.12). This may be explained by decreased DTI velocities at lateral level.

Furthermore, RV structure and RA volume did not differ between TRV groups as well. Although there was a trend towards RV and RA enlargement with increasing estimated pulmonary pressures, RV systolic function was preserved at higher pressures, suggesting no evidence of resting RV functional impairment (Table 4.14) . No differences were found between TRV groups regarding LV and RV strain and strain rate data (Appendix VII).

Table 4.14 - Cardiac structure and function in patients with SCD according to TRV groups

Variable	TRV < 2.5 m/s		TRV ≥ 2.5 m/s		Diff. Mean	99% CI of Difference		p-value ŧ
	(N)	Mean ± SD	(N)	Mean ± SD		Lower	Upper	
LV Structure								
LV septum diameter (mm)	28	9.54 ± 1.37	29	10.29 ± 1.34	-0.74	-1.44	-0.05	0.04
LV posterior wall diameter (mm)	29	9.80 ± 1.57	29	10.34 ± 1.65	-0.54	-1.37	0.28	0.19
LV 2D diastolic volume indexed (ml/m2)	26	72.30 ± 17.24	27	75.73 ± 25.62	-3.44	-14.66	7.79	0.54
LV 2D systolic volume indexed (ml/m2)	29	27.10 ± 9.77	30	25.42 ± 11.37	1.68	-3.76	7.12	0.54
LV mass index (g/m2)	29	86.34 ± 20.76	29	95.39 ± 35.54	-9.05	-25.36	7.26	0.27
RV structure								
RV diastolic area apical view (cm2)	30	19.97 ± 5.21	31	22.09 ± 5.88	-2.12	-4.97	0.73	0.14
RV systolic area apical view (cm2)	30	11.35 ± 3.22	31	12.36 ± 3.20	-1.01	-2.66	0.63	0.22
3D RV end diastolic volume (ml)	29	99.56 ± 23.39	29	120.31 ± 39.15	-20.74	-37.71	-3.78	0.02
3D RV end systolic volume (ml)	29	44.16 ± 14.94	29	55.23 ± 18.46	-11.08	-19.91	-2.24	0.015
LA/RA structure								
Left atrium volume indexed (ml/m2)	30	41.08 ± 12,46	30	47.48 ± 17,13	-6.40	-16.69	3.91	0.10
RA volume indexed (ml/m2)	28	37.99 ± 10.12	29	37.80 ± 13.44	0.20	-6.14	6.53	0.95
LV systolic function								
Global function index lateral	30	0.86 ± 0.21	30	1.10 ± 0.36	-0.24	-0.39	-0.09	**0.003**
Global function index septal	27	1.12 ± 0.27	25	1.30 ± 0.35	-0.17	-0.34	-0.01	0.04
LV 2D Ejection Fraction (%)	30	64.34 ± 6.93	31	67.94 ± 7.20	-3.60	-7.22	0.02	0.05
LV 2D cardiac output (L/min)	28	5.85 ± 1.70	29	6.84 ± 2.24	-0.98	-2.00	0.04	0.06
LV 2D stroke volume (mL)	29	77.40 ± 18.75	29	89.05 ± 27.85	-11.65	-24.00	0.71	0.06
LV S´ wave lateral (cm/s)	30	9.95 ± 1.92	30	8.93 ± 2.55	1.02	-0.16	2.19	0.09
LV S' wave septal (cm/s)	29	8.31 ± 1.24	25	8.25 ± 0.91	0.06	-0.50	0.62	0.84
RV systolic function								
Estimated PVR (Woods unit)	27	1.44 ± 0.35	25	1.67 ± 0.25	-0.23	-0.40	-0.06	0.010
RV MPI by TDI	28	0.34 ± 0.09	29	0.34 ± 0.12	0.00	-0.05	0.06	0.92
RV S´wave (cm/s)	30	14.10 ± 1.99	31	15.50 ± 3.12	-1.41	-2.75	-0.06	0.04
TAPSE (mm)	30	28.03 ± 5.12	30	30.37 ± 5.88	-2.33	-5.18	0.51	0.11
RV fractional area change (%)	30	43.08 ± 9.60	31	43.33 ± 7.92	-0.25	-4.75	4.26	0.91
3D RV Ejection fraction (%)	29	56.15 ± 7.66	29	53.65 ± 6.55	2.50	-1.25	6.25	0.19

Additional analysis was performed to asses LV diastolic function in both TRV groups. In the group of patients with TRV≥ 2.5 m/s, 17 (55%) patients had normal LV diastolic function and 14 patients (45%) had abnormal LV diastolic function. Distribution of patients is summarised in Fig. 4.6.

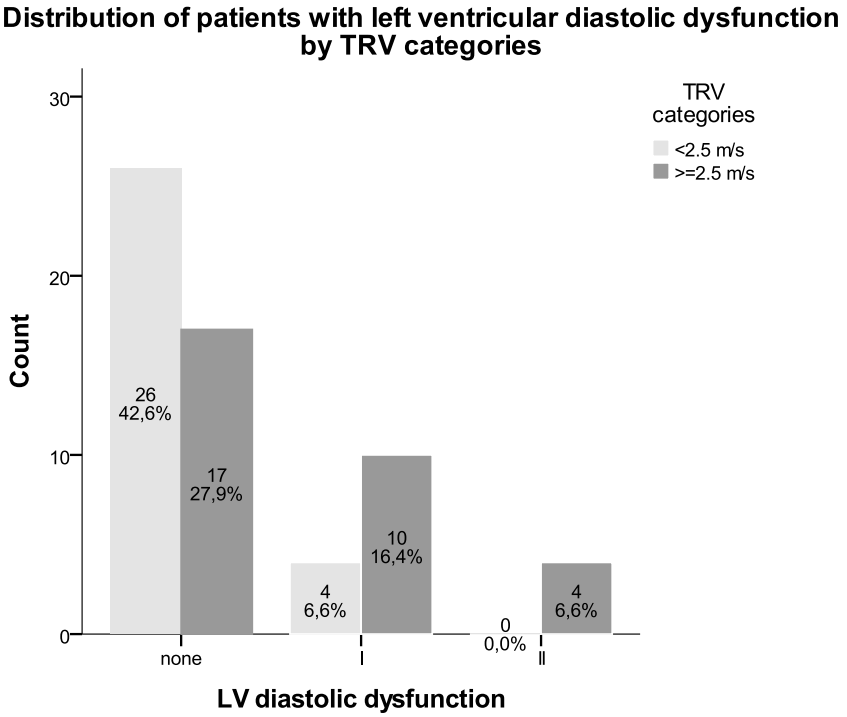

Fig. 4.6 – Detailed distribution by TRV group in patients with SCD.

Further analysis was carried out to assess the estimated LV diastolic filling pressures with the use of LV E/E´ lateral wall, LV E/E´septal and LV E/E´average (mean value from basal septal and lateral walls). All of these LV parameters were significantly increased among TRV groups which therefore seemsto show an association between increased pulmonary pressures with LV diastolic dysfunction. Results are detailed in Table 4.15.

Table 4.15 - Left and right ventricular diastolic assessment in patients with SCD according to TRV groups

Variable	TRV < 2.5 m/s		TRV ≥ 2.5 m/s		Diff. Mean	99% CI of Difference		p-value ŧ
	(N)	Mean ± SD	(N)	Mean ± SD		Lower	Upper	
LV diastolic function								
LV E wave (cm/s)	30	86.46 ± 15.04	31	90.53 ± 14.06	-4.07	-13.99	5.85	0.28
LV E/A ratio	29	1.72 ± 0.55	31	1.35 ± 0.45	0.37	0.02	0.71	**0.006**
MV decelaration time (ms)	29	194.79 ± 39.59	31	207.61 ± 37.88	-12.82	-39.46	13.82	0.21
LV Isovolumic relaxation time (ms)	26	92.53 ± 15.38	29	97.21 ± 18.38	-4.68	-16.97	7.61	0.31
PV a wave duration (ms)	19	114.79 ± 23.70	19	112.42 ± 15.69	2.37	-15.37	20.10	0.72
PV a wave reversal (cm/s)	21	22.10 ± 4.12	24	25.21 ± 6.97	-3.11	-7.80	1.57	0.08
Duration a wave LV	18	117.06 ± 34.34	27	118.77 ± 15.84	-1.71	-22.10	18.68	0.82
LV E´ lateral wall	29	12.70 ± 2.77	31	10.80 ± 2.72	1.90	0.01	3.79	0.01
LV E/E' lateral	29	7.03 ± 1.69	31	8.90 ± 2.57	-1.87	-3.37	-0.36	**0.002**
MV E´ septal (cm/s)	29	9.65 ± 1.87	31	8.90 ± 1.98	0.75	-0.57	2.08	0.14
LV E/E´septal	29	9.13 ± 1.77	31	10.48 ± 2.06	-1.36	-2.68	-0.03	**0.008**
LV E/E´avg	29	8.08 ± 1.51	30	9.71 ± 2.10	-1.63	-2.90	-0.35	**0.001**
RV diastolic function								
RV E wave (cm/s)	28	47.93 ± 10.93	27	46.79 ± 10.21	1.15	-4.58	6.87	0.69
RV E/A	24	1.70 ± 0.43	23	1.34 ± 0.38	0.36	0.11	0.60	**0.005**
RV E´wave (cm/s)	29	11.98 ± 3.46	31	12.29 ± 3.50	-0.31	-2.11	1.49	0.73
RV E´/A´	27	1.27 ± 0.49	28	0.98 ± 0.36	0.29	0.06	0.52	0.01
RV E/E´	28	4.30 ± 1.68	27	4.16 ± 1.77	0.15	-0.78	1.08	0.75
RV isovolumic relaxation time (ms)	25	50.68 ± 26.92	21	71.67 ± 42.20	-20.99	-41.69	-0.28	0.05

ŧTwo-sided P values for continuous variables were calculated with the use of the t-test or spearman correlation according to variable distribution. Significant difference between groups when p<0.01

4.3. Distribution of Clinical and Echocardiography Variables According to LV Diastolic function Groups

The prevalence of LV diastolic dysfunction was 29.5% corresponding to 18 patients. As expected, age was significantly different between Group A1 and Group A2, with an increased mean age value in the Group A2. Global function index lateral, TRV and estimated PVR by echocardiography were all increased in LV diastolic dysfunction patients. Detailed data can be seen in Table 4.16.

Table 4.16 - Cardiac structure and function in patients with SCD according to LV diastolic function

Variable	Group A1 (normal LV diastolic function)				Group A2 (abnormal LV diastolic function)				p-value ŧ
	(N)	Mean	±	SD	(N)	Mean	±	SD	
Demographics									
Age(years)	43	36.70		10.82	18	50.12		8.42	**<0,001**
Height (cm)	43	168.64		9.72	18	169.24		10.51	0.838
Weight (kg)	43	67.77		9.31	18	73.34		13.74	0.149
Body surface area (kg/m^2)	43	1.78		0.15	18	1.85		0.22	0.141
Body Mass Index (kg/m^2)	43	23.92		3.51	18	25.51		3.79	0.134
Heart rate (bpm)	43	74.96		9.52	18	78.88		11.32	0.183
Oxygen saturation on air (%)	43	97.20		3.76	18	97.19		2.46	0.990
Systolic BP (mmHg)	43	118.36		11.17	18	122.75		20.58	0.427
Diastolic BP (mmHg)	43	69.69		9.58	18	73.75		12.04	0.179
LV and RV Structure									
LV septum diameter (mm)	43	9.98		1.39	18	9.75		1.46	0.572
LV posterior wall diameter (mm)	43	10.08		1.67	18	10.11		1.54	0.953
LV 2D diastolic volume indexed (ml/m2)	43	75.11		23.48	18	71.05		16.41	0.527
LV 2D systolic volume indexed (ml/m2)	43	27.02		11.22	18	24.06		8.36	0.339
LV 2D mass index (g/m2)	43	93.41		31.52	18	83.32		21.02	0.304
RV structure									
RV 2D diastolic area apical view (cm2)	43	21.03		5.98	18	21.08		4.62	0.976
RV 2D systolic area apical view (cm2)	43	12.02		3.35	18	11.42		2.92	0.529
RV 3D end diastolic volume (ml)	43	112.64		35.64	18	101.42		25.59	0.281
RV 3D end systolic volume (ml)	43	51.03		18.80	18	45.52		12.53	0.311
LA/RA structure									
Left atrium volume indexed (ml/m2)	43	44.15		17.11	18	44.66		8.31	0.910
RA volume indexed (ml/m2)	43	38.20		12.12	18	37.03		11.28	0.746
LV and RV systolic function									
Global function index lateral	43	0.87		0.23	18	1.28		0.34	**<0,001**
Global function index septal	43	1.15		0.32	18	1.39		0.27	0.010
LV 3D ejection fraction (%)	32	51.38		5.16	11	50.84		4.51	0.759
LV S´ wave lateral (cm/s)	43	9.62		2.50	18	8.88		1.59	0.270
LV S' wave septal (cm/s)	43	8.35		1.18	18	8.07		0.71	0.362
RV systolic function									
Estimated PASP (mmHg)	43	30.61		6.72	18	35.28		5.98	0.017
TRV screening (m/s)	43	2.46		0.28	18	2.72		0.27	**0.002**
Estimated PVR (Woods unit)	43	1.47		0.29	18	1.79		0.30	**0.002**
RV MPI by TDI	43	0.32		0.11	18	0.38		0.10	0.073
RV S´wave (cm/s)	43	14.53		2.36	18	15.60		3.44	0.174
TAPSE (mm)	43	28.84		5.99	18	30.27		4.13	0.398
RV fractional area change (%)	43	42.34		8.82	18	45.66		8.20	0.193
RV 3D Ejection fraction (%)	43	54.95		7.39	18	54.74		6.72	0.924

4.4. Associations between measures of LV diastolic function with Left Ventricular Structure and Function

Body mass index, LV mass index and diastolic blood pressures were strongly associated with increased LV volumes, both systolic and diastolic. A positive correlation was found between LV end diastolic volume and TRV, supporting previous findings. In addition, a negative relationship was found between haemoglobin and LV end-diastolic volume ($p<0.001$, $r=0.51$) (Fig. 4.7).

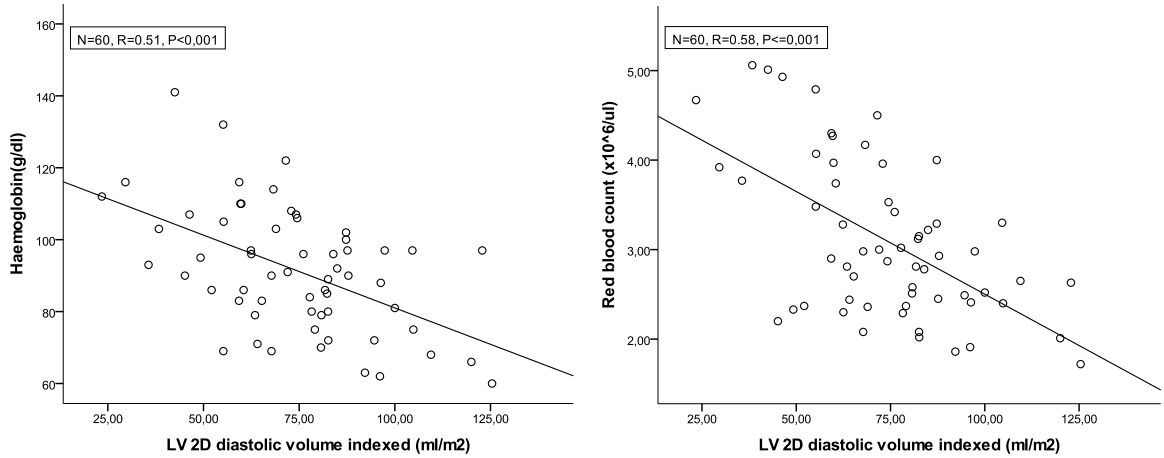

Fig. 4.7 - Relationship between LV end diastolic volume by 2D echocardiography and haemoglobin (p=<0.001; r= -0.51) (top) and red blood count (p=<0.001; r =-0.58) (bottom)

In a univariate analysis (spearman correlation), LV E/E´ lateral ratio was strongly correlated with age (r= 0.41, p=0.001). In addition, there was a negative correlation with platelet count (r= -0.33, p= 0.009) and no association with haemolysis markers. There was a tendency towards a positive relationship with proBNP (r= 0.29, p=0.02) which has been associated with increase pressures in the pulmonary arteries. Supporting this finding, a significant relationship was obtained between LV E/E´lateral, LV E/E´septal, LV E/E´average with TRV (r=0.39, p= 0.002 ; r= 0.35 , p <0.001 ; r= 0.43 , p = 0.007). A comparison between patients with or without clinical features (i.e. smoking and alcohol history, transfusions in lifetime, leg ulcer, vaso-occlusive episodes, lung problems and spleen problems) did not show significant differences between LV diastolic dysfunction parameters, in terms of patients demographics. There was also no association of LV E/E´ratio parameters with LV Strain and Strain rate data.

4.5. Risk Factors for increase TRV

Older age was strongly associated with a TRV ≥ 2.5 m/s (r =0.35; p = 0.005). Mean age was significantly higher in patients with increased TRV compared to TRV< 2.5 m/s (35.91±10.95 vs. 44.38±11.16, p<0.01). As expected, TRV was strongly associated with PVR (r=0.44, p< 0.001) and RV end diastolic (r= 0.43; p= 0.001) and end systolic volumes (r=0.39; p= 0.003) (Table 4.16). Associations of TRV with laboratory tests and

echocardiographic parameters have been explored (Appendix IX). No significant association was found with markers of haemolysis (haemoglobin, lactate dehydrogenase, reticulocytes and total bilirubin). No association was found with BNP (p=0.12). LV systolic function did not correlate significantly with Tricuspid Regurgitation (p=0.1), however there was a tendency for an association with the global function index lateral (r= 0.31; p = 0.017). Moreover, none of the LV and RV myocardial deformation parameters, strain and strain rate, were significantly associated with TRV.

Increased pulmonary pressures have been described extensively in SCD, however its severity is commonly mild and the contribution of LV systolic or diastolic dysfunction remains controversial.

As mentioned earlier, significant differences were found between TRV groups regarding LV diastolic function parameters. Conventional Doppler-derived measurements of LV diastolic filling (i.e., mitral E, E/A, MV DT, and IVRT) were not correlated with TRV velocity. However, mitral E/E´lat and LV E/E´ (average) ratios (Fig. 4.8) were correlated moderately with TRJ velocity which may represent an association increase in LV filling pressures.

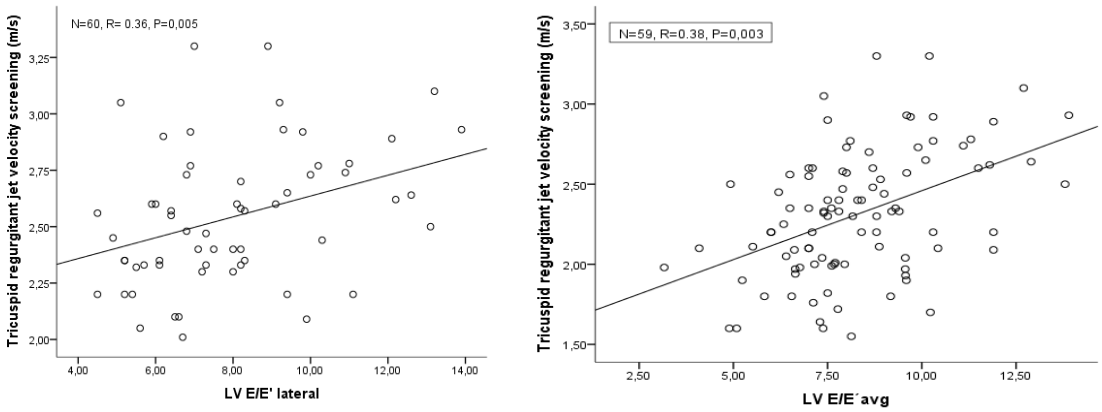

Fig. 4.8 - Positive linear correlation between tricuspid regurgitation velocity and left ventricular E/E´ lateral (r=0.63; p= 0.005) and LV E/E´average (r= 0.38; p=0.0038)

Associations with Chi-Square non parametric test, between LV diastolic function groups (with and without dysfunction) and the TRV groups, has shown that patients who have LV diastolic dysfunction also tend to have increased pulmonary pressures. A strong

association was found in 14 (77.8%) of the subjects with LV DD (n=18) which had a TRV ≥ 2.5 m/s (p= 0.006).

Furthermore, a patient with LV DD had 5.35 times more risk of developing pulmonary hypertension (OR=5.35 ; 95%CI 1.5 – 19.02).

Table 4.17 - Significant associations with TRV, Pearson Rank Correlation Coefficient

Variable	N	Tricuspid regurgitant jet velocity (m/s)	
		Pearson Correlation (*r*)	P-value
Right ventricle E/A	47	-0.40	0.006
Pulmonary vascular resistance (Woods unit)	52	0.50	<0,001
RV base diameter (cm)	59	0.36	0.006
3D RV end diastolic volume	58	0.43	0.001
3D RV end systolic volume	58	0.39	0.003
Tricuspid annular systolic motion (mm)	60	0.38	0.003
Left ventricle E/E' lateral	60	0.36	0.005
Left ventricle E/E´avg	59	0.38	0.003
LV 2D end-diastolic diameter (mm)	61	0.37	0.003

4.5.1. Predictors of Increased tricuspid regurgitant jet velocity

In the logistic regression, LV E/E´ average (p= 0.007) was the only variable that contributed significantly to the model to identify predictors of an association with increased TRV (≥ 2.5 m/s). The chances of developing increased pulmonary pressures (TRV> 2.5 m/s) is 2.2 for each unit of LV E/E´. In other words, the chances of having TRV ≥ 2.5 m/s increases 120% for each unit of LV E/E´average.

Table 4.18 - Independent predictor of TRV ≥2.5 m/s

Variable in the equation			Constant
LV E/E´avg	B	0.788	-6.34
	S.E.	0.29	2.414
	Wald	7.403	6.895
	df	1	1
	p-value	0.007	0.009
	Exp(B)	2.2	0.002
	95% C.I.for EXP(B)		
	Lower	1.247	
	Upper	3.881	

Table 4.19 - Variables not in the equation of the model

Variables not in the equation	Score	df	P-value
Age	.889	1	.346
LV E/E' lateral	.540	1	.462
Left atrium volume indexed (ml/m2)	3.027	1	.082
Duration a wave LV	.878	1	.349
LV E´ lateral wall	.169	1	.681
LV E wave (cm/s)	.021	1	.884
LV E/A ratio	1.662	1	.197
LV E/E´septal	.597	1	.440
LV Isovolumic relaxation time (ms)	.148	1	.701
MV E´ septal (cm/s)	.290	1	.590
MV decelaration time (ms)	.370	1	.543
Overall Statistics	10.496	11	.486

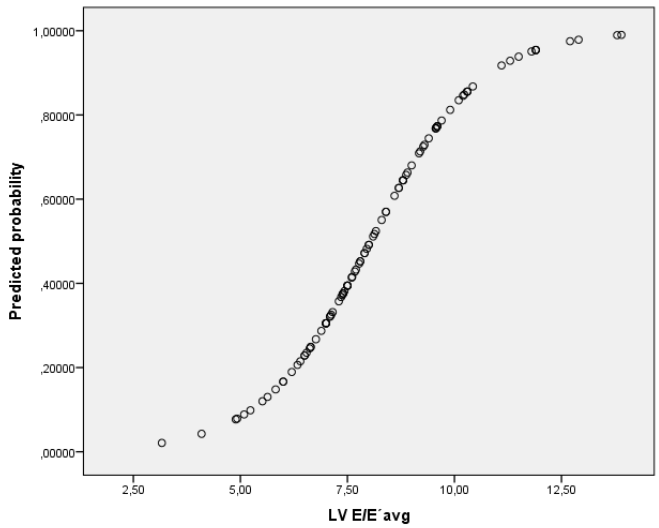

Fig. 4.9 - Predictive effect of LV E/E´ ratio average into TRV≥ 2.5 m/s

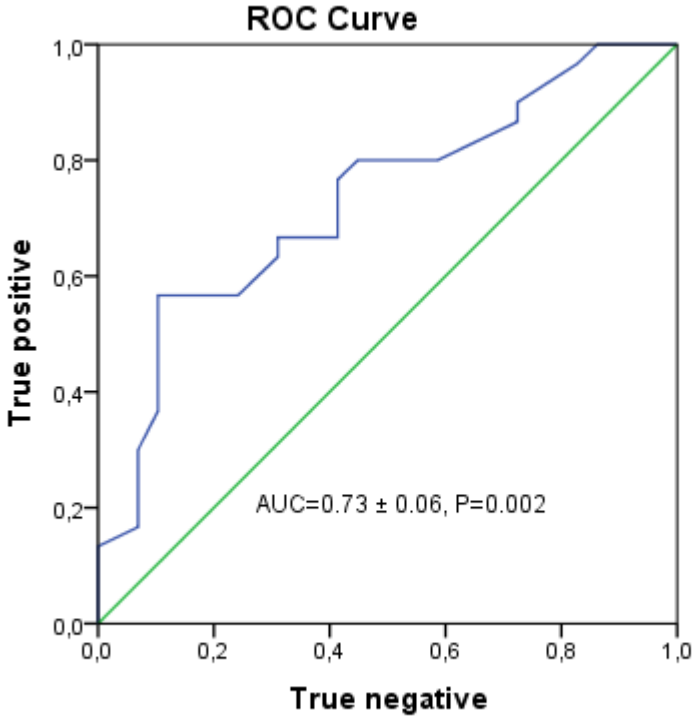

Fig. 4.10 – Receiving operator curve for the LV average E/E´ for predicting a TRV≥ 2.5 m/s.

The area under the ROC curve for the E/E´ average ratio predicting a TRV≥ 2.5 m/s was 0.7 (95% CI 1.24 – 3.88, P=0.007). An E/E´average ratio > 7 was the optimal cut off, with a sensitivity of 70.8% and a specificity of 64.7%.

4.6. Associations with increasing LV lateral E/E´ ratio

In the univariate and multivariate analysis, 22 independent variables were included in the model for the multiple linear regression analysis which was used to ascertain the most useful independent predictor of elevated LV filling pressures. This model identified 4 echocardiographic variables which determine increasing LV lateral E/E´ ratio. Global function index lateral (p=0.000), haemoglobin (p=0.000), global function index septal (p=0.006) and left atrium volume indexed (p=0.035) were each independently associated with a higher LV lateral E/E´ratio. These model explains 92% of the increase of LV E/E´lateral (R2=0.92). Table 4.20 summarizes this analysis.

Table 4.20 - Independent preditors of Left ventricular lateral wall E/E' ration in Multiple Linear Regression analysis (n=34)

Variables	Beta	95% CI	*P*-value	R^2	ANOVA F	*P*- value
Global function index lateral	1.063	(6.74 to 8.74)	0.000	0.917	(4. 29) 91.887	0.000
Haemoglobin(g/dl)	-0.28	(-0.54 to -0.20)	0.000			
Global function index septal	-0.207	(-2.33 to -0.43)	0.006			
Left atrium volume indexed (ml/m2)	-0.14	(-0.03 to -0.001)	0.035			

4.7. Prospective serial study

The mean duration of follow up was 17.13±3 months with a range of 10-23 months. No significant change in the usage of hydroxyurea or participation in a chronic transfusion program was found. The prevalence of elevated tricuspid regurgitation velocity at follow-up was 45% compared to 51% at baseline.

4.7.2. Changes from baseline to follow-up results

In our 5 year survival retrospective published cross-sectional analysis, we observed that TRV was associated with the risk of death by more than four-fold.

In the present study, we evaluated how baseline screening observations change at follow-up. The same echocardiographic protocol was repeated. All 61 patients at baseline had measurable TRV at follow-up.

The difference in values between the screening and follow-up time points was analysd. The choice of statistical method was dependent on the nature of the variable being compared.

The analysis results are summarised in Table 4.19. The figures presented are the number of patients in the analysis, along with the mean and standard deviation at each time point. The mean change over time is also presented, along with a corresponding confidence interval. Due to the large number of variables, Table 4.21 includes only

variables with a significant change between the two time points. Complete data is presented inthe Appendix section.

Table 4.21 - Difference in mean values between the screening and follow-up time points

Variables	N	Screening	Follow-up	Change	*P*-value
		Mean (SD)	Mean (SD)	Mean (99% CI)	
Right ventricle					
RV end diastolic volume 3D	55	110 (34)	118 (41)	8 (4, 12)	**<0.001**
RV end systolic volume 3D	55	49.3 (17.9)	53.0 (2.9)	3.7 (1.8, 5.7)	**<0.001**
RV Global strain (average of 6 segments)	54	-16.3 (8.6)	-20.8 (4.1)	-4.6 (-8.1, -1.0)	**0.001**
RV longitudinal strain basal septum	46	-10.8 (8.3)	-17.5 (6.8)	-6.7 (-11.0, -2.3)	**<0.001**
RV longitudinal strain median septum	54	-14.5 (8.3)	-18.8 (5.7)	-4.3 (-8.3, -0.4)	**0.005**
Left ventricle					
Inter ventricular septum diameter (mm)	61	9.9 (1.4)	10.5 (1.3)	0.6 (0.2, 1.0)	**<0.001**
LV 2D end-diastolic diameter (mm)	61	50.9 (6.7)	49.4 (7.0)	-1.4 (-2.4, -0.4)	**<0.001**
Ejection Fraction by 2D (%)	60	66.3 (7.2)	63.4 (5.8)	-2.9 (-5.5, -0.4)	**0.003**
LV 3D ejection fraction (%)	41	51.3 (5.1)	48.5 (5.3)	-2.7 (-4.9, -0.6)	**0.001**
LV 3D Strain					
LV 3DST median segments average	41	-34.1 (5.0)	-31.7 (5.1)	2.4 (0.5, 4.4)	**0.002**
LV 3DST global average of all segments	41	-32.4 (3.9)	-30.5 (4.5)	1.9 (0.2, 3.6)	**0.003**
LV longitudinal strain median segments average	41	-18.6 (3.5)	-16.5 (2.5)	2.1 (0.7, 3.6)	**<0.001**
LV longitudinal strain global average of all segments	41	-18.1 (2.9)	-16.5 (2.2)	1.6 (0.4, 2.8)	**<0.001**
LV radial strain median segments average	39	74.9 (17.8)	64.0 (12.3)	-10.8 (-17.9, -3.8)	**<0.001**
LV radial strain apical segments average	40	83.1 (32.1)	63.9 (17.4)	-19.2 (-33.4, -5.0)	**<0.001**
LV radial strain global average of all segments	41	69.7 (15.9)	58.9 (10.1)	-10.7 (-16.4, -5.1)	**<0.001**
LV longitudinal strain rate global	41	-0.10 (0.01)	-0.10 (0.01)	0.01 (0.00, 0.02)	**0.006**
LV Diastolic function					
LV E/E' lateral	58	8.0 (2.4)	8.9 (2.7)	0.9 (0.1, 1.7)	**0.005**
LV E´ lateral wall	58	11.7 (2.9)	10.6 (3.3)	-1.2 (-1.9, -0.4)	**<0.001**
LV E/A ratio	60	1.53 (0.53)	1.38 (0.45)	-0.15 (-0.30, -0.01)	**0.007**
MV decelaration time	60	201 (39)	217 (37)	16 (1, 31)	**0.006**
Blood tests					
Aspartate aminotransferase (u/l)	55	41 (23)	52 (26)	11 (3, 18)	**<0.001**
Platelet count (x10^3 cells/ul)	58	333 (173)	291 (127)	-42 (-79, -5)	**0.003**
Demographics					
Systolic blood pressue	60	118.8 (14.3)	123.2 (16.3)	4.3 (0.5, 8.6)	**0.009**

Left ventricular function, analysed by 2D and 3D Ejection fraction, has decreased at follow up (p=0.003 and p=0.001 respectively). In respect to myocardial deformation, all global values (Area Strain, longitudinal and radial strain) decrease at follow-up. Although not significant, there was also a tendency for change in the mean value of LV Circumferential Strain (p=0.02).

Right ventricular volumes were significantly increased at follow-up (p<0.001) while RV Free wall Strain, besides normal values, has significantly decreased (p=0.001).

4.7.3. Increase in tricuspid regurgitation velocity during follow up

Four patients (6.6%) with a baseline tricuspid regurgitation velocity of less than 2.50 m/sec had a follow-up elevation (TRV≥ 2.5 m/sec). Seven patients (11.5%) who had at the baseline, a TRV≥2.5 m/s, reduced to < 2.5 m/s at follow-up (Table 4.22).

Table 4.22 - Tricuspid regurgitant velocity change at follow-up

TRV change screening to follow-up		
	Frequency	Percent
Regular (kept TRV <2.5 m/s)	26	42.60%
Stable (kept TRV >=2.5 m/s)	24	39.3%
worsened (increased TRV >=2.5 m/s)	4	6.6%
Improved (decreased TRV <2.5 m/s)	7	11.5%
N=	61	100%

The mean (SD) follow-up tricuspid regurgitation velocity was 2.54 (±0.30) m/sec and was not significantly different when compared to the mean TRV at baseline of 2.54±30 (p=0.39). Further analysis was performed to evaluate changes between TRV groups at the 2 time points. However no significant changes were found.

4.7.4. Predictor of increased LV lateral E/E´at follow-up

At follow-up, 24 patients had LV Diastolic dysfunction, from where 15 patients on Grade I (24.6%) and 9 patients in Grade 9 (14.8%). Analysis was done for the change in LV diastolic dysfunction and NYHA class at follow-up. Eight patients had worsened LV DD class at follow-up, corresponding to 9.8% of the study subjects (p=0.002). Nine patients worsened in the NHYA functional class (p<0.001) (Table 4.23).

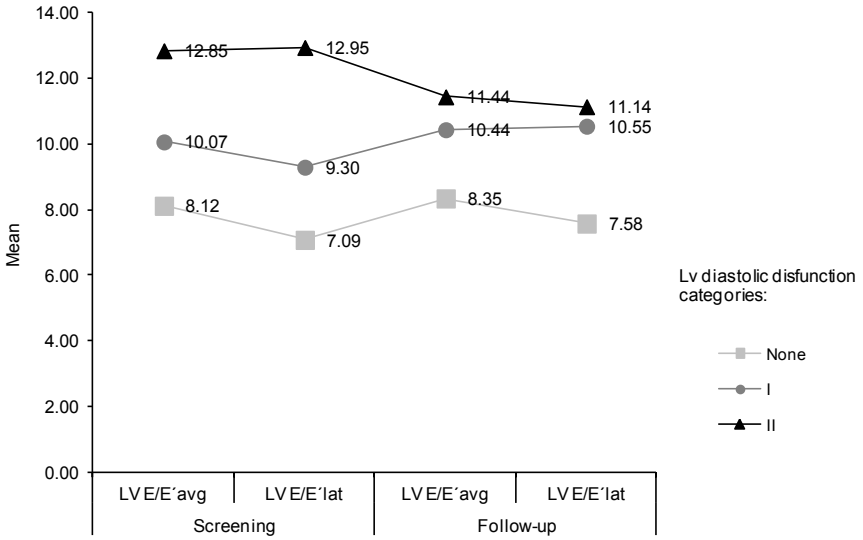

Fig. 4.11 – LV diastolic dysfunction grade and mean LV lateral and average E/E´ratios from screening to follow-up.

Table 4.23 - Change in NYHA class from screening to follow-up

	Category	Screening N (%)	Follow-up N (%)	P-value
NYHA class	Class I	31 (51%)	22 (36%)	**<0.001**
	Class II	24 (39%)	29 (48%)	
	Class III	6 (10%)	10 (16%)	

In a univariate and multivariate analysis, 22 independent variables were included in the model for the multiple linear regression analysis which was used to ascertain the most useful independent predictor of elevated LV filling pressures at follow-up. This model identified only 2 echocardiographic variables which determine increasing LV lateral E/E´ ratio. Global function index lateral ($p<0.001$) (already a predictor at baseline) and blood urea nitrogen (mmol/L) which was new finding comparing to baseline model, both were independently associated with a higher LV lateral E/E´ratio. This model explains 73.7% of the increase of LV E/E´lateral (R2=0.74). Table 4.24 summarises this analysis.

Table 4.24 - Independent predictors of Left ventricular lateral wall E/E' ratio in Multiple Linear Regression analysis (n=34)

Variables	N	Beta	95% CI	*P*-value	R^2	ANOVA F	*P*- value
Global function index lateral	34	0.64	(4.23 to 6.83)	**p<0.001**	0.74	(2.31) 47.18	**p<0.001**
Blood urea nitrogen (mmol/L)	34	0.12	(0.06 to 0.54)	0.017			

4.7.5. Change in LV diastolic function Grade

The change in LV diastolic dysfunction grade was measured according to the LV E/E' lateral ratio. The analysis was performed using linear regression and a normal distribution was found. Subsequently, univariate analysis was performed between each factor and the outcome.

Initially the separate association between each factor and the outcome was examined in a series of univariate analyses, and the results are summarised in the table 4.25. The figures presented are the regression coefficients, along with their corresponding confidence intervals. For predictor variables measured on a categorical scale, the coefficients represent the difference in the outcome between categories. For predictor variables measured on a continuous scale, the coefficients represent how the outcome varies for a one-unit increase in the predictor variable, unless otherwise indicated. Effects for other sized increases are reported where one-unit was either a very small or large change in the predictor variable. P-values indicating the significance of the results are also present.

Table 4.25 - Multivariate analysis for the association with change in Diastolic function

Variable	Coefficient (95% CI)	P-value
E/E Lat (screening)	-0.33 (-0.57, -0.10)	**0.007**
Age (***)	0.38 (-0.13, 0.88)	0.14
Male gender	-0.75 (-1.96, 0.46)	0.22
BMI (**)	0.01 (-0.83, 0.84)	0.99
Systolic blood pressure (***)	0.37 (-0.05, 0.79)	0.08
Hydorxyurea (currently use)	1.06 (-0.33, 2.45)	0.13
Bun blood urea nitrogen (mmol/l)	0.43 (0.11, 0.75)	**0.009**
Hematocrit (*)	-0.24 (-1.56, 1.07)	0.71
Haemoglobin	-0.10 (-0.45, 0.26)	0.59
Creatinine (***)	0.13 (-0.09, 0.34)	0.24
Right atrium volume indexed (ml/m^2) (***)	0.11 (-0.43, 0.64)	0.69
Left atrium volume indexed (ml/m^2) (***)	0.12 (-0.29, 0.53)	0.88
Right ventricle end diastolic volume (***)	-0.14 (-0.33, 0.05)	0.14
Right ventricle ejection fraction (**)	-0.27 (-0.69, 0.15)	0.2
Left ventricle end diastolic volume (ml) (***)	-0.08 (-0.27, 0.10)	0.36
LV 3D ejection fraction (%) (**)	0.59 (0.15, 1.02)	**0.009**
LV mass index (***)	0.04 (-0.20, 0.28)	0.76
6-minute walk test (****)	-0.21 (-0.61, 0.19)	0.3

(*) Coefficients reported for a 0.1-unit increase in predictor variable
(**) Coefficients reported for a 5-unit increase in predictor variable
(***) Coefficients reported for a 10-unit increase in predictor variable
(****) Coefficients reported for a 50-unit increase in predictor variable

The results suggested that initial LV E/E' lat value was strongly associated with the change in diastolic dysfunction.

The regression results and the graph above suggest that patients with higher blood urea values had a greater change in LV E/E' lat. A 1 mmol/l increase in urea was associated with the change in LV E/E' lat increasing by 0.4 units.

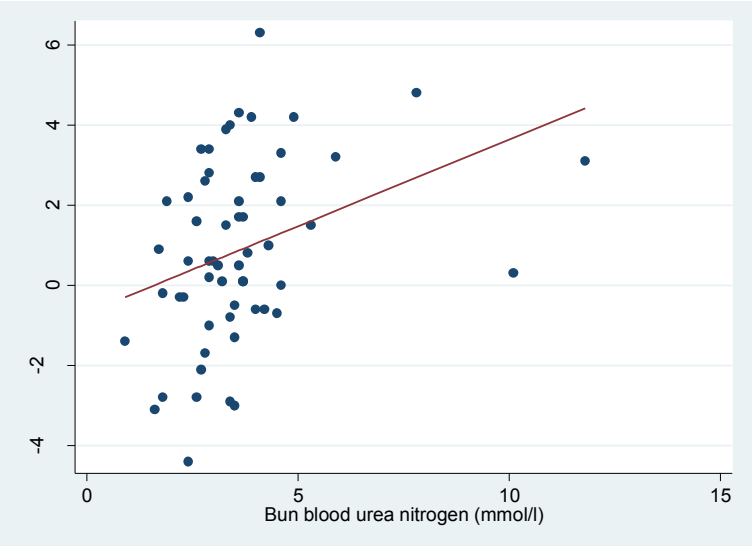

Fig. 4.12 - Regression line for the association between LV E/E´lateral and Blood urea nitrogen (mmo/L).

A third and final statistically significant result was for LV 3D ejection fraction. Here there was also a positive relationship with the change in LV E/E' lat. This suggests that patients with a higher ejection fraction had a greater change in scores. The data also providded some evidence that systolic blood pressure was also associated with the change in diastolic dysfunction. However, the result for these variables was not quite statistically significant.

The second part of the analysis examined the joint effect of the variables in a multivariable analysis. A backwards selection procedure was used to retain only the statistically significant variables, and the final model is summarised in the Table 4.26.

Table 4.26 - Multiple regression for identifying independent predictors of change in LV diastolic function grade

Variable	Coefficient (95% CI)	P-value
E/E Lat (screening)	-0.54 (-0.75, -0.33)	**<0.001**
Age	0.47 (0.02, 0.92)	0.04
Bun blood urea nitrogen (mmol/l)	0.46 (0.19, 0.72)	**0.001**
LV 3D ejection fraction (%) (**)	0.60 (0.25, 0.95)	**0.001**

The results of the selection procedure indicated that, as in the univariate analyses, all of LV E/E' lat at screening, blood urea and LV 3D ejection fraction were statistically significant. In addition, age was also found to besignificant. This was not significant in

the univariate analyses, but after adjusting for the other variables in the final model, this variable was now statistically significant.

LV E/E' lat at screening was negatively correlated with the change in LV E/E' lat, with a one-unit increase in LV E/E' lat at baseline was associated with a change that was 0.47 units lower. Age, blood urea and LV 3D EF were all positively associated with the change in LV E/E' lat. A 5% increase in ejection fraction was associated with a 0.6 unit increase in the change in LV E/E' lat.

After adjusting for the effects of these four variables, no further variables were found to be statistically significant.

4.7.6. Change in TRV Groups

An examination of the change in tricuspid regurgitant velocity from screening to follow up was performed. The results are provided on figure 3. Subsequently, univariate analysis was performed in order to demonstrate the individual association between each factor and the change in tricuspid regurgitant velocity. The results suggested that there was no strong evidence that any of the variables examined was strongly associated with the change in TRV. However, there was a small amount of evidence that creatinine was associated with the change in TRV ($p=0.05$). Higher creatinine values were associated with a greater change in TRV. A 10-unit increase in creatinine was associated with a 0.02 m/s increase in TRV.

When multivariate analysis was performed, only creatinine was slightly associated with the change in TRJV. After adjusting for this variable, no further variables were statistically significant.

Chapter 5: Associations with short term clinical outcomes

Chapter 5 Associations with short term clinical outcomes

5.1. Associations with short term clinical outcomes

The aim of this chapter is to analyse how the level of LV diastolic dysfunction is associated with three patient outcomes.
The factors of interest were a measure of the patient's diastolic dysfunction. This was assessed in two different ways. Firstly the LVDD at screening was used, and secondly the change in LV diastolic dysfunction from screening to follow-up. Diastolic dysfunction at screening was originally measured in three categories (none, grade I, grade II) (Nagueh et al., 2009a). However, there were only a small number of grade II patients, and so these were combined with the class I patients for the purposes of analysis. The change in LV DD was categorised as patients worsening their dysfunction (i.e. a higher grade), or there being no change or improved dysfunction.

The first set of analyses examined if the LV DD groups differed in terms of the demographics of the patients in each group. This was examined, as if there were differences between groups, then these differences could potentially confound the relationships between dysfunction and the outcomes.

The next analyses examined the associations between the LV DD measures and the three patient outcomes. The patient outcomes were increased NYHA class, the number of hospital admissions and a high TRV value at follow-up (≥2.5 m/s) .

For each outcome two sets of analyses were performed. Initially a simple analysis was performed to examine the association between LV DD and the outcome. Subsequently regression methods were used to examine the same relationships, but this time to adjust for potentially confounding variables, where necessary.

Increased NYHA class and a high TRV value were binary outcomes. Therefore, the initial analyses were performed using Fisher's exact test, with logistic regression used for the subsequent analysis. For the TRV outcome, an additional adjustment was made in the regression analyses for TRV category at screening, because it is likely that patients with high TRV values at follow-up might also have high TRV values at baseline.

The number of admissions were measured on a continuous scale, and were found to have a highly skewed distribution, which could not be transformed to normality. Therefore, the Mann-Whitney test was used for the initial analyses, and Poisson regression used for the further analyses. This is a regression method suited to positively skewed data.

5.1.1. Association between diastolic dysfunction and possible confounding variables

The analyses were initially performed to compare between the LV DD at baseline categories, and the results are summarised in table 5.1. The results suggested that there was a significant difference between the two LV diastolic dysfunction groups in terms of their age and body mass index (BMI). Patients with class I or II dysfunction were older and had higher BMI values. Additionally patients with class I or II dysfunction were more likely to use hydroxyurea, although this result was not quite statistically significant. As there were some evidence of a difference between the two groups for these factors, it was necessary to consider adjusting for these factors in the subsequent comparison between the two groups.

Table 5.1 - Association of potential confounding factors with Left ventricular diastolic function groups.

Variable	No LV DD(n=43) Mean (SD) or N(%)	LV DD grade I /II (n=18) Mean (SD) or N(%)	P-value
Age (years)	36.0 (10.4)	50.4 (8.3)	**<0.007**
Male gender	19 (44%)	8 (44%)	1.00
BMI (kg/m^2)	23.6 (3.2)	26.1 (4.0)	**0.01**
Systolic blood pressure (mmHg)	118.2 (11.3)	122.6 (19.5)	0.27
Hydroxyurea (current use)	7 (16%)	7 (39%)	0.09

A similar set of analyses was performed to compare the demographics of patients who had worsening LV DD between baseline and follow-up, and those whose LV DD showed no change or was better. No significant differences between the two groups in terms of the patient demographics were found. As there were no differences between the two groups for these factors, it was not necessary to consider adjusting for any of the demographic factors in the subsequent comparison between the two groups.

5.1.2. Increase in NYHA

It was investigated how LV diastolic dysfunction variables were associated with whether there was an increase in New York Heart Association class (NYHA) from screening to follow-up. The data suggested that of the 61 patients, there was an increase in NYHA class in 13 patients (21%), and no change in the remaining 48 patients. The results are demonstrated on Table 5.2. The results indicated that there was no association between the LV dysfunction at screening and the change in NYHA class. However, there was a significant association between the change in LV dysfunction and the change in NYHA class. Patients with worsening LV dysfunction from screening to follow-up had a higher likelihood of an increase in NYHA class. 70% of patients in this group had an increase in class, compared to only 12% of patients whose LV dysfunction did not worsen.

Table 5.2 - Associations between LV diastolic dysfunction change and NYHA functional class.

Variable	LV DD grade	NYHA no change N (%)	NYHA increase N(%)	P-value
LV diastolic dysfuntion at Screening	None	33 (77%)	**10 (23%)**	0.74
	Class I/II	15 (83%)	3 (17%)	
Change in LV diastolic dysfunction	Same / no change	45 (88%)	6 (12%)	**<0.001**

Worsening	3 (30%)	7 (70%)

Logistic regression was employed to analyse the same relationships. After adjusting for potentially confounding variables, there was little change in the difference in outcome between those with and without LV DD at screening. Patients with a change in LV DD were again at an increased risk of an increase in NYHA class. ($p<0.001$).

5.1.3. Number of admissions

The next set of analyses examined how diastolic dysfunction was associated with the number of admissions. The number of admissions was found to have a positively skewed distribution. Initially a simple comparison of the number of admissions between dysfunction groups was made and the results suggested that there was no significant difference in the number of admissions depending on patients LV DD at screening, or on their change in dysfunction from screening to follow-up.

Regression analysis examined the association between LV DD and the number of admissions. The analysis results are summarised in the Table 5.3. Due to the analysis used, the differences between groups are reported in the form of ratios. These are given as the number of admissions in patients with dysfunction relative to the number in patients without dysfunction. The results for dysfunction in screening suggested no significant difference when potentially confounding variables were not considered. However, after adjusting for age, BMI and hydroxyurea, there was now slight evidence of an association, although this result was only of borderline statistical significance ($p=0.06$). Patients with LV DD at screening (grade I or II) had a larger number of admissions, around twice as many as patients without LV DD at screening. There was again no evidence of an association between the change in diastolic dysfunction and the number of admissions.

Table 5.3 - Associations between LV diastolic dysfunction change and NYHA functional class.

Variable	Adjustments	Ratio (95% CI)	P-value
LV diastolic dysfunction at screening	None	1.24 (0.76, 2.02)	0.38
	Age, BMI, hydroxurea	1.97 (0.98, 3.97)	0.06
Change in LV diastolic dysfunction grade	None	0.91 (0.47, 1.78)	0.79

5.1.4. Increase in tricuspid regurgitant velocity

The final set of analyses examined if the measures of dysfunction were associated with TRV ≥ 2.5m/s at follow-up. Initially a simple analysis was performed using Fisher's exact test, and the results are summarised in Table 5.4. The results indicated that LV DD at screening was significantly associated with TRV at follow-up. Patients with class I/II dysfunction had a higher occurrence of TRV above 2.5. 72% of patients with dysfunction had a high TRV value, compared to only 35% of patients with no dysfunction.

There was no significant association between the change in LV DD and the TRV category at follow-up. Logistic regression was further used to examine the association between dysfunction and TRV, adjusting for potentially confounding variables. The analyses were performed unadjusted, and then adjusted for TRV category at screening. Additional adjustments were made for three potentially confounding demographics as well as for LV DD at screening.

Table 5.4 - Associations between LV diastolic dysfunction change and NYHA functional class.

Variable	Adjustments	Odds Ratio (95% CI)	P-value
Dysfunction at screening	None	4.85 (1.45, 16.2)	**0.01**
	TRV at screening	2.52 (0.57, 11.2)	0.22
	Age, BMI, hydroxurea	2.42 (0.36, 16.5)	0.37
Change in dysfunction	None	1.98 (0.50, 7.87)	0.33
	TRV at screening	1.16 (0.20, 6.70)	0.87

The results of the unadjusted analysis suggested that patients with dysfunction at screening were significantly more likely to have a high TRV value. The difference between the two groups was no longer found to be significant after adjusting for whether the patient had a TRV above 2.5 at screening. Although the result was no longer statistically significant, those with LV DD had a higher occurrence of a high TRV value at follow-up.

Furthermore, there was no significant association between the change in dysfunction and a high TRV value, both before and after adjusting for the TRV category at baseline.

5.2. Associations between haemolysis markers and patients outcomes

The association between the haemolysis markers (haemoglobin, lactate dehydrogenase, reticulocytes and total bilirubin) and the patients´ outcomes was assessed by comparing the values of the markers between outcome groups. For haemoglobin, which was normally distributed, the unpaired t-test was used for the analyses. For the three remaining markers, with skewed distributions, the Mann-Whitney test was used for the analyses. The fourth outcome, number of hospital admissions, was measured on a continuous scale, and was found to be heavily positively skewed in its distribution. As a result, Spearman's rank correlation was used to examine the association with the markers.

Table 5.5 - Associations between haemolysis markers and TRV category at follow-up.

Haemolysis Marker	TRJV < 2.5 m/s	TRJV ≥ 2.5 m/s	P-value
Haemoglobin	9.2 (1.5)	9.1 (2.0)	0.74
Lactate dehydrogenase	317 (269, 418)	387 (319, 636)	0.05
Reticulocytes	7.6 (3.9, 12.4)	8.4 (5.3, 11.7)	0.73
Total Bilirubin	32 (15, 60)	41 (28, 82)	0.05

The results suggested that none of the four markers of haemolysis was significantly associated with the change in NYHA class, number of admission and change in diastolic

dysfunction. As expected, the results suggested slight evidence that both LDH (p=0.05) and bilirubin (p=0.05) were associated with TRV category at follow-up (Table 5.5). However, both results were only of borderline statistical significance. Patients with a high TRV value had higher LDH and higher bilirubin values than patients with lower TRV values.

Chapter 6: Reproducibility Study

Chapter 6 Reproducibility Study

6.1. Reproducibility Data for 3D Left Ventricular Strain analysis

A group of 37 patients (randomly selected) with SCD underwent a series of 3D strain measurements for the assessment of inter-observer, intra-observer and test re-test of the LV Strain variables. Data sets measurements and analysis were performed at least 2 weeks apart in random order.

6.1.1. Inter-observer variability

A second observer (J.G.) with equal experience in echocardiography performed the measurement of inter-observer variability of 3D- left ventricular strain analysis. The analysis consisted of 37 patients.

Left ventricular volumes, ejection fraction and stroke volume

As is demonstrated in Fig. 6.1 the results of the original evaluation and those from observer 2 are lower when compared to the first observer. Rather than being distributed evenly around the fitted line (which shows equal values for the two observers), for most outcomes the second observer seems to have values which are consistently higher or lower.

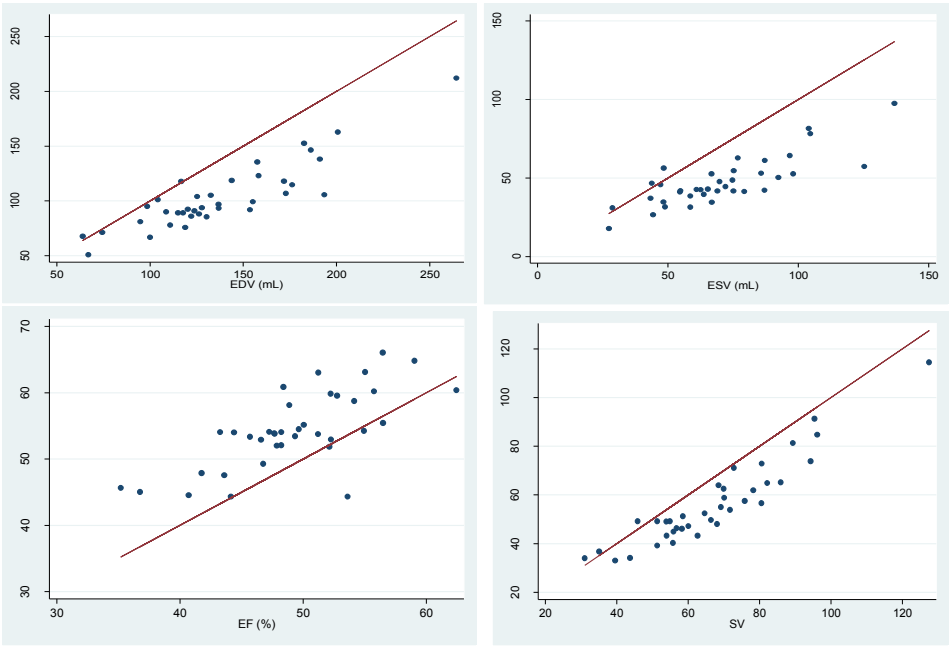

Fig. 6.1 – Reliability of left ventricular volumes, ejection fraction and stroke volume measurements by linear regression.

Bland-Altman graphs, as demonstrated on figure Fig. 6.2, employ the inter-observer agreement for LV end-diastolic volume (EDV), LV end-systolic volume (ESV), LV stroke volume and LV ejection fraction.

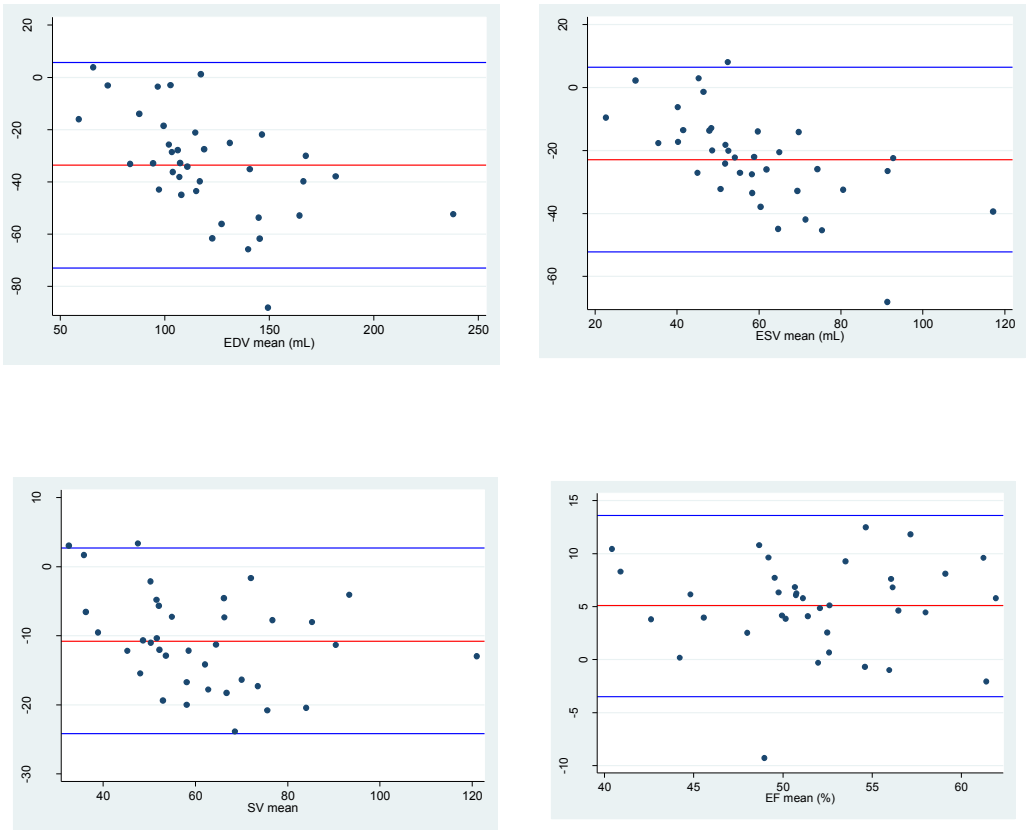

Fig. 6.2 - Inter-observer agreement for LV end-diastolic volume (EDV) , LV end-systolic volume (ESV), LV stroke volume (SV), LV ejection fraction (EF) for the same values (N = 37 patients)
LV global longitudinal strain, LV twist (Twist), LV torsion (Torsion), LV 3D strain (3D strain)

Fig. 6.3 demonstrates the inter-observer agreement for LV strain variables (Global, 3D Strain, Circumferential, Longitudinal and Radial), LV twist (Twist), LV torsion.

The mean difference between measurements is shown along with the Bland-Altman limits of agreement. The Bland-Altman results suggest that generally there were mean differences between the results from the two observers. This suggests that there was consistent tendency of one or both observers to under or overestimate the results.

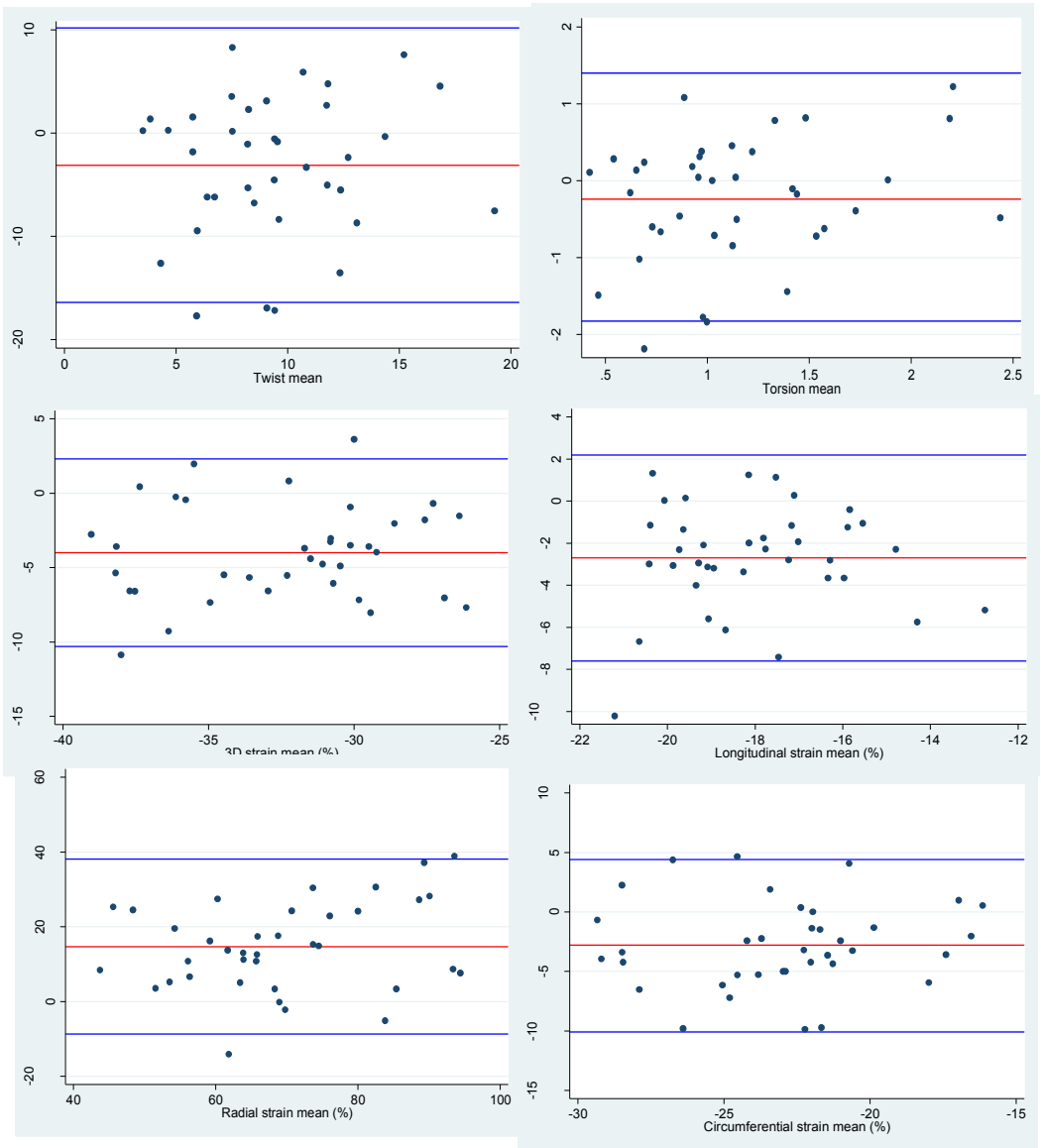

Fig. 6.3 - Inter-observer agreement for LV LV twist (Twist), LV torsion, LV strain variables (3D Strain, Longitudinal, Circumferential and Radial), for the same values (N = 37 patients)

The ICC value is also reported using both methods in the table 6.1. The ICC values suggest that using the first (more standard) method the ICC values were all fairly poor, with values generally below 0.6. There was relatively good agreement for LV SV with an ICC value over 0.9, and a relatively high value for LV EDV. However, the agreement was not so good for the other variables. The agreement was especially poor for twist and torsion, and also not very high for any of the 4 strain variables.

Variable	Label	Bland-Altman Results		ICC	
		Mean difference	95% B-A limits	Method 1 (†)	Method 2 (††)
EDV	LV 3D end diastolic volume (ml)	-33.60	(-73.0, 5.7)	0.59	0.85
ESV	LV 3D end systolic volume (ml)	-22.90	(-52.2, 6.5)	0.45	0.73
SV	LV 3D Stroke volume (ml)	-10.80	(-24.2, 2.7)	0.79	0.93
EF	LV 3D ejection fraction (%)	5.10	(-3.5, 13.6)	0.52	0.72
GLS	Global longitudinal strain (%)	-2.40	(-6.9, 2.0)	0.38	0.57
Twist	3D LV strain twist (degree)	-3.10	(-16.4, 10.2)	0.05	0.06
Torsion	3D LV strain torsion (degree/cm)	-0.24	(1.83, 1.40)	0.18	0.19
3D strain (*)	LV 3D Strain (Area strain)	-4.00	(-10.3, 2.3)	0.48	0.70
Circumferential strain (*)	LV 3D Circumferential global strain	-2.80	(-10.1, 4.4)	0.46	0.57
Longitudinal strain (*)	LV 3D Longitudinal global strain	-2.70	(-7.6, 2.2)	0.26	0.42
Radial strain (*)	LV 3D Radial global strain	14.70	(-8.7, 38.1)	0.48	0.69

Table 6.1 – Inter-observer reliability of left ventricular volumes and function measurements using 3D speckle tracking echocardiography

6.1.2. Intra-observer variability

Both the Bland-Altman and ICC methods were used to examine the agreement between the original and the repeat measurements, and the results are summarised in Table 6.2.

Variable	Bland-Altman Results		ICC
	Mean difference	95% B-A limits agreement	
LV 3D end diastolic volume (ml)	0.10	(-16.7, 17.0)	0.98
LV 3D end systolic volume (ml)	-0.20	(-15.9, 15.4)	0.95
LV 3D Stroke volume (ml)	0.30	(-6.2, 6.9)	0.99
LV 3D ejection fraction (%)	0.10	(-6.1, 6.4)	0.86
Global longitudinal strain (%)	0.10	(-3.2, 3.4)	0.78
3D LV strain twist (degree)	-0.60	(-13.3, 12.1)	0.31
3D LV strain torsion (degree/cm)	-0.05	(-1.51, 1.40)	0.39
LV 3D Strain (Area strain)	-0.10	(-5.5, 5.3)	0.80
LV 3D Circumferential global strain	-0.10	(-5.3, 5.2)	0.78
LV 3D Longitudinal global strain	0.00	(-3.7, 3.6)	0.73
LV 3D Radial global strain	-1.20	(-24.2, 21.8)	0.81

Table 6.2 – Intra-observer reliability of left ventricular volumes and function measurements using 3D speckle tracking echocardiography

The Bland-Altman results suggest that generally there were little average differences between the two sets of results. This suggests that there was no consistent tendency for the repeat measurements to be higher or lower than the original measurements.

The ICC values suggest very good agreement for LV EDV, ESV and SV, with values over 0.9. There was also a relatively high value for EF. However, agreement was poor for twist and torsion, with ICC values of less than 0.4. Agreement was moderate, although not that strong, for the strain variables, with the ICC values typically around 0.8.

6.1.3. Test re-test reproducibility

A group of patients with SCD underwent a series of 3D strain measurements. These patients were then re-tested one hour after the first set of acquisitions. The aim of the analysis was to examine the agreement between the two sets of measurements. All 3D strain outcomes were measured on a continuous scale. Table 6.3 summarises the test retest analysis results.

Variable	Bland-Altman Results		ICC
	Mean difference	95% B-A limits agreement	
LV 3D end diastolic volume (ml)	-1.40	(-24.6, 21.8)	0.96
LV 3D end systolic volume (ml)	0.20	(-17.1, 17.4)	0.93
LV 3D Stroke volume (ml)	-1.60	(-14.1, 10.9)	0.94
LV 3D ejection fraction (%)	-0.70	(-7.8, 6.4)	0.77
Global Longitudinal strain (%)	0.20	(-3.0, 3.5)	0.71
3D LV strain twist (degree)	-1.60	(-14.9, 11.8)	0.16
3D LV strain torsion (degree/cm)	-0.20	(1.76, 1.37)	0.18
LV 3D Strain (Area strain)	0.00	(-5.6, 5.6)	0.76
LV 3D Circumferential global strain	0.20	(-7.0, 7.5)	0.55
LV 3D Longitudinal global strain	0.20	(-3.1, 3.5)	0.67
LV 3D Radial global strain	-1.00	(-27.5, 25.6)	0.65

Table 6.3 – Test re-test reliability of left ventricular volumes and function measurements using 3D speckle tracking echocardiography

Test retest agreement was very poor for twist and torsion and moderate for circumferential, longitudinal and radial strain. LV 3D strain (area strain) had the best ICC value reflecting good reliability.

6.2. Agreement for 4D Right ventricle volumes

A group of 56 patients with SCD (randomly selected) underwent a series of 3D strain measurements for RV volumes. Data sets measurements and analysis were performed at least 2 weeks apart in random order. As for the LV 3D strain analysis, these patients were then re-assessed by the same observer again, retest again, and also observed by second observer. The aim of the analysis was to examine the agreement between the various measurements.

6.2.1. Inter-Observer Agreement

The agreement analyses were repeated for this data, and the results are shown in the table 6.4. The results suggested that for diastolic volume, the second observer tended to give values that were slightly higher than the first observer, with a mean difference of 5ml. There was also a slight difference for systolic volume, but little average difference for ejection fraction.

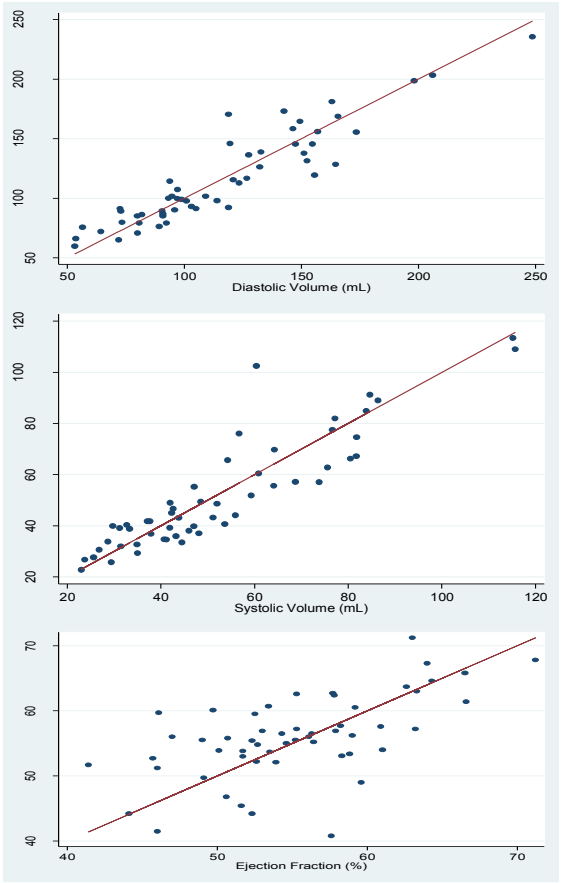

Fig. 6.4 - Reliability of right ventricular volumes and ejection fraction measurements by linear regression.

The ICC values for diastolic and systolic volume were very high, suggesting very good agreement between the two observers, with values of 0.95 or higher. There was a much lower value for ejection fraction, suggesting fairly poor agreement between the two observers.

Table 6.4 - Inter-observer, intra-observer and test re-test reliability of right ventricular volumes and function measurements using 4D echocardiography.

Inter-observer agreement	**Bland-Altman Results**		**ICC**
	Mean difference	**95% B-A limits**	
Right Ventricular end-diastolic volume (ml)	5.10	(-15.8, 26.1)	0.96
Right Ventricular end-systolic volume (ml)	2.00	(-11.0, 15.0)	0.95
RV 4D Ejection Fraction (%)	-0.20	(-10.1, 9.7)	0.60
Intraobserver agreement	**Bland-Altman Results**		**ICC**
	Mean difference	**95% B-A limits**	
Right Ventricular end-diastolic volume (ml)	-0.10	(-30.9, 30.7)	0.92
Right Ventricular end-systolic volume (ml)	-0.70	(-19.8, 18.3)	0.90
RV 4D Ejection Fraction (%)	0.70	(-10.3, 11.8)	0.61
Test-re test agreement	**Bland-Altman Results**		**ICC**
	Mean difference	**95% B-A limits**	
Right Ventricular end-diastolic volume (ml)	-0.40	(-40.8, 40.0)	0.86
Right Ventricular end-systolic volume (ml)	-0.10	(-21.5, 21.3)	0.85
RV 4D Ejection Fraction (%)	-0.20	(-11.5, 11.1)	0.45

6.2.2. Intra-observer agreement

The initial graphs suggest that the agreement between the two sets of results of the two observers is quite high for systolic and diastolic volume, as the values typically lie close to the fitted line (which shows equal values for the two measurements). The agreement appears less good for ejection fraction, where the values are scattered further away from the line of equality.

The ICC values suggest that there was good agreement between the two measurements for diastolic and systolic volume, with high values of 0.9 or higher (Table 6.4). There was poor agreement for ejection fraction, with the value of 0.6 suggesting that a relatively large proportion of the total variation was due to differences of repeat measurements of the same patients.

The result can be also be displayed graphically in a series of Bland-Altman plots, which plot the differences in the pairs of values against the average of the two values. The Bland-Altman graphs suggest that generally there was little average difference between the two sets of measurements. This suggests that the second measurements were not consistently higher or lower than the first.

6.2.3. Test-Retest Agreement

The results suggested little average difference between the two sets of measurements, which implies no consistent bias in the results. The width of the limits of agreement were slightly wider than those obtained for the intra-observation variation. The ICC values (Table 6.4) were relatively high for diastolic and systolic volume, although low for ejection fraction. The ICC value below 0.5 suggests that there was more variation between repeat measurements of the same patient than there was between patients.

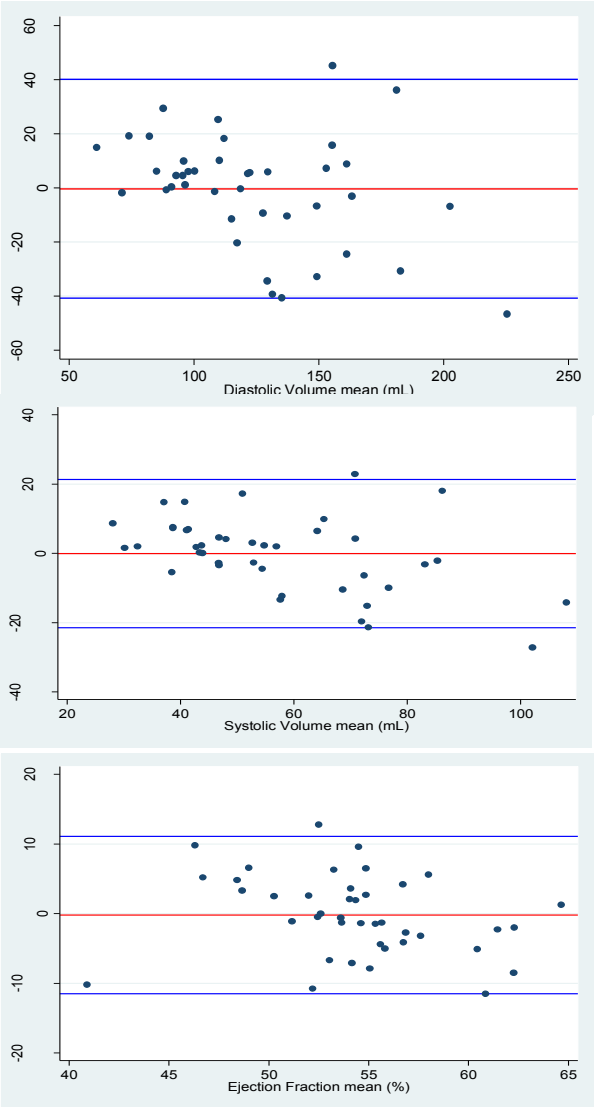

Fig. 6.5 - Test re-test agreement for RV volumes and ejection fraction by 4D echocardiography, for the same values (N = 56 patients)

6.3. Comparison between LV 2D speckle tracking and 3D speckle tracking for myocardial deformation

A subgroup of 52 randomly selected patients with SCD had LV strain measures using two methods: 2D and 3D speckle tracking .The aim of the analysis was to examine the agreement between the two modalities.

Table 6.5 – Mean difference between 2D Strain and 3D Strain parameters according to Longitudinal and Circumferential showing Bias between the methods.

	Mean ± SD	*p* value	BIAS (%)	Limit of agreement	ICC (95% CI)
LV_2DLSTbasalAvg	-16.29 ± 3.27	0.14	0.76 (5%)	3.63 (22%)	0.41
LV_2DLSTmedianAvg	-19.14 ± 3,49	**0.000**	-2.60 (14%)	3.91 (20%)	0.15
2DLSTApicalAvg	-17.08 ± 3,80	0.32	-0.67 (4%)	4.79 (28%)	0.11
LV_2DLongglobalST	-30.50 ± 2.54	**0.003**	-13.82 (45%)	2.77 (9%)	0.02
LV_2DCSTbasalAvg	-23.29 ± 7.32	**0.000**	-6.76 (29%)	7.37 (32%)	0.13
LV_2DCSTmedianAvg	-25.63 ± 9.32	0,06	-3.91 (15%)	14.32 (56%)	-0.10
LV_2DCSTApicalAvg	-29.97 ± 12.61	**0.000**	-7.28 (24%)	15.36 (51%)	-0.07
LV_2DCircunfglobalST	-26.08 ± 6.72	0.16	-4.71 (18%)	7.36 (28%)	0.10

Table 6.5 presents the difference between 2D and 3D measures (2D mean - 3D mean), the standard deviation of the difference, the confidence interval of the difference and the result of hypothesis testing that the mean value of 2D measure is the same as the mean value of 3D measure. If the mean of 2D measure is the same as the mean of 3D measure, one would expect to observe a small mean difference (positive or negative), zero within confidence interval and a *p* value greater than 0.05.

If the *p* value is less than 0.05 that means the 2D mean is not the same as 3D mean. Paired t-test has been used for this hypothesis testing as each patient provides both 2D and 3D measures. About half of the measures in the above table have *p* value less than 0.05 and hence suggest that the mean difference between 2D and 3D methods are statistically significant. There are only 6 segments (19%) that have significant but weak agreement between 2D and 3D evaluation method.

Chapter 7: Discussion

Chapter 7 Discussion

7.1. Retrospective survival study

Raised tricuspid regurgitant velocity occurs in approximately 30% of adults with sickle cell disease and has been shown to be an independent risk factor for death. In our 5 year retrospective follow-up study of adults with sickle cell disease, TRV was assessed in 164 SCD patients who were subsequently followed up for survival (Zimbarra Cabrita et al., 2013a). Higher values of TRV were associated with a greater than 4 fold increased risk of death (HR: 4.48, 99%CI 1.01-19.8), although we showed a lower overall mortality rate (16.67% in patients with a TRV ≥2.5 m/s) than has been shown in previous studies. Importantly, in our cohort TRV was not an independent risk factor for death. We have confirmed the association between raised TRV and mortality in a UK SCD population whose disease severity appears to be less than that reported in previous studies (Gladwin et al., 2004, Sutton et al., 1994).

Castro et al. (Castro et al., 2003) in a study with 34 adults patients, reported a 2 year mortality rate of 55% in patients with a raised mean pulmonary artery pressure (> 25 mmHg) obtained by right heart catheterisation, compared to a mortality rate of 21% in SCD without raised mean pulmonary artery pressure (≤25 mmHg) .

Two older studies also reported increased mortality. Sutton et al found that a raised TRV was associated with a 40% mortality rate at 22 months in 60 patients, with an odds ratio for death of 7.86 (2.63-23.4) (Sutton et al., 1994). Powars et al found a mean survival of 2.5 years in patients with chronic lung disease and elevated TRV (Powars et al., 1988).

In order to extend our analysis, we have re-analysed the data using the conservative cut off value of TRV ≥ 3 m/s. Interestingly, we have found no change in the results. Of the 164 patients included in our study, only 10 patients (6, 1%) had a TRV value of 3.0 m/s or higher. Using the same time point as Gladwin´s Study (24 months) we have found similar survival estimates of 99% for TRV<3.0 m/s and 80% for TRV≥3.0 m/s. Nonetheless, using a time point of 68 months, there was no significant difference (p=0.125) in the survival estimates: 95% for TRV<3.0 m/s and 80% for TRV≥3.0 m/s.

We also found that patients with higher TRV values had a higher risk of death (HR: 6.52; 95% CI 2.97-20.6; p=0.001) when other factors are not considered (in comparison to a HR of 11.14 found in Gladwin's Study). However, this risk disappears after adjustment for other variables associated with survival.

There was no significant difference in the sickle cell genotypes between the two studies (HbSS p=0.45; HbSC p=0.7; *HbS β thalassemia* p=0.68) and no significant difference in the mean TRV (p=0.15). In both studies the overall number of deaths was small which is reflected by the width of the CI for TRV ≥2.5 m/s relative to TRV<2.5 m/s. This means that the true hazard ratio in Gladwin's study could be from 2.2 to 47 (p<0.001), whereas in our study the limits are from 0.71 to 10.4 although not significant (p=0.06). One explanation could be that the National Health Service in the UK ensures that health care is free at the point of access and this may lead to patients with milder phenotypic disease being more likely to attend outpatients clinic and increase the number of patients with milder disease (and lower mortality) in the UK cohorts. On the other hand, we speculate that easier NHS access to specialist sickle cell centres in the UK may result in better outcomes in terms of severity and overall quality of life.

In addition, the mortality figures from the US data seem very high when compared with the UK experience. Although there are not sufficient longitudinal data for mortality of patients with SCD in the UK. The recent National Confidential Enquiry into Patient Outcome and Death (Lucas et al., 2008), report which collected data on all deaths in patients with haemoglobinopathies between January 2005 and December 2006, had only 81 reported deaths, which in an estimated population of 12,000 for SCD in the UK, is a very low mortality rate. In essence, the reasons for this difference in mortality with United States cohorts is not explained by the clinical measurements which were made and further studies to confirm our findings are necessary.

In conclusion, we have confirmed the association between raised TRV and mortality in a UK SCD population attending two North West London specialist SCD centres, whose disease severity appears less than that reported in previous studies.

7.2. Prospective study – heart characterisation

In the prospective study, the mean follow-time was 17.13±3 months with a range of 10-23 months. The prevalence of increased TRV defined as a TRV≥ 2.5 m/s, was 51% at baseline and 45% at follow-up. We have decided to use TRV as a dichotomous variable, following the methodology of several previous studies ((Parent et al., 2011, Fonseca et al., 2012, Gladwin et al. 2004), allowing for the possibility of groups comparison (high and low TRV) to assess associations between clinical and echocardiographic parameters.

In our study cohort, no significant change in the usage of hydroxyurea or participation in a chronic transfusion program was found between the two time points. In addition, as has been previously described we have found a tendency for the association of history of lung problems (e.g. asthma, COPD, bronchitis, emphysema, pneumonia, tuberculosis) with increased TRV. These independent factors may have contributed to the development of PH in this population, but the results were not statistically significant.

2D echocardiography, pulsed-wave Doppler-derived mitral and tricuspid inflow velocities, as well as DTI, were used to assess cardiac structure and function in adult patients with SCD and in race-age matched controls.
Compared with the control group, subjects with SCD had larger LA and RA volumes, increased LV mass and LV volumes. Furthermore, LA dilatation was severe in 64% of the patients.
Also, right heart chambers were larger in the SCD subjects compared to controls, where 48% of the patients had increased RV end-diastolic volume.
Although the presence of left ventricular diastolic dysfunction in patients with SCD is well established, it is not clear whether they have subtle LV systolic dysfunction despite preserved ejection fraction. In our study, we used three-dimensional speckle tracking echocardiography to assess changes in both systolic and diastolic LV function and it demonstrated minor differences between patients and controls regarding LV strain. These results are in agreement with previous studies where global LV systolic function was not only preserved but increased compared to controls (Ahmad et al., 2012).

Additionally, RV longitudinal strain was universally increased in all free wall segments and significantly different from the healthy subjects. This was the first study to use 3DSTE for the evaluation of systolic LV function in patients with SCD in UK.

As expected, parameters of LV and RV function were normal in both groups and increased stroke volumes and cardiac output were found among patients with SCD. The results suggested that chronic anaemia and the increased intravascular volume in patients with SCD, are primarily contributing factors for the findings regarding cardiac structure and systolic function. It is well known that the increasing circulating blood volume due to chronic anaemia in SCD (Bunn, 1997, Varat et al., 1972, Raphael, 2005).

7.3. Increase in LV lateral E/E´ratio during follow up

Echocardiographic estimation of pulmonary artery pressure by measuring the tricuspid regurgitant jet velocity has been validated as a useful screening method for pulmonary hypertension in adult patients with sickle cell disease (Gladwin et al., 2004). A TRV of 2.5 m/sec or more has been used for research purposes to define elevated pulmonary artery pressure in adults with sickle cell disease (Kenneth I. Ataga, 2006). The prevalence and natural history of elevated jet velocity in adults with sickle cell disease at steady state are mostly unknown, despite the mild elevations in pulmonary artery pressure that have been reported.

In subjects with SCD, a positive correlation was found between TRV and LV end diastolic volume. LV lateral E/E´, an important estimator of increased left ventricular filling pressures, was strongly correlated with age, as expected but no association with haemolysis markers was found which may suggest that cardiac adaptations to anaemia have more of an effect on diastolic function than direct effects of haemolysis. These findings are consistent with the study by Sachdev et al (Sachdev et al., 2007) .

In our study, with a prevalence of LV DD of 29.5 %, as assessed by Doppler echocardiography, we have shown that a patient with LV DD had five times more risk of developing pulmonary hypertension. Of note, these patients had diastolic dysfunction based on current guidelines (Nagueh et al., 2009a), using 2D and Doppler criteria, and the prevalence of diastolic dysfunction was considerably higher than reported in previous studies using older criteria.

Furthermore, in this study, elevations of both TRV and LV lateral E/E´ ratio were associated with NYHA functional severity.

This SCD study confirms independent associations of increased TRV with elevated LV filling pressure. Renal dysfunction may have an important role in contributing to LV diastolic dysfunction in SCD patients. In mean pulmonary artery pressure addition we have found slight evidence that creatinine was associated with the change of TRV group (≥2.5 m/s) at follow-up. The vascular involvement of the microvascular circulation where the sickling process takes place may explain specific haemodynamics alterations and arterial stiffness in SCD may warrant further investigations. Furthermore, the independent association of increased blood urea nitrogen and global function index lateral with an increased LV lateral E/E´ ratio is consistent with previous reports (Gordeuk et al., 2008) suggesting an association of renal disease with LV diastolic dysfunction which may lead to elevated pulmonary pressures.

Our present findings confirm that echocardiographic markers of LV DD are prevalent in SCD and point to independent associations of older age, worse haemoglobin levels, and elevated left atrial volume index with an elevated LV lateral E/E´ratio.

The results are supportive of echocardiographic screening for increased tricuspid regurgitation and early identification of LV diastolic dysfunction, a marker of increased mortality in adults with SCD (Sachdev et al., 2007). These observations may have functional and prognostic relevance in terms of assessing sub-clinical identification of early myocardial impairment.

7.4. Ventricular myocardial deformation

Several studies have used 2DST to assess myocardial strain in different pathologies. 2DSTE can only track motion within the imaging plane, while through-plane motion adversely compromises endocardial tracking when speckles move out of imaging plane (Kleijn et al., 2012a) the accuracy of this technique becomes limited. 3D speckle tracking echocardiography has been initially applied to the left ventricle and used for the myocardial motion analysis that aims to overcome the limitations of 2D speckle tracking

(Abate et al., 2012, Gorcsan and Tanaka, 2011). It proved excellent reproducibility with CMR left ventricular ejection fraction (Kleijn et al., 2012b) and also it has proven predictive value in patients who recover from myocardial infarction (Abate et al., 2012). From the current literature, 3D speckle tracking appears to be superior to 2-dimensional speckle tracking and it is promising for the regional myocardial analysis of the left ventricle. Furthermore, our finding concerning the poor agreement between LV 2D strain and 3D strain, confirm that careful use of 2D strain data must be take into consideration, in particular in dilated chambers, which is very frequent in SCD.

Our hypothesis was that this novel methodology could detect subtle changes in systolic myocardial deformation, which may presumably be present in these patients despite preserved LV EF. Our results have shown a significant decrease in all global LV strain parameters from baseline to follow-up. Such early signs of systolic dysfunction could potentially be used to predict which patients are likely to develop more overt systolic dysfunction in the future.

As in several studies that reported normal systolic function in patients with SCD (Westwood et al., 2007, Ahmad et al., 2012), in our patients, global systolic function was not only preserved but there was even a tendency for increased values when compared to healthy volunteers. This may be explained by compensatory mechanisms within the cardiovascular system aimed at maintaining adequate oxygenation in the anaemic patients.

7.5. Reproducibility study

This study assessed the different components of strain values in 16 LV segments, by using newly developed 3D strain imaging, and comparing the data with those measured by conventional 2D strain imaging. Our results showed that the 3D myocardial tracking technique is a simple, feasible, and reproducible method to measure LV strains. However, the mean strain values of 16 segments between 3DT and 2DT showed discordant values in a large number of segments. The reason for these discordant results can be explained by the influence of large LV volumes and increased LVEF. On the other hand, the lower frame rate of 3D technique may have effected the discordance between 3DT and 2DT.

Chapter 8: Conclusions

Chapter 8 Conclusions

8.1. Conclusions and Contributions of this Research Study

This thesis includes two major studies. In the retrospective 5 year-survival study, an association between raised TRV and mortality in a UK SCD population was confirmed. It was found that higher values of TRV were associated with a greater than 4 fold increased risk of death (HR: 4.48, 99%CI 1.01-19.8). However, it showed a lower overall mortality rate than has been shown in previous studies. Importantly, TRV was not an independent risk factor for death and we have confirmed the association between raised TRV and mortality in a UK SCD population whose disease severity appears to be less than that reported in previous studies.

In the prospective study, 61 patients with SCD and 42 healthy volunteers were evaluated with a mean follow-up duration of 17.13±3 months. Significant changes were found between patients and healthy subjects in terms of systolic blood pressure, right and left ventricular structure. Twenty-three percent of the patients had decreased global longitudinal strain, as assessed by 3DSTE. In the serial echocardiographic study, left ventricular average E/E´ ratio was independently associated with an increased tricuspid regurgitation velocity (p=0.007). In addition, blood urea nitrogen and global function index lateral showed independent association with an increased LV lateral E/E´ ratio. Biventricular myocardial deformation by 2D and 3D speckle tracking revealed significant changes in the serial measurements of systolic function. In addition, inter-observer, intra-observer and Test-retest provided good reproducibility and superiority when compared to 2DSTE. 3DSTE is considered as a new tool in the cardiac assessment of SCD that combines the usefulness of wall motion tracking with a better integration of the anatomic structures of the heart. No myocardial fibroses or iron overload was found in the sub-group of patients with LV DD.

These findings provide novel insight into the pathophysiology of the cardiovascular complications of SCD and support the implementation of echocardiographic screening of adult patients with SCD to identify high-risk individuals for further evaluation.

8.2. Limitations of the study

This study had several notable limitations. For the retrospective survival study, the main weakness was in collecting patient records from two different centres with limited access to echocardiographic data. Also, patient´s echocardiograms were requested according to clinical indications, creating a bias in favour of more symptomatic patients, Therefore, the reported prevalence of increased TRV should be interpreted with caution. Also, the echocardiograms were performed with different equipment and the protocol was different in the centres (e.g. left atrial area was not measured in one centre).

For the prospective study important limitations concerning referral bias are important to address. Firstly, the patients were identified through the WALK-PHaSST study where patients that were participating in the interventional study could not take part in my study, potentially excluding patients with increased TRV.

In addition, SCD is a complex genetic disorder with multisystem manifestations and where the conventional cardiac risk factors are powerful risk factors for SCD and may have complex interactions. The stratification of populations based on clinical phenotype and risk factor would be important for the individualized risk assessment in SCD, which has not been done in this study. Another limitation of the study is the fact that the healthy volunteer's values could have been used as reference values for the SCD group. When the healthy volunteers TRV data was analyzed the reference values (Mean±2*SD) were TRV<1,86 m/s and TRV>2,06 m/s. According to SCD patient´s data, only 2 patients had a TRV < 2,06 m/s.

Left ventricle diastolic function

Guidelines for assessing left ventricle diastolic function by echocardiography have been continuously updated and the ability to use the latest recommendations effectively in

SCD population, has been challenging because of loading conditions and anaemia status which my interfere in the results.. In this study, algorithms for interpretation of diastolic grade have been used according to the current Recommendations for the Evaluation of Left Ventricular Diastolic Function by Echocardiography (Nagueh et al, 2009a). This approach has important limitations, since it requires the integration of multiple parameters. Additionally, for the purposes of sample size and power calculation, due to the reduced number of published results in SCD, we have used exclusively the parameter E/E´ average of lateral and septal walls, which may have underestimated the sample size, since its use alone and not integrated with other parameters such as LV E/A, may be not reliable in the SCD population. A meticulous search for the underlying aetiology and precipitant causes of LV diastolic dysfunction is needed for an individualized treatment approach.

Right ventricular assessment

In order to acquire a full-volume dataset that encompasses the complete RV, four high-resolution sub volumes were acquired over consecutive heartbeats in a short breath-hold. These sub volumes were subsequently assembled by the computer to build a complete 3DE dataset. Thus, although RT3DE data acquisition and display are fast (6 to 8 s in the present study), it is not intrinsically Real Time.

In this study, 3DSTE could not be applied for RV strain analyses since its complex anatomy does not allow reliable endocardial tracking of the RV Free wall. 2DSTE has been used to analyse RV myocardial deformation parameters.

3-Dimensional Speckle tracking

One might view the lack of an independent reference technique to compare the 3DSTE-derived measurements as a limitation of our study. As far as myocardial strain is concerned, there is no noninvasive “gold standard” technique that can be used in humans to validate strain in three dimensions.

Another limitation was the fact that we did not use 3DSTE for the assessment of LV diastolic function. The inter-observer variability in measuring the diastolic component

of the strain curves was tested prior to the study starts, and a poor agreement was found.

Cardiac magnetic resonance

The original intention was to include a larger number of patients so that regression analyses could be performed to investigate independent predictors of LV DD. The small sample size that was eventually recruited did not allow this. Moreover, no sufficient data was obtained for a reliable comparison between LV 2D strain and myocardial tagging. Therefore, further studies are needed to confirm the superiority of 2DSE data over that of CMR in the assessment of regional strain.

8.3. Further Research

3-Dimensional Strain Validation

The ability to obtain comparable data with other equipment need to be evaluated. A validation study is currently in place to demonstrate the agreement of different platforms and to establish normal values for LV and RV strain parameters.

Regional heart motion abnormality detection via multiview fusion in cine cardiac MR images would give precise information from several other long-axis image sequence i.e., 2-chamber, 3-chamber and 4-chamber magnetic resonance images.

Finally genomic signatures as potential biomarkers in sickle cell disease maybe clinical useful. Desai et al found that genome-wide gene and miRNA expression profiles were correlated against TRV, yielding 631 transcripts and 12 miRNAs. In addition, support vector machine analysis identified a 10-gene signature including *GALNT13* (encoding polypeptide *N*-acetylgalactosaminyltransferase) that discriminates patients with and without increased TRV with 100% accuracy (Desai et al., 2012).

These genomic signatures may provide a novel approach as a biomarker for increased TRV in patients with SCD.

Chapter 9: References

Chapter 9 References

References

2002. ATS statement: guidelines for the six-minute walk test. *Am J Respir Crit Care Med,* 166, 111-7.

2008. Consensus statement on the management of pulmonary hypertension in clinical practice in the UK and Ireland. *Heart,* 94 Suppl 1, i1-41.

ABATE, E., HOOGSLAG, G. E., ANTONI, M. L., NUCIFORA, G., DELGADO, V., HOLMAN, E. R., SCHALIJ, M. J., BAX, J. J. & MARSAN, N. A. 2012. Value of three-dimensional speckle-tracking longitudinal strain for predicting improvement of left ventricular function after acute myocardial infarction. *Am J Cardiol,* 110, 961-7.

ABBAS, A. E., FORTUIN, F. D., SCHILLER, N. B., APPLETON, C. P., MORENO, C. A. & LESTER, S. J. 2003. A simple method for noninvasive estimation of pulmonary vascular resistance. *J Am Coll Cardiol,* 41, 1021-7.

ACAR, P., MAUNOURY, C., DE MONTALEMBERT, M. & DULAC, Y. 2003. [Abnormalities of myocardial perfusion in sickle cell disease in childhood: a study of myocardial scintigraphy]. *Arch Mal Coeur Vaiss,* 96, 507-10.

AESSOPOS, A., FARMAKIS, D., TSIRONI, M., DIAMANTI-KANDARAKIS, E., MATZOURANI, M., FRAGODIMIRI, C., HATZILIAMI, A. & KARAGIORGA, M. 2007. Endothelial function and arterial stiffness in sickle-thalassemia patients. *Atherosclerosis,* 191, 427-432.

AHMAD, H., GAYAT, E., YODWUT, C., ABDUCH, M. C., PATEL, A. R., WEINERT, L., DESAI, A., TSANG, W., GARCIA, J. G., LANG, R. M. & MOR-AVI, V. 2012. Evaluation of myocardial deformation in patients with sickle cell disease and preserved ejection fraction using three-dimensional speckle tracking echocardiography. *Echocardiography,* 29, 962-9.

AHMED, S., SIDDIQUI, A. K., SADIQ, A., SHAHID, R. K., PATEL, D. V. & RUSSO, L. A. 2004. Echocardiographic abnormalities in sickle cell disease. *Am J Hematol,* 76, 195-8.

AKGUL, F., YALCIN, F., SEYFELI, E., UCAR, E., KARAZINCIR, S., BALCI, A. & GALI, E. 2007. Pulmonary hypertension in sickle-cell disease: comorbidities and echocardiographic findings. *Acta Haematologica,* 118, 53-60.

ALIYU, Z. Y., GORDEUK, V., SACHDEV, V., BABADOKO, A., MAMMAN, A. I., AKPANPE, P., ATTAH, E., SULEIMAN, Y., ALIYU, N., YUSUF, J., MENDELSOHN, L., KATO, G. J. & GLADWIN, M. T. 2008. Prevalence and risk factors for pulmonary artery systolic hypertension among sickle cell disease patients in Nigeria. *Am J Hematol,* 83, 485-90.

ALMEIDA, A. G., ARAUJO, F., REGO, F., DAVID, C., LOPES, M. G. & DUCLA-SOARES, J. 2008. Abnormal myocardial flow reserve in sickle cell disease: a myocardial contrast echocardiography study. *Echocardiography,* 25, 591-9.

ALPENDURADA, F., SMITH, G. C., CARPENTER, J. P., NAIR, S. V., TANNER, M. A., BANYA, W., DESSI, C., GALANELLO, R., WALKER, J. M. & PENNELL, D. J. 2012.

Effects of combined deferiprone with deferoxamine on right ventricular function in thalassaemia major. ***J Cardiovasc Magn Reson,*** **14, 8.**

AMIN, M. G., TIGHIOUART, H., WEINER, D. E., STARK, P. C., GRIFFITH, J. L., MACLEOD, B., SALEM, D. N. & SARNAK, M. J. 2004. Hematocrit and left ventricular mass: the Framingham Heart study. ***Journal of the American College of Cardiology,*** **43, 1276-1282.**

AMUNDSEN, B. H., HELLE-VALLE, T., EDVARDSEN, T., TORP, H., CROSBY, J., LYSEGGEN, E., STOYLEN, A., IHLEN, H., LIMA, J. A., SMISETH, O. A. & SLORDAHL, S. A. 2006. Noninvasive myocardial strain measurement by speckle tracking echocardiography: validation against sonomicrometry and tagged magnetic resonance imaging. ***J Am Coll Cardiol,*** **47, 789-93.**

ANTHI, A., MACHADO, R. F., JISON, M. L., TAVEIRA-DASILVA, A. M., RUBIN, L. J., HUNTER, L., HUNTER, C. J., COLES, W., NICHOLS, J., AVILA, N. A., SACHDEV, V., CHEN, C. C. & GLADWIN, M. T. 2007b. Hemodynamic and Functional Assessment of Patients with Sickle Cell Disease and Pulmonary Hypertension. ***Am. J. Respir. Crit. Care Med.,*** **175, 1272-1279.**

ASAKURA, T., MATTIELLO, J. A., OBATA, K., ASAKURA, K., REILLY, M. P., TOMASSINI, N., SCHWARTZ, E. & OHENE-FREMPONG, K. 1994. Partially oxygenated sickled cells: sickle-shaped red cells found in circulating blood of patients with sickle cell disease. ***Proc Natl Acad Sci U S A,*** **91, 12589-93.**

ATAGA, K. I., MOORE, C. G., JONES, S., OLAJIDE, O., STRAYHORN, D., HINDERLITER, A. & ORRINGER, E. P. 2006. Pulmonary hypertension in patients with sickle cell disease: a longitudinal study. ***British Journal of Haematology,*** **134, 109-15.**

ATAGA, K. I., SOOD, N., DE GENT, G., KELLY, E., HENDERSON, A. G., JONES, S., STRAYHORN, D., LAIL, A., LIEFF, S. & ORRINGER, E. P. 2004. Pulmonary hypertension in sickle cell disease. ***The American Journal of Medicine,*** **117, 665-9.**

ATSUMI, A., ISHIZU, T., KAMEDA, Y., YAMAMOTO, M., HARIMURA, Y., MACHINO-OHTSUKA, T., KAWAMURA, R., ENOMOTO, M., SEO, Y. & AONUMA, K. 2013. Application of 3-dimensional speckle tracking imaging to the assessment of right ventricular regional deformation. ***Circ J,*** **77, 1760-8.**

AUTHORS/TASK FORCE MEMBERS, GALIE, N., HOEPER, M. M., HUMBERT, M., TORBICKI, A., VACHIERY, J.-L., BARBERA, J. A., BEGHETTI, M., CORRIS, P., GAINE, S., GIBBS, J. S., GOMEZ-SANCHEZ, M. A., JONDEAU, G., KLEPETKO, W., OPITZ, C., PEACOCK, A., RUBIN, L., ZELLWEGER, M., SIMONNEAU, G., ESC COMMITTEE FOR PRACTICE GUIDELINES , VAHANIAN, A., AURICCHIO, A., BAX, J., CECONI, C., DEAN, V., FILIPPATOS, G., FUNCK-BRENTANO, C., HOBBS, R., KEARNEY, P., MCDONAGH, T., MCGREGOR, K., POPESCU, B. A., REINER, Z., SECHTEM, U., SIRNES, P. A., TENDERA, M., VARDAS, P., WIDIMSKY, P., DOCUMENT REVIEWERS, AL ATTAR, N., ANDREOTTI, F., ASCHERMANN, M., ASTEGGIANO, R., BENZA, R., BERGER, R., BONNET, D., DELCROIX, M., HOWARD, L., KITSIOU, A. N., LANG, I., MAGGIONI, A., NIELSEN-KUDSK, J. E., PARK, M., PERRONE-FILARDI, P., PRICE, S., DOMENECH, M. T. S., VONK-NOORDEGRAF, A. & ZAMORANO, J. L. 2009. Guidelines for the diagnosis and treatment of pulmonary hypertension: The Task Force for the Diagnosis and Treatment of Pulmonary Hypertension of the European Society of Cardiology (ESC) and the European Respiratory Society (ERS), endorsed by

the International Society of Heart and Lung Transplantation (ISHLT). ***Eur Heart J*****, ehp297.**

AXEL, L. & DOUGHERTY, L. 1989. MR imaging of motion with spatial modulation of magnetization. ***Radiology,*** **171, 841-5.**

BARRETT, O., JR., SAUNDERS, D. E., JR., MCFARLAND, D. E. & HUMPHRIES, J. O. 1984. Myocardial infarction in sickle cell anemia. ***Am J Hematol,*** **16, 139-47.**

BAUMGARTNER, H., HUNG, J., BERMEJO, J., CHAMBERS, J. B., EVANGELISTA, A., GRIFFIN, B. P., IUNG, B., OTTO, C. M., PELLIKKA, P. A. & QUINONES, M. 2009. Echocardiographic assessment of valve stenosis: EAE/ASE recommendations for clinical practice. ***Eur J Echocardiogr,*** **10, 1-25.**

BEET, E. A. 1949. The genetics of the sickle-cell trait in a Bantu tribe. ***Ann Eugen,*** **14, 279-84.**

BIGLANDS, J. D., RADJENOVIC, A. & RIDGWAY, J. P. 2012. Cardiovascular magnetic resonance physics for clinicians: part II. ***J Cardiovasc Magn Reson,*** **14, 66.**

BLAND, J. M. & ALTMAN, D. G. 1986. Statistical methods for assessing agreement between two methods of clinical measurement. ***Lancet,*** **1, 307-10.**

BLONDHEIM, D. S., BEERI, R., FEINBERG, M. S., VATURI, M., SHIMONI, S., FEHSKE, W., SAGIE, A., ROSENMANN, D., LYSYANSKY, P., DEUTSCH, L., LEITMAN, M., KUPERSTEIN, R., HAY, I., GILON, D., FRIEDMAN, Z., AGMON, Y., TSADOK, Y. & LIEL-COHEN, N. 2010. Reliability of Visual Assessment of Global and Segmental Left Ventricular Function: A Multicenter Study by the Israeli Echocardiography Research Group. ***Journal of the American Society of Echocardiography,*** **23, 258-264.**

BLOOM, M. 1995 ***Understanding Sickle Cell Disease*****, Univ. Press of Mississippi.**

BRAWLEY, O. W., CORNELIUS, L.J., EDWARDS, L.R., GAMBLE, V.N., GREEN, B.L., INTURRISI, C.,, JAMES, A. H., LARAQUE, D., MENDEZ, M., MONTOYA, C.J., POLLOCK, B.H., ROBINSON, L., & SCHOLNIK, A. P. S., M. 2008. National Institutes of Health Consensus Development Conference statement: hydroxyurea treatment for sickle cell disease. ***Annals of Internal Medicine,*** **148 pp.932-938.**

BRITTENHAM, G. M., SCHECHTER, A. N. & NOGUCHI, C. T. 1985. HEMOGLOBIN-S POLYMERIZATION - PRIMARY DETERMINANT OF THE HEMOLYTIC AND CLINICAL SEVERITY OF THE SICKLING SYNDROMES. ***Blood,*** **65, 183-189.**

BUCHALTER, M. B., WEISS, J. L., ROGERS, W. J., ZERHOUNI, E. A., WEISFELDT, M. L., BEYAR, R. & SHAPIRO, E. P. 1990. Noninvasive quantification of left ventricular rotational deformation in normal humans using magnetic resonance imaging myocardial tagging. ***Circulation,*** **81, 1236-44.**

BUNN, H. F. 1997. Pathogenesis and Treatment of Sickle Cell Disease. ***New England Journal of Medicine,*** **337, 762-769.**

BYDDER, M., LARKMAN, D. J. & HAJNAL, J. V. 2002. Combination of signals from array coils using image-based estimation of coil sensitivity profiles. ***Magn Reson Med,*** **47, 539-48.**

CALDAS, M. C., MEIRA, Z. A. & BARBOSA, M. M. 2008a. Evaluation of 107 patients with sickle cell anemia through tissue Doppler and myocardial performance index. ***J Am Soc Echocardiogr,*** **21, 1163-7.**

CARPENTER, J. P., HE, T., KIRK, P., ROUGHTON, M., ANDERSON, L. J., DE NORONHA, S. V., SHEPPARD, M. N., PORTER, J. B., WALKER, J. M., WOOD, J. C., GALANELLO, R., FORNI, G., CATANI, G., MATTA, G., FUCHAROEN, S., FLEMING, A., HOUSE, M. J., BLACK, G., FIRMIN, D. N., ST PIERRE, T. G. & PENNELL, D. J.

2011. On T2* magnetic resonance and cardiac iron. *Circulation,* 123, 1519-28.

CASTRO, O., HOQUE, M. & BROWN, B. D. 2003. Pulmonary hypertension in sickle cell disease: cardiac catheterization results and survival. *Blood,* 101, 1257-1261.

CLASTER, S. & VICHINSKY, E. P. 2003. Managing sickle cell disease. *BMJ,* 327, 1151-5.

COVITZ, W., ESPELAND, M., GALLAGHER, D., HELLENBRAND, W., LEFF, S. & TALNER, N. 1995. The Heart in Sickle Cell Anemia: The Cooperative Study of Sickle Cell Disease (CSSCD). *Chest,* 108, 1214-1219.

DE CASTRO, L. 2004. Pulmonary hypertension in SS, SC and S thalassemia:prevalence,associated clinical syndromes, and mortality. *Blood,* 104, 462a.

DE CASTRO, L. M., JONASSAINT, J. C., GRAHAM, F. L., ASHLEY-KOCH, A. & TELEN, M. J. 2008. Pulmonary hypertension associated with sickle cell disease: clinical and laboratory endpoints and disease outcomes. *American Journal of Hematology,* 83, 19-25.

DE MONTALEMBERT, M. 2008. Management of sickle cell disease. *BMJ,* 337, a1397.

DE VINUESA, P. G., DEL CASTILLO, S. V., TORRES, R. A. & BARDERA, J. C. 2008. Update on cardiac imaging techniques. Echocardiography, cardiac magnetic resonance and multidetector computed tomography. *Rev Esp Cardiol,* 61 Suppl 1, 109-31.

DESAI, A. A., ZHOU, T., AHMAD, H., ZHANG, W., MU, W., TREVINO, S., WADE, M. S., RAGHAVACHARI, N., KATO, G. J., PETERS-LAWRENCE, M. H., THIRUVOIPATI, T., TURNER, K., ARTZ, N., HUANG, Y., PATEL, A. R., YUAN, J. X., GORDEUK, V. R., LANG, R. M., GARCIA, J. G. & MACHADO, R. F. 2012. A novel molecular signature for elevated tricuspid regurgitation velocity in sickle cell disease. *Am J Respir Crit Care Med,* 186, 359-68.

DI TULLIO, M. R. 2008. Diastolic dysfunction does ethnicity matter? *J Am Coll Cardiol,* 52, 1022-3.

DUERDEN, R. M., POINTON, K. S. & HABIB, S. 2006. Review of clinical cardiac MRI. *Imaging,* 18, 178-186.

EDLER I FAU - HERTZ, C. H. & HERTZ, C. H. The use of ultrasonic reflectoscope for the continuous recording of the movements of heart walls. 1954.

EL-BESHLAWY, A., ABD EL RAOUF, E., MOSTAFA, F., TALAAT, M., ISMA'EEL, H., AOUN, E., HOFFBRAND, A. V. & TAHER, A. 2006. Diastolic Dysfunction and Pulmonary Hypertension in Sickle Cell Anemia: Is There a Role for L - Carnitine Treatment? *Acta Haematologica,* 115, 91-96.

EVANGELISTA, A., FLACHSKAMPF, F., LANCELLOTTI, P., BADANO, L., AGUILAR, R., MONAGHAN, M., ZAMORANO, J. & NIHOYANNOPOULOS, P. 2008. European Association of Echocardiography recommendations for standardization of performance, digital storage and reporting of echocardiographic studies. *Eur J Echocardiogr,* 9, 438-48.

FAYAD, Z. A., FERRARI, V. A., KRAITCHMAN, D. L., YOUNG, A. A., PALEVSKY, H. I., BLOOMGARDEN, D. C. & AXEL, L. 1998. Right ventricular regional function using MR tagging: normals versus chronic pulmonary hypertension. *Magn Reson Med,* 39, 116-23.

FEIGENBAUM, H. 1996. Evolution of Echocardiography. *Circulation,* 93, 1321-1327.

FERRONE, F. A. 2004. Polymerization and sickle cell disease: a molecular view. *Microcirculation,* 11, 115-28.

FISCHER, S. E., MCKINNON, G. C., MAIER, S. E. & BOESIGER, P. 1993. Improved myocardial tagging contrast. *Magn Reson Med,* 30, 191-200.

FITZHUGH, C. D., LAUDER, N., JONASSAINT, J. C., TELEN, M. J., ZHAO, X., WRIGHT, E. C., GILLIAM, F. R. & DE CASTRO, L. M. 2010. Cardiopulmonary complications leading to premature deaths in adult patients with sickle cell disease. *American Journal of Hematology,* 85, 36-40.

FONSECA, G. H., SOUZA, R., SALEMI, V. M., JARDIM, C. V. & GUALANDRO, S. F. 2012. Pulmonary hypertension diagnosed by right heart catheterisation in sickle cell disease. *European Respiratory Journal,* 39, 112-8.

FRENETTE, P. S. & ATWEH, G. F. 2007. Sickle cell disease: old discoveries, new concepts, and future promise. *J Clin Invest,* 117, 850-8.

GAASCH, W. H. 1994. DIAGNOSIS AND TREATMENT OF HEART-FAILURE BASED ON LEFT-VENTRICULAR SYSTOLIC OR DIASTOLIC DYSFUNCTION. *Jama-Journal of the American Medical Association,* 271, 1276-1280.

GASTON, M. & ROSSE, W. F. 1982. The cooperative study of sickle cell disease: review of study design and objectives. *Am J Pediatr Hematol Oncol,* 4, 197-201.

GEORGE R. SUTHERLAND, L. H., PIET CLAUS JAN D'HOOGE, BART BIJNENS 2006. *Doppler Myocardial Imaging-A Textbook*, BSWK.

GERRY JR, J. L., BULKLEY, B. H. & HUTCHINS, G. M. 1978. Clinicopathologic analysis of cardiac dysfunction in 52 patients with sickle cell anemia. *The American Journal of Cardiology,* 42, 211-216.

GHIO, S., RECUSANI, F., KLERSY, C., SEBASTIANI, R., LAUDISA, M. L., CAMPANA, C., GAVAZZI, A. & TAVAZZI, L. 2000. Prognostic usefulness of the tricuspid annular plane systolic excursion in patients with congestive heart failure secondary to idiopathic or ischemic dilated cardiomyopathy. *Am J Cardiol,* 85, 837-42.

GLADWIN, M. T., BARST, R. J., GIBBS, J. S. R., HILDESHEIM, M., SACHDEV, V., NOURAIE, M., HASSELL, K. L., LITTLE, J. A., SCHRAUFNAGEL, D. E., KRISHNAMURTI, L., NOVELLI, E. M., GIRGIS, R. E., ZHANG, Y., MORRIS, C. R., ROSENZWEIG, E. B., BADESCH, D. B., LANZKRON, S., CASTRO, O. L., TAYLOR, J. G., GOLDSMITH, J. C., GORDEUK, V. R., KATO, G. J. & MACHADO, R. 2012. Risk Factors for Death in 632 Patients with Sickle Cell Anemia in the United States and United Kingdom. *ASH Annual Meeting Abstracts,* 120, 3240-.

GLADWIN, M. T., SACHDEV, V., JISON, M. L., SHIZUKUDA, Y., PLEHN, J. F., MINTER, K., BROWN, B., COLES, W. A., NICHOLS, J. S., ERNST, I., HUNTER, L. A., BLACKWELDER, W. C., SCHECHTER, A. N., RODGERS, G. P., CASTRO, O. & OGNIBENE, F. P. 2004. Pulmonary hypertension as a risk factor for death in patients with sickle cell disease. *The New England Journal of Medicine,* 350, 886-95.

GOPAL, A. S., KING, J. D. L., KING, D. L., KELLER, A. M. & RIGLING, R. 1993. Left ventricular volume and endocardial surface area by three-dimensional echocardiography: Comparison with two-dimensional echocardiography and nuclear magnetic resonance imaging in normal subjects. *Journal of the American College of Cardiology,* 22, 258-270.

GORCSAN, J., 3RD & TANAKA, H. 2011. Echocardiographic assessment of myocardial strain. *J Am Coll Cardiol,* 58, 1401-13.

GORDEUK, V. R., SACHDEV, V., TAYLOR, J. G., GLADWIN, M. T., KATO, G. & CASTRO, O. L. 2008. Relative systemic hypertension in patients with sickle cell disease is associated with risk of pulmonary hypertension and renal insufficiency. ***Am J Hematol,*** **83, 15-8.**

GOTTDIENER, J. S., BEDNARZ, J., DEVEREUX, R., GARDIN, J., KLEIN, A., MANNING, W. J., MOREHEAD, A., KITZMAN, D., OH, J., QUINONES, M., SCHILLER, N. B., STEIN, J. H. & WEISSMAN, N. J. 2004. American Society of Echocardiography recommendations for use of echocardiography in clinical trials. ***Journal of the American Society of Echocardiography,*** **17, 1086-119.**

GRAMIAK, R. & SHAH, P. M. 1971. Cardiac ultrasonography. A review of current applications. ***Radiologic clinics of North America,*** **9, 469-90.**

GREENWOOD, J. P., MAREDIA, N., YOUNGER, J. F., BROWN, J. M., NIXON, J., EVERETT, C. C., BIJSTERVELD, P., RIDGWAY, J. P., RADJENOVIC, A., DICKINSON, C. J., BALL, S. G. & PLEIN, S. 2012. Cardiovascular magnetic resonance and single-photon emission computed tomography for diagnosis of coronary heart disease (CE-MARC): a prospective trial. ***The Lancet,*** **379, 453-460.**

HATLE, L., ANGELSEN, B. A. & TROMSDAL, A. 1981. Non-invasive estimation of pulmonary artery systolic pressure with Doppler ultrasound. ***British Heart Journal,*** **45, 157-165.**

HEGDE, N., RICH, M. W. & GAYOMALI, C. 2006. The cardiomyopathy of iron deficiency. ***Tex Heart Inst J,*** **33, 340-4.**

HEIMDAL, A., STØYLEN, A., TORP, H. & SKJÆRPE, T. 1998. Real-Time Strain Rate Imaging of the Left Ventricle by Ultrasound. ***Journal of the American Society of Echocardiography,*** **11, 1013-1019.**

HELLE-VALLE, T., CROSBY, J., EDVARDSEN, T., LYSEGGEN, E., AMUNDSEN, B. H., SMITH, H. J., ROSEN, B. D., LIMA, J. A., TORP, H., IHLEN, H. & SMISETH, O. A. 2005. New noninvasive method for assessment of left ventricular rotation: speckle tracking echocardiography. ***Circulation,*** **112, 3149-56.**

HERRICK, J. B. 1910. Peculiar elongated and sickle shaped red blood corpuscules in a case of severe anemia. ***Arch.Int.Med.,*** **6, 517-521.**

HERRICK, J. B. 1924. . Abstract of discussion. ***JAMA. 83:16*****.**

HICKMAN, M., MODELL, B., GREENGROSS, P., CHAPMAN, C., LAYTON, M., FALCONER, S. & DAVIES, S. C. 1999. Mapping the prevalence of sickle cell and beta thalassaemia in England: estimating and validating ethnic-specific rates. ***British Journal of Haematology,*** **104, 860-867.**

HO, S. Y. & NIHOYANNOPOULOS, P. 2006. Anatomy, echocardiography, and normal right ventricular dimensions. ***Heart,*** **92, i2-i13.**

HOEPER, M. M., BARBERA, J. A., CHANNICK, R. N., HASSOUN, P. M., LANG, I. M., MANES, A., MARTINEZ, F. J., NAEIJE, R., OLSCHEWSKI, H., PEPKE-ZABA, J., REDFIELD, M. M., ROBBINS, I. M., SOUZA, R., TORBICKI, A. & MCGOON, M. 2009. Diagnosis, assessment, and treatment of non-pulmonary arterial hypertension pulmonary hypertension. ***J Am Coll Cardiol,*** **54, S85-96.**

HOFFMANN, U., GLOBITS, S., SCHIMA, W., LOEWE, C., PUIG, S., OBERHUBER, G. & FRANK, H. 2003. Usefulness of magnetic resonance imaging of cardiac and paracardiac masses. ***Am J Cardiol,*** **92, 890-5.**

HOWARD, L. S., GRAPSA, J., DAWSON, D., BELLAMY, M., CHAMBERS, J. B., MASANI, N. D., NIHOYANNOPOULOS, P. & SIMON R. GIBBS, J. 2012. Echocardiographic assessment of pulmonary hypertension: standard operating procedure. ***European Respiratory Review,*** **21, 239-248.**

HUNG, J., LANG, R., FLACHSKAMPF, F., SHERNAN, S. K., MCCULLOCH, M. L., ADAMS, D. B., THOMAS, J., VANNAN, M., RYAN, T. & ASE 2007. 3D echocardiography: a review of the current status and future directions. ***J Am Soc Echocardiogr,*** **20, 213-33.**

INGRAM, V. M. 1958. Abnormal human haemoglobins: I. The comparison of normal human and sickle-cell haemoglobins by "fingerprinting". ***Biochimica et Biophysica Acta,*** **28, 539-545.**

INGRAM, V. M. 2004. Sickle-cell anemia hemoglobin: the molecular biology of the first "molecular disease"--the crucial importance of serendipity. ***Genetics,*** **167, 1-7.**

J SIMON R GIBBS, A. S., WEI LI 2009. Pulmonary hypertension in clinical echocardiography. ***In:*** **PETROS NIHOYANNOPOULOS, J. A. K. (ed.)** ***Echocardiography.*** **Springer.**

JACOBS, L. D., SALGO, I. S., GOONEWARDENA, S., WEINERT, L., COON, P., BARDO, D., GERARD, O., ALLAIN, P., ZAMORANO, J. L., DE ISLA, L. P., MOR-AVI, V. & LANG, R. M. 2006. Rapid online quantification of left ventricular volume from real-time three-dimensional echocardiographic data. ***European Heart Journal,*** **27, 460-468.**

JENKINS, C., BRICKNELL, K., HANEKOM, L. & MARWICK, T. H. 2004. Reproducibility and accuracy of echocardiographic measurements of left ventricular parameters using real-time three-dimensional echocardiography. ***J Am Coll Cardiol,*** **44, 878-86.**

JENKINS, C., CHAN, J., HANEKOM, L. & MARWICK, T. H. 2006. Accuracy and Feasibility of Online 3-Dimensional Echocardiography for Measurement of Left Ventricular Parameters. ***Journal of the American Society of Echocardiography,*** **19, 1119-1128.**

KAPETANAKIS, S., BHAN, A., MURGATROYD, F., KEARNEY, M. T., GALL, N., ZHANG, Q., YU, C. M. & MONAGHAN, M. J. 2011. Real-time 3D echo in patient selection for cardiac resynchronization therapy. ***JACC Cardiovasc Imaging,*** **4, 16-26.**

KATO, G. J., GLADWIN, M. T. & STEINBERG, M. H. 2007. Deconstructing sickle cell disease: reappraisal of the role of hemolysis in the development of clinical subphenotypes. ***Blood Rev,*** **21, 37-47.**

KENNETH I. ATAGA, C. G. M., SUSAN JONES, OLUDAMILOLA OLAJIDE, DELL STRAYHORN, ALAN HINDERLITER, EUGENE P. ORRINGER, 2006. Pulmonary hypertension in patients with sickle cell disease: a longitudinal study. ***British Journal of Haematology,*** **134, 109-115.**

KIM, W.-J., LEE, B. H., KIM, Y. J., KANG, J. H., JUNG, Y. J., SONG, J.-M., KANG, D.-H. & SONG, J.-K. 2009. Apical Rotation Assessed by Speckle-Tracking Echocardiography as an Index of Global Left Ventricular Contractility / CLINICAL PERSPECTIVE. ***Circulation: Cardiovascular Imaging,*** **2, 123-131.**

KIRK, P., CARPENTER, J. P., TANNER, M. A. & PENNELL, D. J. 2011. Low prevalence of fibrosis in thalassemia major assessed by late gadolinium enhancement cardiovascular magnetic resonance. ***J Cardiovasc Magn Reson,*** **13, 8.**

KISSLO, J., FIREK, B., OTA, T., KANG, D. H., FLEISHMAN, C. E., STETTEN, G., LI, J., OHAZAMA, C. J., ADAMS, D., LANDOLFO, C., RYAN, T. & VON RAMM, O. 2000. Real-Time Volumetric Echocardiography. ***Echocardiography,*** **17, 773-779.**

KLEIJN, S. A., ALY, M. F., TERWEE, C. B., VAN ROSSUM, A. C. & KAMP, O. 2012a. Reliability of left ventricular volumes and function measurements using

three-dimensional speckle tracking echocardiography. *Eur Heart J Cardiovasc Imaging,* 13, 159-68.

KLEIJN, S. A., BROUWER, W. P., ALY, M. F., RUSSEL, I. K., DE ROEST, G. J., BEEK, A. M., VAN ROSSUM, A. C. & KAMP, O. 2012b. Comparison between three-dimensional speckle-tracking echocardiography and cardiac magnetic resonance imaging for quantification of left ventricular volumes and function. *Eur Heart J Cardiovasc Imaging,* 13, 834-9.

KNIGHT-PERRY, J. E., DE LAS FUENTES, L., WAGGONER, A. D., HOFFMANN, R. G., BLINDER, M. A., DAVILA-ROMAN, V. G. & FIELD, J. J. 2011. Abnormalities in cardiac structure and function in adults with sickle cell disease are not associated with pulmonary hypertension. *J Am Soc Echocardiogr,* 24, 1285-90.

KROEKER, C. A. G., TYBERG, J. V. & BEYAR, R. 1995. Effects of Load Manipulations, Heart Rate, and Contractility on Left Ventricular Apical Rotation: An Experimental Study in Anesthetized Dogs. *Circulation,* 92, 130-141.

KÜHL, H. P., SCHRECKENBERG, M., RULANDS, D., KATOH, M., SCHÄFER, W., SCHUMMERS, G., BÜCKER, A., HANRATH, P. & FRANKE, A. 2004. High-resolution transthoracic real-time three-dimensional echocardiographyQuantitation of cardiac volumes and function using semi-automatic border detection and comparison with cardiac magnetic resonance imaging. *Journal of the American College of Cardiology,* 43, 2083-2090.

LAMERS, L., ENSING, G., PIGNATELLI, R., GOLDBERG, C., BEZOLD, L., AYRES, N. & GAJARSKI, R. 2006. Evaluation of Left Ventricular Systolic Function in Pediatric Sickle Cell Anemia Patients Using the End-Systolic Wall Stress-Velocity of Circumferential Fiber Shortening Relationship. *J Am Coll Cardiol*, j.jacc.2006.03.005.

LANG, R. M., BIERIG, M., DEVEREUX, R. B., FLACHSKAMPF, F. A., FOSTER, E., PELLIKKA, P. A., PICARD, M. H., ROMAN, M. J., SEWARD, J., SHANEWISE, J. S., SOLOMON, S. D., SPENCER, K. T., SUTTON, M. S. & STEWART, W. J. 2005. Recommendations for chamber quantification: a report from the American Society of Echocardiography's Guidelines and Standards Committee and the Chamber Quantification Writing Group, developed in conjunction with the European Association of Echocardiography, a branch of the European Society of Cardiology. *Journal of the American Society of Echocardiography,* 18, 1440-63.

LANZARINI, L., FONTANA, A., LUCCA, E., CAMPANA, C. & KLERSY, C. 2002. Noninvasive estimation of both systolic and diastolic pulmonary artery pressure from Doppler analysis of tricuspid regurgitant velocity spectrum in patients with chronic heart failure. *American Heart Journal,* 144, 1087-94.

LANZER, P., BARTA, C., BOTVINICK, E. H., WIESENDANGER, H. U., MODIN, G. & HIGGINS, C. B. 1985. ECG-synchronized cardiac MR imaging: method and evaluation. *Radiology,* 155, 681-6.

LEBBY, R. 1846. Case od Absence Spleen. *Southern Journal of Medical Pharmacology,* 1, 481-483.

LEE, M. T., SMALL, T., KHAN, M. A., ROSENZWEIG, E. B., BARST, R. J. & BRITTENHAM, G. M. 2009. Doppler-defined pulmonary hypertension and

the risk of death in children with sickle cell disease followed for a mean of three years. ***Br J Haematol,*** **146, 437-41.**

LESTER, L. A., SODT, P. C., HUTCHEON, N. & ARCILLA, R. A. 1990. Cardiac abnormalities in children with sickle cell anemia. ***CHEST Journal,*** **98, 1169-1174.**

LESTER, S. J., TAJIK, A. J., NISHIMURA, R. A., OH, J. K., KHANDHERIA, B. K. & SEWARD, J. B. 2008. Unlocking the mysteries of diastolic function: deciphering the Rosetta Stone 10 years later. ***Journal of the American College of Cardiology,*** **51, 679-89.**

LIEM, R. I., YOUNG, L. T. & THOMPSON, A. A. 2007a. Tricuspid regurgitant jet velocity is associated with hemolysis in children and young adults with sickle cell disease evaluated for pulmonary hypertension. ***Haematologica,*** **92, 1549-1552.**

LINDSAY J, J. M. J. C. P. R. H. 1974. THe cardiovascular manifestations of sickle cell disease. ***Archives of Internal Medicine,*** **133, 643-651.**

LOPEZ-CANDALES, A., DOHI, K., RAJAGOPALAN, N., SUFFOLETTO, M., MURALI, S., GORCSAN, J. & EDELMAN, K. 2005. Right ventricular dyssynchrony in patients with pulmonary hypertension is associated with disease severity and functional class. ***Cardiovasc Ultrasound,*** **3, 23.**

LORCH, D., SPEVACK, D. & LITTLE, J. 2011. An elevated estimated pulmonary arterial systolic pressure, whenever measured, is associated with excess mortality in adults with sickle cell disease. ***Acta Haematologica,*** **125, 225-9.**

LORENZ, C. H., WALKER, E. S., MORGAN, V. L., KLEIN, S. S. & GRAHAM, T. P., JR. 1999. Normal human right and left ventricular mass, systolic function, and gender differences by cine magnetic resonance imaging. ***J Cardiovasc Magn Reson,*** **1, 7-21.**

LUCAS, S. B., MASON, D. G., MASON, M. & WEYMAN, D. 2008. ***A Sickle Crisis? A report for the National Confidential Enquiry into Patient Outcome and Death (NCEPOD),*** **London, United Kingdom, NCEPOD.**

MACHADO, R. F. & GLADWIN, M. T. 2010. Pulmonary hypertension in hemolytic disorders: pulmonary vascular disease: the global perspective. ***Chest,*** **137, 30S-38S.**

MAFFESSANTI, F., NESSER, H.-J., WEINERT, L., STERINGER-MASCHERBAUER, R., NIEL, J., GORISSEN, W., SUGENG, L., LANG, R. M. & MOR-AVI, V. 2009. Quantitative Evaluation of Regional Left Ventricular Function Using Three-Dimensional Speckle Tracking Echocardiography in Patients With and Without Heart Disease. ***The American Journal of Cardiology,*** **104, 1755-1762.**

MANSI, I. A. & ROSNER, F. 2002. Myocardial infarction in sickle cell disease. ***J Natl Med Assoc,*** **94, 448-52.**

MARTIN, C. R., JOHNSON, C. S., COBB, C., TATTER, D. & HAYWOOD, L. J. 1996. Myocardial infarction in sickle cell disease. ***J Natl Med Assoc,*** **88, 428-32.**

MARWICK, T. H., LEANO, R. L., BROWN, J., SUN, J.-P., HOFFMANN, R., LYSYANSKY, P., BECKER, M. & THOMAS, J. D. 2009a. Myocardial Strain Measurement With 2-Dimensional Speckle-Tracking Echocardiography: Definition of Normal Range. ***JACC: Cardiovascular Imaging,*** **2, 80-84.**

MAURER, M. S., SPEVACK, D., BURKHOFF, D. & KRONZON, I. 2004. Diastolic dysfunction: can it be diagnosed by Doppler echocardiography? ***J Am Coll Cardiol,*** **44, 1543-9.**

MCLAUGHLIN, V. V., ARCHER, S. L., BADESCH, D. B., BARST, R. J., FARBER, H. W., LINDNER, J. R., MATHIER, M. A., MCGOON, M. D., PARK, M. H., ROSENSON, R. S., RUBIN, L. J., TAPSON, V. F. & VARGA, J. 2009. ACCF/AHA 2009 Expert Consensus Document on Pulmonary HypertensionA Report of the American College of Cardiology Foundation Task Force on Expert Consensus Documents and the American Heart Association Developed in Collaboration With the American College of Chest Physicians; American Thoracic Society, Inc.; and the Pulmonary Hypertension Association. ***Journal of the American College of Cardiology,*** **53, 1573-1619.**

MODELL, B., KHAN, M., DARLISON, M., WESTWOOD, M. A., INGRAM, D. & PENNELL, D. J. 2008. Improved survival of thalassaemia major in the UK and relation to T2* cardiovascular magnetic resonance. ***J Cardiovasc Magn Reson,*** **10, 42.**

MONAGHAN, M. J. 2006. Role of real time 3D echocardiography in evaluating the left ventricle. ***Heart,*** **92, 131-6.**

MOORE, C. C., LUGO-OLIVIERI, C. H., MCVEIGH, E. R. & ZERHOUNI, E. A. 2000b. Three-dimensional Systolic Strain Patterns in the Normal Human Left Ventricle: Characterization with Tagged MR Imaging1. ***Radiology,*** **214, 453-466.**

MOR-AVI, V., LANG, R. M., BADANO, L. P., BELOHLAVEK, M., CARDIM, N. M., DERUMEAUX, G., GALDERISI, M., MARWICK, T., NAGUEH, S. F., SENGUPTA, P. P., SICARI, R., SMISETH, O. A., SMULEVITZ, B., TAKEUCHI, M., THOMAS, J. D., VANNAN, M., VOIGT, J.-U. & ZAMORANO, J. L. 2011. Current and Evolving Echocardiographic Techniques for the Quantitative Evaluation of Cardiac Mechanics: ASE/EAE Consensus Statement on Methodology and Indications Endorsed by the Japanese Society of Echocardiography. ***European Journal of Echocardiography,*** **12, 167-205.**

N.C. HUGHES-JONES, S. N. W., C.HATTON (ed.) 2004. ***Lectures on Haematology*****: Blackwell Publishing.**

NAEHLE, C. P., STRACH, K., THOMAS, D., MEYER, C., LINHART, M., BITARAF, S., LITT, H., SCHWAB, J. O., SCHILD, H. & SOMMER, T. 2009. Magnetic Resonance Imaging at 1.5-T in Patients With Implantable Cardioverter-Defibrillators. ***Journal of the American College of Cardiology,*** **54, 549-555.**

NAGUEH, S. F., APPLETON, C. P., GILLEBERT, T. C., MARINO, P. N., OH, J. K., SMISETH, O. A., WAGGONER, A. D., FLACHSKAMPF, F. A., PELLIKKA, P. A. & EVANGELISTA, A. 2009c. Recommendations for the evaluation of left ventricular diastolic function by echocardiography. ***J Am Soc Echocardiogr,*** **22, 107-33.**

NEEL, J. V. 1949a. The Inheritance of Sickle Cell Anemia. ***Science,*** **110, 64-6.**

NG, M. L., LIEBMAN, J., ANSLOVAR, J. & GROSS, S. 1967. Cardiovascular Findings in Children with Sickle Cell Anemia. ***CHEST Journal,*** **52, 788-799.**

NIEMANN, P. S., PINHO, L., BALBACH, T., GALUSCHKY, C., BLANKENHAGEN, M., SILBERBACH, M., BROBERG, C., JEROSCH-HEROLD, M. & SAHN, D. J. 2007. Anatomically oriented right ventricular volume measurements with dynamic three-dimensional echocardiography validated by 3-Tesla magnetic resonance imaging. ***J Am Coll Cardiol,*** **50, 1668-76.**

NOTOMI, Y., LYSYANSKY, P., SETSER, R. M., SHIOTA, T., POPOVIĆ, Z. B., MARTIN-MIKLOVIC, M. G., WEAVER, J. A., ORYSZAK, S. J., GREENBERG, N. L., WHITE, R. D. & THOMAS, J. D. 2005. Measurement of Ventricular Torsion by Two-

Dimensional Ultrasound Speckle Tracking Imaging. ***Journal of the American College of Cardiology,*** **45, 2034-2041.**

NÚÑEZ, J., ZAMORANO, J. L., PÉREZ DE ISLA, L., PALOMEQUE, C., ALMERÍA, C., RODRIGO, J. L., CORTEZA, J., BANCHS, J. & MACAYA, C. 2004. Differences in regional systolic and diastolic function by Doppler tissue imaging in patients with hypertrophic cardiomyopathy and hypertrophy caused by hypertension. ***Journal of the American Society of Echocardiography : official publication of the American Society of Echocardiography,*** **17, 717-722.**

O'MALLEY, P. D. 2006. ***New Developments in Sickle Cell Disease Research*****, Nova Science Pub Incorporated.**

O'REGAN, D. P., ARIFF, B., BAKSI, A. J., GORDON, F., DURIGHEL, G. & COOK, S. A. 2013. Salvage assessment with cardiac MRI following acute myocardial infarction underestimates potential for recovery of systolic strain. ***Eur Radiol,*** **23, 1210-7.**

ODD, B.-H., NEDIM, S., BENGT, R. & JONAS, W. 2009. Doppler Echocardiography Can Provide a Comprehensive Assessment of Right Ventricular Afterload. ***Journal of the American Society of Echocardiography*** **22, 1360-1367.**

OH, J. K., HATLE, L., TAJIK, A. J. & LITTLE, W. C. 2006. Diastolic Heart Failure Can Be Diagnosed by Comprehensive Two-Dimensional and Doppler Echocardiography. ***J Am Coll Cardiol*****, j.jacc.2005.09.032.**

OLIVEIRA, E. & GÓMEZ-PATINO, N. 1963. Falcemic cardiopathy: Report of a case. ***The American Journal of Cardiology,*** **11, 686-688.**

ONI, L., DICK, M., SMALLING, B. & WALTERS, J. 2006. Care and management of your child with sickle cell disease: a parent's guide. ***London: The NHS sickle cell & thalassaemia screening program*****.**

OSMAN, N. F., KERWIN, W. S., MCVEIGH, E. R. & PRINCE, J. L. 1999. Cardiac motion tracking using CINE harmonic phase (HARP) magnetic resonance imaging. ***Magn Reson Med,*** **42, 1048-60.**

PANNU, R., ZHANG, J., ANDRAWS, R., ARMANI, A., PATEL, P. & MANCUSI-UNGARO, P. 2008. Acute myocardial infarction in sickle cell disease: a systematic review. ***Crit Pathw Cardiol,*** **7, 133-8.**

PARENT, F., BACHIR, D., INAMO, J., LIONNET, F., DRISS, F., LOKO, G., HABIBI, A., BENNANI, S., SAVALE, L., ADNOT, S., MAITRE, B., YAICI, A., HAJJI, L., O'CALLAGHAN, D. S., CLERSON, P., GIROT, R., GALACTEROS, F. & SIMONNEAU, G. 2011. A hemodynamic study of pulmonary hypertension in sickle cell disease. ***The New England Journal of Medicine,*** **365, 44-53.**

PATEL, A., AHMAD, H., DESAI, A., THIRUVOIPATI, T., TURNER, K., WEINERT, L., YODWUT, C., CZOBOR, P., ARTZ, N., TREVINO, S., MOR-AVI, V., MACHADO, R., GARCIA, J. & LANG, R. 2012. Mechanistic insights and characterization of cardiomyopathy due to Sickle Cell Disease. ***Journal of Cardiovascular Magnetic Resonance,*** **14, 1-2.**

PATTYNAMA, P. M., LAMB, H. J., VAN DER VELDE, E. A., VAN DER GEEST, R. J., VAN DER WALL, E. E. & DE ROOS, A. 1995. Reproducibility of MRI-derived measurements of right ventricular volumes and myocardial mass. ***Magn Reson Imaging,*** **13, 53-63.**

PAULING, L. 1964. Molecular disease and evolution. ***Bull N Y Acad Med,*** **40, 334-42.**

PAULING, L., ITANO, H.A., SINGER, S.J., AND WELLS, & I.C. 1949. Sickle cell anemia, a molecular disease. ***Science.*****, 543-548.**

PEREZ DE ISLA, L. V., D., ZAMORANO J. 2008. Three-dimensional speckle tracking. ***Current Cardiovascular Imaging Reports,*** **1, 25-29.**

PERK, G., TUNICK, P. A. & KRONZON, I. 2007. Non-Doppler Two-dimensional Strain Imaging by Echocardiography–From Technical Considerations to Clinical Applications. ***Journal of the American Society of Echocardiography,*** **20, 234-243.**

PETITJEAN, C., ROUGON, N., CLUZEL, P., PRETEUX, F. & GRENIER, P. 2004. Quantification of myocardial function using tagged MR and cine MR images. ***Int J Cardiovasc Imaging,*** **20, 497-508.**

PIRAT, B., KHOURY, D. S., HARTLEY, C. J., TILLER, L., RAO, L., SCHULZ, D. G., NAGUEH, S. F. & ZOGHBI, W. A. 2008. A Novel Feature-Tracking Echocardiographic Method for the Quantitation of Regional Myocardial Function: Validation in an Animal Model of Ischemia-Reperfusion. ***Journal of the American College of Cardiology,*** **51, 651-659.**

PLATT, O. S., BRAMBILLA, D. J., ROSSE, W. F., MILNER, P. F., CASTRO, O., STEINBERG, M. H. & KLUG, P. P. 1994a. Mortality In Sickle Cell Disease -- Life Expectancy and Risk Factors for Early Death. ***The New England Journal of Medicine,*** **330, 1639-1644.**

POPP, R. L. & HARRISON, D. C. 1970. Ultrasonic Cardiac Echography for Determining Stroke Volume and Valvular Regurgitation. ***Circulation,*** **41, 493-502.**

POWARS, D., WEIDMAN, J. A., ODOM-MARYON, T., NILAND, J. C. & JOHNSON, C. 1988. Sickle cell chronic lung disease: prior morbidity and the risk of pulmonary failure. ***Medicine (Baltimore),*** **67, 66-76.**

QUINN, C. T., ROGERS, Z. R., MCCAVIT, T. L. & BUCHANAN, G. R. 2010. Improved survival of children and adolescents with sickle cell disease. ***Blood,*** **115, 3447-52.**

QUIÑONES, M. A., DOUGLAS, P. S., FOSTER, E., GORCSAN III, J., LEWIS, J. F., PEARLMAN, A. S., RYCHIK, J., SALCEDO, E. E., SEWARD, J. B., STEVENSON, J. G., THYS, D. M., WEITZ, H. H., ZOGHBI, W. A., CREAGER, M. A., WINTERS JR, W. L., ELNICKI, M., HIRSHFELD JR, J. W., LORELL, B. H., RODGERS, G. P. & TRACY, C. M. 2003. ACC/AHA clinical competence statement on echocardiography : A Report of the American College of Cardiology/American Heart Association/American College of Physicians–American Society of Internal Medicine Task Force on Clinical Competence Developed in Collaboration with the American Society of Echocardiography, the Society of Cardiovascular Anesthesiologists, and the Society of Pediatric Echocardiography. ***Journal of the American College of Cardiology,*** **41, 687-708.**

QUINONES, M. A., OTTO, C. M., STODDARD, M., WAGGONER, A. & ZOGHBI, W. A. 2002. Recommendations for quantification of Doppler echocardiography: a report from the Doppler Quantification Task Force of the Nomenclature and Standards Committee of the American Society of Echocardiography. ***Journal of the American Society of Echocardiography,*** **15, 167-84.**

RAMAN, S. V., SIMONETTI, O. P., CATALAND, S. R. & KRAUT, E. H. 2006. Myocardial ischemia and right ventricular dysfunction in adult patients with sickle cell disease. ***Haematologica,*** **91, 1329-35.**

RAPHAEL, R. I. 2005. Pathophysiology and treatment of sickle cell disease. ***Clin Adv Hematol Oncol,*** **3, 492-505.**

RIDGWAY, J. P. 2010. Cardiovascular magnetic resonance physics for clinicians: part I. ***J Cardiovasc Magn Reson,*** **12, 71.**

ROBERTO F. MACHADO, M. T. G. 2005. Chronic sickle cell lung disease: new insights into the diagnosis, pathogenesis and treatment of pulmonary hypertension. ***British Journal of Haematology,*** **129, 449-464.**

RODGERS, G. P. 1997. Overview of pathophysiology and rationale for treatment of sickle cell anemia. ***Semin Hematol,*** **34, 2-7.**

ROSENTHAL, R. H. G. A. M. D. 2006. ***Clinical Studies in Medical Biochemistry*****, Paperback.**

RUBLER, S. & FLEISCHER, R. A. 1967. Sickle cell states and cardiomyopathy: Sudden death due to pulmonary thrombosis and infarction∗. ***The American Journal of Cardiology,*** **19, 867-873.**

RÜSSEL, I. K., GÖTTE, M. J. W., BRONZWAER, J. G., KNAAPEN, P., PAULUS, W. J. & VAN ROSSUM, A. C. 2009. Left Ventricular Torsion: An Expanding Role in the Analysis of Myocardial Dysfunction. ***JACC: Cardiovascular Imaging,*** **2, 648-655.**

RUSSO, C., JIN, Z., HOMMA, S., RUNDEK, T., ELKIND, M. S. V., SACCO, R. L. & DI TULLIO, M. R. 2010. Race/ethnic disparities in left ventricular diastolic function in a triethnic community cohort. ***American Heart Journal,*** **160, 152-158.**

SACHDEV, V., KATO, G. J., GIBBS, J. S., BARST, R. J., MACHADO, R. F., NOURAIE, M., HASSELL, K. L., LITTLE, J. A., SCHRAUFNAGEL, D. E., KRISHNAMURTI, L., NOVELLI, E. M., GIRGIS, R. E., MORRIS, C. R., ROSENZWEIG, E. B., BADESCH, D. B., LANZKRON, S., CASTRO, O. L., TAYLOR, J. G. T., HANNOUSH, H., GOLDSMITH, J. C., GLADWIN, M. T. & GORDEUK, V. R. 2011. Echocardiographic markers of elevated pulmonary pressure and left ventricular diastolic dysfunction are associated with exercise intolerance in adults and adolescents with homozygous sickle cell anemia in the United States and United Kingdom. ***Circulation,*** **124, 1452-60.**

SACHDEV, V., MACHADO, R. F., SHIZUKUDA, Y., RAO, Y. N., SIDENKO, S., ERNST, I., ST PETER, M., COLES, W. A., ROSING, D. R., BLACKWELDER, W. C., CASTRO, O., KATO, G. J. & GLADWIN, M. T. 2007. Diastolic dysfunction is an independent risk factor for death in patients with sickle cell disease. ***J Am Coll Cardiol,*** **49, 472-9.**

SACHPEKIDIS, V., BHAN, A., PAUL, M., GIANSTEFANI, S., SMITH, L., REIKEN, J., WALKER, N., HARRIES, D., PEARSON, P. & MONAGHAN, M. J. 2011. The additive value of three-dimensional derived left atrial volume and carotid imaging in dobutamine stress echocardiography. ***Eur J Echocardiogr,*** **12, 46-53.**

SCAPELLATO, F., TEMPORELLI, P. L., ELEUTERI, E., CORRA, U., IMPARATO, A. & GIANNUZZI, P. 2001. Accurate noninvasive estimation of pulmonary vascular resistance by Doppler echocardiography in patients with chronic failure heart failure. ***J Am Coll Cardiol,*** **37, 1813-9.**

SCHILLER, N. B., SHAH, P. M., CRAWFORD, M., DEMARIA, A., DEVEREUX, R., FEIGENBAUM, H., GUTGESELL, H., REICHEK, N., SAHN, D., SCHNITTGER, I. & ET AL. 1989. Recommendations for quantitation of the left ventricle by two-dimensional echocardiography. American Society of Echocardiography Committee on Standards, Subcommittee on Quantitation of Two-Dimensional Echocardiograms. ***J Am Soc Echocardiogr,*** **2, 358-67.**

SCHINDERA, S. T., MEHWALD, P. S., SAHN, D. J. & KECECIOGLU, D. 2002. Accuracy of real-time three-dimensional echocardiography for quantifying right ventricular volume: static and pulsatile flow studies in an anatomic in vitro model. ***J Ultrasound Med,*** **21, 1069-75.**

SCHULTZ WH, W. R. 2003. Malignancy in patients with sickle cell disease. . ***American Journal of Hematology*** **74, 249-253.**

SEO, Y., ISHIZU, T., ENOMOTO, Y., SUGIMORI, H., YAMAMOTO, M., MACHINO, T., KAWAMURA, R. & AONUMA, K. 2009. Validation of 3-dimensional speckle tracking imaging to quantify regional myocardial deformation. ***Circ Cardiovasc Imaging,*** **2, 451-9.**

SERJEANT, G. R. 1997. Sickle-cell disease. ***Lancet,*** **350, 725-30.**

SHAH, A. M. & SOLOMON, S. D. 2012. Myocardial Deformation Imaging: Current Status and Future Directions. ***Circulation,*** **125, e244-e248.**

SHARP, A., TAPP, R., FRANCIS, D. P., MCG. THOM, S. A., HUGHES, A. D., STANTON, A. V., ZAMBANINI, A., CHATURVEDI, N., BYRD, S., POULTER, N. R., SEVER, P. S. & MAYET, J. 2008. Ethnicity and Left Ventricular Diastolic Function in Hypertension: An ASCOT (Anglo-Scandinavian Cardiac Outcomes Trial) Substudy. ***Journal of the American College of Cardiology,*** **52, 1015-1021.**

SHEHATA, M. L., CHENG, S., OSMAN, N. F., BLUEMKE, D. A. & LIMA, J. A. 2009. Myocardial tissue tagging with cardiovascular magnetic resonance. ***J Cardiovasc Magn Reson,*** **11, 55.**

SHERMAN, S. C. & SULE, H. P. 2004. Acute myocardial infarction in a young man with sickle cell disease. ***J Emerg Med,*** **27, 31-5.**

SMEDEMA, J. P., SNOEP, G., VAN KROONENBURGH, M. P., VAN GEUNS, R. J., DASSEN, W. R., GORGELS, A. P. & CRIJNS, H. J. 2005. Evaluation of the accuracy of gadolinium-enhanced cardiovascular magnetic resonance in the diagnosis of cardiac sarcoidosis. ***J Am Coll Cardiol,*** **45, 1683-90.**

SOHN, D., CHAI, I., LEE, D., KIM, H., KIM, H., OH, B., LEE, M., PARK, Y., CHOI, Y., SEO, J. & LEE, Y. 1997. Assessment of mitral annulus velocity by Doppler tissue imaging in the evaluation of left ventricular diastolic function. ***J Am Coll Cardiol,*** **30, 474-480.**

STØYLEN, A. 2011. ***Strain rate imaging. Cardiac deformation imaging by ultrasound / echocardiography Tissue Doppler and Speckle tracking (Online)*** **[Online]. Norwegian University of Science and Technology Available: http://folk.ntnu.no/stoylen/strainrate/#Website index [Accessed November 2012.**

STREETER, D. D., SPOTNITZ, H. M., PATEL, D. P., ROSS, J. & SONNENBLICK, E. H. 1969. Fiber Orientation in the Canine Left Ventricle during Diastole and Systole. ***Circulation Research,*** **24, 339-347.**

STREETLY, A. 2000. NHS Sickle Cell and Thalassaemia Screening Programme. ***Health Technology Assessment*** **4.**

STREETLY, A., LATINOVIC, R. & HENTHORN, J. 2010. Positive screening and carrier results for the England-wide universal newborn sickle cell screening programme by ethnicity and area for 2005-07. ***J Clin Pathol,*** **63, 626-9.**

SUGENG, L., WEINERT, L. & LANG, R. M. 2003. Left ventricular assessment using real time three dimensional echocardiography. ***Heart,*** **89, iii29-iii36.**

SUTTON, L. L., CASTRO, O., CROSS, D. J., SPENCER, J. E. & LEWIS, J. F. 1994. Pulmonary hypertension in sickle cell disease. ***American Journal of Cardiology,*** **74, 626-8.**

TASK FORCE OF THE EUROPEAN SOCIETY OF CARDIOLOGY, I. C. W. T. A. O. E. P. C. 1998. The clinical role of magnetic resonance in cardiovascular disease. ***European Heart Journal,*** **19, 19-39.**

TELFER, P., COEN, P., CHAKRAVORTY, S., WILKEY, O., EVANS, J., NEWELL, H., SMALLING, B., AMOS, R., STEPHENS, A., ROGERS, D. & KIRKHAM, F. 2007. Clinical outcomes in children with sickle cell disease living in England: a neonatal cohort in East London. ***Haematologica,*** **92, 905-12.**

TESKE, A. J., DE BOECK, B. W., OLIMULDER, M., PRAKKEN, N. H., DOEVENDANS, P. A. & CRAMER, M. J. 2008. Echocardiographic assessment of regional right ventricular function: a head-to-head comparison between 2-dimensional and tissue Doppler-derived strain analysis. ***J Am Soc Echocardiogr,*** **21, 275-83.**

THOMAS H MARWICK, C.-M. Y., JING PING SUN 2009. ***Myocardial Imaging: Tissue Doppler and Speckle Tracking Book*****, Kindle Edition.**

THOMAS, J. D. & POPOVIC, Z. B. 2006. Assessment of Left Ventricular Function by Cardiac Ultrasound. ***J Am Coll Cardiol,*** **48, 2012-2025.**

URHEIM, S., EDVARDSEN, T., TORP, H., ANGELSEN, B. & SMISETH, O. A. 2000. Myocardial Strain by Doppler Echocardiography: Validation of a New Method to Quantify Regional Myocardial Function. ***Circulation,*** **102, 1158-1164.**

UZSOY, N. K. 1964. CARDIOVASCULAR FINDINGS IN PATIENTS WITH SICKLE CELL ANEMIA. ***Am J Cardiol,*** **13, 320-8.**

VARAT, M. A., ADOLPH, R. J. & FOWLER, N. O. 1972. Cardiovascular effects of anemia. ***Am Heart J,*** **83, 415-426.**

VICTOR, B. M. & BARRON, J. T. 2010. Diastolic Heart Failure Versus Diastolic Dysfunction: Difference in Renal Function. ***Clinical Cardiology,*** **33, 770-774.**

VOGEL, M., ANDERSON, L. J., HOLDEN, S., DEANFIELD, J. E., PENNELL, D. J. & WALKER, J. M. 2003. Tissue Doppler echocardiography in patients with thalassaemia detects early myocardial dysfunction related to myocardial iron overload. ***Eur Heart J,*** **24, 113-119.**

VOGELSBERG, H., MAHRHOLDT, H., DELUIGI, C. C., YILMAZ, A., KISPERT, E. M., GREULICH, S., KLINGEL, K., KANDOLF, R. & SECHTEM, U. 2008. Cardiovascular magnetic resonance in clinically suspected cardiac amyloidosis: noninvasive imaging compared to endomyocardial biopsy. ***J Am Coll Cardiol,*** **51, 1022-30.**

WANG, H., LASLETT, L. J., RICHMAN, C. M. & WUN, T. 2004. Acute myocardial infarction in hemoglobin SC disease. ***Ann Hematol,*** **83, 622-4.**

WANG, J., KHOURY, D. S., THOHAN, V., TORRE-AMIONE, G. & NAGUEH, S. F. 2007a. Global Diastolic Strain Rate for the Assessment of Left Ventricular Relaxation and Filling Pressures. ***Circulation,*** **115, 1376-1383.**

WESTWOOD, M. A., SHAH, F., ANDERSON, L. J., STRANGE, J. W., TANNER, M. A., MACEIRA, A. M., HOWARD, J., PORTER, J. B., WALKER, J. M., WONKE, B. & PENNELL, D. J. 2007. Myocardial tissue characterization and the role of chronic anemia in sickle cell cardiomyopathy. ***J Magn Reson Imaging,*** **26, 564-8.**

WETHERS, D. L. 2000. Sickle cell disease in childhood: Part I. Laboratory diagnosis, pathophysiology and health maintenance. ***American Family Physician,*** **62, 1013-20, 1027-8.**

WHO. 2006 October. ***Sickle-cell anaemia: Report by the secretariat*** **[Online]. Available: https://apps.who.int/gb/ebwha/pdf_files/WHA59/A59_9-en.pdf.**

WOOD, J. C. 2008. Cardiac iron across different transfusion-dependent diseases. ***Blood Reviews,*** **22, S14-S21.**

WU, Y. & KOVÁCS, S. J. 2006. Frequency-based analysis of the early rapid filling pressure-flow relation elucidates diastolic efficiency mechanisms. ***American Journal of Physiology - Heart and Circulatory Physiology,*** **291, H2942-H2949.**

YODWUT C , L. R., WEINERT L,AHMAD H, MOR-AVI V 2012. Three-dimensional echocardiographic quantitative evaluation of left ventricular diastolic function using analysis of chamber volume and myocardial deformation. ***Int J Cardiovasc Imaging*****.**

YU, C.-M., SANDERSON, J. E., MARWICK, T. H. & OH, J. K. 2007. Tissue Doppler Imaging: A New Prognosticator for Cardiovascular Diseases. ***J Am Coll Cardiol,*** **49, 1903-1914.**

ZERHOUNI, E. A., PARISH, D. M., ROGERS, W. J., YANG, A. & SHAPIRO, E. P. 1988. Human heart: tagging with MR imaging--a method for noninvasive assessment of myocardial motion. ***Radiology,*** **169, 59-63.**

ZILBERMAN, M. V., DU, W., DAS, S. & SARNAIK, S. A. 2007. Evaluation of left ventricular diastolic function in pediatric sickle cell disease patients. ***Am J Hematol,*** **82, 433-8.**

ZIMBARRA CABRITA, I., MOHAMMED, A., LAYTON, M., GHORASHIAN, S., GILMORE, A., CHO, G., HOWARD, J., ANIE, K. A., DESFORGES, L., BASSETT, P., GRAPSA, J., HOWARD, L., MAHALINGAM, G., DAWSON, D., PINTO, F. J., NIHOYANNOPOULOS, P., DAVIES, S. C. & GIBBS, J. S. R. 2013a. The association between tricuspid regurgitation velocity and 5-year survival in a North West London population of patients with sickle cell disease in the United Kingdom. ***British Journal of Haematology,*** **162, 400-408.**

ZIMBARRA CABRITA, I., RUISANCHEZ, C., DAWSON, D., GRAPSA, J., NORTH, B., HOWARD, L. S., PINTO, F. J., NIHOYANNOPOULOS, P. & GIBBS, J. S. 2010. Right ventricular function in patients with pulmonary hypertension; the value of myocardial performance index measured by tissue Doppler imaging. ***Eur J Echocardiogr,*** **11, 719-24.**

ZIMBARRA CABRITA, I., RUISANCHEZ, C., GRAPSA, J., DAWSON, D., NORTH, B., PINTO, F. J., GIBBS, J. S. & NIHOYANNOPOULOS, P. 2013b. Validation of the isovolumetric relaxation time for the estimation of pulmonary systolic arterial blood pressure in chronic pulmonary hypertension. ***Eur Heart J Cardiovasc Imaging,*** **14, 51-5.**

ZOGHBI, W. A., ENRIQUEZ-SARANO, M., FOSTER, E., GRAYBURN, P. A., KRAFT, C. D., LEVINE, R. A., NIHOYANNOPOULOS, P., OTTO, C. M., QUINONES, M. A., RAKOWSKI, H., STEWART, W. J., WAGGONER, A. & WEISSMAN, N. J. 2003. Recommendations for evaluation of the severity of native valvular regurgitation with two-dimensional and Doppler echocardiography. ***J Am Soc Echocardiogr,*** **16, 777-802.**

ZWANENBURG, J. J., GOTTE, M. J., MARCUS, J. T., KUIJER, J. P., KNAAPEN, P., HEETHAAR, R. M. & VAN ROSSUM, A. C. 2005. Propagation of onset and peak time of myocardial shortening in time of myocardial shortening in ischemic

versus nonischemic cardiomyopathy: assessment by magnetic resonance imaging myocardial tagging. ***J Am Coll Cardiol,*** **46, 2215-22.**

Appendices

Appendix I: Research Ethics Committee Approval letter

National Research Ethics Service
Hammersmith and Queen Charlotte's & Chelsea Research Ethics Committee
Room 4W/12, 4th Floor
Charing Cross Hospital
Fulham Palace Road
London
W6 8RF
Telephone: 020 3311 7258
Facsimile: 020 3311 7280

Miss Ines Z P G Cabrita
Research Echocardiographer
Imperial College London
Sir John McMichael Centre
Hammersmith Hospital

08 December 2009

Dear Miss Cabrita

Study Title:	**The heart in sickle cell disease. Role of non invasive cardiac imaging by advanced echocardiography and cardiac magnetic resonance assessment of myocardial function.**
REC reference number:	**09/H0707/73**
Protocol number:	**1.0**

Thank you for your letter of 15 October 2009, responding to the Committee's request for further information on the above research and submitting revised documentation.

The further information has been considered on behalf of the Committee by the Chair.

Confirmation of ethical opinion

On behalf of the Committee, I am pleased to confirm a favourable ethical opinion for the above research on the basis described in the application form, protocol and supporting documentation as revised, subject to the conditions specified below.

Ethical review of research sites

The favourable opinion applies to all NHS sites taking part in the study, subject to management permission being obtained from the NHS/HSC R&D office prior to the start of the study (see "Conditions of the favourable opinion" below).

The Committee has not yet been notified of the outcome of any site-specific assessment (SSA) for the non-NHS research site(s) taking part in this study. The favourable opinion does not therefore apply to any non-NHS site at present. I will write to you again as soon as one Research Ethics Committee has notified the outcome of a SSA. In the meantime no study procedures should be initiated at non-NHS sites.

Conditions of the favourable opinion

The favourable opinion is subject to the following conditions being met prior to the start of the study.

Management permission or approval must be obtained from each host organisation prior to

the start of the study at the site concerned.

For NHS research sites only, management permission for research ("R&D approval") should be obtained from the relevant care organisation(s) in accordance with NHS research governance arrangements. Guidance on applying for NHS permission for research is available in the Integrated Research Application System or at http://www.rdforum.nhs.uk. *Where the only involvement of the NHS organisation is as a Participant Identification Centre, management permission for research is not required but the R&D office should be notified of the study. Guidance should be sought from the R&D office where necessary.*

Sponsors are not required to notify the Committee of approvals from host organisations.

It is the responsibility of the sponsor to ensure that all the conditions are complied with before the start of the study or its initiation at a particular site (as applicable).

Approved documents

The final list of documents reviewed and approved by the Committee is as follows:

Document	*Version*	*Date*
REC application		06 August 2009
Protocol	1.0	06 August 2009
Investigator CV	Ines Zimbarra de Pinho Galvao Cabrita	07 August 2009
Participant Information Sheet: healthy volunteers	1.0	05 August 2009
GP/Consultant Information Sheets	1.0	05 August 2009
Advertisement	1.0	05 August 2009
study design	1.0	14 July 2009
Dr Gibbs CV		07 August 2009
Participant Information Sheet: Patients - Group A1	3	02 December 2009
Participant Information Sheet: Patients - Group A2	3	02 December 2009
Participant Consent Form	2	02 December 2009
Response to Request for Further Information		15 October 2009

Statement of compliance

The Committee is constituted in accordance with the Governance Arrangements for Research Ethics Committees (July 2001) and complies fully with the Standard Operating Procedures for Research Ethics Committees in the UK.

After ethical review

Now that you have completed the application process please visit the National Research Ethics Service website > After Review

You are invited to give your view of the service that you have received from the National Research Ethics Service and the application procedure. If you wish to make your views known please use the feedback form available on the website.

The attached document *"After ethical review – guidance for researchers"* gives detailed

guidance on reporting requirements for studies with a favourable opinion, including:

- Notifying substantial amendments
- Adding new sites and investigators
- Progress and safety reports
- Notifying the end of the study

The NRES website also provides guidance on these topics, which is updated in the light of changes in reporting requirements or procedures.

We would also like to inform you that we consult regularly with stakeholders to improve our service. If you would like to join our Reference Group please email referencegroup@nres.npsa.nhs.uk.

09/H0707/73	**Please quote this number on all correspondence**

Yours sincerely

cc

Professor A George
Chair

Email: clive.collett@imperial.nhs.uk

Enclosures: "After ethical review – guidance for researchers"

Copy to: *Mr Gary Roper*

Appendix II: Supporting documents for Ethical Approval

Imperial College London

Imperial College Healthcare NHS
NHS Trust

AHSC Joint Research Office
Hammersmith Hospital
1st Floor
Ham House
Hammersmith Hospital
Du Cane Road
London W12 0HS
Tel:
Fax: 020 8383 4957

Miss Ines Z P G Cabrita
Research Echocardiographer
Sir John McMichael Centre
Hammersmith Hospital
Du Cane Road
LONDON
W12 0HS

26 January 2010

Dear Miss Cabrita

RE: Trust Approval - Research Governance Registration

Project Title: The heart in sickle cell disease. Role of non invasive cardiac imaging by advanced echocardiography and cardiac magnetic resonance assessment of myocardial function

Our Project Reference: ZIMI1001
Ethics Reference: 09/H0707/73

With regard to the above, we are pleased to confirm that your project complies with all necessary research governance registration requirements and is therefore officially recognised and approved.

We wish you every success in the progression of this project. Please note our reference number and use it in all future communications.

If you have any questions or need clarification please contact Patrik Pettersson (020 8383 4959) patrik.pettersson@imperial.nhs.uk) or Susana Murphy (020 8383 3329) susana.murphy@imperial.nhs.uk.

Yours sincerely

Michelle Quaye
Research Governance Manager, Imperial College and Imperial College Healthcare NHS Trust

Imperial College
London

Faculty of Medicine
Imperial College London

G02 Sir Alexander Fleming Building
South Kensington Campus
London, SW7 2AZ
Tel: +44 (0)20 7594 1188 Fax: +44 (0)207 594 1792

gary.roper@imperial.ac.uk
www.icl.ac.uk/clinicalresearchgovernanceoffice

Gary Roper
Head of Regulatory Compliance

Our ref: CRO1375
31st July 2009

Miss Ines Cabrita
Research Echocardiographer
Walk Phasst Office
Commonwealth Building
Imperial College London
Hammersmith Campus

Dear Miss Cabrita,

Re: **The Heart in Sickle Cell Disease.Role of non invasive cardiac imaging by advanced echocardiography and cardiac magnetic resonance assessment of myocardial function.**

This is to confirm that the above named research project utilises human participants, their organs, tissue and/or data as defined under the sponsorship requirements of the Research Governance Framework for Health and Social Care 2005, incorporating the Medicines for Human Use (Clinical Trials) Regulations 2004.

On behalf of Imperial College of Science, Technology and Medicine, we undertake to act as the identified Research Sponsor for this project.

This letter confirms:

- The research proposal has been discussed, assessed and registered with Imperial College Clinical Research Governance Office and provisional sponsor approval granted.
- The Chief Investigator has undergone a process of scientific critique commensurate with the scale of the project.
- Indemnity and insurance arrangements have been put in place to cover the project.
- Resources and support are available to the research team to aid delivery of the research as proposed.
- Management, monitoring and reporting responsibilities for the research have been approved.
- Imperial College will undertake and enforce those sponsor duties set out in the NHS Research Governance Framework for Health and Social Care.

Imperial College Sponsorship is conditional on the project receiving applicable ethical and regulatory approval for all research related aspects of its conduct. It is also conditional on successful contract and agreement negotiations and sign off via Research Services and the Contracting Office, where relevant, and before the study commences.

A copy of the ethics approval letter **must** be sent to the Research Governance Manager prior to the study commencing. Sponsorship is dependant on obtaining R&D Office approval for all NHS sites where the research is being conducted.

Yours sincerely

Gary Roper
Head of Regulatory Compliance
Faculty of Medicine
Imperial College London

Date: (dd/mm/yyyy)

Declaration by the sponsor's representative

If there is more than one sponsor, this declaration should be signed on behalf of the co-sponsors by a representative of the sponsor nominated to take the lead for the REC application.

I confirm that:

1. This research proposal has been discussed with the Chief Investigator and agreement in principle to sponsor the research is in place.
2. An appropriate process of scientific critique has demonstrated that this research proposal is worthwhile and of high scientific quality.*
3. Any necessary indemnity or insurance arrangements, as described in question A35, will be in place before this research starts.
4. Arrangements will be in place before the study starts for the research team to access resources and support to deliver the research as proposed.
5. Arrangements to allocate responsibilities for the management, monitoring and reporting of the research will be in place before the research starts.
6. The duties of sponsors set out in the NHS Research Governance Framework for Health and Social Care will be undertaken in relation to this research.**
7. I understand that the lay summary of this study will be published on the website of the National Research Ethics Service (NRES) as it appears in this application. Publication will take place no earlier than 3 months after issue of the ethics committee's final opinion or the withdrawal of the application.

* Not applicable to student research (except doctoral research).
** Not applicable to research outside the scope of the Research Governance Framework.

Signature: .....

Print Name: G.C. ROPER

Post: Head of Regulatory Compliance

Organisation: Imperial College London

Date: (dd/mm/yyyy) 07.08.09

Imperial College Healthcare NHS
NHS Trust

Participant Informed Consent Form:

Title of project:
THE HEART IN SICKLE CELL DISEASE. ROLE OF NON INVASIVE CARDIAC IMAGING BY ADVANCED ECHOCARDIOGRAPHY AND CARDIAC MAGNETIC RESONANCE ASSESSMENT OF MYOCARDIAL FUNCTION.

Chief Investigator: Ines Zimbarra Cabrita

Please initial in the boxes

1. I confirm that I have read and understand the subject information sheet dated ..... version ..... for the above study and have had the opportunity to ask questions which have been answered fully. ☐
2. I understand that my participation is voluntary and I am free to withdraw at any time, without giving any reason, without my medical care or legal rights being affected. ☐
3. I understand that sections of any of my medical notes may be looked at by responsible individuals from Hammersmith Hospitals NHS Trust or from regulatory authorities where it is relevant to my taking part in this research. I give permission for these individuals to access my records that are relevant to this research. ☐
4. I give permission to the investigators of this study the use of the data collected during the Walk-PHaSST study. ☐
5. **Group A only:** I give permission to take blood samples as part of this study ☐
6. I agree to take part in the above study ☐

OPTIONAL
7. I agree to my GP being informed of my participation in the study ☐
8. 'I understand that information held by the NHS and records maintained by The NHS Information Centre and the NHS Central Register may be used to help contact me and provide information about my health status'. ☐

Name of Subject	Signature	Date
Name of Person taking consent (if different from Chief Investigator)	Signature	Date
Chief Investigator	Signature	Date

1 copy for subject; 1 copy for Principal Investigator; 1copy to be kept with hospital notes

Version 2.0 –02-DEC-09

INFORMATION SHEET FOR RESEARCH PARTICIPANTS (PATIENTS GROUP A1)

TITLE OF THE STUDY:

THE HEART IN SICKLE CELL DISEASE. ROLE OF NON INVASIVE CARDIAC IMAGING BY ADVANCED ECHOCARDIOGRAPHY AND CARDIAC MAGNETIC RESONANCE ASSESSMENT OF MYOCARDIAL FUNCTION.

Invitation to participate in the Study

You are being invited to take part in a research study at the Hammersmith Hospital that will study the heart in sickle cell disease (SCD). Before you decide it is important for you to understand why the research is being done and what it will involve. Please take time to read the following information carefully and discuss with friends, relatives and your GP if you wish. Please ask us if there is anything that is not clear or if you would like more information. Take time to decide whether or not you wish to take part.

Whether you decide to take part or not, your treatment will not be affected by your decision. You are free to withdraw at any time without explanation and your subsequent treatment will not be affected.

What is the purpose of the study?

An estimated one-third of adults with SCD have high blood pressure in the lungs (pulmonary hypertension). People with sickle cell disease and pulmonary hypertension (PH) tend to have more complications i.e. shortness of breath, pain crisis, pneumonia) than people with SCD but without pulmonary hypertension.

The heart is frequently enlarged in people with sickle cell anemia. In some people with sickle cell anaemia the heart becomes a bit stiff (**diastolic dysfunction**). A stiff heart cannot relax properly and this can cause pulmonary hypertension. We want to look at whether you have any abnomalities in your heart. In particular, we will study the relaxation of your heart muscle and in case of any abnormality, if it is contributing to PH. We also want to look if there are any changes in your heart function status and blood pressure in the lungs since your last visit during the Walk-PHaSST study.

We will need to study 2 main groups of people:

Group A: Sickle cell disease patients. This group will be divided into 2 sub-groups.

Group A1: Patients with normal diastolic function
Group A2: Patients with diastolic dysfunction

Group B. Healthy people

We need at least 60 patients in Group A for this study to work.

Why have I been invited?

You have been invited because you have participated previously in the Walk−PHaSST study where it was found that your heart is not stiff (normal). We would like to do a follow-up study to assess your heart function one year after the echocardiogram done during the Walk-PHaSST study.

Who are the participants?

This research will be performed in patients with SCD who have already taken part in the screening part of the Walk−PHaSST clinical research trial.

Do I have to take part?

It is up to you to decide whether or not to take part. If you do decide to take part you will be given this information sheet to keep and be asked to sign a consent form. If you decide to take part you are still free to withdraw at any time and without giving a reason. A decision to withdraw at any time, or a decision not to take part, will not affect the standard of care you receive.

What do I have to do?

If you decide to take part in this study, you will need to visit the Hammersmith Hospital for one visit.
This study will be performed after one year of the screening visit of the Walk−PHaSST study and will include the following procedures:

-health status questionnaire (face-to-face interview)
-echocardiogram
-blood tests

Maximum length of visit: 1 hour and 30 minutes.

All these procedures will be performed after you have read and signed the consent form. None of your current medication or treatments will be affected by participation in this part of the study. This study requires no lifestyle changes.

An Explanation of Procedures, Tests, and Their Risks

Echocardiogram: This will be performed in the Sir John McMichael Centre at Hammersmith Hospital. This test involves holding a small probe against your chest wall to obtain pictures of your heart. The probe uses sound waves to detect the structures of your heart and does not involve any radiation. It has no side effects, and does not involve the use of needles or agents. It takes around 30-45 minutes and no special preparation is needed.

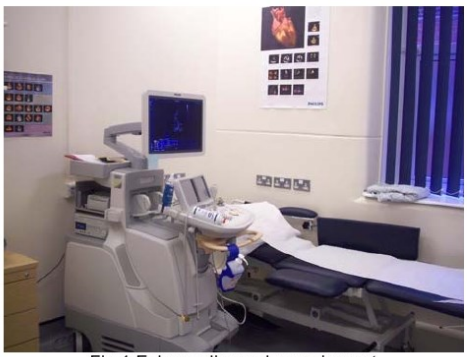

Fig.1 Echocardiography equipment

We are also testing how accurate and reproducible the echo measurements are. For that, we would need to repeat a small part of the echo after an hour after the first acquired images. This will only take 10 minutes.

Blood Sample*:* About 10 ml of blood (three teaspoonfuls) are required for clinical laboratory tests. To draw blood, a needle will be put into the vein of your arm. You may feel some pain at the needle entry site. There is a slight risk of bleeding around the site. This is not dangerous, but it could result in a bruise. Some people experience feelings of lightheadedness or dizziness after having blood taken, we will monitor you closely and

ask you about these symptoms before we allow you to stand up. We will discard the blood once the tests have been completed

In addition to this study, we will request your consent (optional) for the purposes of a long-term follow-up. If you agree, the National Health Service Information Centre for health and social care (NHS IC) and the NHS Central Register will keep us informed about your health status.

What are the benefits of this study?

There is no benefit to be derived from participation in the study. Information obtained during the course of this research study may contribute to a better understanding of your disease.

What are the risks and side effects?

There are no known risks or side effect in having an echo.

Some people experience feelings of lightheadedness or dizziness after having blood taken. There is also a risk of bruising and bleeding around the site.

What would happen if any abnormalities were found during the study?

Any relevant clinical findings may be shared with your GP and Consultant Haematologist. In the event of an acute sickle cell crisis you will be immediately referred to the haematology team at Hammersmith Hospital for treatment.

What if something goes wrong?

Imperial College London holds insurance policies which apply to this study. If you experience harm or injury as a result of taking part in this study, you may be eligible to claim compensation without having to prove that Imperial College is at fault. This does not affect your legal rights to seek compensation.

If you are harmed due to someone's negligence, then you may have grounds for a legal action. Regardless of this, if you wish to complain, or have any concerns about any aspect of the way you have been treated during the course of this study then you should immediately inform the Investigator (Ines Cabrita 02083832269). The normal National Health Service complaint complaints mechanisms are also available to you. If you are still not satisfied with the response, you may contact the Imperial College Joint Research Office

Will I get compensated for my travel expenses?

We will refund travel expenses up to a maximum of £10 pounds per visit. If you travel by public transport you will need to bring your ticket. If you travel by cab please get a receipt from your driver and if you drive to the hospital we will reimburse the cost of fuel for a return journey from your home at 40p per mile.

Will my taking part in this study be kept confidential?

All information which is collected about you during the course of the research will be kept strictly confidential. Any study related information about you which leaves the hospital will have all identifiable information removed so that you cannot be recognised from it.
Research information will be kept in a password-protected computer file that only the investigators (or their designees) can view. If we learn anything of importance during this research, we may publish the results in a medical journal. You will not be identified in the article. The procedures for handling, processing, storage and destruction of your data are compliant with the Data Protection Act 1998.

Who is organising and funding the research?

The Fundação para a Ciência e a Tecnologia is the Portuguese government body responsible for evaluating the study and awarding a doctoral grant for the Chief Investigator. The Chief Investigator will have a monthly allowance to conduct the study. There will be no per patient payments.

Who has reviewed the study?

This study has been given a favourable ethical opinion for conduct in the NHS by Hammersmith, Queen Charlotte's and Chelsea Research Ethics Committee.

Contacts for further information:

Please ask any questions that you wish to. A copy of this information sheet and consent form will be given to you to take away. You can contact Ines Zimbarra Cabrita at any time during this study. She can be contacted through Walk-Phasst office at Hammersmith Hospital (tel: 02083832269 or 02083834068) or through the e-mail : ines.cabrita05@imperial.ac.uk. Thank you for considering this study.

INFORMATION SHEET FOR RESEARCH PARTICIPANTS (PATIENTS GROUP A2)

TITLE OF THE STUDY:

THE HEART IN SICKLE CELL DISEASE. ROLE OF NON INVASIVE CARDIAC IMAGING BY ADVANCED ECHOCARDIOGRAPHY AND CARDIAC MAGNETIC RESONANCE ASSESSMENT OF MYOCARDIAL FUNCTION.

Invitation to participate in the Study

You are being invited to take part in a research study at the Hammersmith Hospital that will study the heart in sickle cell disease (SCD). Before you decide it is important for you to understand why the research is being done and what it will involve. Please take time to read the following information carefully and discuss with friends, relatives and your GP if you wish. Please ask us if there is anything that is not clear or if you would like more information. Take time to decide whether or not you wish to take part.

Whether you decide to take part or not, your treatment will not be affected by your decision. You are free to withdraw at any time without explanation and your subsequent treatment will not be affected.

What is the purpose of the study?

An estimated one-third of adults with SCD have high blood pressure in the lungs (pulmonary hypertension). People with sickle cell disease and pulmonary hypertension (PH) tend to have more complications i.e. shortness of breath, pain crisis, pneumonia) than people with SCD but without pulmonary hypertension.

The heart is frequently enlarged in people with sickle cell anemia. In some people with sickle cell anaemia the heart becomes a bit stiff (**diastolic dysfunction**). A stiff heart cannot relax properly and this can pulmonary hypertension. We want to look at whether you have any abnomalities in your heart. In particular, we will study the relaxation of your heart muscle and in case of any abnormality, if it is contributing to PH. We also want to look if there are any changes in your heart function status and blood pressure in the lungs since your last visit during the Walk-PHaSST study.

We will need to study 2 main groups of people:

Group A: Sickle cell disease patients. This group will be divided into 2 sub-groups.

Group A1: Patients with normal diastolic function
Group A2: Patients with diastolic dysfunction

Group B. Healthy people

We need at least 60 patients in Group A for this study to work.

Why have I been invited?

You have been invited because you have participated previously in the Walk−PHaSST study where it was found that you have a stiff heart. We would like to do a follow-up study and further investigations may assess your heart function better.

Who are the participants?

This research will be performed in patients with SCD who have already taken part in the screening part of the Walk-PHaSST clinical research trial.

Do I have to take part?

It is up to you to decide whether or not to take part. If you do decide to take part you will be given this information sheet to keep and be asked to sign a consent form. If you decide to take part you are still free to withdraw at any time and without giving a reason. A decision to withdraw at any time, or a decision not to take part, will not affect the standard of care you receive.

What do I have to do?

If you decide to take part in this study, you will need to visit the Hammersmith Hospital for one visit.
This study will be performed one year after the screening visit of the Walk−PHaSST study and will include the following procedures:

-health status questionnaire (face-to-face interview)
-echocardiogram
-cardiac magnetic resonance
-blood tests

Maximum length of visit: 2 hour and 30 minutes.

All these procedures will be performed after you have read and signed the consent form. None of your current medication or treatments will be affected by participation in this part of the study. This study requires no lifestyle changes.

An Explanation of Procedures, Tests, and Their Risks

Echocardiogram: This will be performed in the Sir John McMichael Centre at Hammersmith Hospital. This test involves holding a small probe against your chest wall to obtain pictures of your heart. The probe uses sound waves to detect the structures of your heart and does not involve any radiation. It has no side effects, and does not involve the use of needles or agents. It takes around 30-45 minutes and no special preparation is needed.

Fig.1 Echocardiography equipment

We are also testing how accurate and reproducible the echo measurements are. For that, we would need to repeat a small part of the echo after one hour after the first acquired images. This will only take 10 minutes.

Cardiac Magnetic Resonance: This test will be done in the Robert Steiner MR Unit at Hammersmith Hospital.A MRI scanner looks like a long narrow tube that will be used to obtain moving pictures of your heart (fig.2). The test is painless, uses no radiation, and is routinely used in hospitals.

No special preparation is needed before you have an MRI. When applicable, a pregnancy test may be required prior to the MRI.

Before the scan begins we will place monitoring equipment over your chest and you will be given an alarm to hold to press in case you need any assistance. You will lie down on a sliding table that will move into the scanner. You will be asked to lie still and you will hear a knocking noise during the scan. You will be able to communicate with a member of staff at any time using an intercom system. If you do not like being in the scanner for any reason, the scan can be stopped and we will take you out immediately.

During the scan we will give you an injection of a clear fluid (contrast) that helps to show areas of inflammation more clearly. A qualified person will insert a small plastic tube called a cannula into a vein in your arm before the scan begins. You will feel a sharp scratch while the cannula is inserted and there may be some mild bleeding or bruising afterwards.

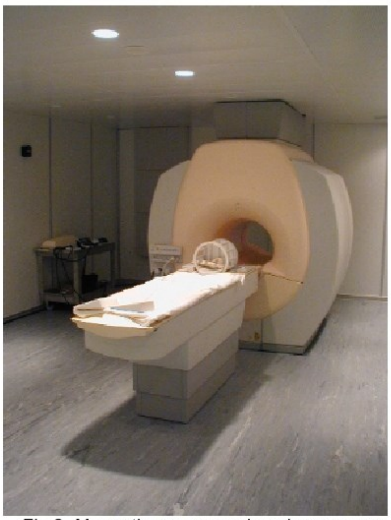

Fig.2- Magnetic resonance imaging scanner

A radiologist will review the images. In the unlikely event that we discover an unexpected abnormality your doctor will contact you to discuss the results. A significant abnormality may require further investigation or treatment. Each MRI scan will take approximately 45-60 minutes. Any relevant clinical findings may be shared with your GP and Consultant.

Blood Sample*:* About 10 ml of blood (three teaspoonfuls) are required for clinical laboratory tests. To draw blood, a needle will be put into the vein of your arm. You may feel some pain at the needle entry site. There is a slight risk of bleeding around the site. This is not dangerous, but it could result in a bruise. Some people experience feelings of lightheadedness or dizziness after having blood taken we will monitor you closely and ask you about these symptoms before we allow you to stand up. We will discard the blood once the tests have been completed.

In addition to this study, we will request your consent (optional) for the purposes of a long-term follow-up. If you agree, the National Health Service Information Centre for health and social care (NHS IC) and the NHS Central Register will keep us informed about your health status.

What are the benefits of this study?

There is no benefit to be derived from participation in the study. Information obtained during the course of this research study may contribute to a better understanding of your disease.

What are the risks and side effects?

There are no known risks or side effect in having an echo.

Some people experience feelings of lightheadedness or dizziness after having blood taken. There is also a risk of bruising and bleeding around the site.

The space inside the MRI scanner is small and occasionally people may find this claustrophobic. MRI scanning is widely performed in many hospitals and is not believed to pose any significant risks. The scanner is operated within the National Radiological Protection Board Guidelines. It is essential that you tell us if you are pregnant or breast-feeding or have any metal objects in or around your body as they may pose a danger to your health when close to the scanner.

Contrast is routinely used when patients have an MRI scan. Symptoms of nausea, headache or taste disturbance occur in less than 1 in 100 patients. Serious allergic reactions requiring treatment have been reported in less than 1 in 1,000 patients. You will not receive contrast if you have had a previous allergic reaction to it, have kidney disease, or certain types of irregular heart beat (arrhythmia).

What would happen if any abnormalities were found during the study?

Any relevant clinical findings may be shared with your GP and Consultant Haematologist. In the event of an acute sickle cell crisis you will be immediately referred to the haematology team at Hammersmith Hospital for treatment.

What if something goes wrong?

Imperial College London holds insurance policies which apply to this study. If you experience harm or injury as a result of taking part in this study, you may be eligible to claim compensation without having to prove that Imperial College is at fault. This does not affect your legal rights to seek compensation.

If you are harmed due to someone's negligence, then you may have grounds for a legal action. Regardless of this, if you wish to complain, or have any concerns about any aspect of the way you have been treated during the course of this study then you should immediately inform the Investigator (Ines Cabrita 02083832269). The normal National Health Service complaint complaints mechanisms are also available to you. If you are still not satisfied with the response, you may contact the Imperial College Joint Research Office

Will I get compensated for my travel expenses?

We will refund travel expenses up to a maximum of £10 pounds per visit. If you travel by public transport you will need to bring your ticket. If you travel by cab please get a receipt from your driver and if you drive to the hospital we will reimburse the cost of fuel for a return journey from your home at 40p per mile.

Will my taking part in this study be kept confidential?

All information which is collected about you during the course of the research will be kept strictly confidential. Any study related information about you which leaves the hospital will have all identifiable information removed so that you cannot be recognised from it.
Research information will be kept in a password-protected computer file that only the investigators (or their designees) can view. Identifiable images from the MRI scan will be stored on a secure hospital database to which only authorised staff has access. If we learn anything of importance during this research, we may publish the results in a medical journal. You will not be identified in the article. The procedures for handling, processing, storage and destruction of your data are compliant with the Data Protection Act 1998.

Who is organising and funding the research?

The Fundação para a Ciência e a Tecnologia is the Portuguese government body responsible for evaluating the study and awarding a doctoral grant for the Chief Investigator. The Chief Investigator will have a monthly allowance to conduct the study. There will be no per patient payments.

Who has reviewed the study?

This study has been given a favourable ethical opinion for conduct in the NHS by Hammersmith, Queen Charlotte's and Chelsea Research Ethics Committee.

Contacts for further information:

Please ask any questions that you wish to. A copy of this information sheet and consent form will be given to you to take away. You can contact Ines Zimbarra Cabrita at any time during this study. She can be contacted through Walk-Phasst office at Hammersmith Hospital (tel: 02083832269 or 02083834068) or through the e-mail : ines.cabrita05@imperial.ac.uk. Thank you for considering this study.

INFORMATION SHEET FOR RESEARCH PARTICIPANTS (VOLUNTEERS)

TITLE OF THE STUDY:

THE HEART IN SICKLE CELL DISEASE. ROLE OF NON INVASIVE CARDIAC IMAGING BY ADVANCED ECHOCARDIOGRAPHY AND CARDIAC MAGNETIC RESONANCE ASSESSMENT OF MYOCARDIAL FUNCTION.

Chief Investigator: Ines Zimbarra Cabrita

Invitation to participate in the Study

You are being invited to take part in a research study at the Hammersmith Hospital that will study the heart in sickle cell disease (SCD). Before you decide it is important for you to understand why the research is being done and what will involve. Please take time to read the following information carefully and discuss with friends, relatives and your GP if you wish. Please ask us if there is anything that is not clear or if you would like more information. Take time to decide whether or not you wish to take part.

What is the purpose of the study?

We are studying the heart in SCD patients. An estimated one-third of adults with SCD have pulmonary hypertension (high blood pressure in the lungs). People with sickle cell disease and pulmonary hypertension (PH) tend to have more complications (shortness of breath, pain crisis, pneumonia, and death) than people with SCD but without pulmonary hypertension.
The research will focus on the study of the heart in patients with SCD and pulmonary hypertension and/or diastolic dysfunction. Diastolic dysfunction is an abnormality in the heart's (i.e. left ventricle) filling during diastole (when it is relaxing).
Echocardiography and cardiac magnetic resonance are important and easy to perform non-invasive tests that will provide important information about the function and structure of the heart, and can detect early signs of heart disease.

We will need to evaluate the function of the heart in **2 groups** of people:

Group A: Sickle cell disease patients
Group B. Healthy volunteers

You have been chosen because you belong to **Group B**. We are looking for healthy volunteers who match our group of patients for age, sex and race in order to obtain normal values in echocardiography. We need at least 35 healthy volunteers to make this study meaning full. Volunteers will be asked to attend the Sir John and McMichael Centre Hospital for **one visit**.

What will happen to me if I take part?

Volunteers in this study will have the following tests:

- Health status questionnaire
- An Echocardiogram

The echocardiogram will be done at the Sir John McMichael Centre of Hammersmith Hospital. This test involves holding a small probe against your chest wall to obtain pictures of your heart. The probe uses sound waves to detect the structures of your heart and does not involve any radiation. It has no known side effects, is harmless and does not involve the use of needles or agents. It takes around 30-45 minutes and not special preparation is needed before you have the test.

We are testing the reproducibility of the echocardiographic measurements of the right ventricle volume. For that, you would need to repeat a small part of the echocardiogram (will take only 10 min), after 1 hour of the first acquired images.
The estimated duration of the visit will be 1 hour and 30 minutes.

Do I have to take part?

It is up to you to decide whether or not to take part. If you do decide to take part you will be given this information sheet to keep and be asked to sign a consent form. If you decide to take part you are still free to withdraw at any time and without giving a reason. A decision to withdraw at any time, or a decision not to take part, will not affect the standard of care you receive.

Are there any risks associated with taking part?

There are no risks associated with taking part in this study. An echocardiogram is a painless and harmless test.

What are the possible benefits of taking part?

There is no intended personal benefit from taking part in the study, although the results will be extremely important to our understanding of the heart in sickle cell disease and the reproducibility of three-dimensional echocardiography.

Will I get compensated for my travel expenses?

We will refund travel expenses up to a maximum of £10 pounds per visit. If you travel by public transport you will need to bring your ticket. If you travel by cab please get a receipt from your driver and if you drive to the hospital we will reimburse the cost of fuel for a return journey from your home at 40p per mile and parking charge.

What if something goes wrong?

Imperial College London holds insurance policies which apply to this study. If you experience harm or injury as a result of taking part in this study, you may be eligible to claim compensation without having to prove that Imperial College is at fault. This does not affect your legal rights to seek compensation.

If you are harmed due to someone's negligence, then you may have grounds for a legal action. Regardless of this, if you wish to complain, or have any concerns about any aspect of the way you have been treated during the course of this study then you should immediately inform the Investigator (Insert name and contact details). The normal National Health Service complaint complaints mechanisms are also available to you. If you are still not satisfied with the response, you may contact the Imperial College Joint Research Office

What will happen to the results of the research study?

Results of the study, including volunteers details will be confidential, will not be divulged to a third party and will be stored securely (under lock and password protected computer file) in the Sir John McMichael Centre at Hammersmith Hospital that only the investigators (or their designees) can view. The results of the study are likely to be published in a scientific journal. Volunteer names will not be used in the publication.

Will my taking part in this study be kept confidential?

All information which is collected about you during the course of the research will be kept strictly confidential. Any information about you which leaves the hospital/surgery will have your name and address removed so that you cannot be recognised from it. The procedures for handling, processing, storage and destruction of your data are compliant with the Data Protection Act 1998.

Who has reviewed the study?

This study was given a favourable ethical opinion for conduct in the NHS by Hammersmith, Queen Charlotte's and Chelsea Research Ethics Committee.

Who is organising and funding the research?

The Fundação para a Ciência e a Tecnologia is the Portuguese government body responsible for evaluating the study and awarding a doctoral grant for the Chief Investigator. The Chief Investigator will have a monthly allowance to conduct the study, there will be no per patient payments.

For further information please contact:

Please ask any questions that you wish to. A copy of this information sheet and consent form will be given to you to take away. You can contact Ines Zimbarra Cabrita at any time during this study. She can be contacted through Sir John McMichael Centre at Hammersmith Hospital (tel: 02083832269 or 02083834068) or through her e-mail : ines.cabrita05@imperial.ac.uk. Thank you for your time considering this study.

Imperial College Healthcare NHS
NHS Trust

RESEARCH STUDY

CALL FOR HEALTHY VOLUNTEERS

We are conducting a study on **healthy volunteers aged 18 years and above**. We are investigating the heart in sickle cell disease, an inherited blood disorder that affects red blood cells and is found more frequently in persons of Middle Eastern, Indian, Mediterranean and African heritage.

We are looking for **healthy volunteers who match our groups of patients for age, sex and race** to obtain normal values in echocardiography in a population matching the group of patients with sickle cell disease that we are studying. An echocardiogram (also called an echo) is similar to the ultrasound scan that is used in pregnancy. An echo uses ultrasound **to examine the heart** and to see how it is functioning. It is a painless and harmless test. There are no known risks from the clinical use of ultrasound during this type of testing.

The study includes **one visit that will last no longer than 1 hour and 30 minutes.** It will consist of a short interview related to your health status followed by an echocardiogram to check the size, shape, and movement of your heart muscle, as well as checking your heart valves are working normally and how blood is flowing through your heart.

If you are interested or would like further information please e-mail/call:

ines.cabrita05@imperial.ac.uk

Tel: 02083832269 / 02083834068

Sir John McMichael Centre

Hammersmith Hospital,

Du Cane Road, W12 0HS London

Version 1. 0-5-Aug-09

Imperial College Healthcare NHS
NHS Trust

Walk-PHaSST office
National Heart and Lung Institute
Hammersmith Campus
Commonwealth building
Du Cane Road
W12 0NN London

Tel: +44 (0) 208 383 2269
e-mail: ines.cabrita05@imperial .ac.uk

Dr [name]
[address]

GP information sheet v1. [date]

Title of project:

THE HEART IN SICKLE CELL DISEASE. ROLE OF NON INVASIVE CARDIAC IMAGING BY ADVANCED ECHOCARDIOGRAPHY AND CARDIAC MAGNETIC RESONANCE ASSESSMENT OF MYOCARDIAL FUNCTION.

REC reference: 09/H0707/73

Dear Dr [name],

Re: [patient's name & address]

This letter is to inform you that your patient has kindly agreed to take part in a research study at Hammersmith Hospital under the supervision of Miss Ines Zimbarra Cabrita.

Your patient has been involved as he/she suffers from sickle cell disease. We aim to study the cardiac function in these patients by new cardiac imaging techniques and correlate it to plasma B-type Natriuretic Peptide levels. He/she has therefore undergone an echocardiography, a blood test and cardiac magnetic resonances scan at the Sir John McMichael Centre and Cardiac Magnetic Resonance Department (Robert Steiner Unit) of Hammersmith Hospital. Your patient's information will be kept secure and confidential.

We hope this study will provide new insights into the objective assessment of cardiac function in sickle cell disease and, therefore, improve the clinical management and monitoring of these patients in the future. We believe that these tests have the potential to do this in a safe and accurate manner. A copy of the patient information sheet is enclosed.

If you have any questions regarding the study, please contact me at the address below.

Many thanks for your attention.

Yours sincerely,

Ines Zimbarra Cabrita

Version 1.0- 5-Aug-09

Appendix III: Two-dimensional and Doppler echocardiography examination protocol

Two-Dimensional and Doppler Echocardiographic Examination Protocol

General procedures

- **Screening visit:** Echo should be done **prior of 6MW**. If not possible there should be **an hour delay** (30 minutes lay down on the echo couch or 10 minutes if 6MW was not performed).
- Studies should be recorded on a DVD and sent to Prosolv.
- Record HR ; Height; Weight; Blood pressure.
- Record **3-5 beats** using harmonic imaging.
- Doppler tracings:
    - recorded at **end-expiration**
    - with **low filter**
    - performed at **50-100 mm/s** sweep speed

3-5 sequential complexes should be include

The echocardiographic examination required the following tomographic views (recorded as listed):

1. Parasternal long axis view
2. Parasternal long axis view right ventricle
3. Parasternal short axis view
3. Apical four chamber view
4. Apical long axis view
5. Apical two chamber view
6. Subcostal long axis view
7. Subcostal short axis view
8. Suprasternal notch view

Echocardiography data to obtain from each view:

1. Parasternal long axis view

   Aortic root diameter
   LV outflow tract diameter for calculation of stroke volume
   LV dimensions (end-diastolic and end-systolic diameter)
   LV wall thickness
   Mitral valve structure/regurgitation
   Wall motion analysis
   Left atrial size
   Aortic valve structure/regurgitation
   Estimation of right ventricular impairment, degree of trabeculation, size and interventricular septal flattening

2. Parasternal long axis view right ventricle inflow and outflow

   RV outflow tract diameter
   Pulmonary artery and branches diameter
   RV isovolumetric contraction and ejection time
   Peak velocity and velocity-time integral of pulmonary artery ejection flow
   Assessment of pulmonary and tricuspid structure/regurgitation

3. Parasternal short axis view

   Basal level
   Papillary muscle level
   Apical level
   M-mode of LV at papillary muscle level
   LV dimensions

4. Apical four chamber view

LV dimensions, long axis dimension

LV volume for single plane and biplane volumes

Mitral regurgitation (colour and continuous wave Doppler)

Tricuspid regurgitation (colour Doppler)

Peak velocity and velocity-time integral of left ventricular outflow tract and aortic flow

LA size and volume

RA size and volume

Measure of RV end-diastolic area

Measure of RV end-systolic area

Separate acquisition of RV including all free wall

Wall motion analysis

Tricuspid regurgitation velocity (continuous wave Doppler)

Time duration from QRS complex to opening of tricuspid valve (start of E wave)

Tricuspid valve inflow

Tissue Doppler of mitral septal and lateral annulus velocity

Tissue Doppler recording of tricuspid annulus velocity

TAPSE: RV tricuspid annulus (sweep speed at 100 m/s)

Diastolic function assessment of left ventricle:

- PW of MV E/A (ate the tips)
- Deceleration time;
- IVRT (include MV inflow and LVOT flow)
- Propagation velocity (Color M-Mode)
- PW of Pulmonary vein (S, D, A reversal waves; A duration)

5. Apical two chamber view

LV volume for biplane volumes

Wall motion analysis

Mitral regurgitation

LA size and volume

6. Sub-costal views

Inferior vena cava

Hepatic vein

6. Apical long axis view

LV outflow tract velocity and velocity time integral

Wall motion analysis

Mitral regurgitation

Aortic regurgitation (colour and continuous wave Doppler) if present

Tricuspid regurgitation velocity (continuous wave Doppler)

7. Sub-costal views

Determination of the diameter of inferior vena cava and its respiratory collapse (ask patient to sniff and record in 2D and M-Mode)

PW of hepatic vein

8. Suprasternal notch view

Aortic Arch

Pulmonary Artery

Descending thoracic aorta

Appendix IV: Three-dimensional echocardiography examination protocol

3D Echocardiography

Optimise ECG tracing to increase R wave peaks.

LEFT VENTRICLE

1. Using 2D imaging, find the best apical window to image the entire left ventricle (use ISCAN)
2. Scan with 3D live; **decrease TGC at apex**, increase gains.
3. Go to "Full Volume" – evaluate whether ventricle fits within sector; readjust transducer position if necessary to include apex. Use **Low scan density** to maximize sector width.
4. Observe image relative to patient's respiration to determine optimal time to acquire.
5. Instruct patient to hold breathing at optimal time and acquire.
6. Countdown as machine acquires and instruct patient to continue breath-hold while acquiring image.
7. Select "autocrop" and inspect for artifact.

RIGHT VENTRICLE

1. Use the best window available in a modified apical transducer location to center the RV. RV free wall must be visible within sector (use ISCAN).
2. Follow steps 2-7 above.

Appendices V to XI: Additional Echocardiography Data

Appendix V. Left ventricular 3-Dimensional Strain and Strain Rate: segmental data

Variable	Patients		Healthy volunteers		Diff. Mean	99% CI of Difference		p-value t
	(N)	Mean ± SD	(N)	Mean ± SD		Lower	Upper	
LV Strain								
3D Frame rate (Hz)	43	18,05 ± 1,65	26	17,23 ± 1,30	0,82	-0,19	1,82	0,04
3D analysis duration (min)	40	10,50 ± 1,28	26	8,54 ± 1,30	1,96	1,10	2,82	**<0.001**
LV 3D end diastolic volume (ml)	43	124,36 ± 39,48	26	96,30 ± 25,36	28,06	5,09	51,04	**0,002**
LV 3D end systolic volume (ml)	43	61,34 ± 22,90	26	46,63 ± 13,13	14,71	1,65	27,76	**0,004**
LV 3DST stroke volume (ml)	43	63,02 ± 18,64	26	49,66 ± 13,85	13,36	2,15	24,56	**0,002**
LV 3DST ejection fraction (%)	43	51,24 ± 4,96	26	51,52 ± 4,75	-0,28	-3,50	2,93	0,82
LV Global longitudinal strain	43	-17,81 ± 3,00	26	-17,23 ± 2,77	-0,58	-2,50	1,34	0,43
LV twist (degree)	43	10,53 ± 6,40	26	10,43 ± 3,97	0,10	-3,60	3,80	0,94
LV torsion (degree/cm)	43	1,28 ± 0,85	26	1,34 ± 0,56	-0,06	-0,55	0,44	0,76
LV 3D Strain (%)								
Basal antero-septal segment	43	-28,51 ± 6,12	26	-30,14 ± 3,38	1,63	-4,72	2,94	0,54
Basal anterior segment	43	-29,59 ± 6,01	26	-30,06 ± 4,42	0,47	-3,13	4,07	0,73
Basal lateral segment	43	-31,21 ± 5,22	26	-31,07 ± 5,06	-0,14	-3,54	3,26	0,91
Basal posterior segment	43	-29,60 ± 6,35	26	-30,00 ± 6,59	0,39	-3,85	4,63	0,81
Basal inferior segment	43	-27,83 ± 6,76	26	-29,35 ± 5,56	1,53	-2,65	5,70	0,34
Basal infero-septal segment	43	-25,83 ± 7,34	26	-31,72 ± 4,14	5,89	1,71	10,06	**<0.001**
Basal segments avg	43	-28,84 ± 3,03	26	-30,05 ± 3,38	1,21	-0,88	3,29	0,13
Median antero-septal segment	42	-34,91 ± 8,32	26	-33,05 ± 6,11	-1,87	-6,87	3,14	0,33
Median anterior segment	43	-35,90 ± 5,48	26	-33,89 ± 7,20	-2,01	-6,08	2,06	0,19
Median lateral segment	43	-34,87 ± 5,44	26	-36,20 ± 6,57	1,32	-2,56	5,20	0,37
Median posterior segment	43	-37,01 ± 6,58	26	-34,87 ± 5,46	-2,14	-6,22	1,94	0,17
Median inferior segment	42	-33,60 ± 7,74	26	-33,56 ± 6,67	-0,04	-4,90	4,83	0,98
Median infero-septal segment	41	-28,12 ± 9,07	26	-30,99 ± 7,96	2,87	-2,89	8,63	0,19
Median segments avg	43	-34,11 ± 4,91	26	-33,76 ± 3,93	-0,36	-3,36	2,65	0,75
Apical anterior segment	42	-35,33 ± 10,06	26	-30,73 ± 8,47	-4,59	-10,87	1,69	0,06
Apical lateral segment	42	-36,05 ± 9,14	26	-32,66 ± 9,60	-3,40	-9,56	2,77	0,15
Apical inferior segment	43	-38,45 ± 11,66	26	-39,53 ± 7,33	1,08	-4,98	7,14	0,64
Apical infero-septal segment	41	-31,16 ± 10,33	24	-31,60 ± 10,22	0,45	-6,58	7,47	0,87
Apical segments avg	43	-35,18 ± 7,26	26	-33,61 ± 5,68	-1,57	-6,00	2,85	0,35
Global (avg of all segments)	43	-32,40 ± 3,83	26	-32,33 ± 3,16	-0,07	-2,44	2,30	0,94
LV Circumferential Strain (CS%)								
Basal antero-septal segment	41	-18,60 ± 6,10	24	-19,23 ± 5,91	0,63	-3,48	4,75	0,68
Basal anterior segment	42	-18,27 ± 5,03	24	-17,36 ± 4,33	-0,90	-4,16	2,35	0,46
Basal lateral segment	41	-20,36 ± 5,81	25	-19,86 ± 5,80	-0,51	-4,42	3,40	0,73
Basal posterior segment	43	-20,49 ± 6,40	25	-22,43 ± 5,89	1,94	-2,21	6,09	0,22
Basal inferior segment	39	-15,88 ± 5,64	25	-16,50 ± 5,70	0,61	-3,24	4,47	0,67
Basal infero-septal segment	42	-17,04 ± 6,26	22	-20,55 ± 6,09	3,51	-0,83	7,84	0,04
Basal segments avg	43	-18,48 ± 3,00	26	-19,22 ± 3,13	0,74	-1,27	2,75	0,33
Median antero-septal segment	43	-26,59 ± 9,26	26	-24,61 ± 5,70	-1,98	-7,33	3,36	0,33
Median anterior segment	43	-30,15 ± 7,30	26	-27,77 ± 7,63	-2,38	-7,28	2,51	0,20
Median lateral segment	43	-29,02 ± 6,69	26	-29,24 ± 9,22	0,22	-4,87	5,31	0,91
Median posterior segment	43	-30,74 ± 6,92	26	-28,67 ± 7,04	-2,07	-6,66	2,51	0,24
Median inferior segment	42	-22,89 ± 8,09	25	-23,56 ± 8,10	0,67	-12,72	1,20	0,03
Median infero-septal segment	35	-18,38 ± 7,60	23	-21,95 ± 7,62	3,57	-6,41	4,52	0,65
Median segments avg	43	-26,52 ± 4,87	26	-26,05 ± 4,29	-0,46	3,58	11,77	**<0.001**
Apical anterior segment	41	-28,07 ± 10,59	26	-23,84 ± 8,99	-4,23	-7,90	2,55	0,17
Apical lateral segment	42	-29,57 ± 9,85	26	-25,61 ± 10,02	-3,96	-9,35	4,45	0,35
Apical inferior segment	42	-29,32 ± 13,36	25	-32,57 ± 8,65	3,25	-3,32	9,32	0,21
Apical infero-septal segment	32	-17,99 ± 9,42	23	-19,22 ± 10,22	1,23	-5,90	8,36	0,65
Apical segments avg	43	-26,75 ± 7,17	26	-25,44 ± 5,12	-1,31	-5,58	2,96	0,42
Global (avg of all segments)	43	-23,48 ± 3,73	26	-23,38 ± 3,51	-0,10	-2,50	2,31	0,92
LV Longitudinal Strain (%)								
Basal antero-septal segment	42	-19,05 ± 4,84	25	-19,85 ± 6,41	0,80	-2,87	4,47	0,57
Basal anterior segment	42	-18,69 ± 5,46	25	-21,79 ± 5,44	3,10	-0,55	6,76	0,03
Basal lateral segment	43	-19,35 ± 5,12	26	-19,09 ± 6,15	-0,26	-3,90	3,38	0,85
Basal posterior segment	41	-16,05 ± 4,49	26	-15,75 ± 6,12	-0,29	-3,74	3,15	0,82
Basal inferior segment	42	-15,43 ± 5,37	26	-18,90 ± 5,49	3,47	-0,11	7,05	0,01
Basal infero-septal segment	41	-15,29 ± 5,03	26	-19,92 ± 4,80	4,63	1,34	7,92	**<0.001**
Basal segments avg	43	-17,31 ± 2,83	26	-19,80 ± 2,56	2,49	0,69	4,29	**<0.001**
Median antero-septal segment	43	-18,68 ± 5,94	26	-16,52 ± 5,24	-2,16	-5,91	1,59	0,13
Median anterior segment	43	-18,65 ± 3,30	26	-19,18 ± 3,63	0,53	-1,73	2,78	0,54
Median lateral segment	43	-19,63 ± 3,15	26	-19,23 ± 3,06	-0,40	-2,45	1,65	0,61
Median posterior segment	43	-17,42 ± 4,04	26	-15,68 ± 3,21	-1,74	-4,22	0,73	0,07
Median inferior segment	43	-18,91 ± 5,72	26	-18,83 ± 4,01	-0,08	-3,47	3,31	0,95
Median infero-septal segment	43	-18,35 ± 4,45	26	-17,89 ± 4,05	-0,46	-3,29	2,38	0,67
Median segments avg	43	-18,61 ± 3,42	26	-17,89 ± 2,51	-0,72	-2,77	1,33	0,36
Apical anterior segment	43	-16,78 ± 4,59	22	-15,52 ± 4,31	-1,26	-4,39	1,88	0,29
Apical lateral segment	43	-18,53 ± 4,24	26	-17,37 ± 4,75	-1,16	-4,08	1,77	0,30
Apical inferior segment	43	-18,72 ± 4,44	25	-19,22 ± 6,13	0,50	-2,92	3,91	0,70
Apical infero-septal segment	43	-19,76 ± 5,77	26	-19,11 ± 5,29	-0,65	-4,33	3,04	0,64
Apical segments avg	43	-18,45 ± 4,01	26	-17,73 ± 4,24	-0,72	-3,41	1,98	0,48
Global (avg of all segments)	43	-18,10 ± 2,79	26	-18,36 ± 2,05	0,26	-1,41	1,94	0,68

Appendix V. Left ventricular 3-Dimensional Strain and Strain Rate: segmental data (cont.)

Variable	Patients		Healthy volunteers		Diff. Mean	99% CI of Difference		p-value ŧ
	(N)	Mean ± SD	(N)	Mean ± SD		Lower	Upper	
LV Radial Strain (%)								
Basal antero-septal segment	43	55,10 ± 17,07	23	50,06 ± 13,27	5,04	-5,84	15,92	0,22
Basal anterior segment	43	56,03 ± 17,52	26	55,79 ± 15,40	0,24	-10,80	11,28	0,95
Basal lateral segment	43	62,08 ± 18,98	25	57,08 ± 14,48	5,00	-6,66	16,66	0,26
Basal posterior segment	42	55,21 ± 16,28	25	54,29 ± 11,96	0,92	-9,03	10,86	0,81
Basal inferior segment	43	48,08 ± 17,92	25	52,15 ± 12,93	-4,07	-14,93	6,79	0,32
Basal infero-septal segment	43	45,64 ± 21,36	26	59,75 ± 14,54	-14,11	-26,69	-1,53	**0,004**
Basal segments avg	43	53,61 ± 9,93	26	55,44 ± 8,67	-1,82	-8,07	4,42	0,44
Median antero-septal segment	43	82,66 ± 36,90	26	68,65 ± 16,65	14,01	-3,27	31,29	0,04
Median anterior segment	43	83,39 ± 22,81	25	74,18 ± 24,38	9,21	-6,39	24,81	0,12
Median lateral segment	43	82,04 ± 22,82	26	83,46 ± 23,28	-1,42	-16,56	13,72	0,80
Median posterior segment	43	85,00 ± 25,70	25	71,62 ± 18,31	13,38	-2,16	28,92	0,03
Median inferior segment	43	75,32 ± 38,72	25	66,86 ± 23,04	8,46	-14,14	31,05	0,32
Median infero-septal segment	43	55,15 ± 25,56	26	60,41 ± 22,09	-5,25	-21,27	10,76	0,39
Median segments avg	43	77,26 ± 20,61	26	71,10 ± 12,16	6,16	-5,64	17,97	0,17
Apical anterior segment	43	82,84 ± 40,01	26	63,95 ± 26,90	18,89	-4,62	42,39	0,04
Apical lateral segment	42	88,53 ± 36,51	26	73,62 ± 34,18	14,91	-8,69	38,50	0,10
Apical inferior segment	41	95,12 ± 45,75	24	92,38 ± 38,44	2,73	-26,78	32,24	0,81
Apical infero-septal segment	43	65,95 ± 37,26	25	62,31 ± 32,45	3,64	-20,10	27,38	0,69
Apical segments avg	43	83,67 ± 31,48	26	72,85 ± 22,23	10,82	-7,87	29,51	0,13
Global (avg of all segments)	43	69,79 ± 15,67	26	65,61 ± 9,99	4,18	-4,93	13,28	0,23
LV 3D Strain Rate (%/ms)								
Basal antero-septal segment	43	-0,19 ± 0,05	26	-0,18 ± 0,05	-0,01	-0,04	0,02	0,46
Basal anterior segment	43	-0,20 ± 0,05	26	-0,19 ± 0,05	-0,01	-0,04	0,03	0,62
Basal lateral segment	43	-0,19 ± 0,04	26	-0,19 ± 0,06	0,00	-0,03	0,03	0,99
Basal posterior segment	43	-0,18 ± 0,04	26	-0,20 ± 0,10	0,02	-0,03	0,06	0,26
Basal inferior segment	43	-0,19 ± 0,05	26	-0,20 ± 0,06	0,01	-0,02	0,04	0,43
Basal infero-septal segment	43	-0,18 ± 0,04	26	-0,22 ± 0,08	0,04	0,00	0,08	0,01
Basal segments avg	43	-0,19 ± 0,02	26	-0,20 ± 0,04	0,01	-0,01	0,03	0,24
Median antero-septal segment	43	-0,20 ± 0,05	26	-0,20 ± 0,06	0,01	-0,03	0,04	0,57
Median anterior segment	43	-0,21 ± 0,04	26	-0,20 ± 0,04	-0,01	-0,04	0,02	0,30
Median lateral segment	43	-0,21 ± 0,05	26	-0,21 ± 0,07	0,00	-0,04	0,04	0,96
Median posterior segment	43	-0,21 ± 0,05	26	-0,18 ± 0,04	-0,03	-0,06	0,01	0,03
Median inferior segment	43	-0,20 ± 0,06	26	-0,21 ± 0,05	0,00	-0,03	0,04	0,75
Median infero-septal segment	43	-0,20 ± 0,06	26	-0,19 ± 0,04	-0,01	-0,05	0,03	0,41
Median segments avg	43	-0,20 ± 0,03	26	-0,20 ± 0,03	-0,01	-0,03	0,01	0,41
Apical anterior segment	43	-0,20 ± 0,05	26	-0,18 ± 0,05	-0,03	-0,06	0,01	0,03
Apical lateral segment	43	-0,23 ± 0,10	26	-0,20 ± 0,09	-0,03	-0,09	0,03	0,19
Apical inferior segment	43	-0,22 ± 0,09	26	-0,24 ± 0,07	0,01	-0,04	0,07	0,50
Apical infero-septal segment	43	-0,23 ± 0,14	26	-0,17 ± 0,05	-0,06	-0,14	0,01	0,03
Apical segments avg	43	-0,22 ± 0,07	26	-0,20 ± 0,04	-0,03	-0,07	0,01	0,06
Global (avg of all segments)	43	-0,20 ± 0,03	26	-0,20 ± 0,03	-0,01	-0,02	0,01	0,46
LV circumferential Strain Rate (%/ms)								
Basal antero-septal segment	43	-0,11 ± 0,03	26	-0,11 ± 0,04	-0,01	-0,03	0,02	0,47
Basal anterior segment	43	-0,12 ± 0,03	26	-0,11 ± 0,04	-0,01	-0,03	0,01	0,22
Basal lateral segment	43	-0,12 ± 0,03	26	-0,12 ± 0,03	0,01	-0,01	0,03	0,36
Basal posterior segment	43	-0,12 ± 0,03	26	-0,13 ± 0,03	0,01	-0,01	0,03	0,30
Basal inferior segment	43	-0,11 ± 0,03	26	-0,12 ± 0,04	0,01	-0,01	0,03	0,29
Basal infero-septal segment	43	-0,11 ± 0,03	26	-0,12 ± 0,04	0,01	-0,01	0,04	0,17
Basal segments avg	43	-0,11 ± 0,02	26	-0,12 ± 0,02	0,00	-0,01	0,02	0,40
Median antero-septal segment	43	-0,16 ± 0,05	26	-0,15 ± 0,04	-0,02	-0,05	0,01	0,11
Median anterior segment	43	-0,18 ± 0,04	26	-0,17 ± 0,05	-0,02	-0,04	0,01	0,17
Median lateral segment	43	-0,17 ± 0,04	26	-0,17 ± 0,06	0,00	-0,03	0,03	0,86
Median posterior segment	43	-0,17 ± 0,05	26	-0,16 ± 0,03	-0,01	-0,04	0,02	0,35
Median inferior segment	43	-0,15 ± 0,05	26	-0,15 ± 0,05	0,00	-0,03	0,03	0,91
Median infero-septal segment	43	-0,14 ± 0,05	26	-0,13 ± 0,05	0,00	-0,03	0,03	0,90
Median segments avg	43	-0,16 ± 0,03	26	-0,16 ± 0,03	-0,01	-0,03	0,01	0,32
Apical anterior segment	43	-0,17 ± 0,06	26	-0,15 ± 0,05	-0,03	-0,06	0,01	0,07
Apical lateral segment	43	-0,18 ± 0,06	26	-0,16 ± 0,06	-0,02	-0,06	0,01	0,10
Apical inferior segment	43	-0,18 ± 0,10	26	-0,18 ± 0,05	0,01	-0,05	0,06	0,77
Apical infero-septal segment	43	-0,16 ± 0,11	26	-0,12 ± 0,06	-0,04	-0,10	0,03	0,14
Apical segments avg	43	-0,17 ± 0,06	26	-0,15 ± 0,03	-0,02	-0,05	0,01	0,13
Global (avg of all segments)	43	-0,10 ± 0,15	26	-0,10 ± 0,01	0,00	-0,02	0,01	0,23

Appendix V. Left ventricular 3-Dimensional Strain and Strain Rate: segmental data (cont.)

Variable	Patients		Healthy volunteers		Diff. Mean	99% CI of Difference		p-value ǂ
	(N)	Mean ± SD	(N)	Mean ± SD		Lower	Upper	
LV Longitudinal Strain Rate (%/ms)								
Basal antero-septal segment	43	-0,12 ± 0,03	26	-0,12 ± 0,03	0,00	-0,02	0,02	0,92
Basal anterior segment	43	-0,11 ± 0,03	26	-0,12 ± 0,03	0,00	-0,02	0,02	0,63
Basal lateral segment	43	-0,12 ± 0,03	26	-0,11 ± 0,03	-0,01	-0,03	0,01	0,25
Basal posterior segment	43	-0,10 ± 0,03	26	-0,10 ± 0,04	0,00	-0,02	0,02	0,92
Basal inferior segment	43	-0,10 ± 0,03	26	-0,11 ± 0,03	0,01	-0,01	0,03	0,35
Basal infero-septal segment	43	-0,11 ± 0,04	26	-0,12 ± 0,04	0,01	-0,02	0,04	0,28
Basal segments avg	43	-0,11 ± 0,02	26	-0,11 ± 0,02	0,00	-0,01	0,02	0,67
Median antero-septal segment	43	-0,11 ± 0,03	26	-0,09 ± 0,03	-0,01	-0,03	0,01	0,10
Median anterior segment	43	-0,09 ± 0,02	26	-0,10 ± 0,02	0,00	-0,01	0,02	0,59
Median lateral segment	43	-0,10 ± 0,02	26	-0,10 ± 0,01	0,00	-0,02	0,01	0,45
Median posterior segment	43	-0,10 ± 0,02	26	-0,08 ± 0,02	-0,01	-0,03	0,00	0,03
Median inferior segment	43	-0,11 ± 0,03	26	-0,10 ± 0,02	0,00	-0,02	0,01	0,54
Median infero-septal segment	43	-0,10 ± 0,03	26	-0,10 ± 0,02	0,00	-0,01	0,02	0,76
Median segments avg	43	-0,10 ± 0,02	26	-0,10 ± 0,01	0,00	-0,01	0,01	0,26
Apical anterior segment	43	-0,08 ± 0,02	26	-0,08 ± 0,02	-0,01	-0,02	0,01	0,28
Apical lateral segment	43	-0,10 ± 0,02	26	-0,09 ± 0,02	-0,01	-0,02	0,01	0,29
Apical inferior segment	43	-0,10 ± 0,02	26	-0,10 ± 0,03	0,00	-0,02	0,01	0,65
Apical infero-septal segment	43	-0,11 ± 0,03	26	-0,10 ± 0,03	-0,01	-0,03	0,01	0,21
Apical segments avg	43	-0,10 ± 0,02	26	-0,09 ± 0,02	-0,01	-0,02	0,01	0,22
Global (avg of all segments)	43	-0,10 ± 0,01	26	-0,10 ± 0,01	0,00	-0,01	0,01	0,42
LV Radial Strain Rate (%/ms)								
Basal antero-septal segment	43	0,31 ± 0,09	26	0,31 ± 0,11	0,01	-0,06	0,07	0,77
Basal anterior segment	43	0,31 ± 0,10	26	0,31 ± 0,11	0,00	-0,07	0,07	0,96
Basal lateral segment	43	0,33 ± 0,09	26	0,31 ± 0,10	0,02	-0,04	0,08	0,42
Basal posterior segment	43	0,30 ± 0,10	26	0,30 ± 0,10	0,00	-0,06	0,07	0,87
Basal inferior segment	43	0,27 ± 0,10	26	0,31 ± 0,13	-0,04	-0,12	0,03	0,14
Basal infero-septal segment	43	0,26 ± 0,13	26	0,35 ± 0,11	-0,09	-0,17	0,00	0,01
Basal segments avg	43	0,30 ± 0,05	26	0,32 ± 0,07	-0,02	-0,06	0,02	0,23
Median antero-septal segment	43	0,50 ± 0,28	26	0,38 ± 0,11	0,11	-0,01	0,24	0,02
Median anterior segment	43	0,45 ± 0,13	26	0,40 ± 0,13	0,05	-0,03	0,13	0,12
Median lateral segment	43	0,43 ± 0,14	26	0,44 ± 0,14	-0,01	-0,10	0,08	0,77
Median posterior segment	43	0,47 ± 0,18	26	0,40 ± 0,11	0,07	-0,04	0,17	0,10
Median inferior segment	43	0,44 ± 0,29	26	0,42 ± 0,19	0,03	-0,14	0,20	0,68
Median infero-septal segment	43	0,34 ± 0,15	26	0,33 ± 0,10	0,01	-0,08	0,10	0,72
Median segments avg	43	0,44 ± 0,14	26	0,39 ± 0,07	0,04	-0,02	0,11	0,08
Apical anterior segment	43	0,51 ± 0,37	26	0,36 ± 0,17	0,16	-0,05	0,36	0,05
Apical lateral segment	43	0,51 ± 0,28	26	0,41 ± 0,20	0,10	-0,07	0,26	0,12
Apical inferior segment	43	0,72 ± 1,19	26	0,54 ± 0,26	0,18	-0,45	0,81	0,45
Apical infero-septal segment	43	0,43 ± 0,37	26	0,37 ± 0,23	0,06	-0,15	0,28	0,43
Apical segments avg	43	0,55 ± 0,50	26	0,40 ± 0,11	0,14	-0,12	0,41	0,15
Global (avg of all segments)	43	0,41 ± 0,16	26	0,37 ± 0,06	0,04	-0,05	0,13	0,22

ǂTwo-sided P values for continuous variables were calculated with the use of the t-test. Significant difference between groups when p<0.01

Appendix VI - LV Diastolic Function and 3D LV strain parameters according to age and gender

Table 1 - LV Diastolic Function parameters

Variable	Female			Male			Both Gender		
	<= 40 y	> 40 y	P-value	<= 40 y	> 40 y	P-value	<= 40 y	> 40 y	P-value
	Mean ± SD	Mean ± SD		Mean ± SD	Mean ± SD		Mean ± SD	Mean ± SD	
Left atrium volume indexed (ml/m2)	38,28 ± 13,81	45,12 ± 15,91	0,20	49,06 ± 17,02	44,56 ± 12,43	0,45	43,67 ± 16,19	44,89 ± 14,39	0,76
LV E wave (cm/s)	95,86 ± 11,20	83,80 ± 14,02	0,01	92,94 ± 12,90	81,34 ± 16,45	0,05	94,40 ± 11,96	82,85 ± 14,79	**0,001**
LV E/A ratio	1,85 ± 0,49	1,32 ± 0,41	**0,002**	1,82 ± 0,48	1,09 ± 0,32	**<0.001**	1,84 ± 0,48	1,23 ± 0,39	**0,000**
LV Isovolumic relaxation time (ms)	85,48 ± 14,62	100,50 ± 17,30	0,02	93,38 ± 18,52	100,50 ± 13,96	0,29	89,29 ± 16,77	100,50 ± 15,67	0,01
MV decelaration time (ms)	191,40 ± 39,65	204,44 ± 37,82	0,34	195,93 ± 38,79	216,25 ± 39,60	0,19	193,67 ± 38,61	209,17 ± 38,31	0,12
LV E´ lateral wall	14,33 ± 2,31	9,98 ± 1,68	**<0.001**	12,97 ± 2,57	9,51 ± 1,84	**0,001**	13,65 ± 2,50	9,79 ± 1,73	**0,000**
MV E´ septal (cm/s)	10,46 ± 1,67	8,12 ± 1,56	**<0.001**	10,48 ± 1,50	7,93 ± 1,45	**<0.001**	10,47 ± 1,56	8,05 ± 1,50	**0,000**
LV E/E' lateral	6,87 ± 1,42	8,71 ± 2,61	0,02	7,49 ± 2,04	8,94 ± 2,77	0,13	7,18 ± 7,00	8,80 ± 2,63	**0,007**
LV E/E´septal	9,41 ± 1,97	10,49 ± 2,14	0,14	8,97 ± 1,47	10,43 ± 2,21	0,05	9,19 ± 1,72	10,47 ± 2,13	0,01
LV E/E´avg	8,13 ± 1,55	9,61 ± 2,08	0,03	8,16 ± 1,57	9,68 ± 2,31	0,06	8,15 ± 1,53	9,64 ± 2,14	**0,003**
Mitral A wave - PV a wave (difference)	-19,67 ± 10,23	-8,10 ± 22,31	0,26	-5,18 ± 50,13	-23,24 ± 45,83	0,45	-10,29 ± 40,67	-14,34 ± 33,57	0,75
Pulmonary veins a wave reversal (cm/s)	21,06 ± 3,55	25,38 ± 7,07	0,07	22,80 ± 3,74	26,61 ± 8,22	0,17	21,93 ± 3,68	25,85 ± 7,35	0,03

Table 2 - LV 3D Strain and Strain Rate

Variable	Female			Male			Both Gender		
	<= 40 y	> 40 y	P-value	<= 40 y	> 40 y	P-value	<= 40 y	> 40 y	P-value
	Mean ± SD	Mean ± SD		Mean ± SD	Mean ± SD		Mean ± SD	Mean ± SD	
LV global longitudinal strain (%)	-20,25 ± 2,32	-16,30 ± 1,92	0,00	-18,18 ± 3,32	-16,37 ± 2,67	0,19	-19,22 ± 2,99	-16,34 ± 2,25	0,00
3D LV strain twist (degree)	9,05 ± 4,76	14,69 ± 7,69	0,05	9,23 ± 5,87	9,02 ± 5,79	0,94	9,14 ± 5,22	12,00 ± 7,28	**0,146**
3D LV strain torsion (degree/cm)	1,10 ± 0,57	1,89 ± 1,05	**0,041**	1,03 ± 0,73	1,07 ± 0,77	**0,906**	1,07 ± 0,64	1,50 ± 0,99	**0,097**
LV 3D strain global (%)	-33,07 ± 2,95	-35,13 ± 3,02	0,12	-30,99 ± 3,87	-30,23 ± 3,83	0,66	-32,03 ± 3,52	-32,80 ± 4,18	0,52
LV circunferential strain global (%)	-23,38 ± 3,58	-26,72 ± 2,18	0,02	-21,37 ± 3,50	-22,35 ± 3,48	0,53	-22,37 ± 3,60	-24,64 ± 3,58	0,04
LV longitudinal strain global (%)	-19,85 ± 2,24	-17,33 ± 2,33	**0,017**	-18,27 ± 3,50	-16,84 ± 2,21	**0,281**	-19,06 ± 2,98	-17,09 ± 2,23	**0,019**
LV radial strain global (%)	73,19 ± 13,22	78,04 ± 16,11	**0,449**	65,81 ± 15,30	61,37 ± 14,39	**0,503**	69,50 ± 14,46	70,10 ± 17,20	**0,901**
LV 3D strain rate (%/ms)	-0,20 ± 0,02	-0,22 ± 0,03	0,01	-0,20 ± 0,03	-0,19 ± 0,03	0,88	-0,20 ± 0,02	-0,21 ± 0,03	**0,140**
LV circumferential strain rate (%/ms)	-0,14 ± 0,02	-0,16 ± 0,03	0,05	-0,14 ± 0,02	-0,14 ± 0,03	0,47	-0,14 ± 0,02	-0,15 ± 0,03	0,06
LV longitudinal strain rate (%/ms)	-0,11 ± 0,01	-0,10 ± 0,01	0,35	-0,10 ± 0,02	-0,10 ± 0,02	0,93	-0,10 ± 0,02	-0,10 ± 0,01	**0,608**
LV radial strain rate (%/ms)	0,40 ± 0,07	0,51 ± 0,27	0,21	0,37 ± 0,10	0,36 ± 0,10	0,72	0,39 ± 0,08	0,44 ± 0,22	0,32

ŧTwo-sided P values for continuous variables were calculated with the use of the t-test. Significant difference between groups when p<0.01

Appendix VII – Cardiac structure and clinical conditions in patients with SCD according to TRV groups

Table 1 - Cardiac structure and function in patients with SCD according to TRV groups

Variable	TRV < 2.5 m/s		TRV ≥ 2.5 m/s		Diff. Mean	99% CI of Difference		p-value ǂ
	(N)	Mean ± SD	(N)	Mean ± SD		Lower	Upper	
LV Structure								
LV septum diameter (mm)	28	9,54 ± 1,37	29	10,29 ± 1,34	-0,74	-1,44	-0,05	0,04
LV posterior wall diameter (mm)	29	9,80 ± 1,57	29	10,34 ± 1,65	-0,54	-1,37	0,28	0,19
LV 2D diastolic volume indexed (ml/m2)	26	72,30 ± 17,24	27	75,73 ± 25,62	-3,44	-14,66	7,79	0,54
LV 2D systolic volume indexed (ml/m2)	29	27,10 ± 9,77	30	25,42 ± 11,37	1,68	-3,76	7,12	0,54
LV mass index (g/m2)	29	86,34 ± 20,76	29	95,39 ± 35,54	-9,05	-25,36	7,26	0,27
RV structure								
RV diastolic area apical view (cm2)	30	19,97 ± 5,21	31	22,09 ± 5,88	-2,12	-4,97	0,73	0,14
RV systolic area apical view (cm2)	30	11,35 ± 3,22	31	12,36 ± 3,20	-1,01	-2,66	0,63	0,22
3D RV end diastolic volume (ml)	29	99,56 ± 23,39	29	120,31 ± 39,15	-20,74	-37,71	-3,78	0,02
3D RV end systolic volume (ml)	29	44,16 ± 14,94	29	55,23 ± 18,46	-11,08	-19,91	-2,24	0,015
LA/RA structure								
Left atrium volume indexed (ml/m2)	30	41,08 ± 12,46	30	47,48 ± 17,13	-6,40	-16,69	3,91	0,10
RA volume indexed (ml/m2)	28	37,99 ± 10,12	29	37,80 ± 13,44	0,20	-6,14	6,53	0,95
LV systolic function								
Global function index lateral	30	0,86 ± 0,21	30	1,10 ± 0,36	-0,24	-0,39	-0,09	**0,003**
Global function index septal	27	1,12 ± 0,27	25	1,30 ± 0,35	-0,17	-0,34	-0,01	0,04
LV 2D Ejection Fraction (%)	30	64,34 ± 6,93	31	67,94 ± 7,20	-3,60	-7,22	0,02	0,05
LV 2D cardiac output (L/min)	28	5,85 ± 1,70	29	6,84 ± 2,24	-0,98	-2,00	0,04	0,06
LV 2D stroke volume (mL)	29	77,40 ± 18,75	29	89,05 ± 27,85	-11,65	-24,00	0,71	0,06
LV S´ wave lateral (cm/s)	30	9,95 ± 1,92	30	8,93 ± 2,55	1,02	-0,16	2,19	0,09
LV S' wave septal (cm/s)	29	8,31 ± 1,24	25	8,25 ± 0,91	0,06	-0,50	0,62	0,84
RV systolic function								
Estimated PVR (Woods unit)	27	1,44 ± 0,35	25	1,67 ± 0,25	-0,23	-0,40	-0,06	0,010
RV MPI by TDI	28	0,34 ± 0,09	29	0,34 ± 0,12	0,00	-0,05	0,06	0,92
RV S´wave (cm/s)	30	14,10 ± 1,99	31	15,50 ± 3,12	-1,41	-2,75	-0,06	0,04
TAPSE (mm)	30	28,03 ± 5,12	30	30,37 ± 5,88	-2,33	-5,18	0,51	0,11
RV fractional area change (%)	30	43,08 ± 9,60	31	43,33 ± 7,92	-0,25	-4,75	4,26	0,91
3D RV Ejection fraction (%)	29	56,15 ± 7,66	29	53,65 ± 6,55	2,50	-1,25	6,25	0,19
LV 3D Strain								
LV 3D ejection fraction (%)	30	50,88 ± 5,06	30	51,61 ± 4,94	-0,73	-3,81	2,35	0,64
LV global longitudinal strain (%)	22	-18,38 ± 3,19	21	-17,22 ± 2,74	-1,16	-3,61	1,30	0,21
LV 3D strain global (%)	22	-31,70 ± 3,57	21	-33,14 ± 4,04	1,43	-1,70	4,57	0,22
LV circunferential strain global (%)	22	-22,54 ± 3,43	21	-24,47 ± 3,85	1,93	-1,07	4,93	0,09
LV longitudinal strain global (%)	22	-18,30 ± 2,89	21	-17,89 ± 2,74	-0,40	-2,73	1,92	0,64
LV radial strain global (%)	22	67,01 ± 13,39	21	72,71 ± 17,60	-5,70	-18,54	7,14	0,24
LV 3D strain rate (%/ms)	22	-0,20 ± 0,02	21	-0,21 ± 0,04	0,01	-0,02	0,03	0,34
LV circumferential strain rate (%/ms)	22	-0,14 ± 0,02	21	-0,15 ± 0,03	0,01	-0,01	0,03	0,19
LV longitudinal strain rate (%/ms)	22	-0,10 ± 0,01	21	-0,10 ± 0,02	0,00	-0,01	0,01	0,70
LV radial strain rate (%/ms)	22	0,37 ± 0,06	21	0,45 ± 0,22	-0,08	-0,21	0,05	0,09
LV RV Strain								
RV longitudinal strain free wall_avg	23	-23,63 ± 11,12	26	-23,46 ± 9,61	-0,17	-4,30	3,97	0,91
RV longitudinal strain basal free wall	19	-21,42 ± 11,58	24	-21,71 ± 10,51	0,29	-6,02	6,60	0,90
RV longitudinal strain median free wall	22	-25,77 ± 13,00	22	-24,00 ± 12,82	-1,77	-9,06	5,51	0,51
RV longitudinal strain apical free wall	22	-23,00 ± 11,62	21	-25,52 ± 12,52	2,52	-3,97	9,02	0,30
RV longitudinal strain basal septum	19	-12,79 ± 8,25	23	-14,57 ± 7,97	1,78	-3,84	7,39	0,40
RV longitudinal strain median septum	23	-18,22 ± 8,82	25	-17,16 ± 8,19	-1,06	-5,24	3,13	0,50
RV longitudinal strain apical septum	21	-13,90 ± 8,39	25	-17,52 ± 9,53	3,62	-2,23	9,46	0,10
All septum segments_avg	23	-15,20 ± 4,35	26	-16,42 ± 5,24	1,22	-2,50	4,94	0,16
RV Global strain (avg of 6 segments)	23	-19,37 ± 8,98	26	-19,80 ± 7,98	0,42	-2,78	3,62	0,72

ǂTwo-sided P values for continuous variables were calculated with the use of the t-test. Significant difference between groups when p<0.01

Appendix VIII - Pearson correlation of clinical and laboratory variables with LV 2D volumes in Univariate analysis

Variable	N	LV 2D systolic volume indexed (ml/m2)		LV 2D diastolic volume indexed (ml/m2)	
		r	P-value	*r*	P-value
Age (years)	61	-0,36	0,00	-0,30	0,02
Heart rate echo (bpm)	61	-0,17	0,18	-0,11	0,41
Body mass index (kg/m^2)	61	-0,41	**0,001**	-0,43	**0,001**
LV mass index (g/m2)	53	0,59	**<0.001**	0,69	**<0.001**
Systolic blood pressue (mmHg)	61	-0,31	0,01	-0,26	0,04
Diastolic blood pressue (mmHg)	61	-0,50	**<0.001**	-0,54	**<0.001**
TRV screening (m/s)	61	0,04	0,76	0,23	0,08
ProBNP, log 10	60	0,20	0,13	0,27	0,04
Clinical history					
Alcohol history	55	0,01	0,96	0,05	0,69
Total number of transfusion in lifetime	46	-0,04	0,81	-0,13	0,37
Leg ulcers	54	-0,05	0,72	0,11	0,42
Vaso-occl, pain crisis	52	-0,06	0,65	-0,07	0,60
History of smoking	55	-0,02	0,90	-0,03	0,81
Lung problems	55	0,19	0,17	0,20	0,14
Spleen problems	55	-0,15	0,28	-0,07	0,58
Blood Tests					
Alkaline phosphatase (uL)	58	0,24	0,07	0,25	0,05
Absolute reticulocyte count (x10^3 cells/lL)	60	0,51	**<0.001**	0,58	**<0.001**
Aspartate aminotransferase (u/L)	57	0,46	**<0.001**	0,58	**<0.001**
Blood urea nitrogen (mmol/L)	60	-0,14	0,30	-0,24	0,06
Creatinine (umol/l)	60	0,05	0,73	-0,12	0,36
Hematocrit (SI units)	59	-0,27	0,04	-0,51	**<0.001**
Haemoglobin(g/dl)	60	-0,30	0,02	-0,51	**<0.001**
LDH (IU/l)	53	0,49	**<0.001**	0,64	**<0.001**
Mean cell volume (fl)	60	0,24	0,06	0,29	0,03
oxygen saturation on air	61	-0,29	0,02	-0,47	**<0.001**
Platelet count (x10^3 cells/ul)	60	0,32	0,01	0,35	**0,006**
Red blood count (x10^6/ul)	60	-0,38	**0,003**	-0,58	**<0.001**
Red cell distribution width (%)	58	0,22	0,10	0,40	**0,002**
Reticulocytes (%)	60	0,55	**<0.001**	0,67	**<0.001**
Total bilirubin (umol/l)	58	0,42	**0,001**	0,47	**<0.001**
White blood cell count (x10^3 cells/ul)	60	0,25	0,05	0,34	**0,007**
LV Diastolic function					
LV E wave (cm/s)	61	0,16	0,21	0,26	0,05
LV E/A ratio	60	0,18	0,18	0,16	0,21
MV decelaration time (ms)	60	0,14	0,30	0,07	0,60
LV Isovolumic relaxation time (ms)	55	-0,02	0,88	0,01	0,93
LV E´ lateral wall	60	0,13	0,33	0,08	0,55
LV E/E' lateral	60	-0,03	0,84	0,08	0,56
MV E´ septal (cm/s)	60	0,23	0,08	0,28	0,03
LV E/E´septal	60	-0,09	0,47	-0,08	0,52
LV E/E´avg	59	-0,07	0,58	0,00	0,99
Left atrium volume indexed (ml/m2)	60	0,36	**0,005**	0,54	**<0.001**

ŧTwo-sided P values for continuous variables were calculated with the use of the t-test. Significant difference between groups when p<0.01

Appendix IX – Associations with Haemolysis markers

Variables	Markers of Hemolysis											
	Hemoglobin (g/dl)			LDH (IU/l)			Total bilirubin (umol/l)			Reticulocytes (%)		
	N	*r*	*P*-value	N	*r*	*P*-value	N	*r*	*P*-value	N	*r*	*P*-value
LV function and structure												
Global function index lateral	60	-0,01	0,94	53	-0,12	0,37	58	0,08	0,56	60	-0,12	0,37
Global function index septal	60	0,18	0,18	53	-0,20	0,13	58	-0,01	0,94	60	-0,20	0,13
LV 3D ejection fraction (%)	43	-0,04	0,82	37	-0,11	0,47	42	-0,14	0,36	43	-0,11	0,47
LV S´ wave lateral (cm/s)	60	-0,21	0,10	53	0,18	0,16	58	-0,19	0,15	60	0,18	0,16
LV S' wave septal (cm/s)	60	-0,43	**0,001**	53	0,36	**0,005**	58	0,15	0,25	60	0,36	**0,005**
LV 2D diastolic volume indexed (ml/m2)	60	-0,51	**<0,001**	53	0,67	**<0,001**	58	0,47	**<0,001**	60	0,67	**<0,001**
LV 2D systolic volume indexed (ml/m2)	60	-0,30	0,02	53	0,55	**<0,001**	58	0,42	**0,001**	60	0,55	**<0,001**
LV mass index (g/m2)	52	-0,22	0,12	45	0,27	0,05	50	0,22	0,13	52	0,27	0,05
Left ventricular strain and strain rate												
3D LV strain twist (degree)	43	0,02	0,92	37	-0,01	0,93	42	0,11	0,50	43	-0,01	0,93
3D LV strain torsion (degree/cm)	43	0,07	0,68	37	-0,08	0,61	42	0,05	0,74	43	-0,08	0,61
LV 3DST global avg of all segments	43	0,09	0,58	37	0,14	0,36	42	0,17	0,27	43	0,14	0,36
LV longitudinal strain global avg of all segments	43	0,13	0,40	37	-0,15	0,32	42	0,00	0,99	43	-0,15	0,32
LV circunferential strain global	43	0,11	0,48	37	0,21	0,17	42	0,03	0,84	43	0,21	0,17
LV radial strain global avg of all segments	43	-0,03	0,87	37	-0,16	0,30	42	-0,09	0,57	43	-0,16	0,30
LV 3D Strain rate global	43	-0,04	0,81	37	0,18	0,24	42	0,12	0,45	43	0,18	0,24
LV longitudinal strain rate global	43	0,05	0,75	37	-0,03	0,85	42	0,10	0,51	43	-0,03	0,85
LV circunferential strain rate global	43	-0,07	0,66	37	0,33	0,03	42	0,12	0,44	43	0,33	0,03
LV radial strain rate global	43	0,18	0,24	37	-0,31	0,05	42	-0,17	0,28	43	-0,31	0,05
Right ventricular function												
Tricuspid regurgitant jet velocity screening (m/s)	60	-0,22	0,10	53	0,18	0,17	58	0,27	0,04	60	0,18	0,17
Estimated pulmonary systolic pressure (mmHg)	60	-0,21	0,11	53	0,18	0,16	58	0,31	0,02	60	0,18	0,16
Pulmonary vascular resistance (Woods unit)	51	-0,03	0,84	47	0,02	0,88	49	0,07	0,62	51	0,02	0,88
RA volume indexed 2D (ml/m2)	56	-0,40	**0,002**	49	0,50	**<0,001**	54	0,28	0,04	56	0,50	**<0,001**
3D RV Ejection fraction (%)	57	-0,20	0,13	51	0,14	0,30	56	0,01	0,94	57	0,14	0,30
3D RV end diastolic volume	57	-0,19	0,16	51	0,40	**0,002**	56	0,46	**<0,001**	57	0,40	**0,002**
3D RV end systolic volume	57	-0,08	0,55	51	0,28	0,03	56	0,38	**0,004**	57	0,28	0,03
RV diastolic area apical view (cm2)	60	-0,23	0,08	53	0,43	**0,001**	58	0,40	**0,002**	60	0,43	**0,001**
RV systolic area apical view (cm2)	60	-0,04	0,77	53	0,27	0,04	58	0,42	**0,001**	60	0,27	0,04
RV fractional area change (%)	60	-0,30	0,02	53	0,21	0,12	58	-0,04	0,78	60	0,21	0,12
RV E wave (cm/s)	55	0,05	0,72	49	-0,01	0,93	53	-0,11	0,45	55	-0,01	0,93
RV E/A	47	0,28	0,05	43	-0,10	0,48	45	-0,25	0,09	47	-0,10	0,48
RV E´/A´	55	0,13	0,36	48	0,05	0,74	54	-0,01	0,94	55	0,05	0,74
RV E´wave (cm/s)	60	-0,16	0,22	53	0,26	0,05	58	0,15	0,28	60	0,26	0,05
RV E/E´	55	0,23	0,09	49	-0,25	0,06	53	-0,18	0,21	55	-0,25	0,06
RV isovolumic relaxation time (ms)	46	-0,24	0,10	42	0,19	0,21	44	0,06	0,72	46	0,19	0,21
RV myocardial performance index by TDI	57	-0,16	0,23	50	0,03	0,81	55	0,06	0,66	57	0,03	0,81
RV S´wave (cm/s)	60	-0,39	**0,002**	53	0,30	0,02	58	0,26	0,05	60	0,30	0,02
Tricuspid annular systolic motion (mm)	59	-0,43	**0,001**	52	0,38	**0,003**	57	0,04	0,75	59	0,38	**0,003**
RV longitudinal strain free wall_avg	59	0,03	0,80	52	0,04	0,75	57	-0,05	0,69	49	0,24	0,10
RV Global strain (avg of 6 segments)	59	0,09	0,52	52	-0,01	0,97	57	-0,05	0,70	49	0,15	0,32
LV diastolic function												
LV E wave (cm/s)	60	-0,20	0,13	53	0,12	0,39	58	0,15	0,25	60	0,32	0,014
MV decelaration time (ms)	60	-0,11	0,40	53	0,13	0,36	58	0,21	0,11	60	0,10	0,44
LV Isovolumic relaxation time (ms)	55	0,00	0,99	49	0,26	0,07	53	-0,03	0,83	55	-0,16	0,23
LV E/A ratio	60	0,07	0,57	53	-0,14	0,31	58	-0,01	0,93	60	0,17	0,20
LV E/E' lateral	60	-0,20	0,12	53	0,13	0,34	58	0,17	0,21	60	0,02	0,89
LV E/E´septal	60	-0,06	0,65	53	0,00	0,99	58	0,13	0,33	60	-0,01	0,94
LV E/E´avg	59	-0,16	0,23	52	0,09	0,53	57	0,17	0,21	59	0,01	0,96

Appendix X - Associations with TRV by Pearson Rank Correlation Coefficient

Variable	N	Tricuspid regurgitant jet velocity (m/s)	
		Pearson Correlation (*r*)	*P*-value
LV systolic function			
Global function index lateral	60	0,31	0,02
Global function index septal	60	0,21	0,11
LV 3D ejection fraction (%)	43	0,05	0,77
LV S´ wave lateral (cm/s)	60	-0,21	0,11
LV S' wave septal (cm/s)	60	0,05	0,69
LV 2D diastolic volume indexed (ml/m2)	61	0,23	0,08
LV 2D systolic volume indexed (ml/m2)	61	0,04	0,76
Interventricular septum diameter (mm)	61	0,17	0,19
LV posterior wall diameter (mm)	61	0,25	0,05
LV 2D end-diastolic diameter (mm)	61	0,37	**0,003**
LV 2D end-systolic diameter (mm)	61	0,14	0,28
LV 2D Ejection fraction (%)	61	0,25	0,05
LV mass index (g/m2)	53	0,28	0,04
LV 2D stroke volume	60	0,32	0,01
LV cardiac output (L/min)	61	0,32	0,01
Right ventricular function:			
Pulmonary vascular resistance (Woods unit)	52	0,50	**<0,001**
RA volume indexed 2D (ml/m2)	57	0,28	0,04
3D RV Ejection fraction (%)	58	-0,10	0,46
3D RV end diastolic volume	58	0,43	**0,001**
3D RV end systolic volume	58	0,39	**0,003**
RV base to apex diamater (cm)	59	0,22	0,10
RV base diameter (cm)	59	0,36	**0,006**
RV mid diamater (cm)	59	0,27	0,04
RV diastolic area apical view (cm2)	61	0,28	0,03
RV systolic area apical view (cm2)	61	0,16	0,21
RV fractional area change (%)	61	0,14	0,28
RV E wave (cm/s)	55	0,02	0,91
RV E/A	47	-0,40	**0,006**
RV E´/A´	55	-0,31	0,02
RV E´wave (cm/s)	60	0,04	0,74
RV E/E´	55	-0,05	0,72
RV isovolumic relaxation time (ms)	46	0,22	0,14
RV myocardial performance index by TDI	57	0,07	0,59
RV S´wave (cm/s)	61	0,27	0,04
Tricuspid annular systolic motion (mm)	60	0,38	**0,003**
Pulmonary valve accelaration time (ms)	60	-0,03	0,82
RV longitudinal strain free wall_avg	60	0,01	0,93
RV Global strain (avg of 6 segments)	60	0,00	1,00
LV diastolic function variables			
LV E wave (cm/s)	61	0,14	0,29
LV E/A ratio	60	-0,28	0,03
MV decelaration time (ms)	60	0,19	0,14
LV Isovolumic relaxation time (ms)	55	0,09	0,53
LV E ´ lateral wall	60	-0,29	0,02
Left ventricle E/E' lateral	60	0,36	**0,005**
MV E´ septal (cm/s)	60	-0,17	0,20
LV E/E´septal	60	0,31	0,02
Left ventricle E/E´avg	59	0,38	**0,003**
Mitral A wave - PV a wave (difference)	34	-0,09	0,60
Pulmonary veins a wave reversal (cm/s)	45	0,22	0,15
Left atrium volume indexed (ml/m2)	60	0,31	0,02
LV Strain 3D variables			
3D LV strain twist (degree)	43	0,33	0,03
3D LV strain torsion (degree/cm)	43	0,31	0,05
LV 3DST global avg of all segments	43	-0,06	0,71
LV longitudinal strain global avg of all segments	43	0,09	0,56
LV circunferential strain global	43	-0,15	0,34
LV radial strain global avg of all segments	43	0,08	0,60
LV 3D Strain rate global	43	-0,11	0,49
LV longitudinal strain rate global	43	0,00	0,99
LV circunferential strain rate global	43	-0,03	0,85
LV radial strain rate global	43	0,13	0,39

Appendix XI - Cardiac structure and function in patients with SCD according to LV diastolic function (COMPLETE)

Variable	Group A1 (normal LV diastolic fucntion)			Group A2 (abnormal LV diastolic function)			p-value ŧ
	(N)	Mean ±	SD	(N)	Mean ±	SD	
Demographics							
Age(years)	43	36,70	10,82	18	50,12	8,42	**<0,001**
Height (cm)	43	168,64	9,72	18	169,24	10,51	0,838
Weight (kg)	43	67,77	9,31	18	73,34	13,74	0,149
Body surface area (kg/m^2)	43	1,78	0,15	18	1,85	0,22	0,141
Body Mass Index (kg/m^2)	43	23,92	3,51	18	25,51	3,79	0,134
Heart rate (bpm)	43	74,96	9,52	18	78,88	11,32	0,183
Oxygen saturation on air (%)	43	97,20	3,76	18	97,19	2,46	0,990
Systolic BP (mmHg)	43	118,36	11,17	18	122,75	20,58	0,427
Diastolic BP (mmHg)	43	69,69	9,58	18	73,75	12,04	0,179
LV and RV Structure							
LV septum diameter (mm)	43	9,98	1,39	18	9,75	1,46	0,572
LV posterior wall diameter (mm)	43	10,08	1,67	18	10,11	1,54	0,953
LV 2D diastolic volume indexed (ml/m2)	43	75,11	23,48	18	71,05	16,41	0,527
LV 2D systolic volume indexed (ml/m2)	43	27,02	11,22	18	24,06	8,36	0,339
LV 2D mass index (g/m2)	43	93,41	31,52	18	83,32	21,02	0,304
RV structure							
RV 2D diastolic area apical view (cm2)	43	21,03	5,98	18	21,08	4,62	0,976
RV 2D systolic area apical view (cm2)	43	12,02	3,35	18	11,42	2,92	0,529
RV 3D end diastolic volume (ml)	43	112,64	35,64	18	101,42	25,59	0,281
RV 3D end systolic volume (ml)	43	51,03	18,80	18	45,52	12,53	0,311
LA/RA structure							
Left atrium volume indexed (ml/m2)	43	44,15	17,11	18	44,66	8,31	0,910
RA volume indexed (ml/m2)	43	38,20	12,12	18	37,03	11,28	0,746
LV and RV systolic function							
Global function index lateral	43	0,87	0,23	18	1,28	0,34	**<0,001**
Global function index septal	43	1,15	0,32	18	1,39	0,27	0,010
LV 3D ejection fraction (%)	32	51,38	5,16	11	50,84	4,51	0,759
LV S´ wave lateral (cm/s)	43	9,62	2,50	18	8,88	1,59	0,270
LV S' wave septal (cm/s)	43	8,35	1,18	18	8,07	0,71	0,362
RV systolic function							
Estimated PASP (mmHg)	43	30,61	6,72	18	35,28	5,98	0,017
TRV screening (m/s)	43	2,46	0,28	18	2,72	0,27	**0,002**
Estimated PVR (Woods unit)	43	1,47	0,29	18	1,79	0,30	**0,002**
RV MPI by TDI	43	0,32	0,11	18	0,38	0,10	0,073
RV S´wave (cm/s)	43	14,53	2,36	18	15,60	3,44	0,174
TAPSE (mm)	43	28,84	5,99	18	30,27	4,13	0,398
RV fractional area change (%)	43	42,34	8,82	18	45,66	8,20	0,193
RV 3D Ejection fraction (%)	43	54,95	7,39	18	54,74	6,72	0,924
Strain and Strain Rate							
LV global longitudinal strain (%)	32	-18,22	3,09	11	-16,62	2,46	0,130
LV 3D strain global (%)	32	-32,44	3,77	11	-32,30	4,18	0,920
LV circunferential strain global (%)	32	-23,14	3,79	11	-24,47	3,52	0,314
LV longitudinal strain global (%)	32	-18,31	3,02	11	-17,48	1,97	0,400
LV radial strain global (%)	32	69,90	16,00	11	69,48	15,40	0,940
LV 3D strain rate (%/ms)	32	-0,20	0,02	11	-0,20	0,04	0,774
LV circumferential strain rate (%/ms)	32	-0,14	0,02	11	-0,15	0,04	0,396
LV longitudinal strain rate (%/ms)	32	-0,10	0,02	11	-0,10	0,01	0,832
LV radial strain rate (%/ms)	32	0,40	0,10	11	0,46	0,28	0,279
RV 2D Strain							
RV Global strain	43	-15,66	8,25	15	-17,04	9,45	0,591
RV Free wall (average)	43	-18,56	9,84	15	-21,21	11,96	0,396
RV Septum (average)	37	-15,60	4,62	12	-16,64	5,59	0,521
Markers of hemolysis							
Haemoglobin (g/dl)	43	9,23	1,88	16	8,93	1,28	0,564
Lactate dehydrogenase (IU/l)	43	408,37	219,66	15	431,27	195,12	0,726
Reticulocytes (%)	43	8,99	5,46	16	7,75	3,70	0,405
Total bilirubin (umol/l)	43	45,17	31,92	16	54,31	48,93	0,407
Hematocrit (SI units)	43	0,26	0,05	16	0,25	0,03	0,663
Creatinine (umol/l)	43	68,75	31,65	16	75,88	13,20	0,388
Blood urea nitrogen (mmol/L)	43	3,93	3,38	16	4,29	2,09	0,690
Aspartate aminotransferase (U/L)	43	40,76	22,02	16	41,44	28,50	0,923
Urate (mmol/L)	40	0,33	0,12	15	0,35	0,12	0,513

ŧTwo-sided P values for continuous variables were calculated with the use of the t-test. Significant difference between groups when p<0.01